WAVE INTERACTIONS IN PERIODIC STRUCTURES AND PERIODIC DIELECTRIC WAVEGUIDES

Thesis by

Avraham Gover (Graubart)

In Partial Fulfillment of the Requirements

for the Degree of

Doctor of Philosophy

California Institute of Technology

Pasadena, California

1976

(Submitted November 26, 1975)

ACKNOWLEDGMENTS

I want to express my appreciation to Dr. Yariv for his superb guidance. His keen scientific intuition led me to directions of worthwhile research problems and to ways toward their solutions. He provided me with considerable patience, attention and advice and at the same time allowed me enough freedom to develop my research ideas. I will always be grateful for all I have learned from him.

I would also like to express my gratitude for the excellent scientific education that I have received at Caltech from the professors of the Electrical Engineering Department, Prof. Carver Mead, Prof. Charles Papas and Prof. Nicholas George.

During this work I have benefited greatly from many discussions with Dr. A. Rose, Prof. R. Feynman, Dr. A. Barybin and many of the professors of the Electrical Engineering Department. I am grateful for the opportunity I had to enjoy their expertise.

The financial support of the Office of Naval Research made this research possible. Miss Dian Rapchak and Mrs. Ruth Stratton invested hard work in the typing of the manuscript. Their efforts are greatly appreciated.

Last, but not least, I want to acknowledge my dear wife, Joan, for her support and help in many ways during this research.

ABSTRACT

This work is concerned with a general analysis of wave interactions in periodic structures and particularly periodic thin film dielectric waveguides.

The electromagnetic wave propagation in an asymmetric dielectric waveguide with a periodically perturbed surface is analyzed in terms of a Floquet mode solution. First order approximate analytical expressions for the space harmonics are obtained. The solution is used to analyze various applications: (1) phase matched second harmonic generation in periodically perturbed optical waveguides; (2) grating couplers and thin film filters; (3) Bragg reflection devices; (4) the calculation of the traveling wave interaction impedance for solid state and vacuum tube optical traveling wave amplifiers which utilize periodic dielectric waveguides. Some of these applications are of interest in the field of integrated optics.

A special emphasis is put on the analysis of traveling wave interaction between electrons and electromagnetic waves in various operation regimes. Interactions with a finite temperature electron beam at the collision-dominated, collisionless, and quantum regimes are analyzed in detail assuming a one-dimensional model and longitudinal coupling.

The analysis is used to examine the possibility of solid state traveling wave devices (amplifiers, modulators), and some monolithic structures of these devices are suggested, designed to operate at the submillimeter-far infrared frequency regime. The estimates of

attainable traveling wave interaction gain are quite low (on the order of a few inverse centimeters). However, the possibility of attaining net gain with different materials, structures and operation condition is not ruled out.

The developed model is used to discuss the possibility and the theoretical limitations of high frequency (optical) operation of vacuum electron beam tube; and the relation to other electron-electromagnetic wave interaction effects (Smith-Purcell and Cerenkov radiation and the free electron laser) are pointed out. Finally, the case where the periodic structure is the natural crystal lattice is briefly discussed. The longitudinal component of optical space harmonics in the crystal is calculated and found to be of the order of magnitude of the macroscopic wave, and some comments are made on the possibility of coherent bremsstrahlung and distributed feedback lasers in single crystals.

TABLE OF CONTENTS

CHAPTER 1

INTRODUCTION

Propagation of waves in periodic structure is a long standing physics research subject which aroused the interest of many distinguished physicists and has been investigated from different aspects through the last century [e.g. Lord Rayleigh, 1887, Brillouin 1946, Pierce 1950, 1974].

The periodically reviving interest in this problem results from the existence of few general phenomena in wave interaction in periodic structures, which are characteristic of the periodic structure and independent of the kinds of interacting waves. With the advancement of technology different kinds of waves in new kinds of structures and operation regimes are constantly found to exhibit these phenomena.

Some of the most important common characteristics of wave propagation in periodic structures are Bragg reflection, forbidden bands and the existence of space harmonics (wave components which can propagate with phase velocities very different from that in the uniform medium). These phenomena occur to electromagnetic waves in the microwave regime, optical regime or x-ray regime. They occur with acoustic waves, electron waves and plasma waves. They may be observed in natural occurring periodic structures - like the crystal lattice - as well as artificial periodic structures like periodic waveguides and optical gratings.

Many physical phenomena may be described as the result of

interaction between two, three or more waves. Suppose we have two traveling plane waves

$$A_1(\underline{r},t) = A_1(\underline{q}_1,\omega_1)e^{i(\omega_1 t-\underline{q}_1\underline{r})}$$
$$A_2(\underline{r},t) = A_2(\underline{q}_2,\omega_2)e^{i(\omega_2 t-\underline{q}_2\underline{r})} \qquad \text{(I-1)}$$

Using very general terms to describe a vast class of phenomena, we may say that the "coupling strength" or the "interaction rate" between the two waves will be proportional to the time-space overlap of the two field waves (assuming the coupling mechanism is uniform in space and time)

$$A_1A_2^*\iint e^{i[(\omega_1-\omega_2)t - (\underline{q}_1-\underline{q}_2)\underline{r}]}d^3rdt \qquad \text{(I-2)}$$

This overlap integral will be maximal when

$$\omega_1 = \omega_2 \qquad \text{(I-3)}$$

$$\underline{q}_1 = \underline{q}_2 \qquad \text{(I-4)}$$

These conditions can be referred to as temporal and spatial "phase matching" and are equivalent to the familiar conditions of energy conservation and momentum conversation.

We may clarify this concept a little more by considering a familiar example - quantum mechanical radiative transition of an electron. This example (which will be broadly discussed later in Chapter VI) can be described as a three wave interaction. Instead of (I-2) the transition rate will be proportional to a term like

$$A_1A_2^*A_3^*\iint e^{i[(\omega_1-\omega_2-\omega_3)t - (\underline{q}_1-\underline{q}_2-\underline{q}_3)\underline{r}]}d^3rdt \qquad \text{(I-5)}$$

where $\omega_1 \equiv \mathcal{E}_1/\hbar$, $\omega_2 \equiv \mathcal{E}_2/\hbar$, $\mathcal{E}_1$ and $\mathcal{E}_2$ are the energies of the electron in the initial and final states respectively, and ω_3 is the radiation frequency. The phase matching condition

$$\omega_1 - \omega_2 - \omega_3 = 0 \tag{I-6}$$

$$\underline{q}_1 - \underline{q}_2 - \underline{q}_3 = 0 \tag{I-7}$$

are equivalent to the familiar energy and momentum conservation conditions respectively $\mathcal{E}_1 - \mathcal{E}_2 = \hbar\omega_3$, $\underline{p}_1 - \underline{p}_2 = \hbar\underline{q}_3$, where $\underline{p}_1 \equiv \hbar\underline{q}_1$, $\underline{p}_2 \equiv \hbar\underline{q}_2$ are the electron momenta at the initial and final states respectively and $\underline{q}_3$ is the propagation vector of the radiation.

The significance of periodic structures in supporting different wave interactions which can be described in the above mentioned manner, can now be appreciated. The mode solutions of a field wave equation in a spatially periodic medium is given according to the Floquet (or Bloch) theorem by

$$\underline{A}(\underline{r},t) = \sum_{\underline{G}} \underline{A}_{\underline{G}}(\underline{q},\omega) e^{i(\omega t - \underline{q}_{\underline{G}} \underline{r})} \tag{I-8}$$

$$\underline{q}_{\underline{G}} = \underline{q} + \underline{G} \tag{I-9}$$

where $\underline{G}$ are the vectors of the reciprocal lattice of the periodic structure. (In the one dimensional periodicity case $|\underline{G}| = m\,2\pi/L$, $m = 0,\pm1,\pm2,\ldots$ and L is the period.) We call the elements of the sum in Eq. (I-8) space harmonics and the zero order space harmonic $\underline{G} = 0$ the fundamental.

Since each wave in a periodic structure has an infinite number of space harmonics with different momenta, momentum conservation

condition (or spatial phase matching) can occur between waves which are normally unmatched in an homogeneous medium, and hence the interaction between them can be largely increased. This phase matching can occur between modes of the same kind of wave (ordinary Bragg reflection can be described this way) as well as interaction between different kinds of waves (like electron- photon interaction in periodic structure which will be discussed in Chapters VI, VII). Deliberate phase matching is possible in artificial periodic structures where the periodicity L can be chosen in advance so that the lattice momentum $|\underline{G}| = m\frac{2\pi}{L}$ will provide spatial phase matching between particular waves of interest.

In the present work I intend to present some interactions in periodic structures with special emphasis on interactions between electron and electromagnetic waves in different physical regimes.

In Chapter II I present a Floquet mode approximate solution of electromagnetic wave propagation in a periodic dielectric waveguide and in particular, thin film dielectric waveguide with a periodically perturbed surface (Fig. 1). This last structure is of particular interest to Caltech's Quantum Electronics research group, which has recently demonstrated its fabrication with a new state of the art period as short as 1000Å and with lengths of the order of centimeter [Garvin 1973]. This structure is also fitting for integration in future monolithic integrated optics circuits which is one of this group's research objectives. The third chapter presents analyses of several applications of this structure utilizing the results of Chapter II.

Inclusive analysis of the interaction between electrons and

electromagnetic waves in periodic semiconductor structures is given in Chapters IV to VI. A classical collision dominated regime is analyzed in Chapter IV, Chapter V presents classical analysis in the collisionless kinetic regime, and in Chapter VI we present a quantum mechanical extension of the theory. The three different treatments are then discussed in Chapter VII, showing their mutual consistency and their consistency and relation with conventional traveling wave interaction analysis and related effects like Smith-Purcell radiation, Cerenkov radiation, free electron laser, coherent bremstrahlung in the crystal lattice, superlattice effects and the distributed feedback single crystal x-ray laser.

CHAPTER II

ANALYSIS OF ELECTROMAGNETIC MODES IN PERIODIC THIN FILM DIELECTRIC WAVEGUIDES

1. Introduction

Wave equations and particularly the Maxwell equations were previously solved in the crystal lattice and in stratified media in some operational regimes by several authors [e.g. Brillouin 1946, Tamir 1964, Elachi 1971, 1972]. However, the problem of periodic thin film dielectric waveguide is different from the case of stratified media, because of the need to match boundary conditions transversely to the periodicity direction, which complicates the mathematical solution.

Following the recent interest in propagation of light waves in periodic thin film dielectric waveguide (with particular reference to application in integrated optics) several analyses of some particular cases of this problem were recently presented. These analyses were usually based on computer calculation and solve particular cases (symmetric waveguide, Bragg reflection regime, leaky waveguides) [Dabby 1972, Sakuda 1973, Peng 1973, 1974].

It is our goal in this chapter to present an approximate analytic solution for electromagnetic wave propagation in a periodic waveguide and in particular in a structure like that in Fig. 1. The analytic approximate expressions that we will derive in this chapter for the space harmonics of the electromagnetic wave will be used in Chapter III to evaluate different applications in different regimes with convenience and transparency that are not achievable by a computer calculation.

The structure which is under investigation (Fig. 1) is an asymmetric dielectric waveguide with a thin periodically perturbed surface layer. The importance of this case is that it corresponds to practically producible periodic thin film waveguides. The structure is composed of a substrate, waveguide, and superstrate layers (for example, GaAlAs, GaAs and air correspondingly), and a surface perturbation layer that can be introduced, for instance, by surface corrugation. The realization of similar structures was recently demonstrated by our research group [Garvin 1973, Nakamura 1973, 1974, Yen 1973]. The shortest periods available so far are of the order of 1000Å and achievement of periods of the order of several hundred Angstroms are anticipated [Bjorklund 1974]. Hence this structure has the advantages of ease of production, compatibility with future monolithic integrated optics layout, and also as an alternative way to achieve long superlattice structures and related effects (discussed later in Chapter VII, Appendix B).

Our model of a periodically perturbed thin film waveguide is described schematically in Fig. 1 . The periodic perturbation is accounted for by an effective layer of thickness a, whose index of refraction varies along the propagation direction z (see Fig. 1) according to

$$n_L^2 = n_{L0}^2 + n_{L1}^2 \cos \frac{2\pi}{L} z \qquad \text{(II-1)}$$

This layer represents, as an example, a corrugation of a dielectric waveguide or any other periodic perturbation of the index of refraction of a dielectric waveguide.

Fig. 1 Dielectric waveguide with periodic perturbation layer of sinusoidally varying dielectric constant.

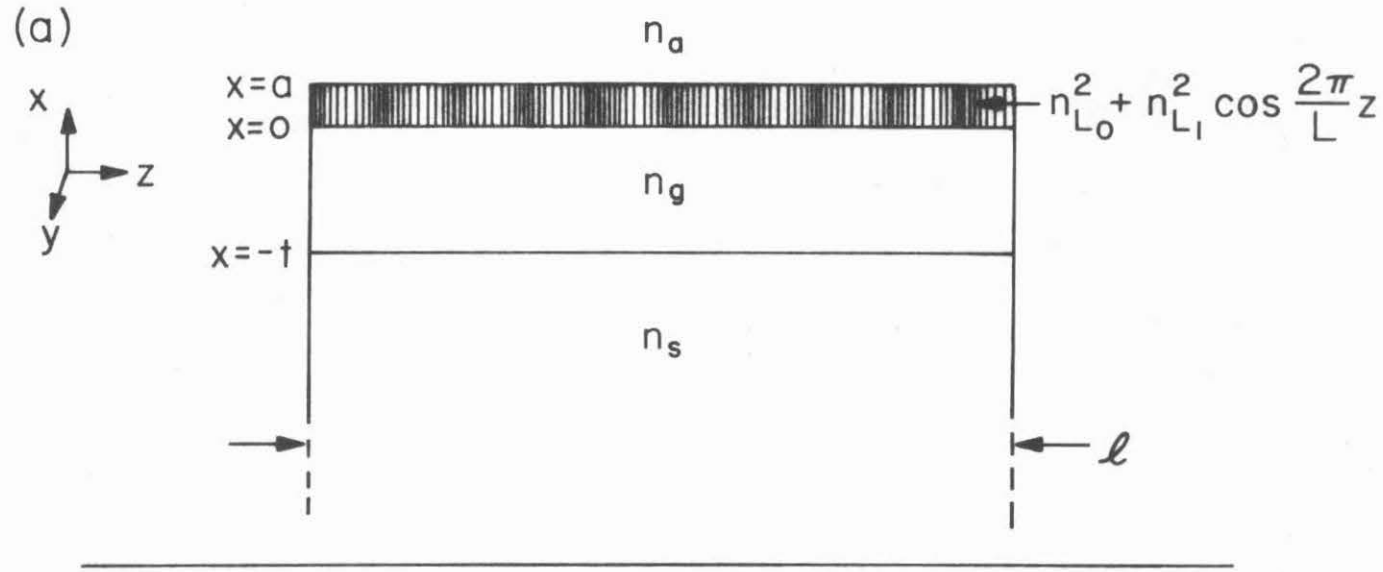

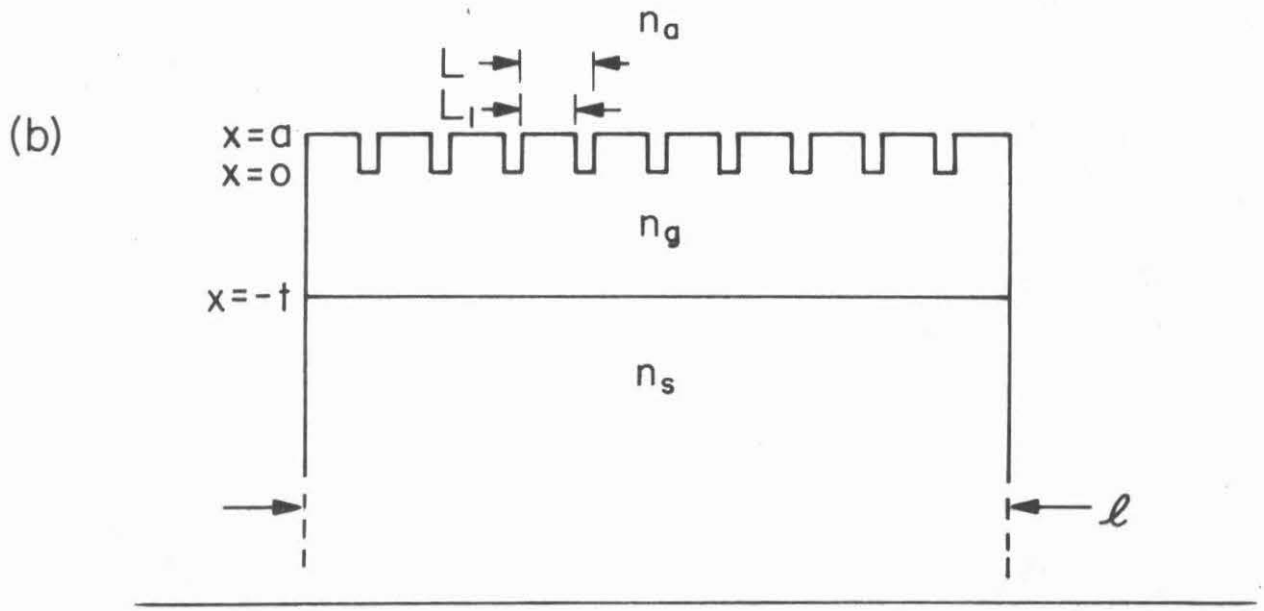

Fig. 2 Periodic waveguide with rectangular corrugation.

In the case of rectangular corrugation of the thin film surface with period L (see Fig. 2) n_{L0}^2 and n_{L1}^2 are the zero and first order Fourier coefficients of the step function:

$$n_{L0}^2 = n_a^2 + (n_g^2 - n_a^2)\frac{L_1}{L} \tag{II-2}$$

$$n_{L1}^2 = \frac{2}{\pi}(n_g^2 - n_a^2)\sin\left(\pi\frac{L_1}{L}\right) \tag{II-3}$$

The higher Fourier components of the corrugation function can be treated by methods similar to those presented below.

In the following we will consider in particular the case of a symmetric corrugation ($L_1 = \frac{L}{2}$) so that:

$$n_{L0}^2 = \frac{n_g^2 + n_a^2}{2} \tag{II-4}$$

$$n_{L1}^2 = \frac{2}{\pi}(n_g^2 - n_a^2) \tag{II-5}$$

In the present analysis the treatment is limited to two dimensional waveguides and no variation in the y direction is assumed. The results will be approximately valid for three dimensional guides and especially those with a large transverse aspect ratio.

2. Derivation of the Mode Equations

TE Modes

From Maxwell's equations:

$$\nabla \times \mathcal{E} = -i\omega\mu\mathcal{H} \tag{II-6}$$

$$\nabla \times \mathcal{H} = i\omega\varepsilon\mathcal{E} \tag{II-7}$$

we obtain

$$\nabla^2\mathcal{E} + \omega^2\mu\varepsilon\mathcal{E} = 0 \tag{II-8}$$

Taking

$$\varepsilon_i = \varepsilon_o[n_{io}^2 + n_{i1}^2 \cos(\tfrac{2\pi}{L} z)] \qquad \text{(II-9)}$$

i = s,g,L,a refers to the different layers of Figs. 1,2

$$k^2 \equiv \omega^2 \mu \varepsilon_o \qquad \text{(II-10)}$$

The equation for $\mathcal{E}_y$ in layer i is:

$$\frac{\partial^2 \mathcal{E}_y}{\partial x^2} + \frac{\partial^2 \mathcal{E}_y}{\partial z^2} + k^2\left[n_{io}^2 + n_{i1}^2 \cos(\tfrac{2\pi}{L} z)\right]\mathcal{E}_y = 0 \qquad \text{(II-11)}$$

Because of the periodicity of the dielectric constant, $\mathcal{E}_y(x,z)$ must possess the Floquet form

$$\mathcal{E}_y = \sum_{m=-\infty}^{\infty} a_m(x) e^{-i\beta_m z} \qquad \text{(II-12)}$$

where:

$$\beta_m = \beta_o + m\,\frac{2\pi}{L} \qquad \text{(II-13)}$$

When we substitute (II-12) into (II-11) and rearrange the order of summation we get

$$e^{-i\beta_o z} \sum_{m=-\infty}^{\infty} e^{-im\frac{2\pi}{L}z}\left[a_m'' + (n_{io}^2 k^2 - \beta_m^2)a_m + \tfrac{1}{2} n_{i1}^2 k^2 (a_{m-1} + a_{m+1})\right] = 0 \qquad \text{(II-14)}$$

where the primes mean differentiation with respect to the argument x.

Due to the uniqueness theorem of the Fourier expansion

$$a_m'' + (n_{io}^2 k^2 - \beta_m^2)a_m + \tfrac{1}{2} n_{i1}^2 k^2 (a_{m-1} + a_{m+1}) = 0 \qquad \text{(II-15)}$$

This is an infinite set of equations which couples each space harmonic to the next lower and higher harmonics. The last result may be applied to the different layers i = s,g,L,a of the waveguide (see Fig. 1). When we come to the periodic layer ($0 < x < a$), we have

non-vanishing n_{L1}^2 . The other layers are homogenous and $n_{i1}^2 = 0$. The result is

$$a_m'' - \alpha_m^2 a_m = 0 \qquad x < -t \qquad \text{(II-16)}$$

$$a_m'' + h_m^2 a_m = 0 \qquad 0 > x > -t \qquad \text{(II-17)}$$

$$a_m'' - \delta_m^2 a_m = -\frac{1}{2} n_{L1}^2 k^2 (a_{m-1} + a_{m+1}) \qquad a > x > 0 \qquad \text{(II-18)}$$

$$a_m'' - \gamma_m^2 a_m = 0 \qquad x > a \qquad \text{(II-19)}$$

where we defined

$$\alpha_m^2 = \beta_m^2 - n_s^2 k^2 \qquad \text{(II-20)}$$

$$h_m^2 = n_g^2 k^2 - \beta_m^2 \qquad \text{(II-21)}$$

$$\delta_m^2 = \beta_m^2 - n_{L0}^2 k^2 \qquad \text{(II-22)}$$

$$\gamma_m^2 = \beta_m^2 - n_a^2 k^2 \qquad \text{(II-23)}$$

In addition to equations (II-16÷19) the field solutions need satisfy the continuity conditions of $\mathcal{E}_y$ and $\mathcal{H}_z = (i/\omega\mu)\,\partial\mathcal{E}_y/\partial x$. From (II-12) we get

$$e^{-i\beta_o z} \sum_m a_m(x^-) e^{-im\frac{2\pi}{L}z} = e^{-i\beta_o z} \sum_m a_m(x^+) e^{-im\frac{2\pi}{L}z} \qquad \text{(II-24)}$$

$$e^{-i\beta_o z} \sum_m a_m'(x^-) e^{-im\frac{2\pi}{L}z} = e^{-i\beta_o z} \sum_m a_m'(x^+) e^{-im\frac{2\pi}{L}z} \qquad \text{(II-25)}$$

Applying (II-24,25) at the interfaces x = -t,0,a and equating separately the corresponding Fourier coefficients results in

$$a_m(-t^-) = a_m(-t^+) \qquad \text{(II-26)}$$

$$a_m(0^-) = a_m(0^+) \qquad \text{(II-27)}$$

$$a_m(a^-) = a_m(a^+) \qquad \text{(II-28)}$$

$$a_m'(-t^-) = a_m'(-t^+) \qquad \text{(II-29)}$$

$$a_m'(0^-) = a_m'(0^+) \qquad \text{(II-30)}$$

$$a_m'(a^-) = a_m'(a^+) \qquad \text{(II-31)}$$

The set of equations (II-16) to (II-19) together with the boundary conditions (II-26) to (II-31) and the appropriate conditions for the behavior at $x = \pm \infty$ constitute a well defined problem. Had we allowed, instead of (II-1), a periodic layer with additional Fourier components, the derivation would be similar except that additional higher and lower space harmonics would appear on the right hand side of Eq. (II-18).

TM Modes

The equation for the magnetic field which is derived from the Maxwell equations (II-6,7) is

$$\underline{\nabla}^2 \underline{\mathcal{H}} + (\underline{\nabla} \log \varepsilon) \times (\underline{\nabla} \times \underline{\mathcal{H}}) + \omega^2 \mu \varepsilon \underline{\mathcal{H}} = 0 \qquad \text{(II-32)}$$

Assuming that in a given layer the dielectric constant ε varies only with z, we obtain for the y component :

$$\frac{\partial^2 \mathcal{H}_y}{\partial x^2} + \frac{\partial^2 \mathcal{H}_y}{\partial z^2} - \frac{d \log \varepsilon_i}{dz} \cdot \frac{\partial \mathcal{H}_y}{\partial z} + \omega^2 \mu \varepsilon_i \mathcal{H}_y = 0 \qquad \text{(II-33)}$$

Because of the periodicity, $\mathcal{H}_y$ must have the Floquet form:

$$\mathcal{H}_y = \sum_m a_m(x) e^{-i\beta_m z} \qquad \text{(II-34)}$$

As in the case of the TE mode we use only the first order Fourier expansion to describe the periodic terms. In particular:

$$-\frac{d \log \varepsilon_i}{dz} \simeq \frac{2\pi}{L} g_{i1} \sin\left(\frac{2\pi}{L} z\right) \qquad \text{(II-35)}$$

The first order Fourier coefficient g_{L1} is calculated in Appendix II-B for the two cases of exact sinusoidally varying dielectric constant and symmetric rectangular corrugation. Eqs. (II-34), (II-35) and (II-9) are substituted in (II-33), and the summation order is rearranged to give:

$$e^{-i\beta_o z} \sum_m e^{-im\frac{2\pi}{L}z}\left[a_m'' + (n_{io}^2 k^2 - \beta_m^2)a_m + \frac{1}{2}(n_{i1}^2 k^2 - \beta_{m-1}\frac{2\pi}{L} g_{i1})a_{m-1} + \right.$$

$$\left. + \frac{1}{2}(n_{i1}^2 k^2 + \beta_{m+1}\frac{2\pi}{L} g_{i1})a_{m+1}\right] = 0 \qquad \text{(II-36)}$$

By the uniqueness of the Fourier expansion it follows that

$$a_m'' + (n_{io}^2 k^2 - \beta_m^2)a_m + \frac{1}{2}(n_{i1}^2 k^2 - \beta_{m-1}\frac{2\pi}{L} g_{i1})a_{m-1} + \frac{1}{2}(n_{i1}^2 k^2 + \beta_{m+1}\frac{2\pi}{L} g_{i1})a_{m+1} = 0 \qquad \text{(II-37)}$$

As before, the last equation applies to all the layers in Fig. 1 with $n_{i1}^2 \neq 0$, $g_{i1} \neq 0$ only for the layer L ($0 < x < a$):

$$a_m'' - \alpha_m^2 a_m = 0 \qquad x < -t \qquad \text{(II-38)}$$

$$a_m'' + h_m^2 a_m = 0 \qquad 0 > x > -t \qquad \text{(II-39)}$$

$$a_m'' - \delta_m^2 a_m = -\frac{1}{2}(n_{L1}^2 k^2 - \beta_{m-1}\frac{2\pi}{L} g_{L1})a_{m-1} - \frac{1}{2}(n_{L_1}^2 k^2 + \beta_{m+1}\frac{2\pi}{L} g_{L1})a_{m+1} \qquad \text{(II-40)}$$

$$a > x > 0$$

$$a_m'' - \gamma_m^2 a_m = 0 \qquad x > a \qquad \text{(II-41)}$$

where α_m, h_m, δ_m, γ_m, β_m are given by equations (II-20) to (II-23) and Eq. (II-13).

The boundary conditions for the space harmonics are somewhat more complicated than in the case of the TE modes. The continuity of $\mathcal{H}_y$ results in an equation similar to Eq. (II-24) which similarly involves continuity of the space harmonics $a_m(x)$.

$$a_m(-t^-) = a_m(-t^+) \tag{II-42}$$

$$a_m(0^-) = a_m(0^+) \tag{II-43}$$

$$a_m(a^-) = a_m(a^+) \tag{II-44}$$

The continuity of $\mathcal{E}_z = (-i/\omega\varepsilon)\, \partial\mathcal{H}_y/\partial_x$, however, takes the form

$$\frac{1}{\varepsilon(x^-)} \frac{\partial \mathcal{H}_y(x^-)}{\partial x} = \frac{1}{\varepsilon(x^+)} \frac{\partial \mathcal{H}_y(x^+)}{\partial x} \tag{II-45}$$

In particular at x = 0 we have:

$$[n_{L0}^2 + n_{L1}^2 \cos(\tfrac{2\pi}{L} z)] \sum_m a_m'(0^-) e^{-i\beta_m z} = n_g^2 \sum_m a_m(0^+) e^{-i\beta_m z} \tag{II-46}$$

As in previous cases, rearranging terms and using the uniqueness property, results in

$$a_m'(0^+) = \frac{n_{L0}^2}{n_g^2} a_m'(0^-) + \frac{n_{L1}^2}{2n_g^2} [a_{m-1}'(0^-) + a_{m+1}'(0^-)] \tag{II-47}$$

and in a similar way:

$$a_m'(a^-) = \frac{n_{L0}^2}{n_a^2} a_m'(a^+) + \frac{n_{L1}^2}{2n_a^2} [a_{m-1}'(a^+) + a_{m+1}'(a^+)] \tag{II-48}$$

and :

$$a_m'(-t^+) = \frac{n_g^2}{n_s^2} a_m'(-t^-) \tag{II-49}$$

Again we have a well defined mathematical problem consisting of a set of equations (II-38) to (II-41), boundary conditions (II-42) to

(II-44), (II-47) to (II-49) and appropriate boundary conditions at $x = \pm \infty$. A simultaneous solution of this set for all m gives the values of the different space harmonics a_m which, taken together, constitute the TM mode.

As pointed out in the TE mode case, it is possible also in the TM mode case to allow for second order (and higher) Fourier components. This will add terms to the right hand side of equations (II-40,47,48). However, observe that in the special case when ε has only one Fourier component and is described accurately by equation (II-9), the derivation for the T.E. mode is exact, but for the TM mode the derivation is still approximate since $-d\log\varepsilon/dz$ possesses higher order Fourier components.

3. First Order Solution

TE Modes

The exact solution of the set of equations presented in Section 2 is rather complicated. However, it was found that a first order approximation leads to relatively simple and useful analytical expressions.

In the first order approximation we neglect higher order spatial harmonics relative to lower order ones. Furthermore, we assume that the zero order harmonic is much larger than the other harmonics and is approximately equal to the undisturbed waveguide solution (a = 0), which is derived in Appendix II-A. Analyzing in particular the example of m = 1, the second term on the right hand side of Eq. (II-18)-(a_2), will be neglected relative to the first term-(a_o), and this first term will be approximated by the third of equations (II-A4):

$$a_0(x) \simeq Fe^{-\gamma x} \qquad x > 0 \qquad \text{(II-50)}$$

Equations (II-16) to (II-19) in this case become a simple inhomogeneous set of ordinary differential equations for $a_1(x)$, and its solution is:

$$a_1 = A_1 e^{\alpha_1(x+t)} \qquad x < -t \qquad \text{(II-51)}$$

$$a_1 = B_1\cos(h_1 x) + C_1\sin(h_1 x) \qquad 0 > x > -t \qquad \text{(II-52)}$$

$$a_1 = D_1\cosh(\delta_1 x) + E_1\sinh(\delta_1 x) - \frac{fF}{\gamma^2-\delta_1^2}\, e^{-\gamma x} \qquad a > x > 0 \qquad \text{(II-53)}$$

$$a_1 = F_1 e^{-\gamma_1(x-a)} \qquad x > a \qquad \text{(II-54)}$$

where

$$f \equiv \frac{1}{2} n_{L1}^2 k^2 \qquad \text{(II-55)}$$

When this solution is substituted in the boundary conditions (II-26÷31) the result is a set of algebraic linear inhomogeneous equations which can be readily solved for the coefficients. To avoid complicated expressions we give here only the first order Taylor approximation (in terms of a) of the solution which is valid for

$$\delta_1 a, \gamma_1 a \ll 1 \qquad \text{(II-56)}$$

$$A_1 = \frac{1}{\Delta} h_1 f\cdot F\cdot a \qquad \text{(II-57)}$$

$$B_1 = \frac{1}{\Delta}[\alpha_1\sin(h_1 t) + h_1\cos(h_1 t)]f\cdot F\cdot a \qquad \text{(II-58)}$$

$$C_1 = \frac{1}{\Delta}[\alpha_1\cos(h_1 t) - h_1\sin(h_1 t)]f\cdot F\cdot a \qquad \text{(II-59)}$$

$$F_1 = B_1 \qquad \text{(II-60)}$$

$$\Delta = h_1(\alpha_1+\gamma_1)\cos(h_1 t) - (h_1^2-\alpha_1\gamma_1)\sin(h_1 t) \qquad \text{(II-61)}$$

The vertical profile $a_1(x)$ of the first order space harmonic for the

case of long period L (so that h_1 is real) is plotted in Fig. 3 and compared to the zero order space harmonic profile $a_o(x)$.

The same procedure may be used for any order m, when for finding $a_m(x)$ we use instead of (II-50) the expression for $a_{m-1}(x)$ (if $m > 0$) or $a_{m+1}(x)$ (if $m < 0$) as the driving term on the right hand side of Eq. (II-18). So, every space harmonic can be evaluated in terms of the lower ones which were calculated in the previous steps. The solution described by Eqs. (II-57) to (II-61) is correct also for the -1 harmonic when the subscript 1 is replaced by -1. Similar expressions arise for all other values of m. When $a = 0$ all the space harmonics $m \neq 0$ vanish except for $a_o(x)$ which equals the unperturbed waveguide solution as would be expected.

TM Modes

In a manner similar to that of TE modes, we neglect in the TM mode first order approximation higher order space harmonics relative to lower order ones. Taking in particular $m = 1$, the second term (a_2) on the right hand side of Eq. (II-40) is neglected relative to the first term (a_o), and $a_o(x)$ is approximated by the unperturbed waveguide solution - Eq. (II-A 21).

$$a_o(x) \simeq F\, e^{-\gamma x}, \qquad x > 0 \tag{II-62}$$

Eqs. (II-38) to (II-41) can then be solved as before, and the solution is again given by Eqs. (II-51) to (II-54), but f is now replaced by:

$$f_1 = \frac{1}{2}\left(n_{L1}^2 k^2 + g_{L1}\frac{2\pi}{L}\beta_o\right) \tag{II-63}$$

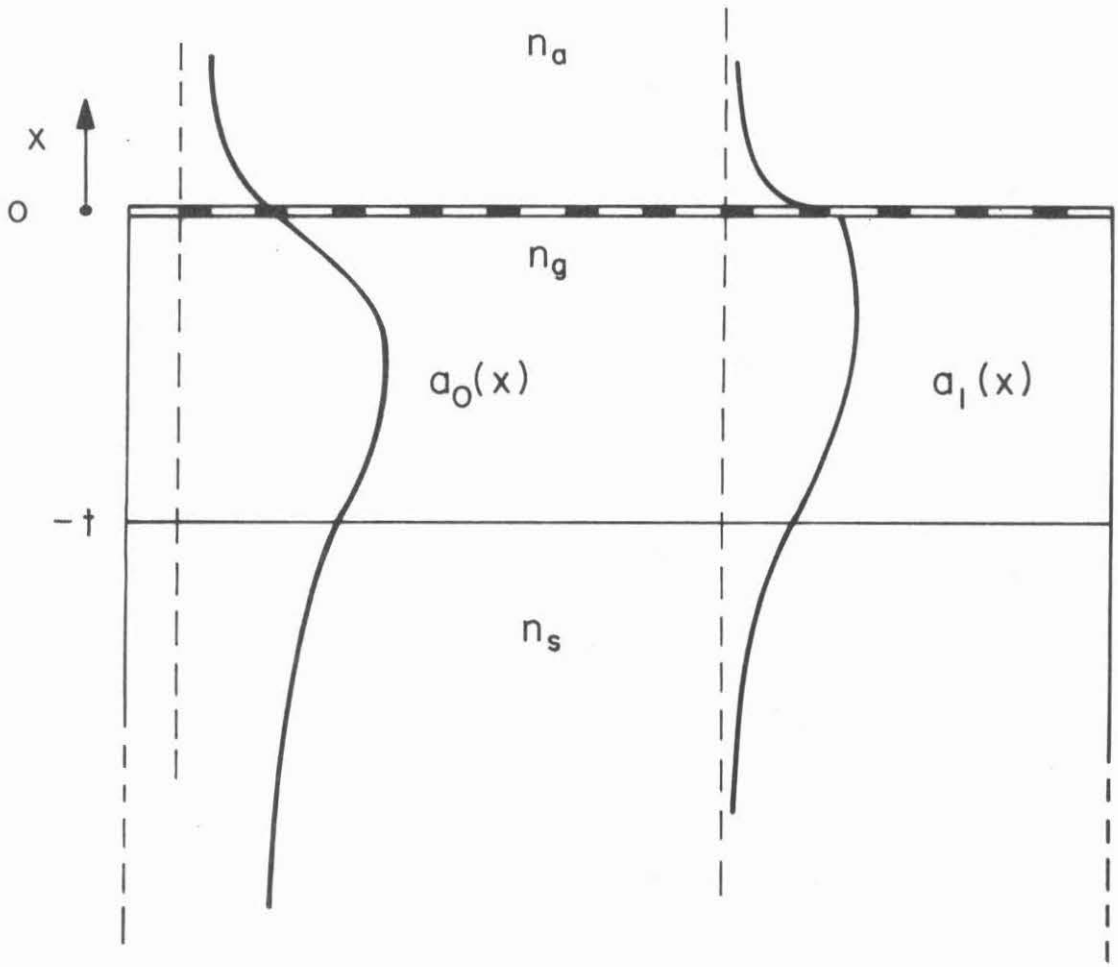

Fig. 3 Profile of the first order space harmonic ($a_1(x)$) in comparison to the fundamental harmonic ($a_0(x)$) of the fundamental TE mode of the periodic waveguide. Notice the discontinuity in the derivative (the magnetic field) at the perturbed surface! (In a case of a TM mode also the electric field is discontinuous).

In equations (II-47) and (II-48) we neglect a_2' relative to a_0' and a_1' and then substitute equations (II-51) to (II-54) in the boundary condition equations (II-42) to (II-44), (II-47) to (II-49). The resulting inhomogeneous set of linear algebraic equations is readily solved and its first order approximation (in terms of a), which is valid in the limit of (II-56), is:

$$A_1 = \frac{1}{\Delta}\left[\frac{n_g^2}{n_{LO}^2} f_1 + \frac{1}{2}\frac{n_{L1}^2}{n_a^2}\gamma\left(\bar{\gamma}_1 + \frac{n_g^2}{n_{LO}^2}\gamma\right)\right] h_1 \cdot F \cdot a \qquad \text{(II-64)}$$

$$B_1 = \frac{1}{\Delta}\left[\frac{n_g^2}{n_{LO}^2} f_1 + \frac{1}{2}\frac{n_{L1}^2}{n_a^2}\gamma\left(\bar{\gamma}_1 + \frac{n_g^2}{n_{LO}^2}\gamma\right)\right]\left[\bar{\alpha}_1 \sin(h_1 t) + h_1 \cos(h_1 t)\right] \cdot F \cdot a \qquad \text{(II-65)}$$

$$C_1 = \frac{1}{\Delta}\left[\frac{n_g^2}{n_{LO}^2} f_1 + \frac{1}{2}\frac{n_{L1}^2}{n_a^2}\gamma\left(\bar{\gamma}_1 + \frac{n_g^2}{n_{LO}^2}\gamma\right)\right]\left[\bar{\alpha}_1 \cos(h_1 t) - h_1 \sin(h_1 t)\right] \cdot F \cdot a \qquad \text{(II-66)}$$

$$F_1 = \frac{1}{\Delta}\left\{\left[\frac{n_g^2}{n_{LO}^2}\left(f_1 + \gamma^2 \frac{n_{L1}^2}{2n_a^2}\right) - \frac{n_{L1}^2}{2n_a^2}\gamma\bar{\alpha}_1\right] h_1 \cos(h_1 t) + \right.$$
$$\left. + \left[\frac{n_g^2}{n_{LO}^2}\left(f_1 + \gamma^2 \frac{n_{L1}^2}{2n_a^2}\right)\bar{\alpha}_1 + \frac{n_{L1}^2}{2n_a^2}\gamma h_1^2\right] \sin(h_1 t)\right\} \cdot F \cdot a \qquad \text{(II-67)}$$

$$\Delta = h_1(\bar{\alpha}_1 + \bar{\gamma}_1)\cos(h_1 t) - (h_1^2 - \bar{\alpha}_1\bar{\gamma}_1)\sin(h_1 t) \qquad \text{(II-68)}$$

where

$$\bar{\alpha}_1 \equiv \frac{n_g^2}{n_s^2}\alpha_1 \qquad \text{(II-69)}$$

$$\bar{\gamma}_1 \equiv \frac{n_g^2}{n_a^2}\gamma_1 \qquad \text{(II-70)}$$

The same results, Eqs. (II-65) to (II-71), apply also for the harmonic m = -1 if all the subscripts 1 are substituted by -1, and f_{-1} is:

$$f_{-1} = \frac{1}{2}\left(n_{L1}^2 k^2 - g_{L1}\frac{2\pi}{L}\beta_o\right) \qquad \text{(II-71)}$$

Similar expressions result for all other values of m.

4. Higher Order Solution

Iterative Methods

We already mentioned in Section 3 that higher order harmonics a_m can be calculated in terms of the lower ones: a_{m-1} (if $m > 0$) or a_{m+1} (if $m < 0$). We may also point out that if $\gamma_m a$, $\delta_m a \ll 1$ the explicit expression of a_m will be proportional to $a^{|m|}$, so for small values of a, the mth space harmonic is of $|m|^{th}$ order when expanded in a.

By substituting our first order solutions back into the differential equation as forcing terms, one gets higher order solutions, and in principle the space harmonics may be completely evaluated in terms of power expansion series by such an iterative procedure. For example, if we already solved a_{-1} and a_1 to the first order, we may substitute them in the right hand side of Eq. (II-18) for the case $m = 0$ and so solve for the second order correction to a_o. Note that the series expansion which is obtained in this way has only odd powers of a for odd harmonics, and even powers of a for even harmonics. Therefore, the first order correction to our first order solution of the first harmonic is of third order!

Another kind of correction which should be considered is that due to higher order Fourier terms of the periodic layer. If Eq. (II-1) or (II-35) include second order Fourier components, then terms proportional to a_{m-2} and a_{m+2} will appear on the right hand side of

Eqs. (II-18, 40, 47, 48). The contribution of the second order Fourier component or any higher order Fourier component can then be calculated independently and added to the first order result due to the linearity of the inhomogeneous set of equations.

In the first order approximation the second order Fourier component does not have a significant effect on the 1st harmonic, since it couples it to the -1 harmonic and contributes a second order correction. It may, however, be significant for the 2nd harmonic (and higher) since it couples it to the zero harmonic and thus contributes a first order term, while the first Fourier component contributes only second order term. Higher order Fourier coefficients may be important in TM modes even in cases when their effect on the TE modes is insignificant. This is because even if ε has no higher Fourier coefficients then the first one (Eq. II-1), $\frac{d\log\varepsilon}{dz}$ may have them.

"Several Harmonics" Approximation

There are physical situations when the assumption used above, that the zero order harmonic is much larger than all the other harmonics, is not valid. If two space harmonics have propagation parameters close to those of the unperturbed waveguide modes (this happens, for example, when $\beta_0 \simeq \pi/L$ because $\beta_{-1} = -\pi/L = -\beta_0$, is the propagation parameter of the same mode, propagating in the opposite direction), then physical considerations indicate that they both may possess comparable amplitudes. In other cases, the assumption that 3 or more harmonics are significant will lead to more accurate results when the first order approximation fails.

In fact we present in the following an exact solution of the TE mode problem, in the case of purely sinusoidally perturbed layer (II-1),

by solving formally the set of Eqs. (II-16) to (II-19) with the boundary conditions (II-26) to (II-31), including any arbitrary number of spatial harmonics. In practice, this solution may be applied by truncation to a finite number of harmonics.

The infinite set of Eqs. (II-18) can be written in a matrix form:

$$\left(\mathcal{I}\frac{d^2}{dx^2} + \mathcal{V}\right)\mathcal{A} = 0 \qquad \text{(II-72)}$$

where

$$\mathcal{V} \equiv \begin{pmatrix} f & \delta_{-1}^2 & f & & \\ & f & \delta_0^2 & f & \\ & & f & \delta_1^2 & f \end{pmatrix} \qquad \text{(II-73)}$$

$\mathcal{I}$ is the unit matrix, and $\mathcal{A}$ is a column matrix whose elements are the space harmonics $a_m(x)(-\infty < m < \infty)$.

Since $\mathcal{V}$ is symmetric, it is possible to diagonalize it by an orthogonal matrix $\mathcal{T}$

$$\mathcal{T}^T\mathcal{T} = \mathcal{I} \qquad \text{(II-74)}$$

$$\mathcal{T}^T\mathcal{V}\mathcal{T} = \Lambda \qquad \text{(II-75)}$$

where T denotes the transpose of the matrix, and Λ is a diagonal matrix whose diagonal elements are:

$$\Lambda_{ii} \equiv \lambda_i^2 \qquad -\infty < i < \infty \qquad \text{(II-76)}$$

Hence λ_i^2 are the eigenvalues of the matrix $\mathcal{V}$.

When we substitute in Eq. (II-72) the transformation

$$\mathcal{A} = \mathcal{T}\bar{\mathcal{A}} \qquad \text{(II-77)}$$

we get:

$$\left(\mathcal{I}\frac{d^2}{dx^2}+\Lambda\right)\bar{\mathcal{A}} = 0 \qquad \text{(II-78)}$$

Since this is a diagonal set it is readily solved for $\bar{a}_i$, the components of $\bar{\mathcal{A}}$

$$\bar{a}_i = D_i\cos\lambda_i x + E_i\sin\lambda_i x \qquad -\infty < i < \infty \qquad \text{(II-79)}$$

then using (II-77):

$$a_m = \sum_{j=-\infty}^{\infty} T_{mj}[D_j\cos\lambda_i x + E_j\sin\lambda_j x] \qquad -t < x < 0 \qquad \text{(II-80)}$$

where T_{mj} are the elements of the matrix $\mathcal{T}$.

For the other layers, as in Section 1:

$$a_m = A_m e^{\alpha_m(x+t)} \qquad x < -t \qquad \text{(II-81)}$$

$$a_m = B_m\cos(h_m x) + C_m\sin(h_m x) \qquad 0 > x > -t \qquad \text{(II-82)}$$

$$a_m = F_m e^{-\gamma_m(x-a)} \qquad x > a \qquad \text{(II-83)}$$

When this is substituted in boundary conditions (II-26) to (II-31), one gets after short manipulation:

$$h_m[\alpha_m\cos(h_m t)-h_m\sin(h_m t)]\sum_j T_{mj}D_j-[\alpha_m\sin(h_m t)+h_m\cos(h_m t)]\sum_j \lambda_j T_{mj}E_j = 0$$

$$\sum_j[\gamma_m\cos(\lambda_j a)-\lambda_j\sin(\lambda_j a)]T_{mj}D_j+\sum_j[\gamma_m\sin(\lambda_j a)+\lambda_j\cos(\lambda_j a)]T_{mj}E_j = 0 \qquad \text{(II-84)}$$

$$(-\infty < m < \infty) \qquad \text{(II-85)}$$

To satisfy the infinite set of Eqs. (II-84,85) the determinant of the coefficients of the unknown D_j, E_j must be equated to zero. This equation gives the dispersion relation of β_o vs. ω. When the dispersion equation is solved, all the coefficients A_m, B_m, C_m, D_m, E_m, F_m may be obtained up to a multiplicative constant, which

may be determined by a normalization condition or by fixing C_o.

In practice, the procedure just discussed may be used to obtain an approximate solution in which m spans a finite number of integral values. Note, that if the dielectric constant of the perturbed layer (Eq. II-1) has additional Fourier component, its only effect will be to add additional symmetric diagonal rows to the matrix (Eq. II-73). A similar procedure may also be used in the case of TM modes. This involves a slightly more complicated derivation and will not be considered further here.

5. Adiabatic Approximation

For very large periods of the spatial perturbation, ($\lambda << L$), a simple approximation can be applied which leads to explicit expressions for all the space harmonics. We will shortly describe this approximation, previously presented in [Somekh 1972].

In the limit $L >> \lambda$ the solution must approach that of the unperturbed waveguide, but with a z-modulated amplitude envelope. Taking for instance the TE mode case the field can be written in the form of

$$E_y = K^p(z)a^p(x)e^{-i\beta z} \qquad \text{(II-86)}$$

where $a^p(x)$ is the normalized solution of the p^{th} TE mode in the unperturbed dielectric waveguide (Appendix II-A) and $K^p(z)$ is the excitation amplitude of mode p.

We regard the periodic layer as a small perturbation $\Delta n^2(x,z)$ to the unperturbed case, then by substitution of (II-86) into equation (II-8) and by making use of the orthogonality of the unperturbed waveguide modes and the normalization (II-A14) obtain [Somekh 1972, Marcuse 1969]:

$$\frac{\partial^2 K^p}{\partial z^2} - 2i\beta \frac{\partial K^p}{\partial z} = -k^2 \frac{\beta}{2\omega\mu} K^p \int_{-\infty}^{\infty} |a^p(x)|^2 \Delta n^2(x,z)dx \qquad \text{(II-87)}$$

where it was assumed that the waveguide carries only the mode p. When Eq. (II-1) is used we receive for Δn^2:

$$\Delta n^2 = \begin{cases} n_{LO}^2 - n_a^2 + n_{L1}^2 \cos(\frac{2\pi}{L} z) & 0 < x < a \\ 0 & \text{otherwise} \end{cases} \qquad \text{(II-88)}$$

For the case $L >> \lambda$ we can neglect the first term in (II-87). If we also assume $a \to 0$, the solution of (II-87) is

$$K^p(z) = K^p(0) e^{-i \frac{k^2}{2\omega\mu} |a^p(0)|^2 (n_{LO}^2 - n_a^2) az} \; e^{-i \frac{k^2}{8\pi\omega\mu} |a^p(0)|^2 n_{L1}^2 aL \sin(\frac{2\pi}{L} z)} \qquad \text{(II-89)}$$

Using a familiar expansion in terms of Bessel functions for the last exponential in (II-89) and substituting back in Eq. (II-86) we get

$$E_y = a^p(x) \sum_{m=-\infty} C_m e^{-i(\beta_o + m \frac{2\pi}{L}) z} \qquad \text{(II-90)}$$

where

$$C_m = K^p(0) J_m(M) \qquad \text{(II-91)}$$

$$M = \frac{k^2}{8\pi\omega\mu} |a^p(0)|^2 n_{L1}^2 La \qquad \text{(II-92)}$$

$$\beta_o = \beta + \frac{k^2}{2\omega\mu} |a^p(0)|^2 (n_{LO}^2 - n_a^2) a \qquad \text{(II-93)}$$

and J_m is the m order Bessel function.*

We thus find that the amplitude of the m space harmonic is proportional to the mth order Bessel function, and for a large argument M it is possible for the higher order space harmonics to have higher amplitude than the zero space harmonic. On the other hand, when a tends to zero all the space harmonics except the zero order become vanishingly small. For $M \ll 1$ we have in particular for a well confined mode (when $\beta \approx n_g k$ and $h \approx \pi/t$) and symmetrical rectangular corrugation (Eq. II-5):

$$\frac{C_1}{C_o} = \frac{J_1(M)}{J_o(M)} \simeq \frac{M}{2} = \frac{1}{4\pi n_g} \frac{L\lambda a}{t^3} \qquad \text{(II-94)}$$

In deriving the last expression we substituted $a(0) = F = -\frac{h}{\gamma}\sqrt{\frac{2}{t}} \cdot \sqrt{\frac{2\omega\mu}{\beta}}$ which results from Eqs. (II-A4, A9, A15).

Note that in this approximation all the harmonics have the same x profile.

---

*The periodic spatial modulation considered here is analogous to that of temporal phase modulation of a carrier wave. In the limit $L \gg \lambda$ we can write instead of (II-86)

$$a^p(x)\exp[-i \int \beta\ (z)dz]$$

where

$$\beta(z) \simeq \beta_o + \frac{\partial\beta}{\partial t}\ a \cos \frac{2\pi}{L} z$$

where t is the height of the guiding layer (See Fig. 1). Substituting the second equation in the first will also give a result in the form of (II-89).

6. Discussion on the Approximations

The first order approximation and the adiabatic approximation provide explicit expressions for the space harmonics, and therefore they are in many cases more useful than the more accurate numerical solution. However, one has to be aware of the limits in which these approximations are valid.

In the first order approximation we neglected higher order space harmonics relative to lower ones. This assumption must be checked after getting the explicit solution. From the solution for the first order harmonic (Eqs. II-57 to II-61 for the TE mode or Eqs. II-64 to II-68 for the TM mode) we note that it will cease being negligible relative to the zero harmonic whenever the determinant Δ which appears in the denominator approaches zero.

Comparing Eq. (II-61) to Eq. (II-A8) and Eq. (II-68) to Eq. (II-A25) one observes that Δ vanishes whenever the propagation parameters of the first space harmonic h_1, α_1, γ_1, β_1 satisfy the dispersion relation of the unperturbed waveguide. There are two cases when this can happen:

1) When $L \to \infty$ then $\beta_1 \to \beta$ and consequently (using Eqs. II-20 ÷ 23) $\alpha_1 \to \alpha$, $\gamma_1 \to \gamma$, $h_1 \to h$.

2) When

$$\frac{2\pi}{L} = \beta^{p'} - \beta^{p} \qquad \text{(II-95)}$$

where $\beta^{p'}$ and β^{p} are the propagation parameters of two separate modes of the unperturbed waveguide, so that $\beta_1^p = \beta^{p'}$ (see Eq. II-13) and consequently $\alpha_1^p = \alpha^{p'}$, $\gamma_1^p = \gamma^{p'}$, $h_1^p = h^{p'}$. Note that this will always be the case whenever $\beta^p = -\frac{\pi}{L}$, because then $\beta^{p'} = +\frac{\pi}{L}$

corresponds to a waveguide mode, and condition (II-95) is satisfied. In a similar way, the first order approximation fails whenever:

$$m \frac{2\pi}{L} = \beta^{p'} - \beta^{p} \qquad \text{(II-96)}$$

It is obvious that the first order approximation fails in cases (1) and (2), because the neglect of all space harmonics relative to the zero order one is not justified. In case (2), whenever Eq. (II-95) is exactly or approximately satisfied, it is physically obvious that the space harmonic a_1 is as significant as a_o, and in the more general case of Eq. (II-96), the space harmonic a_m is as significant as a_o. It is expected that in these cases a "two harmonics" approximation based on the results of Section 4 will provide a satisfactory solution.

The first order approximation fails in case (1), because for longer periods L, more and more space harmonics become significant relative to the zero order one. For large values of L the adiabatic approximation gives that the m space harmonic amplitude becomes proportional to $J_m(M)$ (Eqs. II-91, 92) which for arguments $M > 1$ is not negligible except for high order harmonics which satisfy $m > M$.

For L large enough to allow the adiabatic approximation but not that large to fail the first order approximation, one would expect the two methods to agree. For the adiabatic approximation to hold, the x profile of the space harmonics must be close to the zero one, in particular $h_1 \approx h_o$. Using Eqs. (II-21), (II-A6) the condition to satisfy this requirement is:

$$\frac{2\pi}{L} \cdot \beta_o \ll h_o^2 \qquad \text{(II-97)}$$

which for a well confined mode can be expressed by:

$$L >> 4n_g \frac{t^2}{\lambda} \qquad \text{(II-98)}$$

In this condition it is also possible to expand the results of the first order approximation Eqs. (II-57) to (II-61) to first order in $2\pi/L$. When this is done in particular for symmetrical rectangular corrugation, one gets from Eqs. (II-57, 61, A15) a result identical to Eq. (II-94), which indicates agreement between the two methods. Equation (II-94) is valid of course only as long as the ratio C_1/C_o is small compared to unity, which makes the condition for L:

$$L << 4\pi n_g \frac{t^3}{\lambda a} \qquad \text{(II-99)}$$

Comparing conditions (II-98) and (II-99) indicates the domain in which both the adiabatic and first order approximations are valid and agree with each other. We may mention that in many useful cases condition (II-97) or (II-98) is not satisfied and the adiabatic approximation cannot be used. In general, the first order approximation will be valid in these cases. However, if the first order approximation is not satisfactory enough, higher order approximation with 3, 5 or more harmonics can be used in the way described in Section 4.

It is difficult to find for the general case a simple criterion for the validity of the first order approximation. In general one has to solve explicitly for the space harmonics and then check if the assumptions about their negligibility hold. For small enough perturbation depth the approximation will be valid.

Finally we would like to point out that in general, the different space harmonics in periodically perturbed dielectric waveguides, have different transverse profiles $a_m(x)$ (see Fig. 3 for example). This is what makes this problem much more difficult than the simple problem of periodic stratified media. Except for special cases when simple approximations are justified, it is hard to solve practical structures like Fig. 1 with less complexity.

Appendix II-A: Solution for Unperturbed Waveguide

TE Modes

For asymmetric unperturbed waveguide (see Fig. 1 with a = 0), the TE mode nonvanishing field components are:

$$\mathcal{E}_y = a(x)e^{-i\beta z} \tag{II-A1}$$

$$\mathcal{H}_x = -\frac{i}{\omega\mu}\frac{\partial \mathcal{E}_y}{\partial z} = \frac{\beta}{\omega\mu}a(x)e^{-i\beta z} \tag{II-A2}$$

$$\mathcal{H}_z = \frac{i}{\omega\mu}\frac{\partial \mathcal{E}_y}{\partial x} = \frac{i}{\omega\mu}a'(x)e^{-i\beta z} \tag{II-A3}$$

Solution of Maxwell equations (Eqs. II-6,7) with the appropriate boundary conditions gives:

$$a(x) = A\, e^{\alpha(x+t)} \qquad x < -t$$

$$a(x) = B\cos(hx) + C\sin(hx) \qquad -t < x < 0 \tag{II-A4}$$

$$a(x) = F\, e^{-\gamma x} \qquad x > 0$$

$$\alpha^2 = \beta^2 - n_s^2k^2 \tag{II-A5}$$

$$h^2 = n_g^2k^2 - \beta^2 \tag{II-A6}$$

$$\gamma^2 = \beta^2 - n_a^2k^2 \tag{II-A7}$$

$$\tan(ht) = \frac{h(\gamma+\alpha)}{h^2-\gamma\alpha} \tag{II-A8}$$

$$F = B = -\frac{h}{\gamma}C \tag{II-A9}$$

$$A = -\left[\frac{h}{\gamma}\cos(ht) + \sin(ht)\right]\cdot C \tag{II-A10}$$

and C may be determined by power normalization requirement :

$$\int_{-\infty}^{\infty} a^2(x)dx = \int_{-\infty}^{\infty} |\mathcal{E}_y|^2 dx = \frac{2\omega\mu}{\beta}\frac{P}{w} \tag{II-A11}$$

which gives

$$C = \sqrt{\frac{2}{t_{eff}}} \cdot \sqrt{\frac{2\omega\mu}{\beta}\frac{P}{w}} \qquad \text{(II-A12)}$$

$$t_{eff} \equiv \frac{\gamma^2+h^2}{\gamma^2}\left(t + \frac{1}{\gamma} + \frac{1}{\alpha}\right) \qquad \text{(II-A13)}$$

In many cases it is convenient to normalize the power of the mode to a unit power per unit width of the waveguide

$$\frac{P}{w} = \frac{\beta}{2\omega\mu}\int_{-\infty}^{\infty} |\mathcal{E}_y|^2 dx = 1 \text{ watt/cm} \qquad \text{(II-A14)}$$

in this case

$$C = \sqrt{\frac{2}{t_{eff}}}\sqrt{\frac{2\omega\mu}{\beta}} \qquad \text{(II-A15)}$$

To denote the degree of excitation of the normalized mode we should relate to it an excitation amplitude K, so that the total field is

$$E_y = K\mathcal{E}_y \qquad \text{(II-A16)}$$

Using the normalization (II-A14) it turns out that the total power in the excited mode is

$$P = wK^2 \text{ (watt)} \qquad \text{(II-A17)}$$

where w is the width of the waveguide.

TM Modes

The nonvanishing field components of the TM modes are:

$$\mathcal{H}_y = a(x)e^{-i\beta z} \qquad \text{(II-A18)}$$

$$\mathcal{E}_x = \frac{i}{\omega\varepsilon}\frac{\partial \mathcal{H}_y}{\partial z} = \frac{\beta}{\omega\varepsilon}a(x)e^{-i\beta z} \qquad \text{(II-A19)}$$

$$\mathcal{E}_z = -\frac{i}{\omega\varepsilon}\frac{\partial \mathcal{H}_y}{\partial x} = \frac{i}{\omega\varepsilon}a'(x)e^{-i\beta z} \qquad \text{(II-A20)}$$

where:

$$a(x) = A\, e^{\alpha(x+t)} \qquad x < -t$$

$$a(x) = B\cos(hx) + C\sin(hx) \qquad -t < x < 0 \qquad \text{(II-A21)}$$

$$a(x) = F\, e^{-\gamma x} \qquad x > 0$$

$$\alpha^2 = \beta^2 - n_s^2 k^2 \qquad \text{(II-A22)}$$

$$h^2 = n_g^2 k^2 - \beta^2 \qquad \text{(II-A23)}$$

$$\gamma^2 = \beta^2 - n_a^2 k^2 \qquad \text{(II-A24)}$$

$$\tan(ht) = \frac{h(\bar{\alpha}+\bar{\gamma})}{h^2 - \bar{\alpha}\bar{\gamma}} \qquad \text{(II-A25)}$$

$$\bar{\alpha} \equiv \frac{n_g^2}{n_s^2}\,\alpha \qquad \text{(II-A26)}$$

$$\bar{\gamma} \equiv \frac{n_g^2}{n_a^2}\,\gamma \qquad \text{(II-A27)}$$

$$F = B = -\frac{h}{\bar{\gamma}}\,C \qquad \text{(II-A28)}$$

$$A = -\left[\frac{h}{\bar{\gamma}}\cos ht + \sin ht\right]C \qquad \text{(II-A29)}$$

and C may be determined by normalization requirement:

$$\int_{-\infty}^{\infty} \frac{1}{n^2}\, a^2(x)dx = \int_{-\infty}^{\infty} \frac{1}{n^2}\, |\mathcal{H}_y(x)|^2 dx = \frac{2\omega\varepsilon_o}{\beta}\,\frac{P}{w} \qquad \text{(II-A30)}$$

which results in :

$$C = \sqrt{\frac{2}{t_{eff}}}\,\sqrt{\frac{2\omega\varepsilon_o}{\beta}\,\frac{P}{w}} \qquad \text{(II-A31)}$$

where:

$$t_{eff} \equiv \frac{\bar{\gamma}^2+h^2}{\bar{\gamma}^2}\left[\frac{t}{n_g^2} + \frac{\gamma^2+h^2}{\bar{\gamma}^2+h^2}\cdot\frac{1}{n_a^2\gamma} + \frac{\alpha^2+h^2}{\bar{\alpha}^2+h^2}\cdot\frac{1}{n_s^2\alpha}\right] \qquad \text{(II-A32)}$$

When the mode power is normalized to unit power per unit width of the waveguide

$$\frac{P}{w} = \frac{\beta}{2\omega} \int_{-\infty}^{\infty} \frac{1}{\varepsilon} |\mathcal{H}_y|^2 dx = 1 \text{ watt/cm} \qquad \text{(II-A33)}$$

$$C = \sqrt{\frac{2}{t_{eff}}} \sqrt{\frac{2\omega\varepsilon_o}{\beta}} \qquad \text{(II-A34)}$$

and the total field is

$$\mathcal{H}_y = K\mathcal{H}_y \qquad \underline{E} = K\underline{\mathcal{E}} \qquad \text{(II-A35)}$$

where K is the mode excitation amplitude. The power in the mode is then

$$P = wK^2 \text{ (watt)} \qquad \text{(II-A36)}$$

Appendix II-B: Fourier Coefficient of the Logarithmic Derivative of the Dielectric Constant

The first order Fourier coefficient (g_1) of $-\frac{L}{2\pi}\frac{d \log \varepsilon}{dz}$ is given by

$$g_1 = -\frac{2}{L}\int_{-L/2}^{L/2}\left(\frac{L}{2\pi}\ \frac{\varepsilon'}{\varepsilon}\right)\sin\left(\frac{2\pi}{L}\ z\right)dz \qquad \text{(II-B1)}$$

When ε is given by Eq. (II-9) we obtain from Eq. (II-B1)

$$g_1 = 2\ \frac{n_o^2}{n_1^2}\left(1 - \sqrt{1 - \frac{n_1^2}{n_o^2}}\ \right) \qquad \text{(II-B2)}$$

For the case of symmetrical rectangular corrugation, ε is described by step functions. Describing the step function as the limit of some continuous function allows evaluation of the integral (II-B1). The result is

$$g_1 = \frac{2}{\pi}\ \ell n\ \frac{n_g^2}{n_a^2} \qquad \text{(II-B3)}$$

Appendix II-C: Computation of the Propagation Parameters of a TE Mode in an Asymmetric Dielectric Waveguide

Program 3: This program calculates the propagation parameters and profile parameters of a TE mode using the equations in Appendix II-A. The following notations in the program (left) correspond to different notations in the text:

Input:

$A \rightarrow n_a$ $\qquad$ $L \rightarrow t/\lambda$

$G \rightarrow n_g$ $\qquad$ $K \rightarrow kt = 2\pi t/\lambda$

$S \rightarrow n_s$

Part 1:

Calculates propgation parameters for all modes and does part 2:

$H \rightarrow ht$ $\qquad$ $Q(H) \rightarrow \alpha t$

$B(H) \rightarrow \beta t$ $\qquad$ $T \rightarrow t_{eff}/t$

$P(H) \rightarrow \gamma t$

Part 2:

Calculates profile coefficients for all modes:

$C \rightarrow C\sqrt{t}$

$V \rightarrow B\sqrt{t}$

$E \rightarrow A\sqrt{t}$

```
*USE FILE 1
ROGER.
*RECALL ITEM 3
DONE.
*
*
*TYPE ALL

1.10 TYPE G,A,S,L,K.
1.101 LINE.
1.11 LET B(H)=SQRT((G*K)↑2-H*H).
1.12 LET Q(H)=SQRT((G*G-S*S)*K↑2-H*H).
1.13 LET P(H)=SQRT((G*G-A*A)*K↑2-H*H).
1.14 LET F(X,Y,Z)=SIN(X)/COS(X)-X*(Y+Z)/(X*X-Y*Z).
1.15 SET H=.01.
1.151 SET N=0.
1.16 SET N=N+1.
1.17 SET I=1.
1.171 SET H=H+.001.
1.172 SET C=.1.
1.18 SET J=H+C.
1.181 SET M=SGN(F(H,Q(H),P(H))).
1.182 SET R=SGN(F(J,Q(J),P(J))).
1.19 TO STEP 1.24 IF M+R=0.
1.20 SET I=I+1.
1.21 TO STEP 1.27 IF I=30.
1.22 SET H=J.
1.23 TO STEP 1.18.
1.24 TO STEP 1.261 IF !J-H!<=.001.
1.25 SET C=(J-H)/2.
1.26 TO STEP 1.18.
1.261 TO STEP 1.17 IF !F(J,Q(J),P(J))-F(H,Q(H),P(H))!>1.
1.27 SET I=(1+1/P(H)+1/Q(H))*(P(H)↑2-H*H)/P(H)↑2.
1.28 TYPE N,J,H,B(H),P(H),Q(H),I,C,I,F(J,Q(J),P(J)),F(H,Q(H),P(H)).
1.281 LINE.
1.282 LINE.
1.283 DO PART 2.
1.29 TO PART 6 IF N=10.
1.30 TO STEP 1.16.

2.1 SET C=SQRT(2/I).
2.2 SET V=-H*C/P(H).
2.3 SET E=-(H/P(H)*COS(H)+ SIN(H))*C.
2.4 TYPE H,C,V,E.
2.5 LINE.
2.6 LINE .
2.7 LINE.
2.8 LINE.

3.1 SET K=6.283185*L.
3.2 SET G=3.5.
3.3 SET A=1.
3.4 SET S=3.
3.5 DO PART 1.




3.6 DO PART 2.

4.1 DO PART 1.
4.2 DO PART 2.

6.1 TYPE N.


      B(H):  SQRT((G*K)↑2-H*H)
  F(X,Y,Z):  SIN(X)/COS(X)-X*(Y+Z)/(X*X-Y*Z)
      P(H):  SQRT((G*G-A*A)*K↑2-H*H)
      Q(H):  SQRT((G*G-S*S)*K↑2-H*H)
```

The following is a calculation of modes propagation parameters (α,h,γ,β) and profile parameters (A,B,C,F,t_{eff}) for the following input parameters:

$n_g = 3.5$	$n_a = 1$	$n_s = 3$	$L = t/\lambda = .566$	(2 modes)
$n_g = 3.525$	$n_a = 1$	$n_s = 3.025$	$L = 1.132$	(4 modes)
$n_g = 3.5$	$n_a = 1$	$n_s = 3.3$	$L = .566$	(1 mode)
$n_g = 3.525$	$n_a = 1$	$n_s = 3.325$	$L = 1.132$	(3 modes)

(L = .566 and L = 1.132 correspond to particular case of interest where the wavelength is $\lambda = 10.6\mu$ and $\lambda = 5.3\mu$ correspondingly, and the waveguide thickness is $t = 6\mu$).

```
DO PART 1
          G =          3.5
          A =          1
          S =          3
          L =           .566037736
          K =          3.55651981

          N =          1
          J =          2.5245
          H =          2.52371875
       B(H) =         12.1893006
       P(H) =         11.6589115
       Q(H) =          5.89402677
          T =          1.19660987



          C =           7.8125*10↑(-4)
          I =          13
F(J,Q(J),P(J)) =          .001269312
F(H,Q(H),P(H)) =         -2.06237*10↑(-4)

          H =          2.52371875
          C =          1.29282192
          V =          -.279847644
          E =          -.520829058



          N =          2
          J =          4.96790625
          H =          4.967125
       B(H) =         11.4138457
       P(H) =         10.8456002
       Q(H) =          4.0541802
          T =          1.05803525
          C =          7.8125*10↑(-4)
          I =          6
F(J,Q(J),P(J)) =          .01120533
F(H,Q(H),P(H)) =         -.00522429

          H =          4.967125
          C =          1.37488043
          V =          -.629674968
          E =          1.17184106
```

```
*SET G=3.525
*SET S=3.025
*SET L=6/5.3
*DO STEP 3.1
*DO PART 1
            G =          3.525
            A =          1
            S =          3.025
            L =          1.13207547
            K =          7.11303961

            N =          1
            J =          2.80575
            H =          2.80496875
         B(H) =         24.91607 47
         P(H) =         23.8791844
         Q(H) =         12.5631152
            T =          1.10600142
            C =          7.8125*10↑(-4)
            I =         17
F(J,Q(J),P(J)) =          9.52481*10↑(-4)
F(H,Q(H),P(H)) =         -3.0723*10↑(-5)

            H =          2.80496875
            C =          1.3447 3638
            V =          -.15795947 9
            E =          -.29507 5578

            N =          2
            J =          5.59837 5
            H =          5.59759375
         B(H) =         24.4406541
         P(H) =         23.382691
         Q(H) =         11.5916633
            T =          1.06433303
            C =          7.8125*10↑(-4)
            I =         13
F(J,Q(J),P(J)) =          2.19923*10↑(-4)
F(H,Q(H),P(H)) =          -.001251252

            H =          5.59759375
            C =          1.37080673
            V =          -.328158088
            E =           .613891243

            N =          3
            J =          8.36287 5
            H =          8.36209375
         B(H) =         23.6379782
         P(H) =         22.54237 53
         Q(H) =          9.78647 547
            T =           .98877 3989
            C =          7.8125*10↑(-4)
            I =          8
F(J,Q(J),P(J)) =           .0021124
F(H,Q(H),P(H)) =          -.0016665
```

```
            H =          8.36209375
            C =          1.42221902
            V =          -.52757 2123
            E =          -.98586337 6


            N =          4
            J =          11.26309 38
            H =          11.16309 38
         B(H) =          22.4513689
         P(H) =          21.29480 3
         Q(H) =           6.4097 6216
            T =            .87 239 1247
            C =            .1
            I =          30
F(J,Q(J),P(J)) =          52.297 127 5
F(H,Q(H),P(H)) =          20.1192959


            H =          11.16309 38
            C =           1.5141167
            V =           -.7937 25432
            E =           1.360577 69

*
*SET G=3.5
*SET S=3.3
*SET L=6/10.6
*DO STEP 3.1
*DO PART 1
            G =          3.5
            A =          1
            S =          3.3
            L =           .566037 7 36
            K =          3.5565198 1

            N =          1
            J =          2.34403125
            H =          2.34325
         B(H) =          12.22527 64
         P(H) =          11.6965188
         Q(H) =           3.42222042
            T =           1.322409 25


            C =          7.8125*10↑(-4)
            I =          12
F(J,Q(J),P(J)) =            .0017 4032
F(H,Q(H),P(H)) =         -4.6821*10↑(-4)


            H =          2.34325
            C =          1.2297 9312
            V =           -.2463 7 3539
            E =           -.7088 3557 4
```

```
*SET G=3.525
*SET S=3.325
*SET L=6/5.3
*DO STEP 3.1
*DO PART 1
            G =          3.525
            A =          1
            S =          3.325
            L =          1.13207547
            K =          7.11303961

            N =          1
            J =          2.6995
            H =          2.69871875
         B(H) =         24.9278066
         P(H) =         23.8914255
         Q(H) =          7.87607279
            T =          1.15390934
            C =          7.8125*10↑(-4)
            I =         15
F(J,Q(J),P(J)) =         7.71477*10↑(-4)
F(H,Q(H),P(H)) =        -3.46696*10↑(-4)

            H =          2.69871875
            C =          1.31652513
            V =          -.148711556
            E =          -.429816444


            N =          2
            J =          5.3593125
            H =          5.35853125
         B(H) =         24.4941783
         P(H) =         23.4386313
         Q(H) =          6.37195018


            T =          1.1369089
            C =          7.8125*10↑(-4)
            I =         11
F(J,Q(J),P(J)) =         7.1683*10↑(-4)
F(H,Q(H),P(H)) =         -.00186536

            H =          5.35853125
            C =          1.32633524
            V =          -.303226274
            E =           .876386831


            J =          8.3623875
            H =          8.36209375
         B(H) =         23.6379782
         P(H) =         22.5423753
         Q(H) =          9.78647547
            T =           .988773989
            C =          7.8125*10↑(-4)
            I =          8
F(J,Q(J),P(J)) =           .0021124
F(H,Q(H),P(H)) =          -.0016665
```

N = 3

ht = 7.857

βt = 23.81

CHAPTER III

ANALYSIS FOR PERIODIC THIN FILM WAVEGUIDE APPLICATIONS

1. Introduction

In the previous chapter we presented an approximate solution for the space harmonics of periodically perturbed waveguide electromagnetic modes. In this chapter we utilize this solution in the analysis of a number of potential applications of the structure, including second harmonic generation in thin films, grating coupler, traveling wave amplifier and Bragg reflection devices.

All of the above-mentioned applications involve interaction between two or more waves. As discussed in Chapter I, the periodic perturbation helps to phase match the waves or to keep momentum conservation of the interaction with the aid of the "grating momentum." In practice we can describe the interaction as being carried through one of the electromagnetic wave space harmonics $a_m(x)$ (Eq. II-12) whose propagation constant β_m (Eq. II-13) is made (by appropriate choice of m and L) to match the other interacting waves.

It is clear that the strength of the interaction in each case depends on the profile and the relative power of the phase-matched space harmonics through which the interaction is carried out. These can be found out from Eqs. (II-51) to (II-61) for the TE mode first order space harmonic and Eqs. (II-64) to (II-70) for the TM mode first order space harmonic. Before embarking on a detailed analysis we can learn a good deal about the profile and character of the electromagnetic wave by an

examination of these equations and Eqs. (II-13,20-23). The schematic description of the harmonics profile is given in Fig. 4 for the different cases. It can be understood from general consideration in conjunction with the corresponding momentum charts. It is the apparent advantage of the solution we presented in Chapter II that the space harmonics for all the cases described in Fig. 4 can be given by the same expressions which were derived from this solution (II-51-61,64-70). The only difference between the cases is the different size of the period L which changes the character of the solution.

The condition for the confinement of the fundamental harmonic (or the unperturbed waveguide mode) is

$$n_s k < \beta_o < n_g k \qquad \text{(III-1)}$$

since only then h_o, α_o, γ_o (Eqs. II-20,21,23) are real, and the profile decays exponentially in the bounding media $x > 0$ and $x < -t$ (Fig. 4a).

The condition for any space harmonic to be confined to the waveguide is that its transverse profile will decay into the substrate and superstrate (α_m, γ_m are real). Assuming $n_s > n_a$, we deduce from (II-20,23)

$$|\beta_m| > n_s k \qquad \text{(III-2)}$$

(see Fig. 4e, for example).

In case

$$n_a k < |\beta_m| < n_s k \qquad \text{(III-3)}$$

Fig. 4 Momentum charts and transverse profiles of different space harmonics.

a. The fundamental space harmonic (or the unperturbed waveguide mode). The condition for confinement (sine-cosine solutions in the waveguide and exponential decay in the substrate and superstrate) is $n_s k < \beta_o < n_g k$.

b. The -1 order space harmonic in the case when $n_a k < \beta_{-1} < n_s k$. In this case α_{-1} is imaginary (II-20) and the space harmonic leaks to the substrate. This case is useful for substrate grating light coupler (Sect. 4). Notice also that the solution inside the waveguide is more oscillatory than that of the fundamental space harmonic.

c. The -1 order space harmonic in the case $0 < \beta_{-1} < n_a k$. Both α_{-1} and γ_{-1} are imaginary (II-20,23) and there is leakage to both substrate and superstrate (air). This can be used for coupling to air.

d. The -1 order space harmonic in the case $-n_s k < \beta_{-1} < 0$. It radiates to the substrate only, and only to one direction (other space harmonics are confined, satisfying Eq. III-2). Useful as a highly directional backward substrate coupler.

e. The first and -1 space harmonics in the case $n_s k < \beta_{-1}, \beta_1 < n_g k$. In this case both harmonics are confined (notice though that a_{-1} gets more oscillatory and a_1 less oscillatory). This case is useful for phase matching in second harmonic generation (Sect. 2).

f. The first order space harmonic in the case $\beta_1 >> n_g k$. In this case the profile is very different from $a_o(x)$. It is exponentially decaying from the perturbed surface. This case is useful in traveling wave interaction (Sect. 3).

g. The -1 order harmonic in the case $\beta_{-1} = -\beta_o$. This case corresponds to Bragg reflection (Sect. 5). The profile of $a_{-1}(x)$ is equal to the fundamental $a_o(x)$. But the propagation direction is opposite.

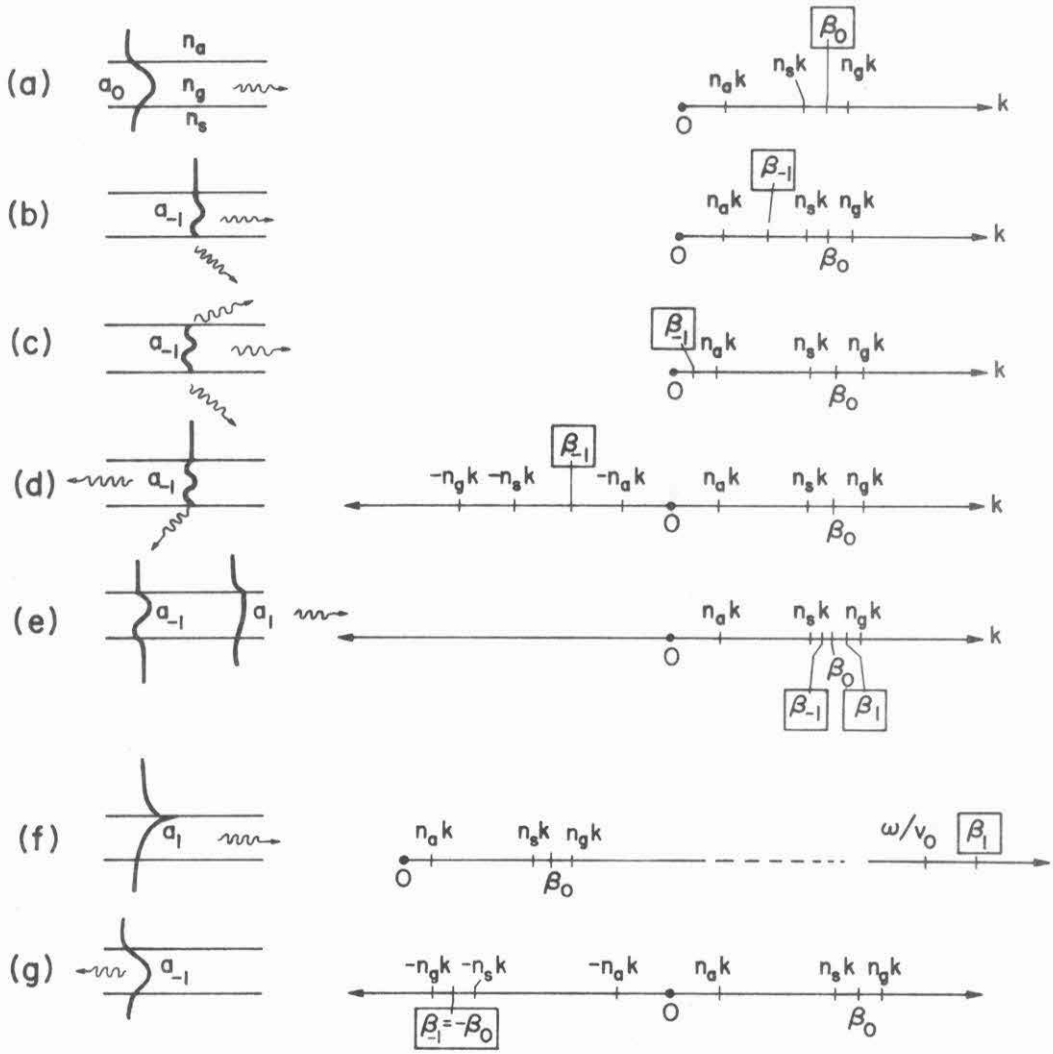
(a)
a_0
n_a
n_g
n_s
β_0
$n_a k$
$n_s k$
$n_g k$
k
O
(b)
a_{-1}
β_{-1}
$n_a k$
$n_s k$
$n_g k$
k
O
β_0
(c)
a_{-1}
β_{-1}
$n_a k$
$n_s k$
$n_g k$
k
O
β_0
(d)
a_{-1}
β_{-1}
$-n_g k$
$-n_s k$
$-n_a k$
$n_a k$
$n_s k$
$n_g k$
k
O
β_0
(e)
a_{-1}
a_1
$n_a k$
$n_s k$
$n_g k$
k
O
β_0
β_{-1}
β_1
(f)
a_1
$n_a k$
$n_s k$
$n_g k$
ω/v_0
β_1
O
β_0
(g)
a_{-1}
$-n_g k$
$-n_s k$
$-n_a k$
$n_a k$
$n_s k$
$n_g k$
$\beta_{-1} = -\beta_0$
O
β_0

the space harmonic will radiate to the substrate (Fig. 4b) since α_m in Eq. (II-20) is imaginary.

When

$$|\beta_m| < n_a k \tag{III-4}$$

radiation to both substrate and air will occur, (Fig. 4c) since both α_m and γ_m are imaginary. Obviously these cases are appropriate for application of light coupling from the waveguide to radiation modes.

Note that the profile of any space harmonic will differ more from the profile of the zero harmonic the bigger is $m \frac{2\pi}{L}$ relative to β_o . In particular, when

$$|\beta_m| > n_g k \tag{III-5}$$

then h_m is imaginary and $a_m(x)$ inside the guide is described by a sum of hyperbolic sine and cosine instead of trigonometric sine and cosine. In the limit $|\beta_m| >> n_g k$ the profile will look exponentially decaying to both sides of the perturbed surface (see Fig. 4f).

2. Second Harmonic Generation

It is well known that nonlinearity of the material dielectric constant may lead to three-photon interactions in which (as a special example) two photons of frequency ω can combine to a photon of frequency 2ω . However, due to material dispersion, and in thin films also due to waveguide dispersion, we generally have for any given electromagnetic mode

$$\beta^{2\omega} > 2\beta^{\omega} \tag{III-6}$$

and because of the phase mismatch (or the nonconservation of momentum) the efficiency of the interaction is rather poor. Since birefringence phase matching cannot be used in optically isotropic material, many materials with high nonlinear coefficients like GaAs are not phase matchable in the bulk and are not used for second harmonic generation.

Furthermore, second harmonic generation in thin film dielectric waveguide seems an attractive possibility for many reasons, particularly because it makes it possible to achieve high power density without diffraction, which increases the conversion efficiency. This application is still retarded mainly because of the problem of phase matching.

Somekh and Yariv [1972] suggested phase matching by introducing in the waveguide a perturbation of period L (Fig. 1) which satisfies

$$\frac{2\pi}{L} = \beta_o^{2\omega} - 2\beta_o^{\omega} \qquad \text{(III-7)}$$

In that paper the authors actually calculated the effective nonlinear optical coefficient d_{eff} using an adiabatic approximation (see Chapter II, Sect. 5) which is valid for long perturbation period L so that (Eq. II-97)

$$\frac{2\pi}{L}\beta_o << h_o^2 \qquad \text{(III-8)}$$

The evaluation of the amplitudes of the space harmonics in the first order approximation which we did in Chapter II allows us to calculate d_{eff} for the more general case, to be used in practical cases when condition (III-8) is not satisfied.

At the present time we will analyze in detail the case of TE modes. The same treatment can be easily extended to the TM case. We

denote the degree of excitation of a mode by premultiplying the normalized mode field (II-12) by a z dependent constant $K^{\omega}(z)$

$$E^{\omega}(x,z) = K^{\omega}(z) \sum_{n} a_n(x)\, e^{-i\beta_n^{\omega} z} \qquad \text{(III-9)}$$

$$E^{2\omega}(x,z) = K^{2\omega}(z) \sum_{n} a_n^{2\omega}(x)\, e^{-i\beta_n^{2\omega} z} \qquad \text{(III-10)}$$

Since the assumed mode normalization (II-A14,A15) corresponds to a power of 1 watt/cm in the fundamental space harmonic (the contribution of the other harmonics is neglected), the field (III-9) corresponds to a power $P^{\omega} = w|K^{\omega}(z)|^2$ watts (Eq. II-A17).

We solve here the problem only in the nondepleted pump approximation, therefore K^{ω} is assumed independent of z, and $K^{2\omega}(z)$ satisfies the initial condition

$$K^{2\omega}(0) = 0 \qquad \text{(III-11)}$$

Since in the first order approximation the power of the mode is predominantly carried by the zero harmonic which is approximated by the normalized mode of the unperturbed waveguide, we get that the power carried by each of the waves is

$$P^{\omega} = w|K^{\omega}|^2 \qquad \text{(III-12)}$$

$$P^{2\omega}(z) = w|K^{2\omega}(z)|^2 \qquad \text{(III-13)}$$

where w is the waveguide width.

The nonlinear coefficient d is defined by [Yariv 1971]

$$p^{2\omega}(x,z) = d \cdot [E^{\omega}(x,z)]^2 \qquad \text{(III-14)}$$

where $p^{2\omega}$ is the 2ω frequency induced polarization. Hence, by substituting Eqs. (III-14), (III-9) and (III-10) into the equation

$$\frac{dP^{2\omega}}{dz} = \omega w \, \mathrm{Im} \int_{-\infty}^{0} E^{2\omega}(p^{2\omega})^* \, dx \qquad \text{(III-15)}$$

we get:

$$\frac{dP^{2\omega}(z)}{dz} = wd \, \mathrm{Im}[K^{2\omega}(z)^*(K^{\omega})^2 \sum_{n,\ell,m} e^{-i(\beta_m^{2\omega}-\beta_n^{\omega}-\beta_\ell^{\omega})z} \cdot \int_{-\infty}^{0} a_n(x) \, a_\ell^{\omega}(x) \, a_m^{2\omega}(x) \, dx \,] \qquad \text{(III-16)}$$

If L is chosen to satisfy Eq. (III-7), then all the terms in Eq. (III-16) that satisfy

$$n + \ell - m = 1 \qquad \text{(III-17)}$$

are phase matched. The main significant synchronous terms are the three first-order triplets: $(n,\ell,m) = (1,0,0), (0,1,0), (0,0,-1)$. The wave vector chart of these three terms is plotted in Fig. 5, describing the two possible ways to balance the momentum conservation equation. Keeping only the three major synchronous terms, substitution of Eqs. (III-12,13) into Eq. (III-16) gives

$$\frac{dP^{2\omega}(z)}{dz} = \frac{4\omega^{5/2} \, \mu^{3/2} \, d_{eff} \, P^{\omega}}{(wt \, \beta^{2\omega})^{1/2} \, \beta^{\omega}} [P^{2\omega}(z)]^{1/2} \qquad \text{(III-18)}$$

where

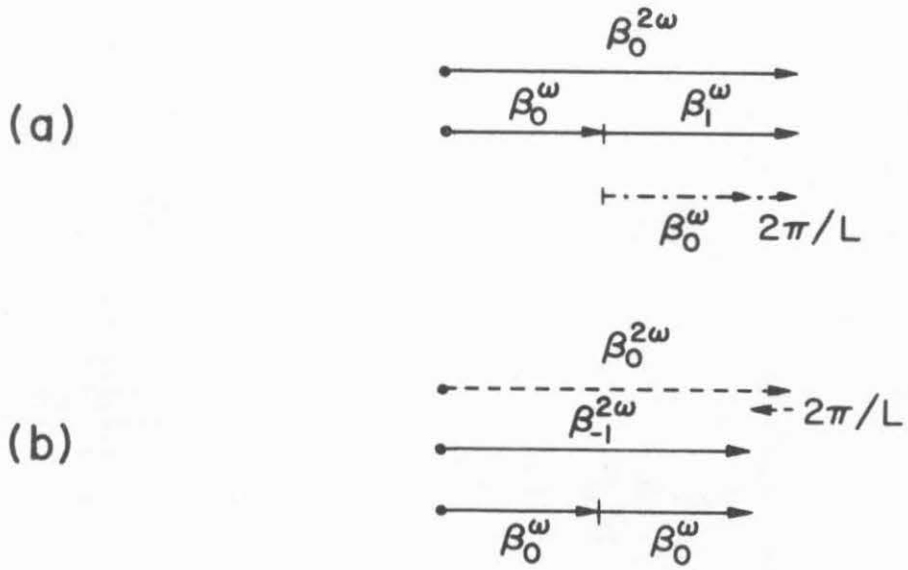

Fig. 5. Forward scheme for phase matching in second harmonic generation.

a. Zero and first order space harmonics of the fundamental frequency phase-matched to the zero order space harmonic of the doubled frequency.

b. Zero order space harmonics of two fundamental frequency photons, phase-matched to the -1 harmonic of the doubled frequency wave.

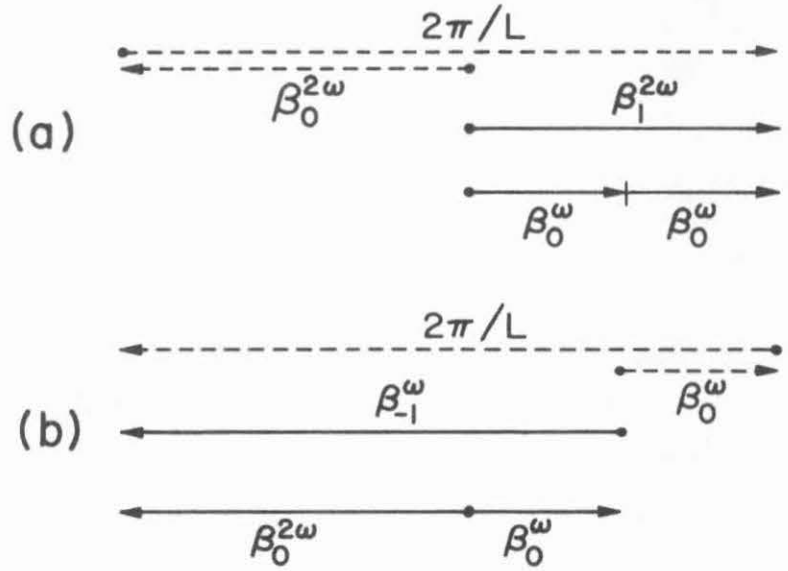

Fig. 6. Backward scheme for phase matching in second harmonic generation.

a. Zero order space harmonics of two fundamental frequency photons, phase matched to the first space harmonic of the doubled frequency wave propagating backward.

b. Zero order and -1 order space harmonics of two fundamental frequency photons, phase matched to zero order space harmonic of the doubled frequency wave propagating backward.

$$d_{eff} = d\sqrt{t}\left\{2\int_{-\infty}^{0} a_0^{\omega}(x)\, a_1^{\omega}(x)\, a_0^{2\omega}(x)dx + \int_{-\infty}^{0} [a_0^{\omega}(x)]^2\, a_{-1}^{2\omega}(x)dx\right\}\left(\sqrt{\frac{\beta^{\omega}}{2\omega\mu}}\right)\sqrt{\frac{\beta^{2\omega}}{4\omega\mu}} \qquad \text{(III-19)}$$

The solution of Eq. (III-18) gives the expression for the conversion efficiency

$$\frac{P^{2\omega}(\ell)}{P^{\omega}} = \frac{4\omega^5\, \mu_o^3\, d_{eff}^2\, \ell^2}{\beta^{2\omega}\, (\beta^{\omega})^2}\, \frac{P^{\omega}}{wt} \qquad \text{(III-20)}$$

In the special case of well confined modes, Eq. (III-20) turns into the familiar expression [Yariv 1971, Somekh 1973]

$$\frac{P^{2\omega}(\ell)}{P^{\omega}(\ell)} = \frac{2\omega^2\, d_{eff}^2\, \ell^2}{(n^{\omega})^2\, n^{2\omega}} \left(\frac{\mu_o}{\varepsilon_o}\right)^{3/2} \frac{P^{\omega}}{wt} \qquad \text{(III-21)}$$

To evaluate the effective nonlinear coefficient d_{eff} (Eq. III-19) we may substitute the expressions for $a_0(x)$, $a_1(x)$, $a_{-1}(x)$ from Eqs. (II-51) to (II-61). The result involves integration of products of trigonometric (or hyperbolic) functions (a scheme for computer calculation of d_{eff} is presented in Appendix III-A).

As an example we calculated a second harmonic generation of a fundamental wave at $\lambda_o = 10.6$, assuming a GaAs epitaxial film (Fig. 2) with $t = 6\mu$, $n_g(\omega) = 3.5$, $n_s(\omega) = 3.3$, using the computer program listed in Appendix III-A. The bulk dispersion in this wavelength [Boyd 1970] and the waveguide dispersion require mismatch compensation: $\frac{2\pi}{L} = \beta^{2\omega} - 2\beta^{\omega} = 0.078\ \mu m^{-1}$ ($L = 80\ \mu m$). Using this data, Eq. (III-19) yields: $d_{eff} = d/15$.

This value is higher than the value calculated by Somekh [1972] in the adiabatic approximation ($d = d_{eff}/25$). The reason is that the adiabatic approximation is hardly valid in this case since Eq. (III-8) is barely satisfied. With input power density $P^{\omega}/wt = 10$ megawatt/cm^2, one gets 10% conversion after length of $\ell = 4.3$ cm.

We may indicate that reduction in the conversion efficiency may arise from radiation loss due to light out coupling through high order negative m harmonics which do not satisfy the confinement condition (III-2). This loss may be calculated in the way described in Section 4. Since the amplitude of higher harmonics is generally small, this loss is believed to be rather low. However, radiation loss can be completely avoided if the backward matching scheme is used (Fig. 6). In this scheme the fundamental components of the ω and the 2ω waves move in opposite directions, so that Eq. (III-7) can be written as:

$$\frac{2\pi}{L} = |\beta_o^{2\omega}| + 2|\beta_o^{\omega}| \qquad \text{(III-22)}$$

Considering Eq. (III-1), this results in

$$\frac{2\pi}{L} > 4\, n_s k \qquad \text{(III-23)}$$

which lets Eq. (III-2) be satisfied for all m in both frequencies ω and 2ω. The expressions for second harmonic generations which were deried above are valid for the case of backward matching as well as for forward matching.

It turns out that technological limitations are the main factor in the device design and in choosing the operation scheme. In practice,

perfect phase matching can only be approached, $\Delta\beta = \beta^{2\omega} - 2\beta^{\omega} - 2\pi/L \neq 0$, because of some inaccuracy in determination of β^{ω}, $\beta^{2\omega}$ or L. If the coherence length

$$\ell_c \equiv \pi/\Delta\beta \qquad \text{(III-24)}$$

is short enough ($\ell_c < \ell$) then the maximum attainable second harmonic power generation is determined by ℓ_c and not by ℓ.* In this sense the process of phase matching can be viewed as increasing the coherence length from its natural value $\ell_c = \pi/(\beta^{2\omega} - 2\beta^{\omega})$ to a longer value, $\ell_c = \pi/(\beta^{2\omega} - 2\beta^{\omega} - 2\pi/L)$, which tends to an infinite value as the phase matching accuracy increases.

The dominant contribution for phase mismatch is inaccuracy in determination of the perturbation period L. (The thin film thickness t may be measured accurately before determination of the periodicity. Also, inaccuracy in t has little effect when the modes are well confined). So, in order to increase the coherence length (decrease the mismatch $\Delta\beta$) relative to their natural value by a factor of ten--from

---

*When $\Delta\beta \neq 0$, Eq. (III-21) does not apply. Instead, the second harmonic power generated in a distance ℓ is proportional to $p^{2\omega}{}_{\alpha} \sin^2(\Delta\beta\ell/2) / (\Delta\beta)^2$. Thus the second harmonic power oscillates as a function of length between zero and some low maximal value which is attained when $\ell = \ell_c \equiv \pi/\Delta\beta$ (see illustration in Fig. 14a and a broader discussion in Yariv [1971].) Hence, for fixed coupling coefficient and input, the maximum attainable gain is proportional to ℓ_c^2 (or inversely proportional to $(\Delta\beta)^2$) as long as an interaction length $\ell = \ell_c$ can be practically realized, and as long as the undepleted pump assumption holds. However, if $\ell \ll \ell_c$ then the sine function can be expanded to first order, resulting again in Eq. (III-21).

ℓ_c = 40 μm (with no phase matching at all, L = ∞) to a value of ℓ_c = 0.4 mm, the periodic perturbation must be introduced within 10% accuracy, when the forward matching scheme is used. Introducing perturbation of L = 80 ± 8 μm can be easily done by conventional masking techniques. On the other hand, if we consider backward phase matching then for the above example, using Eq. (III-22), we get L = 0.765 μm . In order to get in this case elongation of the coherence length (decrease in the mismatch $\Delta\beta$) by a factor of 10, the periodicity must be determined within an accuracy of 0.1%, which is a difficult task, even if the grating fabrication is done by holographic method. It is therefore because of this technological limitation that backward phase matching may be difficult to realize.

3. Traveling Wave Amplifier

When charged particles happen to move in higher velocity than an electromagnetic wave which propagates in the same medium, then under the appropriate conditions, transfer of energy from the particle beam to the electromagnetic field may occur. This principle is the basis of phenomena such as the Cerenkov [e.g., Jackson 1962] and the Smith Purcell radiation [Smith 1953], and of traveling wave amplifiers and oscillators [Pierce 1950] in which accelerated electron beam interacts with a slow electromagnetic wave component which is generated by a periodic waveguide. The period and the electron velocities used in common traveling wave tubes allow for microwave frequency amplification and generation.

The ability to produce dielectric waveguides with very short period perturbation (less than 1 μ) makes it interesting to consider the traveling wave interaction in new operational regimes. Since very short periods provide appreciable slowing down of the electromagnetic wave, it may be possible to amplify higher frequency waves (visible or IR light) or alternatively to use lower velocity charged particle current (like drifting carriers current in solids). The first possibility (see Fig. 7) was investigated in Yariv [1973A], and the second one will be discussed in Chapters IV to VI (see Fig. 8).

Assume that the slow wave component which participates in the interaction is the first order harmonic a_1 or the -1 harmonic a_{-1}. Their propagation parameters are $\beta_{\pm 1} = \beta_o \pm \frac{2\pi}{L}$. The charged particle drift velocity is v_o. The condition for energy transfer into the electromagnetic wave is

$$v_o > v_{Ph \pm 1} = \omega / \left| \beta_o \pm \frac{2\pi}{L} \right| \qquad \text{(III-25)}$$

which can be rearranged to:

$$\frac{\lambda}{L} > \frac{c}{v_o} \pm \frac{\beta_o}{k} \qquad \text{(III-26)}$$

Using Eq. (III-1) and assuming $v_o << c$, it is possible to write this condition approximately as:

$$\frac{\lambda}{L} > \frac{c}{v_o} \qquad \text{(III-27)}$$

Equation (III-26) or (III-27) allows calculating in a very simple way the wavelengths in which one expects amplification in both mentioned applications.

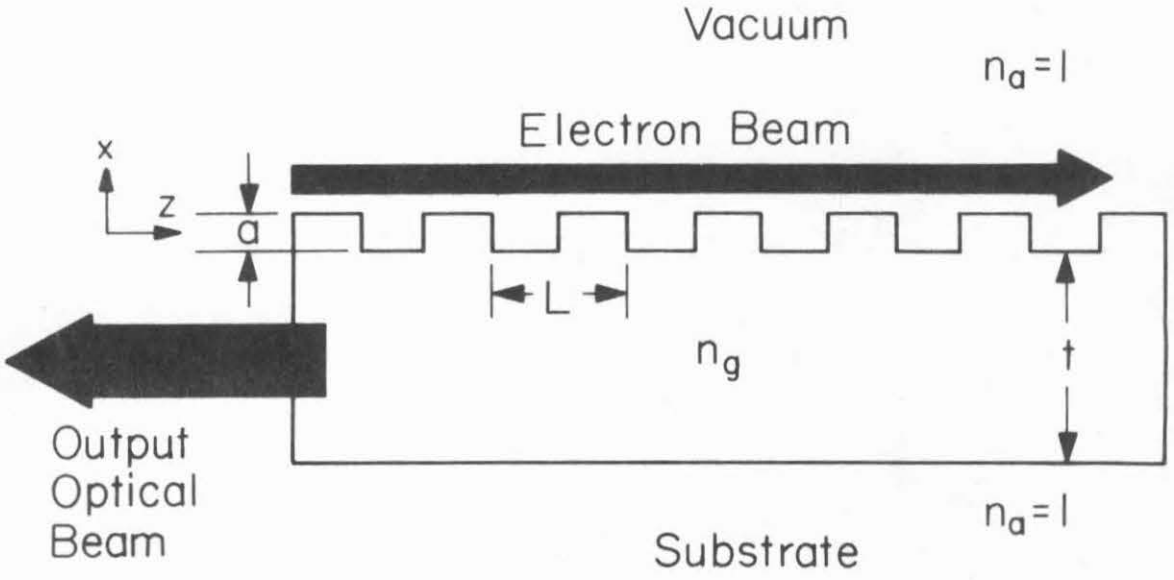

Fig. 7 Schematic diagram of an optical traveling wave oscillator using a corrugated dielectric thin-film waveguide.

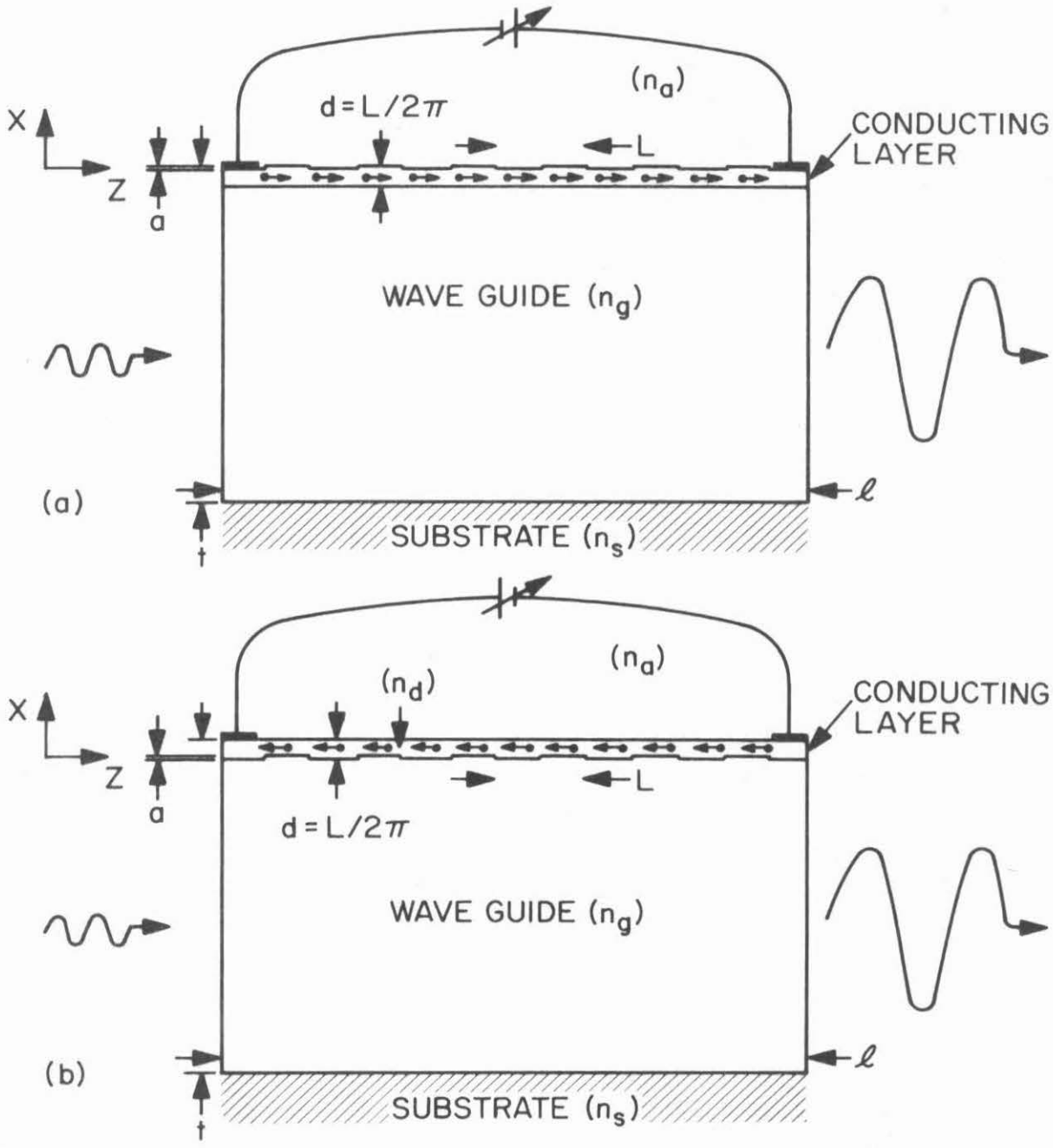

Fig. 8 (a) Monolithic solid-state traveling-wave amplifier with conducting layer beneath the periodic corrugation. (b) Monolithic solid-state traveling-wave amplifier with conducting layer on top of the periodic corrugation.

Consider the case of the vacuum beam optical traveling wave oscillator (Fig. 7) with $L = 1\mu$. Assume that the electron beam is accelerated to a tenth the speed of light, then Eq. (III-27) predicts amplification range:

$$\lambda \gtrsim 10\ \mu m$$

On the other hand, in the solid state traveling wave amplifier (Fig. 8), we want to use drifting carriers for the charged particle beam. Achievable carrier drift velocity may be as high as $v_o \simeq 2 \times 10^7$ cm/sec. When this is substituted in Eq. (III-27) with $L = 1\mu$ we find that the wavelengths which may be amplified in this device are of the order:

$$\lambda \gtrsim 1.5\ mm$$

We may indicate that higher order harmonics may allow proportionally shorter wavelengths in both applications, however their interaction efficiency will also be reduced, and this case will not be considered here. Using shorter corrugation periods [Yen 1973, Bjorklund 1974], the wavelength may be reduced by another order of magnitude.

Let us discuss the traveling wave interaction in more detail. It may be described as a coupled wave problem, where the electromagnetic wave couples to a space-charge wave of the beam. The electromagnetic wave spatially modulates the flowing charged particle plasma and, in turn, the space charge wave induces electromagnetic field into the waveguide structure. The detailed calculation of this process [Pierce 1950, Gould 1955] requires the knowledge of a parameter of the slow wave

structure. This parameter, called the interaction impedance, is a measure of the coupling between the space charge wave and the electromagnetic wave, and is given by

$$K_1 = \frac{|E_1|^2}{2\beta_1^2 P} \qquad \text{(III-28)}$$

where E_1 is the electric field of the slow space harmonic (the first order one in this case) at the point where the interaction with the charged carrier beam takes place, and P is the total power carried by the electromagnetic wave.

We are interested in finding expressions for the interaction impedance in order to use it in the following chapters, as well as in other published works [Yariv 1973A, 1974A, Gover 1974A, 1974B].

In order to find E_1 and the interaction impedance, we can use the expression for the first order space harmonic of the TM wave which was calculated in Chapter II (longitudinal space charge modulation will be performed by the z field component only $E_1 = E_{z_1}$, for this reason we have to use the TM mode).

For large values of $2\pi/L$ which are to be used in the presently discussed applications, the parameter h_1 (II-21) becomes imaginary. We then define

$$\chi_1 \equiv ih_1 = (\beta_1^2 - n_g^2 k^2)^{1/2} \qquad \text{(III-29)}$$

Substituting this instead of h_1 and taking the limit

$$\chi_1 t \gg 1 \qquad \text{(III-30)}$$

Eqs. (II-51, 52, 54, 64-68) turn in this limit into:

$$a_1(x) = B_1 e^{\chi_1 x} \qquad x < 0 \qquad \text{(III-31)}$$

$$a_1(x) = F_1 e^{-\chi_1 x} \qquad x > 0 \qquad \text{(III-32)}$$

$$B_1 = \frac{n_g^2}{n_{LO}^2} \frac{f_1 + \frac{1}{2}\frac{n_{L1}^2}{n_a^2}\gamma_o\left(\gamma_o + \frac{n_{LO}^2}{n_a^2}\gamma_1\right)}{\frac{n_g^2}{n_a^2}\gamma_1 + \chi_1} K F_o a \qquad \text{(III-33)}$$

$$F_1 = \frac{n_g^2}{n_{LO}^2} \frac{f_1 + \frac{1}{2}\frac{n_{L1}^2}{n_a^2}\gamma_o\left(\gamma_o - \frac{n_{LO}^2}{n_g^2}\gamma_1\right)}{\frac{n_g^2}{n_a^2}\gamma_1 + \chi_1} K F_o a \qquad \text{(III-34)}$$

where

$$f_1 = \frac{1}{2}\left(n_{L1}^2 k^2 + g_1 \frac{2\pi}{L}\beta_o\right) \qquad \text{(III-35)}$$

n_{LO}^2, n_{L1}^2, g_1 are defined by Eqs. (II-1,35). The same equations apply also for the -1 harmonic when the subscript 1 is substituted by -1 and

$$f_{-1} = \frac{1}{2}\left(n_{L1}^2 k^2 - g_1 \frac{2\pi}{L}\beta_o\right) \qquad \text{(III-36)}$$

The transverse profile corresponding to this solution is illustrated in Fig. 4f.

We further use the equations:

$$E_{z_{\pm 1}}(0^+) = \frac{i\gamma_{\pm 1}}{\omega\varepsilon_o n_a^2} F_{\pm 1} \cdot K \qquad \text{(III-37)}$$

$$E_{z_{\pm 1}}(0^-) = -\frac{i\chi_{\pm 1}}{\omega\varepsilon_o n_a^2} B_{\pm 1} \tag{III-38}$$

$$F_o = -\frac{n_a^2 h_o}{n_g^2 \gamma_o \sqrt{t_{eff}}} \frac{2\omega\varepsilon_o}{\beta} \tag{III-39}$$

$$P = wK^2 \tag{III-40}$$

(see Appendix II-A). In the limit

$$\frac{2\pi}{L} >> n_g k \tag{III-41}$$

we have:

$$\chi_{\pm 1} \simeq \gamma_{\pm 1} \simeq \frac{2\pi}{L} \tag{III-42}$$

and substitution of Eqs. (III-33) to (III-42) in Eq. (III-28) gives in this limit:

$$K_{\pm 1}(0^+) = \sqrt{\frac{\mu_o}{\varepsilon_o}} \frac{n_a^4}{2n_{LO}^4(n_g^2 + n_a^2)^2} \frac{h_o^2 a^2}{\gamma_o^2 \beta_o k t_{eff} w} (g_1\beta_o \mp \frac{n_{L1}^2}{n_a^2} \frac{n_{LO}^2}{n_g^2} \gamma_o)^2 \tag{III-43}$$

$$K_{\pm 1}(0^-) = \sqrt{\frac{\mu_o}{\varepsilon_o}} \frac{n_a^8}{2n_{LO}^4 n_g^4(n_g^2 + n_a^2)^2} \frac{h_o^2 a^2}{\gamma_o^2 \beta_o k t_{eff} w} (g_1\beta_o \pm \frac{n_{L1}^2 n_{LO}^2}{n_a^4} \gamma_o)^2 \tag{III-44}$$

Equation (III-43) gives the interaction impedance with an electron stream moving outside of the waveguide next to the perturbed surface, and Eq. (III-44) is for interaction with electron stream flowing inside the waveguide next to the surface.

In the case of an electron beam optical oscillator [Yariv 1973A] the electromagnetic wave interacts with an accelerated electron beam flowing outside of the waveguide next to the surface (see Fig. 7). From Eqs. (III-32) and (III-42) we deduce that the space harmonic decays

exponentially away from the surface (Fig. 4f), hence effective interaction occurs only with a beam focused down to $L/2\pi$ thickness. Equation (III-43) indicates also that interaction impedance is bigger for the -1 harmonic than for the +1 harmonic, consequently oscillators and amplifiers of this type should be better designed for "backward wave" coupling.

In the application of solid state traveling wave amplifiers [Gover 1974A, Yariv 1974A] the electromagnetic wave interacts with carrier currents flowing in a thin conducting layer located in the waveguide right beneath the perturbed surface (see Fig. 8a). The conducting layer thickness must be of order $L/2\pi$ in order to get effective interaction. Equation (III-44) which gives the interaction impedance for this case indicates that forward wave amplification is advantageous.

Another way to produce the solid state amplifier is to deposit a thin conducting layer of thickness $L/2\pi$ on top of the perturbed surface (see Fig. 8b). If the layer is thick enough so that the mode penetration through layer n_d is negligible, then we can still use Eq. (III-43) with n_d instead of n_a. However, when $d = L/2\pi << 1/\gamma_o$, then our treatment up to this point does not rigorously describe this case, because an additional layer with index of refraction n_d (which may be quite high) replaces the medium n_a above the perturbation layer. However, with some simplified assumptions we may suggest a rough approximation for this case. The assumption is that the first and -1 harmonics, having short range of penetration, sense only n_d above the waveguide surface and for their calculation n_d is used instead of n_a, but for the zero harmonic calculation the thin layer n_d is neglected

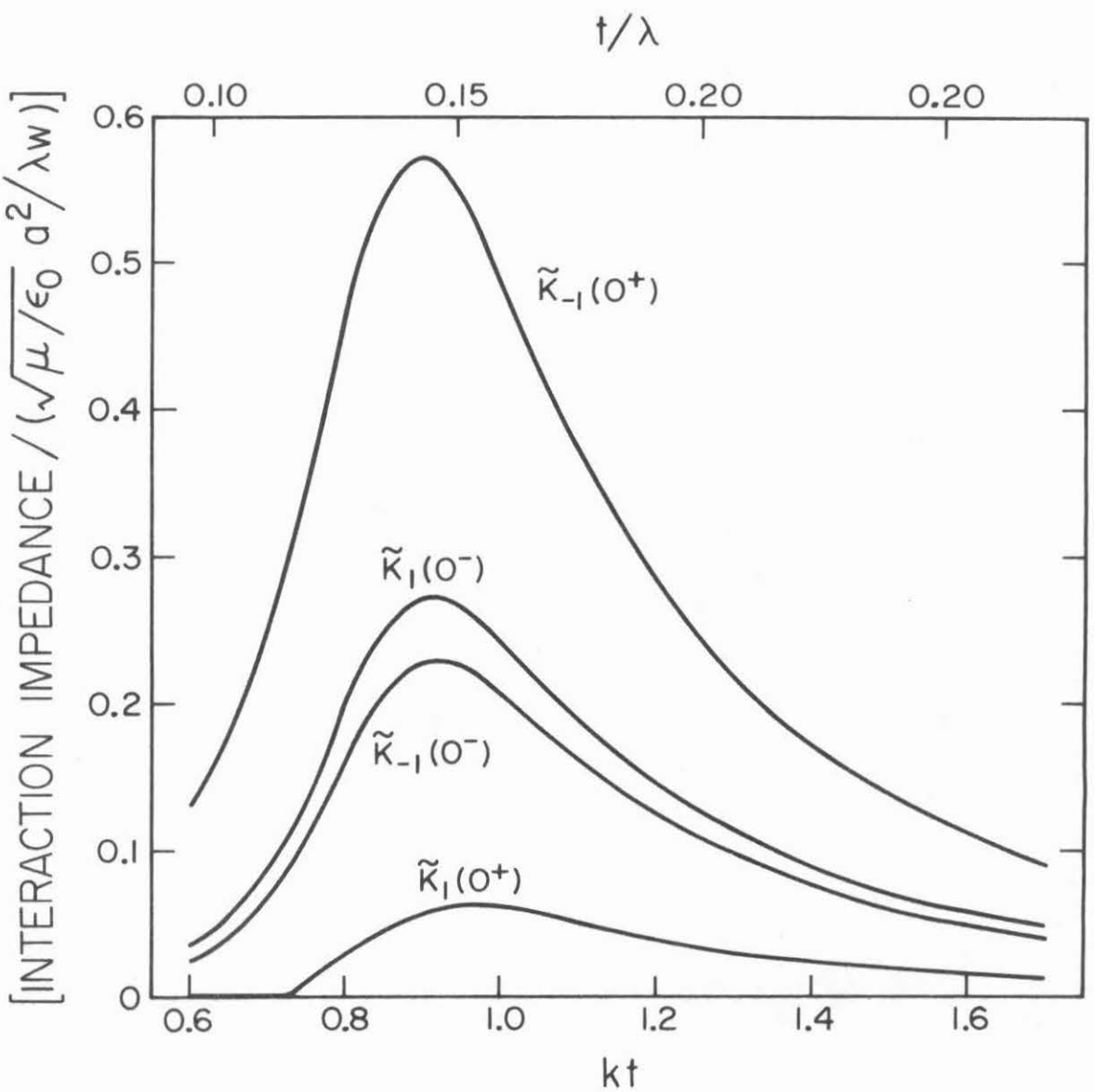

Fig. 9 Normalized interaction impedance (Eqs. III-B5÷B7) for interaction with the fundamental even TM mode in a symmetric waveguide $n_g=3.5$, $n_a=n_s=1$.

and medium n_a only is assumed to be for $x > 0$. The resulting interaction impedance is in this approximation

$$K_{\pm 1}(0^+) = \sqrt{\frac{\mu_o}{\varepsilon_o}} \frac{n_a^4}{2n_{L0}^4(n_g^2 + n_d^2)^2} \frac{h_o^2 a^2}{\gamma_o^2 \beta_o k t_{eff} w} (g_1 \beta_o \mp \frac{n_{L1}^2}{n_d^2} \frac{n_{L0}^2}{n_g^2} \gamma_o)^2 \qquad \text{(III-45)}$$

where g_1, n_{L0}^2, n_{L1}^2 are calculated from (II-4,5,B3) with n_d instead of n_a, but $h_o, \beta_o, \gamma_o, t_{eff}$ are calculated with the assumption $d = 0$. For this case apparently the backward interaction is stronger. Equation (III-45) is based on rough approximations and it is hard to estimate its validity for quantitative indication of the interaction impedance. We will use it further only for qualitative discussion. A more rigorous approximate calculation of the interaction impedance in the case of Fig. 8b (in special operation condition) is presented later in Appendix IV-A.

We use Eq. (III-43) to calculate interaction impedance for a particular example in which the thin waveguiding layer is GaAs - n_g = 3.5 and the periodic perturbation is introduced by "symmetric" corrugation of the surface ($L_1 = L/2$ in Fig. 2):

$$n_{L0}^2 = \frac{1}{2}(n_g^2 + n_a^2) = 6.6 \qquad \text{(III-46)}$$

$$n_{L1}^2 = \frac{2}{\pi}(n_g^2 - n_a^2) = 7.2 \qquad \text{(III-47)}$$

$$g_1 = \frac{2}{\pi} \ell n \frac{n_g^2}{n_a^2} = 1.6 \qquad \text{(III-48)}$$

A numerical calculation of Eqs. (III-43,44) was carried out (see Appendix III-B) and the resulting normalized interaction

impedances (Eqs. III-B5-B7) are displayed in Fig. 9. The electromagnetic mode that was used in the example which is illustrated in Fig. 9 is the first order even TM mode in a symmetric waveguide ($n_g = 3.5$, $n_s = n_a = 1$).

From Fig. 9 it seems that all first order mode interaction impedances attain their maxima about $t/\lambda \simeq 1/7$. For backward wave interaction on top of the corrugation (Fig. 7), the choice of parameters $t/\lambda = 0.1433$ results in the highest value of $K_{-1}(0^+)$. At this condition

$$K_{-1}(0^+) = 0.573 \sqrt{\frac{\mu}{\varepsilon_o}} \frac{a^2}{\lambda w}$$
$$K_{+1}(0^+) = 0.0589 \sqrt{\frac{\mu}{\varepsilon_o}} \frac{a^2}{\lambda w} \qquad \text{(III-49)}$$

For example, for possible operation conditions $a = 1\mu$, $\lambda = 10\mu$, $t = 1.43\mu$, we get $wK_{-1}(0^+) = 2.16 \times 10^{-3}\Omega$ cm. For forward wave interaction beneath the corrugation (Fig. 8a), the choice $t/\lambda = 0.1448$ results in the highest value of $K_1(0^-)$. At this condition

$$K_1(0^-) = 0.272 \sqrt{\frac{\mu}{\varepsilon_o}} \frac{a^2}{\lambda w}$$
$$K_{-1}(0^-) = 0.230 \sqrt{\frac{\mu}{\varepsilon_o}} \frac{a^2}{\lambda w} \qquad \text{(III-50)}$$

For example, for possible operation conditions $a = 1\mu$, $\lambda = 1.5$ mm, $t = 0.22$ mm we get from (III-50): $wK_1(0^-) = 6.84 \times 10^{-6}\Omega$ cm.

The expressions calculated in this section are used in Chapters IV, V and in Refs. [Yariv 1973A, Gover 1974A, 1974B].

4. Grating Coupler and Thin Film Filters

In this section we discuss another application of periodically perturbed thin films: coupling of light between radiation and guided modes. As discussed previously, in the introduction to this chapter, coupling of light out of the waveguide will be performed through harmonic m whenever Eq. (III-3) or (III-4) is satisfied. We get substrate coupling for the case of Eq. (III-3) and air and substrate coupling for Eq. (III-4). If $\beta_m < 0$, the coupling is called backward coupling, since light coupled out propagates in opposite direction to the fundamental guided wave (see Figs. 4b to 4d).

Coupling of light out of the waveguide is due to all the space harmonics that satisfy Eq. (III-3) or (III-4), but we will analyze only the -1 harmonic which couples the dominant part of the power. In most applications we will also prefer having only one harmonic coupling in order to be able to collect the coupled light in one direction. The condition for a single harmonic coupling is satisfaction of Eq. (III-2) for $m = -2$. Using the definition (II-13) we get

$$\frac{2\pi}{L} > \frac{1}{2}(\beta_o + n_s k) \qquad \text{(III-51)}$$

This is certainly satisfied when we have -1 backward coupling for which

$$\frac{2\pi}{L} > \beta_o \qquad \text{(III-52)}$$

Best directionality of light coupling (i.e., light is coupled out only to one direction) is achieved for -1 substrate backcoupling for which

$$\beta_o + n_s k > \frac{2\pi}{L} > \beta_o + n_a k \qquad \text{(III-53)}$$

In this case light is coupled out only through the -1 order space harmonic which is leaking only to the substrate (Fig. 4d).

Besides being used for power coupling in optical dielectric waveguides, grating couplers may be used as transmission filters for guided light [Dabby 1973]. To get a high pass filter which transmits at $\omega > \omega_1$, choose the period L_1 so that

$$\frac{2\pi}{L_1} = \beta_o(\omega_1) - n_s k_1 \qquad \text{(III-54)}$$

For frequencies $\omega < \omega_1$ we then have

$$\beta_{-1} = \beta_o - \frac{2\pi}{L_1} < n_s k \qquad \text{(III-55)}$$

Hence α_{-1} (Eq. II-20) becomes imaginary and the light mode in frequency ω loses power through the -1 harmonic (see Fig. 10). In fact frequencies higher than ω_1 also lose some power through higher order negative harmonics, but this power loss is significantly smaller than the -1 harmonic loss. So, for sufficiently long grating couplers it is possible to achieve considerable filtering of the frequencies $\omega < \omega_1$.

To get low pass filter [Dabby 1973] which transmits $\omega < \omega_2$, the periodicity L_2 must be chosen to satisfy:

$$\frac{2\pi}{L_2} = \beta_o(\omega_2) + n_s k_2 \qquad \text{(III-56)}$$

then for frequencies $\omega > \omega_2$,

$$|\beta_{-1}| = |\beta_o - \frac{2\pi}{L_2}| < n_s k \qquad \text{(III-57)}$$

then Eq. (III-20) becomes imaginary for $m = -1$ and we have power loss at high frequencies $\omega > \omega_2$ (Fig. 11).

Band pass transmission filter can be devised by incorporating two gratings with periods that satisfy Eq. (III-54) and (III-56) on the thin film surface. The two gratings can be put successively, or in the same place. In designing a filter like this, one has to be aware of having a reflection stop band inside the pass band $\omega_1 < \omega < \omega_2$. This stop band occurs for $\beta_o = \frac{\pi}{L}$ (see discussion in the next section). By choosing ω_1 to fall in or above the reflection stop band, one can design a narrow single transmission band (see Fig. 12).

We may mention that the stop band itself can also be used as a very narrow bandpass filter when the reflected light is used. This application is discussed in the next section.

In order to calculate coupling efficiency we are going to use the expression for the -1 harmonic amplitude derived in Chapter II. In using this expression we make the approximation that over few periods only a small portion of the power is coupled out, hence the mode amplitude stays approximately constant. The next step will be to assume exponential decay of the mode amplitude where the decay constant is determined from the power loss rate calculated in the first step. For brevity we henceforth develop the expression for coupling efficiency only for TE mode -1 substrate coupling (either forward or backward). One can easily calculate the appropriate expressions for the other cases by following the same procedure and using for the case of the TM mode the expression

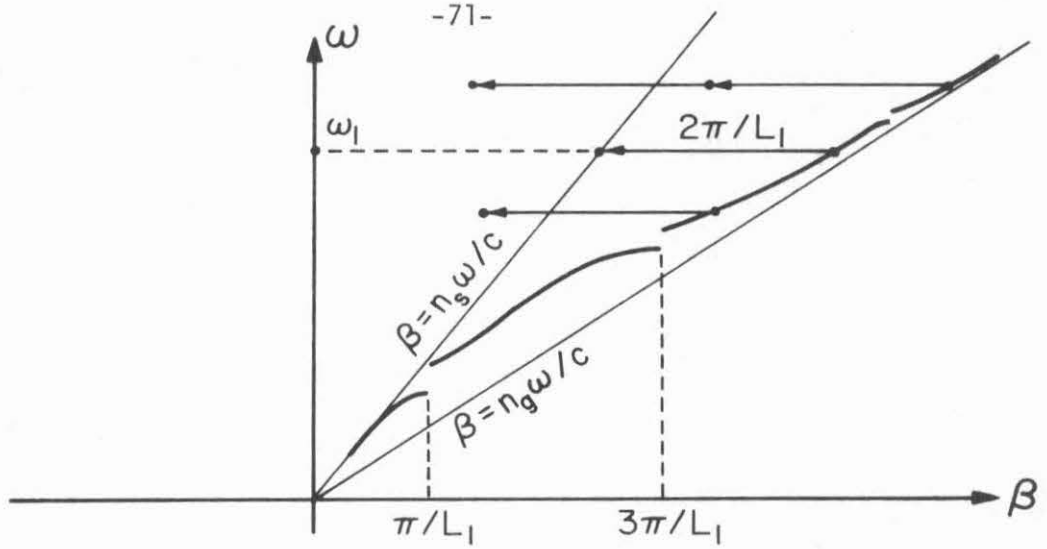

Fig. 10 High pass filter. The condition for leakage via the -1 space harmonic (Eq. III-55) is satisfied only for $\omega < \omega_1$. For $\omega > \omega_1$ the -1 harmonic is confined and there is leakage only through -2 harmonic or higher negative orders.

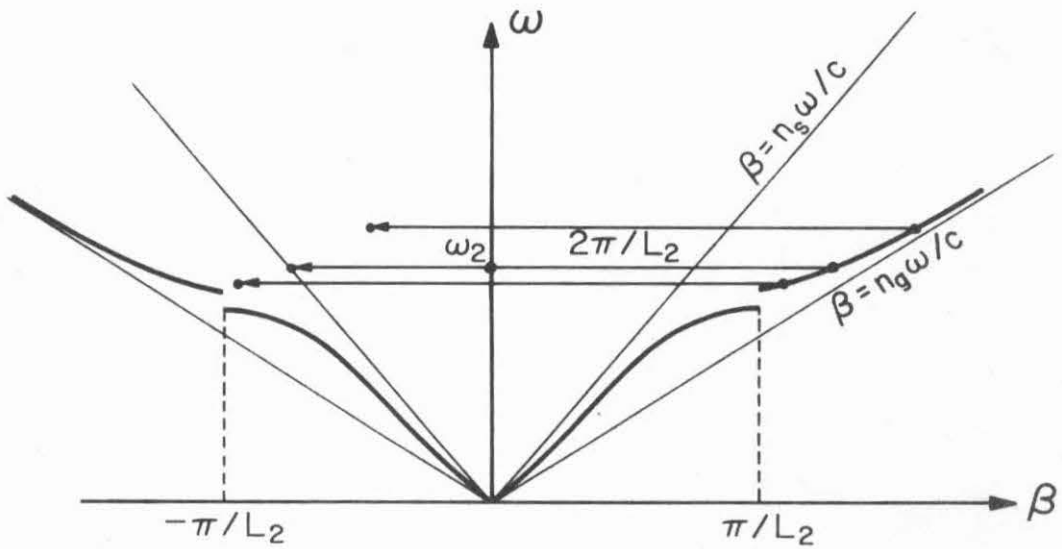

Fig. 11 Low pass filter. The condition for leakage via the -1 space harmonic (Eq. III-57) is satisfied only for $\omega > \omega_2$. For $\omega < \omega_2$ the -1 harmonic is confined and the light is transmitted (except at the stop band).

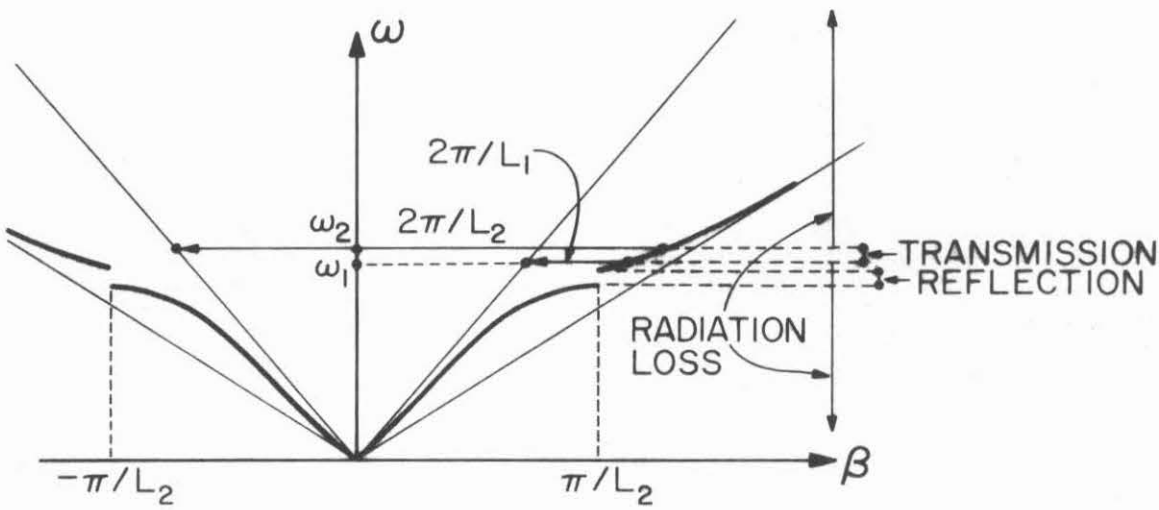

Fig. 12 Band-pass filter application of grating couplers. The period L_1 grating filters out by radiation loss frequencies $\omega < \omega_1$. The period L_2 grating filters out by radiation loss frequencies $\omega > \omega_2$, and also provides filtering by Bragg reflection in a thin reflection band. Light is transmitted without attenuation in the band $\omega_1 < \omega < \omega_2$.

derived in Chapter II.

For -1 order substrate coupling $n_a k < |\beta_{-1}| < n_s k$, hence α_{-1} in Eq. (II-20) is imaginary and we may define real positive q_{-1} :

$$\alpha_{-1} = iq_{-1} = i\sqrt{n_s^2 k^2 - \beta_{-1}^2} \qquad \text{(III-58)}$$

Equation (II-51) then changes into

$$a_{-1}(x) = A_{-1} e^{iq_{-1}(x+t)} \qquad x < -t \qquad \text{(III-59)}$$

while Eqs. (II-52) and (II-54) do not change. All the coefficients A_{-1}, B_{-1}, C_{-1}, F_{-1} calculated in Chapter II become complex. In particular (II-57,61) and (III-58) result in

$$A_{-1} = \frac{\frac{1}{2} n_{L1}^2 k^2 h_{-1} a}{h_{-1}(iq_{-1} + \gamma_{-1})\cos h_{-1} t - (h_{-1}^2 - iq_{-1}\gamma_{-1})\sinh_{-1} t} \cdot F \qquad \text{(III-60)}$$

To find out the power flow into the substrate along a distance $\Delta\ell$, integrate the x component of the Poynting vector in a plane parallel to the waveguide plane which is located in the substrate $x < -t$ (see Fig. 1).

$$\Delta P_{-1}^{out} = \frac{w}{2} \mathrm{Re} \int_0^{\Delta\ell} E_y H_z^* \, dz = \frac{w}{2\omega\mu} \mathrm{Re}\, i \int_0^{\Delta\ell} E_y \frac{\partial E_y^*}{\partial x} \, dz \qquad \text{(III-61)}$$

where the segment $\Delta\ell$ is short enough to neglect the decay of the mode power within its length, but long enough to include several periods of the periodic structure. We substitute in (III-61) a normalized mode

with excitation amplitude K (only the fundamental and -1 space harmonics are kept):

$$E_y \simeq K(a_o(x)\, e^{-i\beta_o z} + a_{-1}(x)\, e^{-i\beta_{-1} z}) \qquad \text{(III-62)}$$

and carry the integration over an integral number of periods, then Eq. (III-61) yields only one nonvanishing term:

$$\Delta P_{-1}^{out} = wK^2 \frac{q_{-1}|A_{-1}|^2}{2\omega\mu} \Delta\ell = -P_o \frac{q_{-1}}{2\omega\mu} |A_{-1}|^2 \Delta\ell \qquad \text{(III-63)}$$

where we used Eq. (III-59) for $a_{-1}(x)$. The minus sign in Eq. (III-63) indicates flow of power to the -x direction. $P_o = wK^2$ is (in the zero order approximation) the total power carried by the mode with excitation amplitude K (II-A14-A17). ΔP_{-1}^{out} is the amount of power coupled to the substrate by the -1 harmonic within the length $\Delta\ell$.

For a long segment $\Delta\ell$, we can no longer assume that the power P_o in the right hand side of Eq. (III-63) is constant. We assume that the differential decrease in the mode power ΔP_o is equal to the power coupled out to the substrate within the short segment $\Delta\ell$

$$-\Delta P_o = \Delta|P_{-1}^{out}| \qquad \text{(III-64)}$$

Substituting (III-63) in (III-64) we can write the result as a differential equation for P_o

$$dP_o = -P_o \frac{q_{-1}}{2\omega\mu} |A_{-1}|^2 d\ell \qquad \text{(III-65)}$$

whose solution is

$$P_o(\ell) = P_o(0)\, e^{-\eta_{-1}\ell} \qquad \text{(III-66)}$$

where (using (III-65,60,IIA9,A15))

$$\eta_{-1} = \frac{q_{-1}}{2\omega\mu}|A_{-1}|^2 = \frac{1}{2}\frac{n_{L1}^4 k^4 h_o^2}{\beta_o \gamma_o^2 t_{eff}} \cdot \frac{q_{-1} h_{-1}^2 a^2}{h_{-1}^2(\gamma_{-1}\cosh_{-1} t - h_{-1}\sinh_{-1} t)^2 + q_{-1}^2(h_{-1}\cosh_{-1} + \gamma_{-1}\sinh_{-1} t)^2} \quad \text{(III-67)}$$

For $2\pi/L$ big enough so that

$$\frac{h_{-1}^2}{q_{-1}^2} = \frac{n_g^2 k^2 - \beta_{-1}^2}{n_s^2 k^2 - \beta_{-1}^2} \simeq 1$$

is a good approximation, this expression can be simplified to

$$\eta_{-1} = \frac{1}{2}\frac{n_{L1}^4}{n_g^2 - n_a^2}\frac{k^2 h_o^2 (n_s^2 k^2 - \beta_{-1}^2)^{1/2} a^2}{\beta_o \gamma_o^2 t_{eff}} \quad \text{(III-68}$$

The direction in which the coupled light is emitted is:

$$\tan\theta = \frac{(n_s^2 k^2 - \beta_{-1}^2)^{1/2}}{\beta_{-1}} \quad \text{(III-69)}$$

For the special case of well confined mode and with the periodic perturbation being introduced by "symmetric" corrugation (Eq. II-5) we can reduce to a very simple working formula:

$$\eta_{-1} = 2\frac{\beta_{-1}}{n_g k}\tan\theta\frac{a^2}{t^3} \quad \text{(III-70)}$$

We calculate an example with

$n_g = 3.5$, $n_s = 3.3$, $t/\lambda = .566$, $L/t = 1.2$

Equation (III-70) leads to

$$\eta_{-1} = 8.6 \times \left(\frac{a}{t}\right)^2 \frac{1}{t}$$

For $\lambda = 10.6\mu m (t = 6\mu m)$ and $a/t = .05$

$$\eta_{-1} = 35.9 \text{ cm}^{-1}$$

so that corrugation of the waveguide surface in a length of $\ell = 280\mu$ is required to couple out $1/e$ of the power in the mode. The angle at which the light will be coupled into the substrate is calculated from Eq. (III-69)

$$\tan\theta = 1.47 \qquad \theta = 56°$$

The simple formulas derived above were found to agree closely with computer calculated coupling efficiencies [Ogawa 1973].

5. Bragg Reflection Devices

When the periodicity L is chosen so that:

$$m\frac{2\pi}{L} = 2\beta_o \tag{III-71}$$

then the propagation parameters of harmonic a_{-m} correspond to a mode of the unperturbed waveguide propagating in the negative direction:

$$\beta_{-m} = \beta_o - m\frac{2\pi}{L} = -\beta_o \tag{III-72}$$

Since both harmonics a_o and a_{-m} are resonant in the waveguide, they will have the same weight in the perturbed structure eigenmodes, and generation of one of them will necessarily involve generation of

the other with opposite phase velocity (see Fig. 4g). This property may be used in different applications which require reflection or feedback, like distributed mirrors, transmission stop band filters (which may be used as reflection band pass filters) and distributed feedback lasers.

We will calculate the structure eigenmodes and the stop band for the example of a TE mode. We cannot in this case use the first order approximation, and will resort to two-harmonic approximation (see Chapter II, Section 4).

$$\mathcal{E}(x,z) = a_0(x)\, e^{-i\beta_0 z} + a_{-1}(x)\, e^{-i\beta_{-1} z} \qquad \text{(III-73)}$$

where right in the Bragg condition

$$\beta_{-1} = -\beta_0 = -\frac{\pi}{L} \qquad \text{(III-74)}$$

Following the derivation in Section 4, Chapter II , we indicate that $a_0(x)$ and $a_{-1}(x)$ in the periodic layer satisfy the differential equation:

$$\left(\mathcal{I}\frac{d^2}{dx^2} + \mathcal{V}\right)\begin{pmatrix} a_{-1} \\ a_0 \end{pmatrix} = 0 \qquad \text{(III-75)}$$

where

$$\mathcal{V} = \begin{pmatrix} \delta^2 & f \\ f & \delta^2 \end{pmatrix} \qquad \text{(III-76)}$$

$$\delta^2 \equiv \delta_{-1}^2 = \delta_0^2 = \left(\frac{\pi}{L}\right)^2 - n_{L_0}^2 k^2 \qquad \text{(III-77)}$$

$$f = \frac{1}{2} n_{L1}^2 k^2 \qquad \text{(III-78)}$$

The solution of Eq. (III-75) in the region $0 < x < a$ (see Fig. 1) is

$$a_{-1} = \frac{1}{\sqrt{2}} (B_A \cos \lambda_A x + C_A \sin \lambda_A x + B_B \cos \lambda_B x + C_B \sin \lambda_B x) \quad \text{(III-79)}$$

$$a_o = \frac{1}{\sqrt{2}} (-B_A \cos \lambda_A x - C_A \sin \lambda_A x + B_B \cos \lambda_B x + C_B \sin \lambda_B x) \quad \text{(III-80)}$$

where λ_A^2, λ_B^2 are the eigenvalues of $\mathscr{V}$

$$\lambda_A^2 = \delta^2 - f \quad \text{(III-81)}$$

$$\lambda_B^2 = \delta^2 + f \quad \text{(III-82)}$$

The solution of the space harmonics in the other (uniform) layers is given by (II-81-83)

$$\begin{aligned} a_m(x) &= A_m e^{\alpha_m (x+t)} && x < -t \\ a_m(x) &= B_m \cos h_m x + C_m \sin h_m x && -t < x < 0 \\ a_m(x) &= F_m e^{-\gamma_m x} && x > 0 \end{aligned} \quad \text{(III-83)}$$

By properly matching the boundary conditions (see Section 4, Chapter II) one derives a set of homogeneous equations which may be reduced into

$$(\alpha \cos ht - h \sin ht) B_B - (\cos ht + \frac{\alpha}{h} \sin ht) \lambda_B C_B = 0 \quad \text{(III-84)}$$

$$(\gamma \cos \lambda_B a - \lambda_B \sin \lambda_B a) B_B + (\gamma \sin \lambda_B a + \lambda_B \cos \lambda_B a) C_B = 0 \quad \text{(III-85)}$$

and another identical set in which A replaces B .

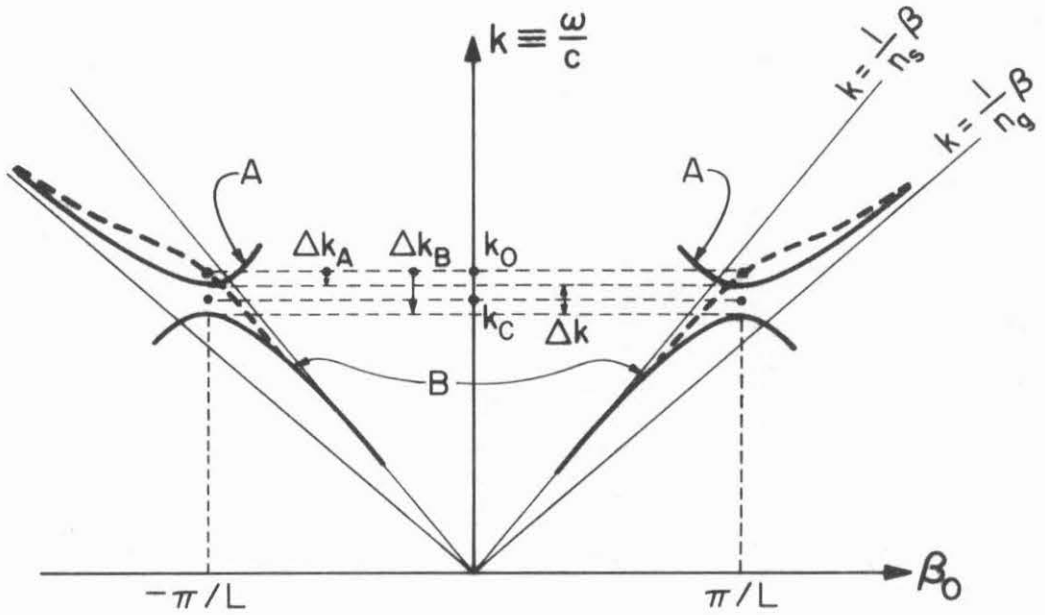

Fig. 13 Brillouin dispersion diagram for periodically perturbed waveguide. The broken line is the unperturbed guide dispersion curve. The perturbation opens a stop band Δk and shifts its center from k_o to k_c.

$$h^2 \equiv h_o^2 = h_{-1}^2 = n_g^2 k^2 - (\frac{\pi}{L})^2 \qquad \text{(III-86)}$$

$$\gamma^2 \equiv \gamma_o^2 = \gamma_{-1}^2 = (\frac{\pi}{L})^2 - n_a^2 k^2 \qquad \text{(III-87)}$$

$$\alpha^2 \equiv \alpha_o^2 = \alpha_{-1}^2 = (\frac{\pi}{L})^2 - n_s^2 k^2 \qquad \text{(III-88)}$$

For a nonvanishing solution of Eqs. (III-84),(III-85), the determinant of the coefficients must vanish:

$$(\alpha \cos ht - h \sin ht)(\gamma \sin \lambda_B a + \lambda_B \cos \lambda_B a) + \lambda_B(\cos ht + \frac{\alpha}{h} \sin ht)(\gamma \cos \lambda_B a - \lambda_B \sin \lambda_B a) = 0 \qquad \text{(III-89)}$$

Equivalent equation results also for the other eigenvalue λ_A

$$(\alpha \cos ht - h \sin ht)(\gamma \sin \lambda_A a + \lambda_A \cos \lambda_A a) + \lambda_A(\cos ht + \frac{\alpha}{h} \sin ht)(\lambda \cos \lambda_A a - \lambda_A \sin \lambda_A a) = 0 \qquad \text{(III-90)}$$

Equations (III-89), (III-90) are the dispersion equations for the frequency ω at $\beta = \pm\frac{\pi}{L}$. Equation (III-89) corresponds to the lower branch of the dispersion curve-curve B, and Eq. (III-90) to the upper branch-curve A (see Fig. 13). When the periodic perturbation layer vanishes, $a = 0$, both Eqs. (III-89) and (III-90) reduce to the dispersion relation of the unperturbed waveguide (compare to Eq. II-A8).

$$h^{(o)}(\alpha^{(o)} + \gamma^{(o)}) \cos h^{(o)}t - (h^{(o)2} - \alpha^{(o)}\gamma^{(o)}) \sin h^{(o)}t = 0 \qquad \text{(III-91)}$$

For $a \neq 0$ we may provide an approximate solution of Eqs. (III-89) and (III-90) by assuming that the thin layer "a" shifts the

frequency ω or the vacuum propagation constant $k \equiv \omega/c$ by a small amount Δk

$$k = k_o + \Delta k \tag{III-92}$$

where $k_o = \frac{\omega_o}{c}$ is the solution of Eq. (III-91) and k is the solution of Eq. (III-89) or (III-90). Then we expand all the parameters, h_1, γ_1, α_1, λ_A, λ_B to first order in Δk using Eqs. (III-77,78,81,82,86-88), and substitute in Eq. (III-89) or (III-90). The zero order parts ($\Delta k = 0$) of both equations turn out to be identically zero when Eq. (III-91) is used, while the first order parts result in:

$$\frac{\Delta k_{A,B}}{k_o} = \frac{\Delta\omega_{A,B}}{\omega_o} = p_{A,B}\, a \tag{III-93}$$

where

$$p_A = \frac{\frac{1}{2} n_{L1}^2 - (n_{L0}^2 - n_a^2)}{n_g^2 - n_a^2} \; \frac{h(o)^2}{\beta^2(\frac{1}{\alpha} + \frac{1}{\gamma}) + n_g^2 k_o^2 t} \tag{III-94}$$

$$p_B = \frac{-\frac{1}{2} n_{L1}^2 - (n_{L0}^2 - n_a^2)}{n_g^2 - n_a^2} \; \frac{h(o)^2}{\beta^2(\frac{1}{\alpha} + \frac{1}{\gamma}) + n_g^2 k_o^2 t} \tag{III-95}$$

The stop band width is then given by the difference of the two branches

$$\frac{\Delta\omega}{\omega_o} = \frac{\Delta\omega_A - \Delta\omega_B}{\omega_o} = \frac{n_{L1}^2}{n_g^2 - n_a^2} \; \frac{h(o)^2 a}{\beta^2(\frac{1}{\alpha} + \frac{1}{\gamma}) + n_g^2 k_o^2 t} \tag{III-96}$$

and the stop band center by

$$\frac{\omega_c}{\omega_o} = 1 + \frac{\Delta\omega_A + \Delta\omega_B}{2\omega_o} = 1 - \frac{n_{LO}^2 - n_a^2}{n_g^2 - n_a^2} \frac{h^{(o)2}_a}{\beta^2(\frac{1}{\alpha}+\frac{1}{\gamma}) + n_g^2 k_o^2 t} \qquad \text{(III-97)}$$

The analysis gave expressions for both the gap separation and a constant down shift of the dispersion curve (see Fig. 13). The two effects may be comparable in magnitude, and the shift effect may be significant in design of some devices.

For the "symmetrically corrugated" layer (Eqs. II-4,5) and well confined mode ($h_n^{(0)} \simeq n\pi/t$, $\frac{1}{\alpha}+\frac{1}{\gamma} \ll t$, $\beta \simeq n_g k$), Eqs. (III-96) and (III-97) simplify into:

$$\frac{\Delta\omega}{\omega_o} = \frac{n^2}{2\pi n_g^2} \frac{\lambda_o^2 a}{t^3} \qquad \text{(III-98)}$$

$$\frac{\omega_c - \omega_o}{\omega_o} = -\frac{n^2}{8n_g^2} \frac{\lambda_o^2 a}{t^3} \qquad \text{(III-99)}$$

where n is the order of the mode.

The perturbation analysis resulted, in addition to the expression for the band gap, an expression for the shift in the dispersion curve (see Fig. 13). This shift is caused by the "DC part" (n_{LO}^2) of the perturbation layer (Eqs. II-1,4). This term has exactly the effect of adding an effective dielectric layer $n_d^2 = n_{LO}^2 = (n_g^2 + n_a^2)/2$ of thickness a. The effect of such a layer is to increase the propagation constant by $\Delta\beta_n = \frac{\pi n^2}{4n_g} \frac{\lambda a}{t^3}$ (see Appendix III-C, and use Eq. III-C8). To find the effect of this layer on $\omega(\beta)$, one should use the relation

$$\frac{\partial\omega}{\partial t} = -\left.\frac{\partial\beta}{\partial t}\right|_\omega \Big/ \left.\frac{\partial\beta}{\partial\omega}\right|_t$$

With $\omega_c - \omega_o = \frac{\partial\omega}{\partial t} a$ $\qquad \Delta\beta_n = \frac{\partial\beta}{\partial t} a = \frac{\pi n^2}{4n_g} \frac{\lambda a}{t^3}$ and $\frac{\partial\beta}{\partial\omega} = \frac{n_g}{c}$ (III-99) gets confirmed by the independent analysis of Appendix III-C.

Consequently we point out that in designing a Bragg reflector for a specific frequency (given laser) one has to be aware of the fact that ω_o, defined by $\beta_o(\omega_o) = \pi/L$ (where $\beta_o(\omega)$ is the propagation constant of the waveguide without the perturbation layer, see Fig. 1, a=0), is not the center of the Bragg reflected frequency band, but it is rather ω_c, defined by $\beta_n(\omega_c) + \Delta\beta_n(\omega_c) = \pi/L$ (see Fig. 13). Equation (III-99) or in more general cases, Eqs. (III-97) or (III-C13), can be used to find ω_c. Notice that the shift $\omega_c - \omega_o$ is of the order of magnitude of the bandgap $\Delta\omega$.

The use of Eqs. (III-98,99) is demonstrated through the following example: n=1, $\lambda_o = 10.6\mu$, $n_g = 3.5$, $n_a = 1$, $t = 6\mu$, $a = 0.3\mu$, $L = 1.5\mu$. One gets from Eq. (III-98) $\Delta\omega/\omega_o = 2 \times 10^{-3}$ or $\Delta\lambda = 215\text{Å}$. From Eq. (III-99) one gets $(\omega_c - \omega_o)/\omega_o = 1.6 \times 10^{-3}$ or $\omega_c = 10.616\mu$.

The use of a Bragg reflector as a narrow band reflection filter has been demonstrated experimentally [Schmidt 1974] with light in the visible region. Fractional bandwidth $\Delta\omega/\omega = 3 \times 10^{-5}$ was achieved there.

We have to point out that expression (III-98) is different from the corresponding expression which was derived by coupled mode technique by Stoll [1973],

$$\frac{\Delta\omega}{\omega} = \frac{2\pi}{3} \frac{n_g^2 - n_a^2}{n_g^2} \left(\frac{a}{t}\right)^3 \qquad \text{(III-100)}$$

The reason for the difference is the use of different approximate assumptions. Although both Eqs. (III-98) and (III-100) were derived for

the case of well confined modes, it was assumed in deriving Eq. (III-98) that the perturbation layer, a , is thin enough so that the field variation across it is negligible and assumed constant, and first order expansion of the parameters in terms of "a" is valid. On the other hand, in deriving Eq. (III-100) the field was assumed to vanish at the surface and vary appreciably (linearly) across the perturbation layer $0 < x < a$. Indeed, when one repeats the coupled mode analysis, avoiding the last assumption, one gets for a well confined mode [Yariv 1973B]

$$\frac{\Delta\omega}{\omega} = \frac{2\pi}{3} \frac{n_g^2 - n_a^2}{n_g^2} \left(\frac{a}{t}\right)^3 \left[1 + \frac{3(\lambda_o/a)}{2\pi(n_g^2 - n_a^2)^{1/2}} + \frac{3(\lambda_o/a)^2}{4\pi^2(n_g^2 - n_a^2)}\right] \quad \text{(III-101)}$$

In the limit:

$$\lambda \gg \pi(n_g^2 - n_a^2)^{1/2} a \quad \text{(III-102)}$$

this expression reduces to Eq. (III-98), and in the opposite limit it reduces to Eq. (III-100), which indicates the limits of validity of each of these approximations. We also realize that at thick enough perturbation layer "a", the first order (in terms of a) solution of Eqs. (III-89,90) stops being valid and higher order solution is required. Condition (III-102) may be too restrictive when the mode is not well confined (the variation of the field across the perturbation layer is then smaller), hence Eqs. (III-96,97) may have somewhat larger scope of validity than indicated by inequality (III-102).

Finally, a few words may be in order concerning the two different approaches in solving Bragg reflection thin film devices. The

coupled mode approach solves the problem in terms of two (contradirectional) modes of the unperturbed (homogeneous) waveguide which are coupled by the periodic perturbation. This approach was first introduced by Kogelnik and Shank [1972], solving for the distributed feedback laser in a one-dimensional model. Following D. Marcuse's coupled mode analysis of perturbed dielectric slab waveguide [Marcuse 1969], A. Yariv et al. showed how to extend the one-dimensional coupled mode approach to the basically three-dimensional problem of Bragg-coupled dielectric-waveguide modes, and how to apply it to specific devices like Bragg reflectors and filters [Stoll 1973, Yariv 1973B] and oscillators [Yariv 1974B].

The approach taken in the present work is based on solving the problem in terms of the eigenmodes of the periodically perturbed waveguide which are Floquet-Bloch modes. To simplify the solution we truncated the Floquet mode series and left only two terms: zero and -1 order space harmonics (Eq. III-73) which are in resonance with the unperturbed waveguide modes. This makes the two approaches completely equivalent!

Claims made by S. Wang in several publications that the truncated Floquet-modes can bring additional results which are not evolving from the coupled modes approach was shown by Yariv and Gover to be unfounded [Yariv 1975, see there references to S. Wang]. The two approaches are equally valid, and fail at the same point when the perturbation is strong enough. At this failure point it is invalid to neglect higher order space harmonics (in one case) or the other unperturbed

waveguide modes (in the other case). In this case it might be more convenient to use the Floquet mode approach, basically following the procedure presented in Sect. 4 of Chapter II and solving the set of equations (II-85) truncated at some high integer. This must be usually done by numerical computation [Dabby 1972, Sakuda 1973, Peng 1974]. We should point out that the elaborate three-dimensional analysis of Sect. 4, Chapter II cannot be substituted in this case by a one-dimensional Floquet mode approximation (as used by S. Wang), since the transverse profile of the higher space harmonics is very different from that of the two fundamental space harmonics.

By matching boundary conditions at the ends of the Bragg reflection device and by introducing complex index of reflection at some of the layers, one can extend the analysis of this section to calculate different parameters of Bragg reflectors, filters and distributed feedback lasers. However, as mentioned above, one should not expect results which are different from the coupled mode formalism. This is well presented in closed form in Stoll [1973] and Yariv [1973B,1974B].

6. Analysis of General Coupling between Floquet Modes

The problems discussed in the previous sections involve different examples of coupling between waves in a periodic dielectric waveguide. We intend, in this section, to generalize the analysis of wave interaction in a periodic structure (using the Floquet-Bloch formalism approach) so that the analysis can be applied to any additional problems of wave coupling in periodic waveguides.

Before embarking on the detailed analysis, we review some of the general qualitative results of coupled-mode theory of wave interactions in dielectric waveguides [Marcuse 1969, Kogelnik 1972, Yariv 1973B, Stoll 1973]. These are descendants of Pierce's coupled mode formalism [Pierce 1954, Louisell 1960].

A detailed and unified coupled-mode formalism for waves in a dielectric waveguide is presented in Yariv [1973B]. Following this reference, some features of the coupled mode interaction (in the case of two waves) are illustrated in Fig. 14a,b. When the waves are not spatially phase matched (which means that there is a difference in their propagation constants $\Delta\beta = \beta^A - \beta^B \neq 0$), then there is recurrent power transfer between the two waves with small amplitude and short oscillation period (or short coherence length; the coherence length defined by Eq. (III-24) $\ell_c = \pi/\Delta\beta$, is the distance between adjacent minima and maxima in the power oscillation--see Fig. 14a). When the waves are nearly phase matched and codirectional, the amplitude of power oscillation and the coherence length both increase. It is possible to get full power transfer from one wave to the other when the waves are exactly phase matched (see Fig. 14a). The period of power oscillation then is maximum and is determined by the coupling coefficient.

The case of contradirectional phase matched coupling is described in Fig. 14b. In this case there is no power oscillation, and full power transfer is approached when the coupling length (ℓ) tends to infinity.

Let us now discuss wave coupling in periodic dielectric waveguides. There are two different approaches to this problem, and to avoid

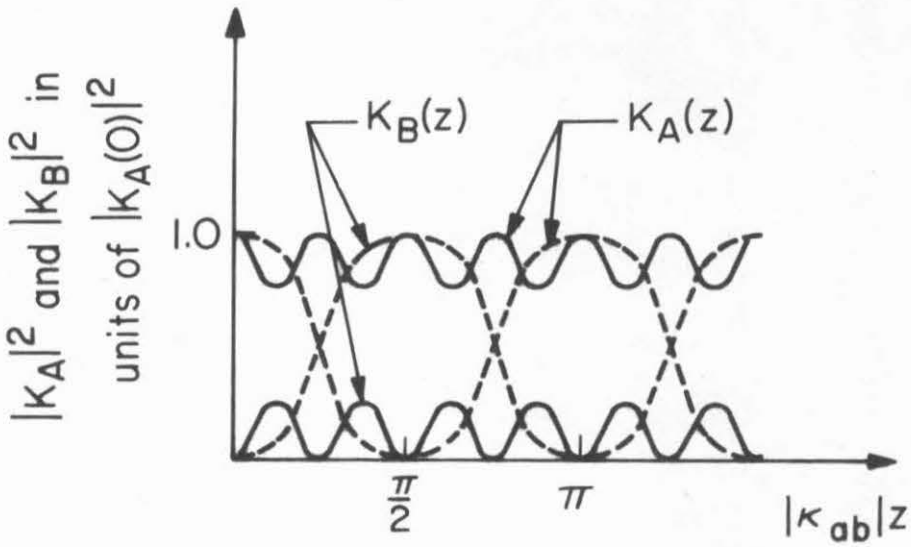

Fig. 14a The variation of the mode power in the case of codirectional coupling for phase-matched (broken line) and unmatched (continuous line) operation.

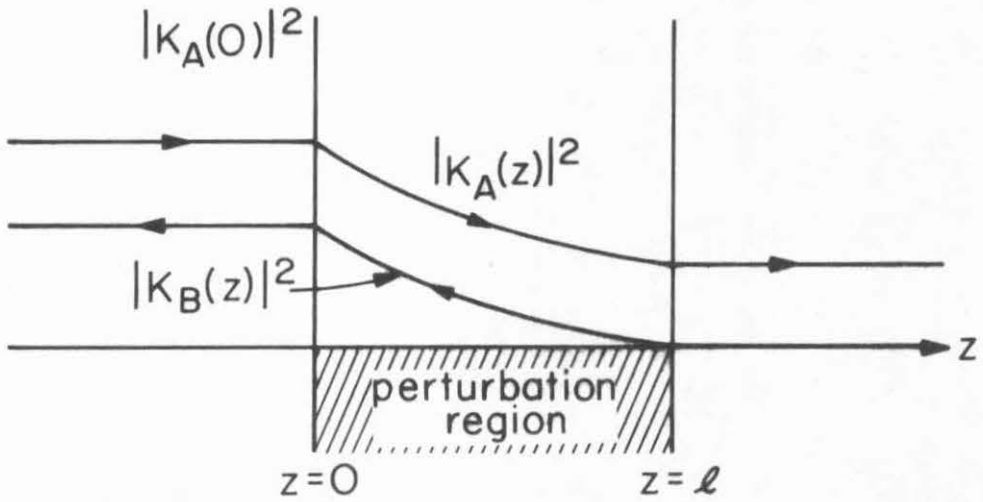

Fig. 14b The transfer of power from an incident forward wave $K_A(z)$ to a reflected wave $K_B(z)$ in the case of contradirectional coupling.

confusion we will briefly clarify their differences. In the usual approach [Yariv 1973B] the eigenmodes of the system, between which coupling takes place, are the eigenmodes of the waveguide without periodic perturbation (uniform waveguide). The periodic perturbation itself is viewed as the coupling perturbation which couples the modes of the uniform waveguide. For example: one TE mode can be coupled to another TE mode by a periodic perturbation of the linear dielectric constant. If the perturbation period L satisfies $2\pi/L = \beta^A - \beta^B$, full conversion between modes A and B can be attained [Marcuse 1969]. Coupling of a TE mode to a TM mode cannot happen unless an anisotropic perturbation in the dielectric constant is introduced (e.g., by the electrooptic effect or the magnetooptic effect). If we apply a uniform anisotropic perturbation, then coupling from TE to TM modes is possible, but full conversion will not be attained because the two modes are usually not phase matched (i.e., they have different propagation constant). This can be avoided if the anisotropic perturbation can be made periodic [Yariv 1973B, Tien 1972, Somekh 1972]. Alternatively, it is possible to add to the uniform anisotropic perturbation a periodic perturbation of the linear dielectric constant. In this case the coupling between the TE and TM mode will be considered to occur through two perturbations--the uniform anisotropic perturbation and the periodic perturbation.

In most of the present work a different approach is used. The eigenmodes between which coupling takes place are the Floquet-Bloch eigenmodes (and not the uniform waveguide modes). Thus different modes can be phase matched through their space harmonics (i.e., they may have

space harmonics with the same β), but by definition, they are not coupled to each other until another perturbation is introduced (like a uniform anisotropic perturbation in the case of electrooptic coupling). This was the approach used in the analysis of second harmonic generation and traveling wave interaction in a periodically perturbed dielectric waveguide (Sects. 2 and 3, respectively.) In this sense, the calculation of grating couplers (Sect. 4) and Bragg reflection (Sect. 5) are not coupled mode problems (since no perturbation in addition to the periodic perturbation is present). They can be viewed as an evaluation of the amplitude of the space harmonic amplitudes and the dispersion relation of the Floquet eigenmodes in special operation regimes.

In the following we present in a generalized form a coupled-mode treatment of Floquet eigenmodes. We specialize the treatment to the case of two-wave coupling and exact phase matching (extension to more general cases is straightforward). We pursue this analysis to the point where standard coupled mode equations are derived (III-118). Once this is done, one may proceed to solve these equations as in the standard coupled mode problem, and the interested reader is referred to Yariv [1973B], Louisell [1960].

As a preliminary step we proceed by proving an orthogonality theorem for Floquet-Bloch modes in a periodic dielectric waveguide.

A Floquet mode A in a structure with a period L can be written as:

$$\underline{\mathcal{E}}_A(x,z) = e^{-i\beta_o^A z}\, \underline{u}_A(x,z) \qquad \text{(III-103)}$$

where

$$\underline{u}_A(x,z+L) = \underline{u}_A(x,z) \qquad \text{(III-104)}$$

We show that this mode is orthogonal to any other mode $\underline{\mathcal{E}}_B(x,z)$ of the periodic waveguide if

$$\beta_o^B - \beta_o^A \neq n\,\frac{2\pi}{L} \qquad \text{(III-105)}$$

$$\iiint_{-\infty}^{\infty} dxdydz\ \underline{\mathcal{E}}_A^*(x,z)\cdot\underline{\mathcal{E}}_B(x,z) = \iiint_{-\infty}^{\infty} dxdydz\ e^{-i(\beta_o^A - \beta_o^B)z}\,\underline{u}_A^*(x,z)\cdot\underline{u}_B(x,z)$$

$$= \sum_{m=-\infty}^{\infty} \int_{mL}^{(m+1)L} dz\ e^{-i(\beta_o^A - \beta_o^B)z} \iint_{-\infty}^{\infty} dxdy\ \underline{u}_A^*(x,z)\cdot\underline{u}_B(x,z)$$

and using Eq. (III-104),

$$= \left[\sum_{m=-\infty}^{\infty} e^{-im(\beta_o^A - \beta_o^B)L}\right]\left[\int_0^L dz\ e^{-i(\beta_o^A - \beta_o^B)z} \iint_{-\infty}^{\infty} dxdy\ \underline{u}_A^*(x,z)\cdot\underline{u}_B(x,z)\right] \qquad \text{(III-106)}$$

$$\left(\beta_o^B - \beta_o^A \neq n\,\frac{2\pi}{L}\right) = 0$$

Contrary to homogeneous waveguides where translation symmetry results in an orthogonality of the modes' transverse profiles, in the periodic waveguide the mode profiles are not orthogonal and the orthogonality involves a three-dimensional integration. Independently of the overlap of the mode profiles, modes with unmatched propagation constants (Eq. III-105) are orthogonal because the first factor in Eq. (III-106) is proportional to a delta function $\delta(\beta_o^B - \beta_o^A - n\,\frac{2\pi}{L})$.

However, when the perturbation is small, also the mode profiles will be nearly orthogonal, which means that also the last coefficient in Eq. (III-106) is close to zero. Modes may be orthogonal even if they are phase matched ($\beta_o^B - \beta_o^A = n\,\frac{2\pi}{L}$) because of other symmetries in the system; for example, a TE mode is (vectorially) orthogonal to any TM mode even if they are phase matched.

We proceed to derive the coupled mode equation. From Maxwell equations (II-6,7) we get the wave equation for the electric field

$$\underline{\nabla} \times \underline{\nabla} \times \underline{E} - \omega^2 \mu \varepsilon \underline{E} = 0 \qquad \text{(III-107)}$$

where $\varepsilon = \varepsilon(\underline{r})$ is periodic with z .

The Floquet modes $\underline{\mathcal{E}}_p(x,z)$ are solutions of the homogeneous equation (III-107). We now introduce a perturbation to the system which causes coupling of the modes (for example an electrooptic or electromagnetic coefficient in the case of TE to TM mode coupling). The perturbation introduces polarization

$$\underline{P}_{pert}(x,z) = \underline{\chi}_{pert}(x)\, \underline{E}(x,z) \qquad \text{(III-108)}$$

which drives the wave equation:

$$\underline{\nabla} \times \underline{\nabla} \times \underline{E} - \omega^2 \mu \varepsilon \underline{E} = \omega^2 \mu\, \underline{P}_{pert} \qquad \text{(III-109)}$$

If the perturbation is small the solution of Eq. (III-109) can be written in terms of the eigenmodes

$$\underline{E} = \sum_p K_p(z)\, \underline{\mathcal{E}}_p(x,z) \qquad \text{(III-110)}$$

where $K_p(z)$ are slowly varying coefficients of the normalized modes

$\underline{\mathcal{E}}_p$.

We substitute Eq. (III-110) and (III-108) in (III-109) and get after some mathematical manipulation:

$$\sum_p K_p''(z)(\underline{\mathcal{E}}_p - \mathcal{E}_{pz}\hat{e}_z) + K_p'(z)(\frac{\partial}{\partial z}\underline{\mathcal{E}}_p - \hat{e}_z \times \underline{\nabla} \times \underline{\mathcal{E}}_p - \hat{e}_z \underline{\nabla} \cdot \underline{\mathcal{E}}_p) =$$

$$= -\omega^2 \mu \sum_p K_p(z) \underline{\chi}_{pert} \underline{\mathcal{E}}_p \quad . \qquad \text{(III-111)}$$

The z component of the first term is identically zero, the other components are neglected because we assume $K_p'(z)$ to vary with z much slower than the eigenmodes. We get:

$$\sum_p K_p'(z) \underline{L}_p(x,z) = -\omega^2 \mu \sum_p K_p(z) \underline{\chi}_{pert}(x) \underline{\mathcal{E}}_p(x,z) \qquad \text{(III-112)}$$

where

$$\underline{L}_p \equiv \frac{\partial}{\partial z}\underline{\mathcal{E}}_p - \hat{e}_z \times \underline{\nabla} \times \underline{\mathcal{E}}_p - \hat{e}_z \underline{\nabla} \cdot \underline{\mathcal{E}}_p =$$

$$= -\hat{e}_z \times \underline{\nabla} \times \underline{\mathcal{E}}_p + (\hat{e}_z \cdot \underline{\nabla})\underline{\mathcal{E}}_p - \hat{e}_z(\underline{\nabla} \cdot \underline{\mathcal{E}}_p) \qquad \text{(III-113)}$$

We assume that two modes which are excited in the waveguide $\underline{\mathcal{E}}_A(x,z)$ and $\underline{\mathcal{E}}_B(x,z)$ are nearly phase matched through an nth order space harmonic

$$\beta_o^B - \beta_o^A \simeq n \frac{2\pi}{L} \qquad \text{(III-114)}$$

We now multiply Eq. (III-112) by $\underline{\mathcal{E}}_A^*$ and $\underline{\mathcal{E}}_B^*$ in turn, and integrate over all space. Since $\underline{L}_p(x,z)$ satisfies Eqs.(III-103,104) the orthogonality theorem (Eq. III-106) can be extended to say that $\underline{\mathcal{E}}_A$ and

$\underline{\mathcal{E}}_B$ are orthogonal to any $\underline{L}_p$ ($p \neq A,B$) which is not phase matched to mode A or B (III-105). The result of the integration is

$$K'_A(z) \int_0^L dz \iint_{-\infty}^{\infty} dxdy\, \underline{\mathcal{E}}_A^*(x,z)\, \underline{L}_A(x,z) =$$

$$= -\omega^2 \mu\, K_B(z)\, e^{-i(\Delta\beta)_n z} \int_0^L dz\, e^{i(\Delta\beta)_n z} \iint_{-\infty}^{\infty} dxdy\, \underline{\mathcal{E}}_A^*(x,z)$$

$$\underline{\chi}_{pert}(x)\, \underline{\mathcal{E}}_B(x,z) \qquad \text{(III-115)}$$

$$(\Delta\beta)_n = \beta_o^B - \beta_o^A - n\,\frac{2\pi}{L} \qquad \text{(III-116)}$$

In deriving (III-115) we had to assume that $K'_A(z)$, $K_A(z)$ and $e^{-i(\Delta\beta)_n z}$ have negligible variation over one period L so that pulling them out of the integral is justified (for the last term this can be expressed as $|2\pi/(\Delta\beta)_n| \gg L$). Also we assumed that $\underline{\mathcal{E}}_A$ is orthogonal to $\underline{L}_B$ and $\underline{\mathcal{E}}_B$ is orthogonal to $\underline{L}_A$, and that the susceptibility $\underline{\chi}_{pert}$ does not couple the modes to themselves. The last two assumptions may not be satisfied in some cases, however, the extension to this case is straightforward, resulting in somewhat more complicated coupled wave equations (two terms are added to both sides of Eq. III-115).

The integrals on the left and right hand sides of Eq. (III-115) are constants (z independent). Hence, with the above assumptions and approximations, and in the special case of exact phase matching,

$$(\Delta\beta)_n = \beta_o^B - \beta_o^A - n\,\frac{2\pi}{L} = 0 \qquad \text{(III-117)}$$

Equation (III-115) and the corresponding equation for K_B' can be written in the form of the standard coupled mode equations

$$K_A'(z) = \kappa_{AB}\, K_B(z)$$
$$K_B'(z) = \kappa_{BA}\, K_B(z) \qquad \text{(III-118)}$$

where

$$\kappa_{AB} = \frac{-\omega^2\mu \int_0^L dz \iint_{-\infty}^{\infty} dxdy\, \underline{\mathcal{E}}_A^*(x,z)\, \underline{\underline{\chi}}(x)\, \underline{\mathcal{E}}_B(x,z)}{\int_0^L dz \iint_{-\infty}^{\infty} dxdy\, \underline{\mathcal{E}}_A^*(x,z) \cdot \underline{L}_A(x,z)} \qquad \text{(III-119)}$$

and κ_{BA} is given by exchanging A and B in Eq. (III-119).

We first proceed to develop the denominator of Eq. (III-119). We use Eq. (III-113) and the identity

$$\underline{\nabla}\cdot(\underline{\mathcal{E}}^* \times \underline{\mathcal{E}} \times \hat{e}_z) \equiv -\hat{e}_z(\underline{\mathcal{E}} \times \underline{\nabla} \times \underline{\mathcal{E}}^*) - \underline{\mathcal{E}}^*(\hat{e}_z \cdot \underline{\nabla})\underline{\mathcal{E}} + \underline{\mathcal{E}}^*\, \hat{e}_z(\underline{\nabla} \cdot \underline{\mathcal{E}}) \qquad \text{(III-120)}$$

to substitute the integrand:

$$\int_0^L \iint_{-\infty}^{\infty} dzdxdy\, \underline{\mathcal{E}}_A^* \cdot \underline{L}_A = \int_0^L \iint_{-\infty}^{\infty} dzdxdy[-\underline{\mathcal{E}}_A^* \cdot (\hat{e}_z \times \underline{\nabla} \times \underline{\mathcal{E}}_A) + \underline{\mathcal{E}}_A^*(\hat{e}_z \cdot \underline{\nabla})\underline{\mathcal{E}}_A - \underline{\mathcal{E}}_A^* \cdot \hat{e}_z(\underline{\nabla} \cdot \underline{\mathcal{E}}_A)] =$$

$$= \int_0^L \iint_{-\infty}^{\infty} dzdxdy[\hat{e}_z \cdot (\underline{\mathcal{E}}_A^* \times \underline{\nabla} \times \underline{\mathcal{E}}_A) - \hat{e}_z \cdot (\underline{\mathcal{E}}_A \times \underline{\nabla} \times \underline{\mathcal{E}}_A^*) - \underline{\nabla} \cdot (\underline{\mathcal{E}}_A^* \times \underline{\mathcal{E}}_A \times \hat{e}_z)] \qquad \text{(III-121)}$$

The third term can be shown to vanish:

$$\int_0^L \iint_{-\infty}^{\infty} dzdxdy\ \underline{\nabla}\cdot(\underline{\mathcal{E}}_A^* \times \underline{\mathcal{E}}_A \times \hat{e}_z) = \oiint_S ds\hat{n}\cdot(\underline{\mathcal{E}}_A^* \times \underline{\mathcal{E}}_A \times \hat{e}_z) = 0 \qquad \text{(III-122)}$$

S is the surface which surrounds the volume of integration, $\hat{n}$ is the unit normal vector to the surface. The integral of (III-122) vanishes at the surfaces $x = \pm\infty$ because $\underline{\mathcal{E}}_A(x = \pm\infty, z) = 0$. It vanishes at the surfaces $y = \pm\infty$ because $\underline{\mathcal{E}}_A$ is independent of y and the normal vectors at these two surfaces are opposite. It vanishes at the surfaces $z = 0, L$ because $\underline{\mathcal{E}}_A(x, z=L) = e^{-i\beta_0 L}\underline{\mathcal{E}}_A(x, z=0)$ (Eqs. III-103, 104) so that the integrand in Eq. (III-120) is the same on these two surfaces, and the integral vanishes because the normals are opposite on these two surfaces.

We substitute in Eq. (III-121) the magnetic field from Maxwell equation (II-6)

$$\int_0^L \iint_{-\infty}^{\infty} dzdxdy\ \underline{\mathcal{E}}_A^* \cdot \underline{\mathcal{L}}_A = -i\omega\mu \int_0^L \iint_{-\infty}^{\infty} dzdxdy\ \hat{e}_z\cdot(\underline{\mathcal{E}}_A^* \times \underline{\mathcal{H}}_A + \underline{\mathcal{E}}_A \times \underline{\mathcal{H}}_A^*)$$

$$= -4i\omega\mu \int_0^L dz \iint_{-\infty}^{\infty} dxdy\ \mathrm{Re}\ S_{zA} = -4i\omega\mu L P_A \qquad \text{(III-123)}$$

Here S_z is the z component of the Poynting vector and P_A is the total average z directed power carried by the mode A defined as:

$$P_A = \frac{1}{L}\int_0^L dz \iint_{-\infty}^{\infty} dxdy \ \mathrm{Re}\ S_{zA} \qquad \text{(III-124)}$$

Notice that the z component of the Poynting power is in general dependent on z. The definition (III-124) associates with the Floquet mode an average power flow in the z direction which is the significant physical quantity in this problem. It reduces to the conventional power definition of a waveguide mode when the periodic perturbation vanishes. An alternative form for (III-124) results when we substitute the Floquet expansion of the mode:

$$\underline{\mathscr{E}}_A(x,z) = \sum_m \underline{\mathscr{E}}_{A_m}(x)\, e^{-i\beta_m z} \qquad \text{(III-125)}$$

where $\beta_m = \beta_o + m\frac{2\pi}{L}$, and a similar equation for $\mathscr{H}_A(x,z)$. When the integration over z is performed in (III-124), the mixed harmonic terms vanish and we get:

$$P_A = \sum_m \iint_{-\infty}^{\infty} dxdy \ \mathrm{Re}\ S_{zA_m} \qquad \text{(III-126)}$$

where

$$S_{zA_m} = \frac{1}{2}\left[\underline{\mathscr{E}}_{A_m}(x) \times \underline{\mathscr{H}}_{A_m}(x)\right]_z \qquad \text{(III-127)}$$

Hence, the average z directed power of the mode defined by Eq. (III-124) is also the sum of the powers carried by the individual space harmonics.

We now go back to the expression for the coupling coefficient (Eq. III-119) and substitute in it the result (III-123). Let us assume that the modes are power normalized ($|P_A|/w$ = 1 watt per cm waveguide width, see Appendix II-A). In fact, if the perturbation is small, and most of

the power is carried by the fundamental harmonic, the normalization is given by Eq. (II-A14) for a TE mode or by Eq. (II-A33) for a TM mode. Assuming the mode propagates in the positive (+z) direction so that its power is positive $P_A/w = +1$ watt/cm, we get

$$\kappa_{AB} = -\frac{i\omega}{4L}\int_0^L dz \int_{-\infty}^{\infty} dx\, \underline{\mathcal{E}}_A^*(x,z)\, \underline{\underline{\chi}}_{pert}(x)\, \underline{\mathcal{E}}_B(x,z) \qquad \text{(III-128)}$$

An alternative expression for the coupling coefficient is achieved using Eqs. (III-103,104). Assuming $\beta_o^B - \beta_o^A = \frac{2\pi}{L}$ (the phase matching condition (III-117) satisfied in first order, $n = 1$) we get

$$\kappa_{AB} = -\frac{i\omega}{4L}\int_0^L dz\, e^{-i\frac{2\pi}{L}z} \int_{-\infty}^{\infty} dx\, \underline{u}_A^*(x,z)\, \underline{\underline{\chi}}_{pert}(x)\, \underline{u}_B(x,z) \qquad \text{(III-129)}$$

Still a third form results when we substitute the Floquet expansion of the modes (III-125):

$$\kappa_{AB} = -\frac{i\omega}{4}\sum_m \int_{-\infty}^{\infty} dx\, \underline{\mathcal{E}}_{A_m}^*(x)\, \underline{\underline{\chi}}_{pert}(x)\, \underline{\mathcal{E}}_{B_{m-1}}(x) \qquad \text{(III-130)}$$

which means that the coupling coefficient is proportional to the amount of overlap (through the susceptibility) of the space harmonics of mode A with the correspondingly phase matched (one order smaller) space harmonics of mode B. If we keep only terms up to first order we get:

$$\kappa_{AB} = -\frac{i\omega}{4}\int_{-\infty}^{\infty} dx[\underline{\mathcal{E}}_{A_o}^*(x)\, \underline{\underline{\chi}}_{pert}(x)\underline{\mathcal{E}}_{B_{-1}}(x) + \underline{\mathcal{E}}_{A_1}^*(x)\, \underline{\underline{\chi}}_{pert}(x)\underline{\mathcal{E}}_{B_o}(x)] \qquad \text{(III-131)}$$

Assuming $\underline{\underline{\chi}}_{pert}$ is a Hermitian matrix, and taking the Hermitian conjugate of Eq. (III-130) results in

$$\kappa_{AB} = -\kappa^*_{BA} \tag{III-132}$$

The solution of the coupled mode equations (III-118) is now straightforward. If $K_B(0) = 0$, we get

$$K_A(z) = K_A(0) \cos \kappa z \tag{III-133}$$

$$K_B(z) = - \frac{\kappa^*_{AB}}{\kappa_{AB}} K_A(0) \sin \kappa z \tag{III-134}$$

where

$$\kappa = |\kappa_{AB}| \tag{III-135}$$

which means that at phase matched codirectional coupling a complete power exchange between modes can take place at $z = \pi/2\kappa$ (Fig. 13a).

Notice that if one of the coupled modes has negative power ($\beta_o < 0$), then in the normalization step (Eq. III-123) we have to normalize the mode average power to -1 watt per cm waveguide width instead of 1 watt. This leads to

$$\kappa_{AB} = \kappa^*_{BA} \tag{III-136}$$

yielding hyperbolic solutions of the coupled mode equations (III-118). In this case we have phase matched contradirectional coupling (backward wave interaction) in which one wave decays in its propagation, and the other wave grows (possibly from zero) in the opposite direction (see Fig. 13b).

When the assumption $(\Delta\beta)_n = 0$ (III-117) is not made, and a slight mismatch is assumed, then in deriving (III-118) from (III-115) the two coupled equations (III-118) get extra oscillatory terms $e^{-i(\Delta\beta)_n z}$ and

$e^{i(\Delta\beta)_n z}$ respectively. This case leads to the oscillatory solution in Fig. 14a. For further discussion of the solutions of the standard coupled mode equations, the interested reader is referred to [Yariv 1973, Pierce 1954, Louisell 1960, Watkins 1958].

Finally we discuss the limits of the approximations used to derive the coupled mode equations. The first coefficient in Eq. (III-106) tends to the limit of a delta function at points $\beta_o^B - \beta_o^A = n\frac{2\pi}{L}$ when the structure is infinite ($-\infty < m < \infty$). When the structure is finite the summation is over the total number of periods $N = \ell/L$ where ℓ is the length of the structure. In this case, the coefficient is still a function with maxima at points $\beta_o^B - \beta_o^A = n\frac{2\pi}{L}$ but the peaks have finite width, $\Delta\beta = \frac{\pi}{NL} = \pi/\ell$.

In order for the orthogonality condition (Eq. III-106) to hold, the separation between unmatched modes p and p' (which satisfy Eq. III-105) should be

$$|\beta_o^p - \beta_o^{p'} - n\frac{2\pi}{L}| << \Delta\beta = \pi/\ell \qquad \text{(III-137)}$$

In deriving Eq. (III-115) we had to assume that $K_p(z)$ changes slowly in order to be able to use the orthogonality condition (Eq. III-106). We can now specify this requirement more quantitatively. The summation in Eq. (III-106) should be performed only on so many periods N within which $K(z)$ does not change appreciably, which means that in Eq. (III-137) we must substitute ℓ by π/κ (if $\pi/\kappa < \ell$):

$$|\beta_o^p - \beta_o^{p'} - n\frac{2\pi}{L}| << \kappa \qquad \text{(III-138)}$$

We should mention that it is possible to extend the analysis of this section to coupling of three or more waves. In this case, instead of doublets of phase matched space harmonics (Eqs. III-130,131) we get triplets of phase matched space harmonics. This is implicitly expressed in the previously derived equations (III-17,19). Those equations refer to the problem of phase matched second harmonic generation which is a special case of three-wave coupling.

In concluding this section we want to indicate an interesting by-product of the present analysis. We will show that it is consistent with the Pierce equation for the electric field induced in a slow wave periodic structure by a space charge current ("the circuit equation" [Pierce 1950])

$$E_1 = i \frac{\beta^2 \beta_1 K_1}{\beta_1^2 - \beta^2} I_1 \qquad \text{(III-139)}$$

where K_1, the interaction impedance is given by Eq. (III-28), β_1 is the propagation constant of the electromagnetic wave first order space harmonic in the absence of interaction, and β is the propagation constant of the external space charge current $I_1(z) = I_1 e^{-i\beta z}$ and of the induced field at the location of the (zero thickness) electron current ($\beta \simeq \beta_1$):

$$E_1(z) = E_1 e^{-i\beta z} \qquad \text{(III-140)}$$

Substitution of Eq. (III-28) into (III-139) gives

$$E_1 = i \frac{\beta^2 |\underline{\mathcal{E}}_{A1}(0)|^2}{2\beta_1^A [(\beta_1^A)^2 - \beta^2] P_A} I_1 \qquad \text{(III-141)}$$

where we specify here to a particular mode $\underline{\mathcal{E}}_A \cdot \underline{\mathcal{E}}_{A_1}(0)$ is the field

of the electromagnetic mode first order space harmonic (in the absence of interaction) at point $x = 0$ where the electron current passes. P_A is the total power of the mode, which is power normalized (Eqs. II-A30,A31).

On the other hand, in the present section we used a slightly different approach. An external current distribution

$$j_1(x,z) = j_1(x)\, e^{-i\beta z} \tag{III-142}$$

or the corresponding polarization

$$\underline{P}_{pert} = -\frac{i}{\omega}\,\underline{j}_1 \tag{III-143}$$

induces, through Eq. (III-109), the eigenmodes of the periodic waveguides. If for a particular mode $\underline{\mathcal{E}}_A$, $\beta_1^A \simeq \beta$, this mode will be predominantly excited and will grow with amplitude $K_A(z)$

$$\underline{E}(x,z) = K_A(z)\,\underline{\mathcal{E}}_A(x,z) \tag{III-144}$$

In particular, the synchronous space harmonic field will vary as

$$\underline{E}_1(x,z) = K_A(z)\,\underline{\mathcal{E}}_{A_1}(x,z) = K_A(z)\,\underline{\mathcal{E}}_{A_1}(x)e^{-i\beta_1^A z} \tag{III-145}$$

To find $K_A(z)$ we solve Eq. (III-109) in the same manner as before, using (III-143) instead of (III-108). An expression similar to (III-115) is readily attained

$$K_A'(z)\int_0^L dz \iint_{-\infty}^{\infty} dxdy\, \underline{\mathcal{E}}_A^*(x,z)\cdot\underline{L}_A(x,z) = i\omega\mu\, e^{-i(\Delta\beta)_1 z} \times \int_0^L dz\, e^{i(\Delta\beta)_1 z} \iint_{-\infty}^{\infty} dxdy\, \underline{\mathcal{E}}_A^*(x,z)\cdot\underline{j}_1(x,z) \tag{III-146}$$

where we assumed in (III-116) $n = 1$ (phase matching through first order space harmonic)

$$(\Delta\beta)_1 = \beta - \beta^A - \frac{2\pi}{L} = \beta - \beta_1^A \qquad \text{(III-147)}$$

Using (III-123) and substituting in the right hand side of (III-146) the Floquet expansion (III-125) and the definitions (III-142,147), we get the result that only the term with the first order space harmonic $\underline{\mathcal{E}}_{A_1}(x)\, e^{-i\beta_1^A z}$ does not vanish in the z integration, and Eq. (III-146) yields

$$K_A'(z) = -\frac{e^{-i(\Delta\beta)_1 z}}{4P_A} \int_{-\infty}^{\infty} dx\, \underline{\mathcal{E}}_{A_1}^*(x) \cdot \underline{j}_1(x) \qquad \text{(III-148)}$$

$$K_A(z) = i\,\frac{e^{i(\beta_1^A - \beta)z}}{4P_A(\beta_1^A - \beta)} \int_{-\infty}^{\infty} dx\, \underline{\mathcal{E}}_{A_1}^*(x) \cdot \underline{j}_1(x) \qquad \text{(III-149)}$$

Now substituting in (III-145) we find

$$\underline{E}_1(x,z) = i\,\frac{1}{4P_A(\beta_1^A - \beta)}\, \underline{\mathcal{E}}_{A_1}(x)\, e^{-i\beta z} \int_{-\infty}^{\infty} dx\, \underline{\mathcal{E}}_{A_1}^*(x) \cdot \underline{j}_1(x) \qquad \text{(III-150)}$$

or

$$\underline{E}_1(x) = \frac{i}{4P_A(\beta_1^A - \beta)}\, \underline{\mathcal{E}}_{A_1}(x) \int_{-\infty}^{\infty} dx\, \underline{\mathcal{E}}_{A_1}^*(x) \cdot \underline{j}_1(x) \qquad \text{(III-151)}$$

Assuming $\beta_1 \simeq \beta$ this can be written as

$$\underline{E}_1(x) = i\,\frac{\beta^2}{2\beta_1^A[(\beta_1^A)^2 - \beta^2]P_A}\, \underline{\mathcal{E}}_{A_1}(x) \int_{-\infty}^{\infty} dx\, \underline{\mathcal{E}}_{A_1}^*(x) \cdot \underline{j}_1(x) \qquad \text{(III-152)}$$

This result is a generalization of Pierce's equation (III-141) to the case of finite width and general transverse profile of the current. It includes transverse field as well as longitudinal field coupling. In the limit where the current is a zero thickness sheet at $x = 0$, and

$$\int_{-\infty}^{\infty} dx \, \underline{\mathcal{E}}_{A_1}^{*}(x) \cdot \underline{j}_1(x) = \underline{\mathcal{E}}_{A_1}^{*}(0) \, I_1 \qquad \text{(III-153)}$$

Equation (III-152) is identical to (III-141).

The confirmation of the Pierce equation (III-139) is of considerable interest to us, since it will be used extensively throughout this work. It is striking that the one-dimensional simple model and transmission line analogy originally used by Pierce [1950] provided expressions which agree well with a three-dimensional rigorous solution of the Maxwell equation.

A similar derivation of Floquet electromagnetic mode coupling to space charge wave can be found in a previous work of Barybin and Ter-Martirosian [1969].

Appendix III-A : Computation of Space Harmonics in a Periodic Asymmetric Dielectric Waveguide and the Effective Nonlinear Coefficient for Second Harmonic Generation

In the following definitions the left-hand side corresponds to notations used in the text while the right-hand side corresponds to notations used in the program.

Input

$n_g^{\omega} \rightarrow G(1)$	$n_g^{2\omega} \rightarrow G(3)$
$n_s^{\omega} \rightarrow Q(1)$	$n_s^{2\omega} \rightarrow Q(3)$
$k^{\omega}t \rightarrow K(1)$	$k^{2\omega}t \rightarrow K(3)$
$\beta^{\omega}t \rightarrow B(1)$	$\beta^{2\omega}t \rightarrow B(3)$
$t_{eff}^{\omega}/t \rightarrow T(1)$	$t_{eff}^{2\omega}/t \rightarrow T(3)$

These parameters can be calculated for any asymmetric waveguide using program 3 (Append. II-C). A TE mode is assumed.

Part 4:

This part calculates the propagation and profile parameters of the four space harmonics that are involved in the phase matched second harmonic generation (Eq. III-19):

$$a_n(x) = B_N \begin{Bmatrix} \cosh(h_N x) \\ \cos(h_N x) \end{Bmatrix} + C_N \begin{Bmatrix} -i \sinh(h_N x) \\ \sin(h_N x) \end{Bmatrix} \quad -t < x < 0$$

$$a_n(x) = A_N e^{\alpha_N(x+t)} \qquad x < -t$$

$$a_n(x) = F_N e^{-\gamma_N x} \qquad x > 0$$

where

N = 1	for	m = 0	frequency	ω
N = 2	for	m = 1	frequency	ω
N = 3	for	m = 0	frequency	2ω
N = 4	for	m = -1	frequency	2ω

$$h_N t = \sqrt{|n_g^2 k^2 - \beta_N^2|}\, t \rightarrow H(N)$$

$$\gamma_N t \rightarrow P(N)$$

$$\alpha_N t \rightarrow A(N)$$

(These parameters are defined in Eqs. II-20,21,23).

$$C_o^{\omega}\sqrt{\frac{\beta^{\omega}}{2\omega\mu}}\,\sqrt{t} = \sqrt{\frac{2t}{t_{eff}^{\omega}}} \rightarrow C(1) = \sqrt{\frac{2}{T(1)}}$$

$$C_1^{\omega}\sqrt{\frac{\beta^{\omega}}{2\omega\mu}}\;\frac{1}{f_{\omega}a\sqrt{t}} \rightarrow C(2)$$

$$C_o^{2\omega}\sqrt{\frac{\beta^{2\omega}}{4\omega\mu}}\,\sqrt{t} = \sqrt{\frac{2t}{t_{eff}^{2\omega}}} \rightarrow C(3) = \sqrt{\frac{2}{T(3)}}$$

$$C_{-1}^{2\omega}\sqrt{\frac{\beta^{2\omega}}{4\omega\mu}}\;\frac{1}{f_{2\omega}a\sqrt{t}} \rightarrow C(4)$$

$$B_o^{\omega} \sqrt{\frac{\beta^{\omega}}{2\omega\mu}}\sqrt{t} \rightarrow V(1) \qquad A_o^{\omega}\sqrt{\frac{\beta^{\omega}}{2\omega\mu}}\sqrt{t} \rightarrow E(1)$$

$$B_1^{\omega} \sqrt{\frac{\beta^{\omega}}{2\omega\mu}}\frac{1}{f_{\omega}a\sqrt{t}} \rightarrow V(2) \qquad A_1^{\omega}\sqrt{\frac{\beta^{\omega}}{2\omega\mu}}\frac{1}{f_{\omega}a\sqrt{t}} \rightarrow E(2)$$

$$B_o^{2\omega} \sqrt{\frac{\beta^{2\omega}}{4\omega\mu}}\sqrt{t} \rightarrow V(3) \qquad A_o^{2\omega}\sqrt{\frac{\beta^{2\omega}}{4\omega\mu}}\sqrt{t} \rightarrow E(3)$$

$$B_{-1}^{2\omega} \sqrt{\frac{\beta^{2\omega}}{4\omega\mu}}\frac{1}{f_{2\omega}a\sqrt{t}} \rightarrow V(4) \qquad A_{-1}^{2\omega}\sqrt{\frac{\beta^{2\omega}}{4\omega\mu}}\frac{1}{f_{2\omega}a\sqrt{t}} \rightarrow E(4)$$

(These parameters are defined in Eqs. (II-55-61) and (II-A9 A10,A12-A15).

The program goes through different schemes in the two different cases of trigonometric or hyperbolic solution inside the waveguide. It indicates a hyperbolic solution by typing O(N) (negative)

$$n_g^2 k^2 - \beta_N^2 \rightarrow O(N)$$

The program types the space harmonics propagation and profile parameters and the wave number mismatch $\Delta\beta = \beta^{2\omega} - 2\beta^{\omega} = 2\pi/L$.

Part 5:

This part calculates terms in the overlap integrals of the different space harmonic profiles.

$$U(1,I,M,N) = \left\{ \int_{-1}^{0} \sin[H_{(I)}u]\sin[H_{(M)}u]\sin[H_{(N)}u]du \right\} C(I)\ C(M)\ C(N)$$

$$U(2,I,M,N) = \left\{ \int_{-1}^{0} \cos[H_{(I)}u]\cos[H_{(M)}u]\cos[H_{(N)}u]du \right\} V(I)\ V(M)\ V(N)$$

$$U(3,I,M,N) = \{ \int_{-1}^{0} \sin[H(I)u]\cos[H(M)u]\cos[H(N)u]du \}\ C(I)\ V(M)\ V(N)$$

$$U(4,I,M,N) = \{ \int_{-1}^{0} \cos[H(I)u]\sin[H(M)u]\sin[H(N)u]du \}\ V(I)\ C(M)\ C(N)$$

$$U(5,I,M,N) = \{ \int_{-1}^{-1} e^{[A(I)+A(M)+A(N)](x+t)}\ dx \}\ E(I)\ E(M)\ E(N)$$

$$U(6,I,M,N) = U(1,I,M,N) + U(2,I,M,N) + U(3,I,M,N) + U(3,M,N,I) +$$

$$+ U(3,N,I,M) + U(4,I,M,N) + U(4,M,N,I) + U(4,N,I,M) +$$

$$+ U(5,I,M,N)$$

Part 6:

This part calculates the effective nonlinear coefficient. It types the two relevant overlap integrals

$$U(6,1,2,3) = [\int_{-\infty}^{0} a_0^{\omega}(x)\ a_1^{\omega}(x)\ a_0^{2\omega}(x)dx] \frac{1}{\sqrt{t}\ a\ f_{\omega}} \left(\sqrt{\frac{\beta^{\omega}}{2\omega\mu}}\right)^2 \sqrt{\frac{\beta^{2\omega}}{4\omega\mu}}$$

$$U(6,1,1,4) = \int_{-\infty}^{0} [a_0(x)]^2 a_{-1}^2(x)dx\ \ \frac{1}{\sqrt{t}\ a\ f_{2\omega}} \left(\sqrt{\frac{\beta^{\omega}}{2\omega\mu}}\right)^2 \sqrt{\frac{\beta^{2\omega}}{4\omega\mu}}$$

and the parameter D

$$D = 2U(6,1,2,3) + 4U(6,1,1,4)$$

from which the effective nonlinear coefficient d_{eff} may be found:

$$d_{eff} = dta\ f_{\omega} D$$

Parts 8,9

These parts calculate the profiles of the four space harmonics which are involved in the interaction; evaluates and types them for points: $x/t = -2,-1.9,-1.8,\cdots,0$.

$$W(1) = a_o^{\omega}(x) \sqrt{\frac{\beta^{\omega}}{2\omega\mu}} \sqrt{t}$$

$$W(2) = a_1^{\omega}(x) \sqrt{\frac{\beta^{\omega}}{2\omega\mu}} \frac{1}{f_{\omega} a \sqrt{t}}$$

$$W(3) = a_o^{2\omega}(x) \sqrt{\frac{\beta^{2\omega}}{4\omega\mu}} \sqrt{t}$$

$$W(4) = a_{-1}^{2\omega}(x) \sqrt{\frac{\beta^{2\omega}}{4\omega\mu}} \frac{1}{f_{2\omega} a \sqrt{t}}$$

The parts also calculate at the same time (by step summation) the overlap integrals:

$$Y(10) = \left[\int_{-2}^{0} a_o^{\omega}\, a_1^{\omega}\, a_o^{2\omega}\, dx\right] \frac{1}{\sqrt{t}\, a\, f_{\omega}} \left(\sqrt{\frac{\beta^{\omega}}{2\omega\mu}}\right)^2 \sqrt{\frac{\beta^{2\omega}}{4\omega\mu}}$$

$$Y(11) = \left[\int_{-2}^{0} (a_o^{\omega})^2\, a_{-1}^{2\omega}\, dx\right] \frac{1}{\sqrt{t}\, a\, f_{\omega}} \left(\sqrt{\frac{\beta^{\omega}}{2\omega\mu}}\right)^2 \sqrt{\frac{\beta^{2\omega}}{4\omega\mu}}$$

from which one can calculate

$$D = Y(10) + 4Y(11)$$

as a check to the calculation of parts 5,6.

LIST PROGRAM 4

2nd Harmonic Generation

```
4.01 LET R(X)=(EXP(X)+EXP(-X))/2.
4.02 LET S(X)=(EXP(X)-EXP(-X))/2.
4.1  SET L=B(3)-2*B(1).
4.11 SET K(2)=K(1).
4.12 SET G(2)=G(1).
4.13 SET Q(2)=Q(1).
4.14 SET B(2)=B(1)+L.
4.15 SET K(4)=K(3).
4.16 SET G(4)=G(3).
4.17 SET Q(4)=Q(3).
4.18 SET B(4)=B(3)-L.
4.19 SET N=1.
4.191 SET O(N)=(G(N)*K(N))↑2-B(N)↑2.
4.192 TO STEP 4.20 IF O(N)>0.
4.193 SET H(N)=SQRT(-O(N)).
4.194 TYPE O(N),H(N).
4.195 LINE.
4.1951 LINE.
4.196 TO STEP 4.21.
4.20 SET H(N)=SQRT((G(N)*K(N))↑2-B(N)↑2).
4.21 SET A(N)=SQRT(B(N)↑2-K(N)↑2*Q(N)↑2).
4.22 SET P(N)=SQRT(B(N)↑2-K(N)↑2).
4.23 SET N=N+1.
4.24 TO STEP 4.191 IF N<=4.
4.3  SET N=1.
4.31 SET C(N)=SQRT(2/T(N)).
4.32 SET V(N)=-H(N)/P(N)*C(N).
4.33 SET E(N)=-(H(N)/P(N)*COS(H(N))+SIN(H(N)))*C(N).
4.34 SET N=N+2.
4.35 TO STEP 4.31 IF N=3.
4.4  SET N=2.
4.401 TO STEP 4.462  IF O(N)<0.
4.41 SET E(9)=H(N)*(A(N)+P(N))*COS(H(N))-(H(N)↑2-A(N)*P(N))*SIN(H(N)).
4.42 SET V(N)=(A(N)*SIN(H(N))+H(N)*COS(H(N)))*V(N-1)/E(9).
4.43 SET C(N)=(A(N)*COS(H(N))-H(N)*SIN(H(N)))*V(N-1)/E(9).
4.46 SET E(N)=H(N)*V(N-1)/E(9).
4.461 TO STEP 4.47.
4.462 SET E(9)=H(N)*(A(N)+P(N))*R(H(N))+(H(N)↑2+A(N)*P(N))*S(H(N)).
4.463 SET C(N)=(A(N)*R(H(N))+H(N)*S(H(N)))*V(N-1)/E(9).
4.464 SET V(N)=(A(N)*S(H(N))+H(N)*R(H(N)))*V(N-1)/E(9).
4.465 DO STEP 4.46.
4.47  SET N=N+2.
4.48 TO STEP 4.401 IF N=4.
4.5  SET N=1.
4.51 TYPE G(N),Q(N),K(N),B(N),H(N),P(N),A(N),C(N),V(N),E(N).
 4.52 LINE.
4.53 SET N=N+1.
4.54 TO STEP 4.51 IF N<=4.
4.55 TYPE L,T(1),T(3).
4.56 LINE.
4.57 LINE.
4.58 LINE.
```

```
5.101 SET I=1.
5.102 SET M=1.
5.103 SET N=1.
5.12 SET Z(1,I,M,N)=H(I)+H(M)-H(N).
5.13 SET Z(2,I,M,N)=H(M)+H(N)-H(I).
5.14 SET Z(3,I,M,N)=H(I)+H(N)-H(M).
5.15 SET Z(4,I,M,N)=H(I)+H(M)+H(N).
5.151 SET J=1.
5.16 SET X(J)=(1-COS(Z(J,I,M,N)))/Z(J,I,M,N).
5.17 SET Y(J)=SIN(Z(J,I,M,N))/Z(J,I,M,N).
5.171 SET J=J+1.
5.172 TO STEP 5.16 IF J<=4.
5.18 SET U(1,I,M,N)=-1/4*(X(1)+X(2)+X(3)-X(4))*C(I)*C(M)*C(N).
5.19 SET U(2,I,M,N)=1/4*(Y(1)+Y(2)+Y(3)+Y(4))*V(I)*V(M)*V(N).
5.20 SET U(3,I,M,N)=-1/4*(X(4)-X(2)+X(1)+X(3))*C(I)*V(M)*V(N).
5.21 SET U(4,I,M,N)=1/4*(Y(3)+Y(1)-Y(4)-Y(2))*V(I)*C(M)*C(N).
5.22 SET U(5,I,M,N)=1/(A(I)+A(M)+A(N))*E(I)*E(M)*E(N).
5.25 SET N=N+1.
5.26 TO STEP 5.12 IF N<=4.
5.27 SET M=M+1.
5.28 TO STEP 5.103 IF M<=4.
5.29 SET I=I+1.
5.30 TO STEP 5.102 IF I<=4.
5.301 SET J=1.
5.31 SET I=1.
5.32 SET M=2.
5.33 SET N=3.
5.34 SET U(6,I,M,N)=U(1,I,M,N)+U(2,I,M,N)+U(3,I,M,N)+U(3,M,N,I).
5.35 SET U(6,I,M,N)=U(6,I,M,N)+U(3,N,I,M)+U(4,I,M,N)+U(4,M,N,I).
5.36 SET U(6,I,M,N)=U(6,I,M,N)+U(4,N,I,M)+U(5,I,M,N).
5.37 SET M=1.
5.38 SET N=4.
5.39 SET J=J+1.
5.40 TO STEP 5.34 IF J=2.

6.1 SET D=2*U(6,1,2,3)+4*U(6,1,1,4).
6.2 TYPE U(6,1,2,3),U(6,1,1,4),D.

7.1 DO PART 4.
7.2 DO PART 5.
7.3 DO PART 6.

8.01 SET N=1.




8.1 TO STEP 8.14 IF O(N)<0.
8.11 SET Z(10)=COS(X(10)).
8.12 SET Z(11)=SIN(X(10)).
8.13 TO STEP 8.16.
8.14 SET Z(10)=R(X(10)).
8.15 SET Z(11)=S(X(10)).
8.16 TO STEP 8.20 IF X(10)>-1.0.
8.17 SET W(N)=E(N)*EXP(A(N)*(X(10)+1)).
8.18 TO STEP 8.22.
8.20 SET W(N)=E(N)*Z(10)+C(N)*Z(11).
8.22 SET N=N+1.
8.221 TO STEP 8.1 IF N<=4.
8.23 SET Y(10)=Y(10)+W(1)*W(2)*W(3)*0.1.
8.24 SET Y(11)=Y(11)+W(1)↑2*W(4)*0.1.
8.25 TYPE W(1),W(2),W(3),W(4),Y(10),Y(11).
8.27 LINE .
8.28 LINE.

9.1 DO PART 4.
9.2 SET Y(10)=0.
9.3 SET Y(11)=0.
9.4 DO PART 8 FOR X(10)=-2(.1)0.0.
9.5 TYPE 2*Y(10)+4*Y(11).
```

```
*DO PART 4
        O(N) =        -6.406068
        H(N) =         2.53102114

        G(N) =         3.5
        Q(N) =         3.3
        K(N) =         3.55651981
        B(N) =        12.2252764
        H(N) =         2.34325031
        P(N) =        11.6965187
        A(N) =         3.42221989
        C(N) =         1.22979312
        V(N) =         -.246373573
        E(N) =         -.70883523

        G(N) =         3.5
        Q(N) =         3.3
        K(N) =         3.55651981
        B(N) =        12.7025302
        H(N) =         2.53102114
        P(N) =        12.194484
        A(N) =         4.85885573
        C(N) =         -.0167864274
        V(N) =         -.0167195898
        E(N) =        -9.13214633*10↑(-4)

        G(N) =         3.525
        Q(N) =         3.325
        K(N) =         7.11303961
        B(N) =        24.9278066
        H(N) =         2.69871914
        P(N) =        23.8914254
        A(N) =         7.87607256
        C(N) =         1.31652513
        V(N) =         -.148711578
        E(N) =         -.429815935

        G(N) =         3.525
        Q(N) =         3.325
        K(N) =         7.11303961
        B(N) =        24.4505528




        H(N) =         5.55419616
        P(N) =        23.3930374
        A(N) =         6.20213745
        C(N) =         -.0266232037
        V(N) =        -3.59543437*10↑(-5)
        E(N) =         -.0177609594

           L =          .4772538
        T(1) =         1.32240925
        T(3) =         1.15390934
```

Appendix III-B Computation of the Propagation Parameters of TM Modes in a Symmetric Waveguide and the Interaction Impedance

We calculate the TM mode parameters of a symmetric dielectric waveguide. This is used in order to calculate the interaction impedance of such a waveguide with periodic perturbation on its surface.

The dispersion relations of a TM mode in an asymmetric waveguide were derived in Appendix II-A. For symmetric waveguides they can be solved and the different propagation parameters can all be written as a function of the normalized propagation parameter ht. For even modes:

$$kt = \frac{(ht)}{(n_g^2 - n_a^2)^{1/2}} \left[1 + \frac{n_a^4}{n_g^4} \tan^2\left(\frac{ht}{2}\right)\right]^{1/2} \qquad \text{(III-B1)}$$

$$\beta t = \frac{n_a(ht)}{(n_g^2 - n_a^2)^{1/2}} \left[1 + \frac{n_a^2}{n_g^2} \tan^2\left(\frac{ht}{2}\right)\right]^{1/2} \qquad \text{(III-B2)}$$

$$\gamma t = \frac{n_a^2(ht)}{n_g^2} \tan\left(\frac{ht}{2}\right) \qquad \text{(III-B3)}$$

The equations for the odd modes are the same with the only change $\tan(ht/2) \rightarrow -\text{ctan}(ht/2)$. The effective mode width t_{eff} can then be found from equation (II-A32).

$$\frac{t_{eff}}{t} = \frac{(\bar{\gamma}t)^2 + (ht)^2}{(\bar{\gamma}t)^2} \left[\frac{1}{n_g^2} + \frac{(\gamma t)^2 + (ht)^2}{(\bar{\gamma}t)^2 + (ht)^2} \frac{2}{n_a^2 \gamma}\right] \qquad \text{(III-B4)}$$

When these parameters are found the interaction impedance can be evaluated using Eqs. (III-43,44).

The propagation parameters γt, kt, βt, t_{eff}/t and the normalized interaction impedances $\tilde{K}_{\pm 1}(0^+)$, $\tilde{K}_{\pm 1}(0^-)$ were computed by computer and hand calculator as a function of (ht) for different values of n_g, n_a. For $n_g = 3.5$, $n_a = 1$ the results are plotted in Figs. 15 to 18 and 9 as function of kt (or t/λ). The normalized interaction impedance $(\tilde{K}_{\pm 1}(0^{\pm}))$ defined by:

$$\tilde{K}_{\pm 1}(0^{\pm}) \equiv K_{\pm 1}(0^{\pm}) \Big/ \left(\frac{a^2}{\lambda w}\sqrt{\frac{\mu}{\varepsilon_o}}\right) \qquad \text{(III-B5)}$$

is given for these values of parameters by:

$$\tilde{K}_{\pm 1}(0^-) = 6.9125 \times 10^{-6} \frac{(h_o t)^2}{(\gamma_o t)^2 (kt)^2 (\beta_o t)(t_{eff}/t)} [(\beta_o t) \pm 29.747(\gamma_o t)]^2 \qquad \text{(III-B6)}$$

$$\tilde{K}_{\pm 1}(0^+) = 1.0373 \times 10^{-3} \frac{(h_o t)^2}{(\gamma_o t)^2 (kt)^2 (\beta_o t)(t_{eff}/t)} [(\beta_o t) \mp 2.4283(\gamma_o t)]^2 \qquad \text{(III-B7)}$$

The curves corresponding to these expressions are plotted in Fig. 9.

The listing of the computer calculation of kt, βt, γt and t_{eff}/t is also given in the end of the appendix.

The following notations in the text (left) correspond to notations in the program (right).

$ht \to h$	$t_{eff}/t \to t$
$kt \to k$	$n_g \to g$
$\beta t \to b$	$n_a \to a$
$\gamma t \to p$	

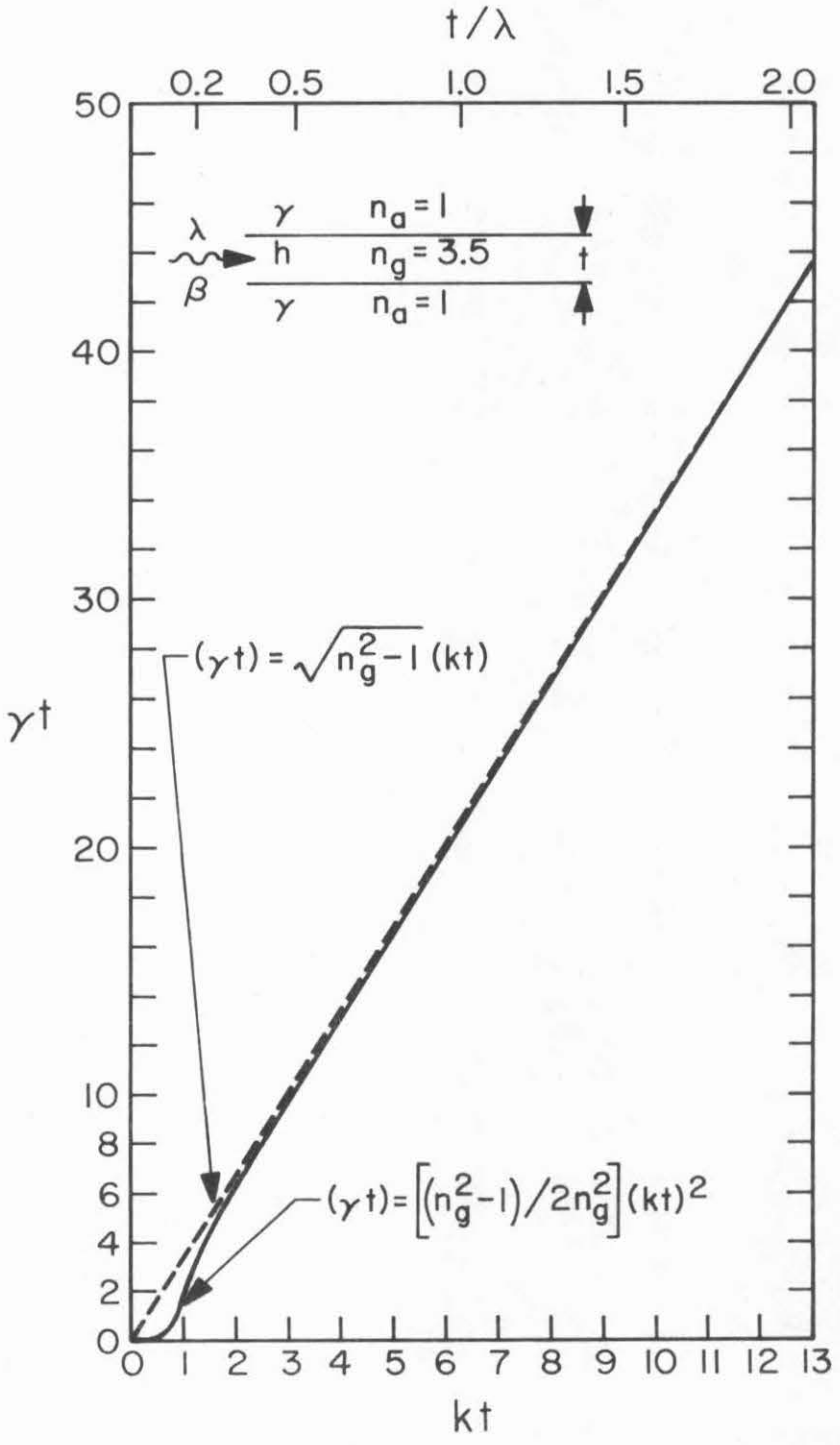

Fig. 15 Dispersion relation-TM 1st order mode (γt).

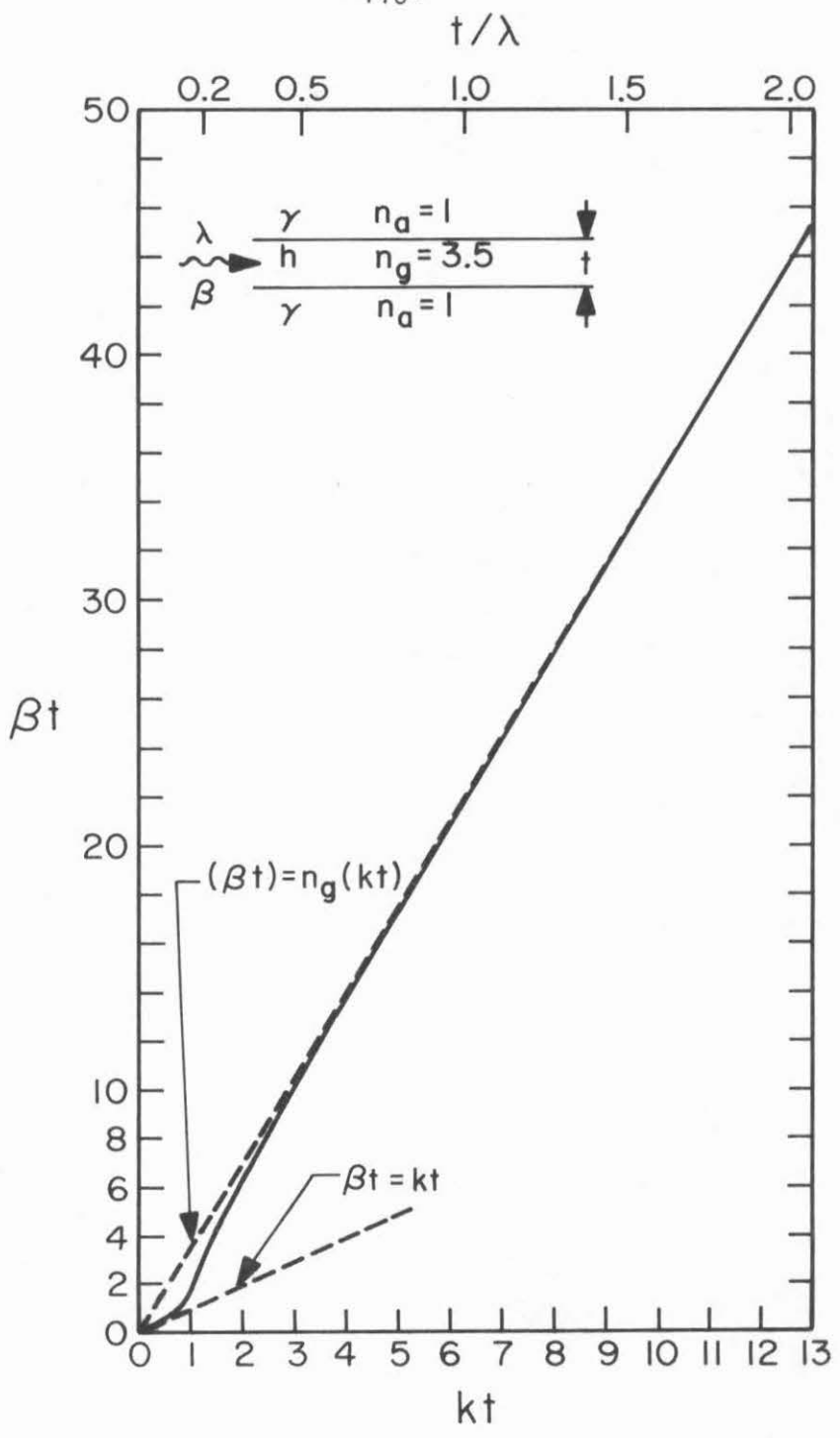

Fig. 16 Dispersion relation—TM 1st order mode (βt).

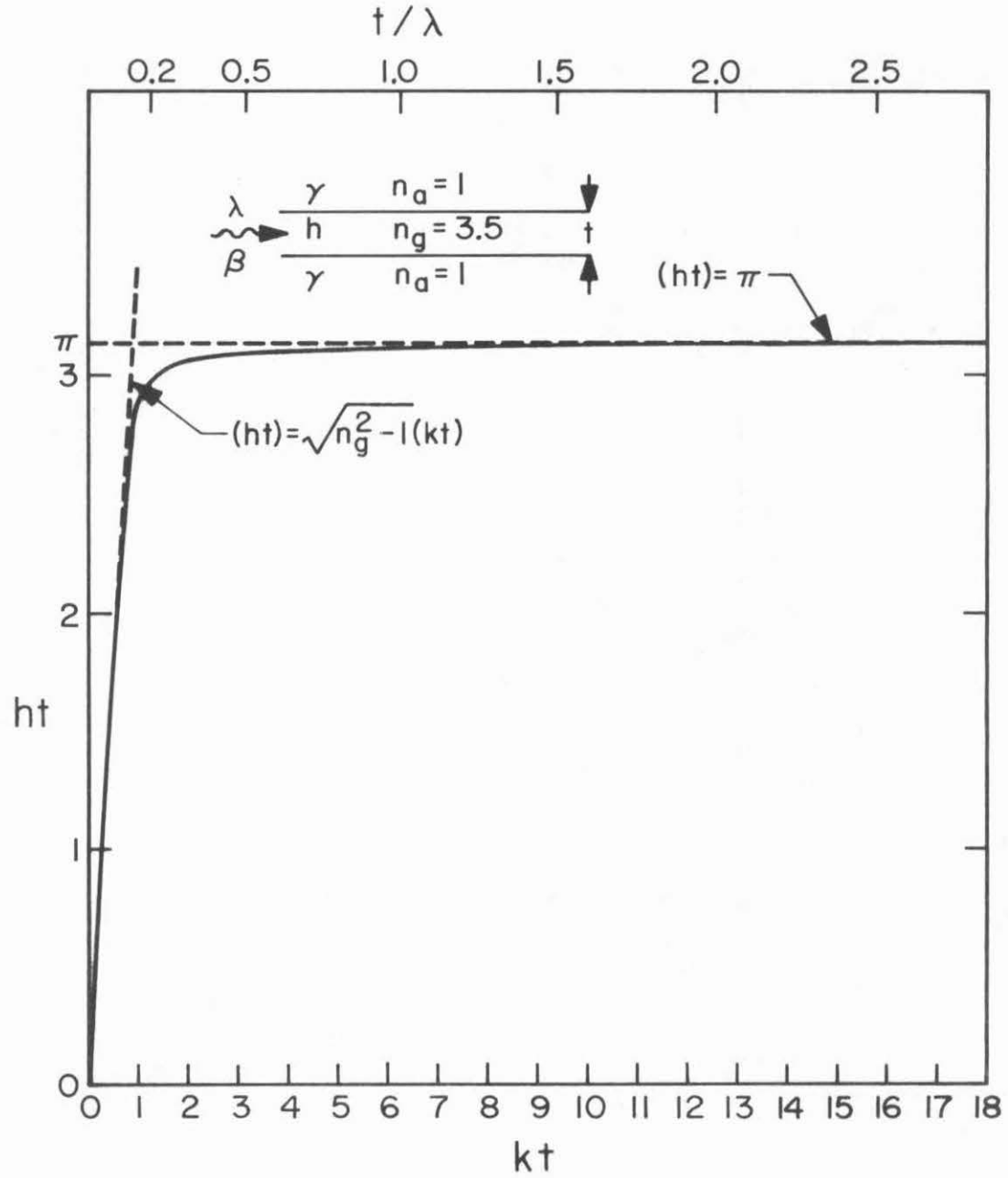

Fig. 17 Dispersion relation—TM 1st order mode (ht).

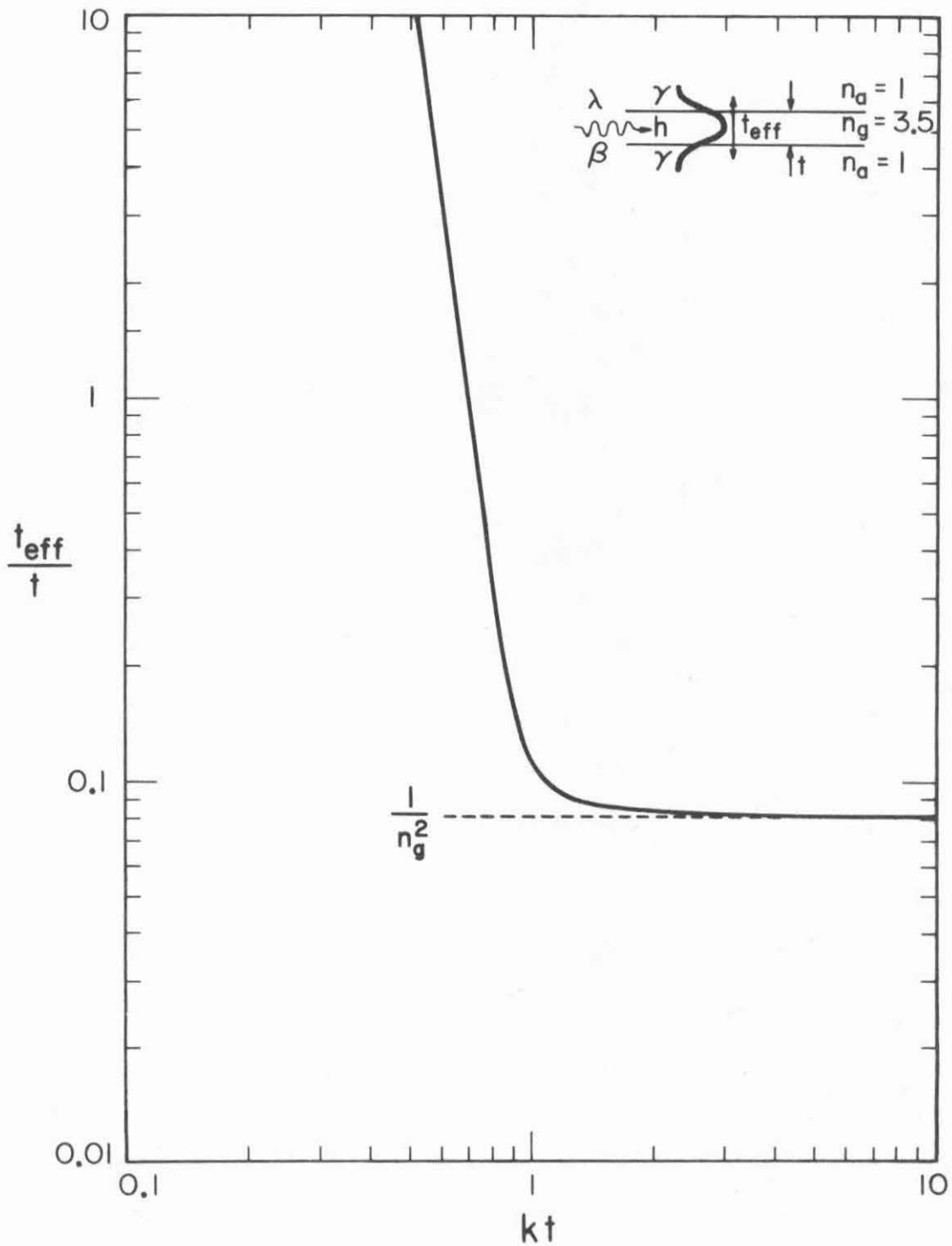

Fig. 18 The effective width (t_{eff}/t) of TM 1st order.

```
  1.1 Set n=sin(h/2)/cos(h/2).
  1.2 Set k=h*sqrt(1+n*n*a^4/c^4)/sqrt(g*c-a*a).
  1.3 Set b=h*sqrt(1+n*n*a*a/c/c)*a/sqrt(g*c-a*a).
  1.4 Set j=h*n*a*a/g/c.
  1.5 Set p=j*g*c/a/a.
  1.6 Set t=(1/c/g+(j*j+n*h)/(p*p+h*h)*2/j/a/a)*(p*p+h*h)/p/p.
  1.7 Set l=log(g*g/a/a)*b.
  1.8 Set m=j*(g^4-a^4)/g/g/a/a/2.
  1.9 Set i=305.6*a*a/(g*c+a*a)^4*h*h/(j*j*b*k*t).
  1.91 Set q=i*(l+m)^2.
  1.92 Set r=i*(l+m)^2.
  1.95 Type h,k,b,j,t,q,r  in form 3.
  *
  *1.96 TYPE h/k,*
  *1.96 TYPE b/k,k/k

  2.02 Line.
  2.03 Type g,a in form 1.
  2.04 Type form 4.
  2.05 Type form 2.
  2.1 Do part 1 for h=.1(.3)3.14.

  3.01 Line.
  3.02 Line.
  3.1 Do part 2 for a=1(.5)g-.1.

  4.01 Line.
  4.02 Line.
  4.1 Do part 3 for g=1.5(1)4.5.

  form 1:
       g=__._^     a=__.__

  form 2:
       h          k          b          j          t          q          r

  form 3:
  ********* ********* ********* ********* ********* ********* *********

  form 4:
       ========   ========

  *DO PART 2

       g= 3.50    a= 1.00
       ========   ========
       h          k          b          j          t          q          r
  1.000-01  2.981-02  2.982-02  4.065-04  1.955 06  1.783-03  2.037-03
            q/k =          .0598048602
            r/k =          .0683204564
  4.000-01  1.193-01  1.195-01  6.619-03  7.357 03  2.316-02  3.963-02
            q/k =          .1943094865
            r/k =          .3339347999
  7.000-01  2.086-01  2.096-01  2.086-02  7.209 02  5.624-02  1.506-01
            q/k =          .2693348849
            r/k =          .7212300777
  1.000 00  2.984-01  3.018-01  4.460-02  1.509 02  8.618-02  3.872-01
            q/k =          .2887747177
            r/k =          1.297309776
  1.300 00  3.863-01  3.966-01  8.067-02  4.329 01  9.767-02  6.511-01
            q/k =          .2515086959
            r/k =          2.191740922
  1.600 00  4.787-01  4.972-01  1.345-01  1.429 01  7.547-02  1.758 00
            q/k =          .1576582064
            r/k =          3.673091155
  1.900 00  5.701-01  6.100-01  2.169-01  4.900 00  1.946-02  3.621 00
            q/k =          .0341323566
```

```
            r/k =          6.35105766
 2.200 00  6.643-01  7.522-01  3.529-01  1.609 00  3.296-02  7.792 00
            q/k =           .049614765
            r/k =         11.7300973
 2.500 00  7.675-01  9.630-01  6.142-01  4.719-01  7.486-01  1.774 01
            q/k =           .975619163
            r/k =         23.1082303
 2.600 00  9.236-01  1.615 00  1.325 00  1.390-01  3.442 00  3.130 01
            q/k =          3.72642911
            r/k =         33.8892008
 3.100 00  3.743 00  1.273 01  1.217 01  8.283-02  2.694-01  1.629 00
            q/k =          .0773236516
            r/k =          .488729163
 3.140 00  9.997 01  3.359 02  3.219 02  8.167-02  4.470-04  2.810-03
            q/k =         4.65747351*10^(-6)
            r/k =         2.92742356*10^(-5)
*
*
*2.1DO PART 1 FOR H=2.5(.05)3.1
Eh?
*2.1 DO PART 1 FOR h=2.5(.05)3.1
*DO PART 2

     g= 3.50     e= 1.00
     =======     =======
     h          k          b          j          l          q          r
 2.500 00  7.675-01  9.630-01  6.142-01  4.719-01  7.486-01  1.774 01
            q/k =           .975619163
            r/k =         23.1082303
 2.550 00  7.871-01  1.042 00  6.631-01  3.806-01  1.056 00  2.027 01
            q/k =          1.34205192
            r/k =         25.7503403
 2.600 00  8.080-01  1.112 00  7.045-01  3.070-01  1.445 00  2.300 01
            q/k =          1.78817104
            r/k =         28.4925868
 2.650 00  8.309-01  1.197 00  8.023-01  2.482-01  1.913 00  2.579 01
            q/k =          2.30276509
            r/k =         31.0394925
 2.700 00  8.566-01  1.303 00  9.820-01  2.019-01  2.442 00  2.839 01
            q/k =          2.85067868
            r/k =         33.1447293
 2.750 00  8.868-01  1.438 00  1.132 00  1.661-01  2.981 00  3.041 01
            q/k =          3.36183816
            r/k =         34.2934269
 2.800 00  9.236-01  1.615 00  1.325 00  1.390-01  3.442 00  3.130 01
            q/k =          3.72642911
            r/k =         33.8892008
 2.850 00  9.722-01  1.859 00  1.564 00  1.190-01  3.702 00  3.049 01
            q/k =          3.80826229
            r/k =         31.3599272
 2.900 00  1.042 00  2.211 00  1.950 00  1.048-01  3.634 00  2.751 01
            q/k =          3.48764838
            r/k =         26.4065313
 2.950 00  1.154 00  2.759 00  2.506 00  9.507-02  3.153 00  2.229 01



            q/k =          2.73174596
            r/k =         19.3115203
 3.000 00  1.304 00  3.713 00  3.453 00  8.881-02  2.201 00  1.529 01
            q/k =          1.87216672
            r/k =         11.2094554
 3.050 00  1.858 00  5.742 00  5.433 00  8.503-02  1.201 00  7.755 00
            q/k =          .846466466
            r/k =         4.17474256
 3.100 00  3.743 00  1.273 01  1.217 01  8.283-02  2.694-01  1.629 00
            q/k =          .0773236516
            r/k =          .488729163
*2.1 DO PART 1 FOR h=2.7(.01)2.8
*DO PART 2
```

```
      g= 3.50     a= 1.00
      =======     =======
     h          k          b          j          t          q          r
 Error at step 2.1:  Eh?
 *2.1 DO PART 1 FOR h=2.7(.01)2.8
 *DO PART 2

      g= 3.50     a= 1.00
      =======     =======
     h          k          b          j          t          q          r
  2.700 00  8.566-01   1.303 00  9.820-01  2.019-01  2.442 00  2.639 01
          q/k =         2.85067866
          r/k =        33.1447293
  2.710 00  8.622-01   1.327 00  1.009 00  1.940-01  2.551 00  2.806 01
          q/k =         2.95880453
          r/k =        33.4689853
  2.720 00  8.680-01   1.353 00  1.036 00  1.865-01  2.660 00  2.929 01
          q/k =         3.06483917
          r/k =        33.7508048
  2.730 00  8.739-01   1.380 00  1.066 00  1.793-01  2.769 00  2.970 01
          q/k =         3.16795918
          r/k =        33.9854333
  2.740 00  8.802-01   1.408 00  1.099 00  1.725-01  2.876 00  3.007 01
          q/k =         3.26727542
          r/k =        34.167974
  2.750 00  8.866-01   1.438 00  1.132 00  1.661-01  2.981 00  3.041 01
          q/k =         3.36183616
          r/k =        34.2934265
  2.760 00  8.934-01   1.469 00  1.167 00  1.601-01  3.083 00  3.069 01
          q/k =         3.45063194
          r/k =        34.3567309
  2.770 00  9.004-01   1.503 00  1.203 00  1.543-01  3.181 00  3.093 01
          q/k =         3.53260343
          r/k =        34.3528609
  2.780 00  9.077-01   1.538 00  1.242 00  1.489-01  3.274 00  3.111 01
          q/k =         3.60664976
          r/k =        34.2768229
  2.790 00  9.155-01   1.575 00  1.282 00  1.438-01  3.361 00  3.124 01
          q/k =         3.67164065
          r/k =        34.1238005

  2.800 00  9.236-01   1.615 00  1.325 00  1.390-01  3.442 00  3.130 01
          q/k =         3.72642911
          r/k =        33.8892068
 *
```

Appendix III-C: Coupled Mode Formulation and the Effect of a Perturbation in the Transverse Structure of the Waveguide

Coupled mode analysis is a very useful tool in analyzing electromagnetic wave propagation in dielectric waveguides [Marcuse 1969,1972, 1973,1974; Yariv 1973B; Stoll 1974]. Some basic formulas which result from this theory will be presented in the present appendix for future reference and they will be subsequently used to derive a simple expression for the change in a mode propagation parameter due to a slight change in the transverse structure of the waveguide.

We wish to start from a general formula which can be reduced to different cases (TE,TM modes). The discontinuity of the normal electric field at the waveguide boundaries imposes some mathematical difficulty which may lead to inaccurate formulas in the case of TM modes [Stoll 1974]. We will use the carefully derived formulas from Marcuse [1974].

The problem in question is the coupling between the eigenmodes $\{\underline{\mathcal{E}}_n(x,y)\}$ of a general cross section dielectric waveguide due to the introduction of a small perturbation to the dielectric constant $(n^2 \rightarrow n^2 + \Delta n^2)$. The field of the perturbed waveguide can be given in terms of the unperturbed modes:

$$\underline{E} = \sum_n K_n(z)\, \underline{\mathcal{E}}_n(x,y)\, e^{-i\beta_n z} \qquad \text{(III-C1)}$$

where $K_n(z)$ is a slowly varying function. After some development of Maxwell equations assuming a solution (III-C1), a set of coupled mode equations is obtained for the coefficients $K_n(z)$ [Marcuse 1974]

$$\frac{dK_n}{dz} = \sum_m \kappa_{nm} K_m e^{i(\beta_n - \beta_m)z} \qquad \text{(III-C2)}$$

where

$$\kappa_{nm} = \frac{\omega\varepsilon_o}{4iP_n} \iint_{-\infty}^{\infty} \Delta n^2 [\underline{\mathcal{E}}^*_{nt} \cdot \underline{\mathcal{E}}_{mt} + \frac{\beta_n\beta_m}{|\beta_n\beta_m|} \frac{n^2}{n^2+\Delta n^2} \mathcal{E}_{mz} \mathcal{E}_{nz}] dxdy \qquad \text{(III-C3)}$$

where in our notation (which is somewhat different from that of Marcuse [1974]), P_n, the power of mode n, is a real number which can assume negative values (when $\beta_n < 0$). $\underline{\mathcal{E}}_{nt}$ is the transverse component of the mode, $\mathcal{E}_{nz}$ is the longitudinal component, and β_n is real (positive or negative).

In the case of a slab waveguide the modes $\underline{\mathcal{E}}_n$ are either TE or TM modes. For TE modes $\mathcal{E}_{nz} = 0$ and $\underline{\mathcal{E}}_{nt} = \mathcal{E}_{ny}\,\hat{e}_y$, then Eq. (III-C3) simplifies to

$$\kappa_{nm} = \frac{\omega\varepsilon_o}{4iP_n} \iint_{-\infty}^{\infty} \Delta n^2\, \mathcal{E}^*_{ny}\, \mathcal{E}_{my}\, dxdy \qquad \text{(III-C4)}$$

For the TM mode there is not much simplification. When $\Delta n^2 << n^2$ then to first order in the perturbation:

$$\kappa_{nm} = \frac{\omega\varepsilon_o}{4iP_n} \iint_{-\infty}^{\infty} \Delta n^2 [\mathcal{E}^*_{ny}\mathcal{E}_{my} + \frac{\beta_n\beta_m}{|\beta_n\beta_m|} \mathcal{E}^*_{nz}\mathcal{E}_{mz}] dxdy \qquad \text{(III-C5)}$$

We now want to specify to the case where $\Delta n^2 = \Delta n^2(x)$, viz. there is only a change in the transverse dependence of the dielectric waveguide. We solve Eq. (III-C2) with the initial condition $C_m(0) = \delta_{mn}$. Equation (III-C2) can be approximated by

$$\frac{dK_n}{dz} = \kappa_{nn} K_n \qquad \text{(III-C6)}$$

which indicates "coupling" of the mode with itself because of the perturbation. This allows us to find the change in the propagation parameter of the mode due to a slight change in the transverse structure of the waveguide. The solution of (III-C6) is

$$K_n(z) = K_n(0)\, e^{\kappa_{nn} z} \qquad \text{(III-C7)}$$

The field can approximately be written as

$$\underline{E}(z) = K_n(z)\, \underline{\mathcal{E}}_n(x)\, e^{-i\beta_n z} = K_n(0)\, \underline{\mathcal{E}}_n(x)\, e^{(\kappa_{nn} - i\beta_n) z} \qquad \text{(III-C8)}$$

which means that the effect of the perturbation is to change the propagation constant of the mode β_n by

$$\Delta\beta_n = i\kappa_{nn} \qquad \text{(III-C9)}$$

for a TE mode we have

$$\Delta\beta_n = \frac{\omega\varepsilon_0}{4P_n} \iint_{-\infty}^{\infty} \Delta n^2 |\mathcal{E}_{ny}|^2 \, dxdy \qquad \text{(III-C10)}$$

and for TM (and TE) modes

$$\Delta\beta_n = \frac{\omega\varepsilon_0}{4P_n} \iint_{-\infty}^{\infty} \Delta n^2 |\underline{\mathcal{E}}_n|^2 \, dxdy \qquad \text{(III-C11)}$$

These equations are useful in many problems of interest.

Let us find for instance the effect of adding a thin uniform dielectric layer n_d of thickness "a" on top of an asymmetric

dielectric slab waveguide. The eigenmodes of the (unperturbed) waveguide are derived in Appendix II-A. We specify to TE modes and to simplify the integration we assume a thin enough perturbation layer so that $\mathcal{E}_{ny}(x)$ does not change considerably through its thickness. So

$$\Delta\beta_n = \frac{(n_d^2 - n_a^2)k^2 \, aw}{4\omega\mu \, P_n} |\mathcal{E}_{ny}(0)|^2 \qquad \text{(III-C12)}$$

Using Eqs. (II-A4, A9, A15) and assuming that the modes are power normalized (II-A14, $P_n/w = 1$ watt) we obtain

$$\mathcal{E}_{ny}(0) = a_n(0) = -\frac{h_n}{\gamma_n}\sqrt{\frac{2}{t_{eff}}}\sqrt{\frac{2\omega\mu}{\beta_n}} \qquad \text{(III-C13)}$$

$$\Delta\beta_n = \frac{(n_d^2 - n_a^2)\, k^2 \, h_n^2 a}{\gamma_n^2 \, \beta_n t_{eff_n}} \qquad \text{(III-C14)}$$

This derivation is equivalent to the adiabatic approximation of Chapter II, Sect. 5 (Eq. II-93).

In the case of well confined modes this equation can be written more explicitly. Substituting $h_n \simeq n\pi/t$, $\beta_n \simeq n_g k$, $\gamma_n \simeq (n_g^2 - n_a^2)^{1/2} k$, $t_{eff_n} \simeq t$, we get

$$\Delta\beta_n = \frac{\pi n^2}{2n_g} \frac{n_d^2 - n_a^2}{n_g^2 - n_a^2} \frac{\lambda a}{t^3} \qquad \text{(III-C15)}$$

As a particular case, the effect of increasing the thickness of the waveguide by "a" ($n_d = n_g$) is found to be

$$\Delta\beta_n = \frac{\pi n^2}{2n_g} \frac{\lambda a}{t^3} \qquad \text{(III-C16)}$$

CHAPTER IV

MONOLITHIC SOLID STATE TRAVELING WAVE AMPLIFIER IN THE COLLISION DOMINATED REGIME

1. Introduction and Description of the Device

The application of periodic structures in traveling wave amplification was discussed briefly in Section 3 of Chapter III. We mentioned there the possibility of travelling wave interaction with drifting carriers in semiconductors, suggested new structures for the embodiment of this interaction (Fig. 8), and calculated the interaction impedance of those structures.

The possibility of solid state travelling wave interaction was discussed by several authors. A simple closed analysis of this interaction was first introduced by L. Solymar and E. A. Ash [1966]. This was a one-dimensional model coupled mode analysis based on earlier analyses of vacuum traveling wave tubes (TWT) presented by Pierce [1950]. Further elaboration of the analysis (three-dimensional) was presented by Masao Sumi [1966, 1967], who has also first demonstrated experimental evidence of this kind of interaction using n type InSb semiconductors [1968]. B. Zotter [1968] presented critical analysis of Sumi's derivations. Another demonstration of the effect in InSb and Ge at 4.2°K was presented by Freeman et al. [1973]. Further elaborations and different approaches are presented in Refs. [Nadan 1967, Hines 1969, Ettenberg 1970, Meyer 1970]. A related work is also that of Swanenburg, who analyzed [1973] and observed [1972] negative conductance in an interdigital electrode structure on a semiconductor surface.

In most of the proposals to date, the solid state amplifier is considered as a straightforward extension of the conventional travelling-wave tube amplifier, where a current conducting semiconductor is placed in close proximity to an external slow-wave circuit (helix or metallic meander line, electrically insulated from the semiconductor.) A different structure (Fig. 8) which was proposed before by Gover and Yariv [1974] is discussed here. This structure has the current and "the external circuit" integrated together in one monolithic semiconductor crystal. The external circuit in this case is really an integral part of the structure, consisting of a periodic perturbation of the dielectric constant (e.g., corrugation). The current conducting layer is placed right next to (or even at the same place as) the periodic layer. It can be introduced by diffusion or ion implantation (Fig. 8a) or epitaxial growth [Nakamura 1974] (Fig. 8b). The electromagnetic wave is guided in a dielectric waveguide and no external cavity is required. At very high frequency operation (millimeter waves, far infrared) where short (submicron) period of the periodic structure is essential, the present structures seem to be much more feasible for fabrication than the previous proposals, and in addition provide closer coupling between the current and the electromagnetic wave. Common use of semiconductor techniques, epitaxial growth, doping, lithography, and waveguiding indicates that these structures have also the advantage of compatibility with electronic and possibly future optical integrated circuits.

The design considerations of any of the structures of Fig. 8 can be aided by the understanding of wave propagation in periodic dielectric waveguides that we achieved in Chapters II and III. The field of the

first or -1 order space harmonic (which carries the interaction) is given by

$$a_{\pm 1}(x) = \begin{cases} a_{\pm 1}(0^+)e^{-(2\pi/L)x} & x > 0 \\ a_{\pm 1}(0^-)e^{(2\pi/L)x} & x < 0 \end{cases} \qquad \text{(IV-1)}$$

where $a_{\pm 1}(0^+) = F_{\pm 1}$, $a_{\pm 1}(0^-) = B_{\pm 1}$ (see Eqs. III-31÷36,42). Hence, effective interaction can occur only in a layer of distance $L/2\pi$ above or below the perturbation layer. For this reason and also to avoid undesirable heating, the conduction layer is confined in both structures (Fig. 8a,b) to thickness $d = L/2\pi$. As follows from the computer numerical calculation (Appendix III-B) for structures made of semiconductor with $n_g \simeq 3.5$, maximum interaction impedance is expected when the thickness of the waveguide is about one-seventh of the operating wavelength $t \simeq \lambda/7$ (see Fig. 9). This should be a preferable choice in the structure design.

In the following sections we present a one-dimensional coupled mode analysis of solid state travelling wave interaction in the collision dominated regime. This analysis proceeds along the same lines as presented by Solimar and Ash [1966] and previously by Pierce [1950] (without collisions and diffusion). However we add here (in Sections 4 and 5) the (non-negligible) effect of interaction with the asynchronous space harmonics, and we also apply (in Section 6) the analysis to a different structure (Fig. 8) whose interaction impedance was calculated in Section 3 of Chapter III.

2. The Dispersion Equation

The line of analysis is as follows : The z-component of a slow wave field component $E_{c_1}(z) = E_{c_1} e^{i(\omega t - \beta z)}$ modulates the drifting carriers

and generates a carriers' plasma wave. The plasma wave in turn induces electromagnetic wave in the corrugated waveguide. Calculating each of the processes separately and substituting them self-consistently results in the dispersion characteristic for the combined excitation travelling in the structure. The imaginary part of the propagation parameter β gives the expected gain.

From any linear plasma response theory it results that an external harmonic field E_{c_1} will induce a plasma current $J_{z_1} = J_1(\beta,\omega) \times e^{i(\omega t-\beta z)}$ which is proportional to the local field E_{z_1}:

$$J_{z_1} = i\omega\chi_p(\beta,\omega)E_{z_1} \qquad \text{(IV-2)}$$

χ_p is the plasma susceptibility to be found later. E_{z_1} is the local field which is experienced by the plasma:

$$E_{z_1} = E_{cz_1} + E_{pz_1} \qquad \text{(IV-3)}$$

where E_{pz_1} is the plasma space charge field given by Poisson equation (rationalized M.K.S. units system is used throughout the derivation):

$$-i\beta E_{pz_1} = \frac{1}{\varepsilon}\rho_1 = \frac{1}{\varepsilon}\frac{\beta}{\omega}J_{z_1} = \frac{i\beta}{\varepsilon}\chi_p E_{z_1} \qquad \text{(IV-4)}$$

where we also used the continuity equation $\beta J_{z_1} = \omega\rho_1$ to derive Eq. (IV-4). We hence obtain

$$E_{z_1} = \varepsilon_p^{-1} E_{c_1} \tag{IV-5}$$

$$\varepsilon_p \equiv 1 + \chi_p/\varepsilon \tag{IV-6}$$

where ε is the dielectric constant of the semiconductor apart from the free carrier plasma contribution.

Equations (IV-2,5,6) give:

$$J_{z_1} = \frac{i\omega\chi_p}{1 + \chi_p/\varepsilon} E_{cz_1} \tag{IV-7}$$

This last result represents the linear plasma response to an external field E_{cz_1}. It includes as a special case the plasma dispersion relation $\varepsilon_p \equiv 1 + \chi_p(\beta,\omega)/\varepsilon = 0$. This follows from requiring that J_{z_1} be finite with zero external field $E_c = 0$ in Eq. (IV-7), which can occur only when the denominator $1 + \chi_p/\varepsilon$ vanishes.

In order to complete the coupled mode analysis we need an expression for the electric field E_{cz_1} which would be induced in the structure (circuit) by an impressed current J_{z_1}. We use the heuristic Pierce expression (Eq. III-139):

$$E_{cz_1} = i \frac{\beta^2 \beta_1 K_1 S}{\beta_1^2 - \beta^2} J_{z_1} \tag{IV-8}$$

where $S = wd$ is the interaction cross section area, d is the thickness of the conducting layer, and w is the width of the waveguide. $\beta_1 = \beta_o + 2\pi/L$ is the propagation constant of the first order space harmonic in the absence of charge carriers (real number). K_1 is the

interaction impedance which is characteristic of the electromagnetic mode (Eq. III-128).

The dispersion equation of the coupled modes is obtained by imposing self-consistency on Eqs. (IV-7,8). This yields:

$$\frac{K_1 S\beta_1\beta^2\omega}{\beta^2-\beta_1^2}\ \frac{\chi_p(\beta,\omega)}{1+\chi_p(\beta,\omega)/\varepsilon} = 1 \qquad \text{(IV-9)}$$

When the coupling vanishes ($K_1 = 0$), the dispersion relation gives the four independent eigenmodes of the system, the electromagnetic waves $\beta = \pm\beta_1$ and two plasma space charge waves which are the solutions of $\varepsilon_p(\beta,\omega) = 0$. For small coupling, Eq. (IV-9) still has four solutions which are slightly different from the uncoupled modes. We can solve for the "electromagnetic-like" mode, using first order expansion of β : $\beta = \beta_1 + \Delta\beta$ (β_1 is the propagation constant of the electromagnetic component with no coupling). Assuming $\varepsilon_p(\beta,\omega)$ does not have a root near $\beta = \beta_1$ we get

$$\Delta\beta = \frac{1}{2} K_1 S\beta_1^2\omega \frac{\chi_p(\beta_1,\omega)}{1+\chi_p(\beta_1,\omega)/\varepsilon} \qquad \text{(IV-10)}$$

In particular:

$$\mathrm{Im}\beta = \mathrm{Im}\Delta\beta = \frac{1}{2} K_1 S\beta_1^2\omega \frac{\mathrm{Im}\chi_p}{|1+\chi_p/\varepsilon|^2} \qquad \text{(IV-11)}$$

This results in an exponential intensity gain constant of $g = 2\,\mathrm{Im}\beta$.

3. First Order Space Harmonic Interaction with Plasma Which is Described by the Macroscopic Equations

The analysis of Section 2 is very general in the sense that it does not impose any limitations on the plasma model as long as the linear relation

(IV-2) holds. In the present chapter we use the standard macroscopic (moment) description of the plasma, in which it is described by its first three velocity moments (carriers density n, average drift velocity v, and thermal velocity v_T or temperature T). The assumption is that in the collision dominated regime collisions are frequent enough to relax the carriers to a steady state distribution keeping the temperature of the plasma a meaningful parameter [Steele 1969, Stix 1972].

The velocity field v(z,t) of negative charge carriers is governed by the force equation (collisions included)

$$\frac{d}{dt} v(z,t) \equiv \frac{\partial v}{\partial t} + v \frac{\partial v}{\partial z} = - \frac{e}{m} E - \frac{D}{n\tau} \frac{\partial n}{\partial z} - \frac{v}{\tau} \qquad \text{(IV-12)}$$

where D is the carrier diffusion coefficient, τ is the collision relaxation time, and m the effective mass of the carrier.

The parameters E, v, and n can be broken into dc and small signal ac (harmonic) parts:

$$E(z,t) = E_o + E_1 e^{i(\omega t - \beta z)} \qquad \text{(IV-13)}$$

$$v(z,t) = v_o + v_1 e^{i(\omega t - \beta z)} \qquad \text{(IV-14)}$$

$$n(z,t) = n_o + n_1 e^{i(\omega t - \beta z)} \qquad \text{(IV-15)}$$

where $|E_1| << |E_o|, |v_1| << |v_o|, |n_1| << |n_o|$. When these are substituted in Eq. (IV-12) and the dc and ac parts are separated we get:

$$v_o = -\frac{e\tau}{m} E_o \tag{IV-16}$$

$$(i\omega - i\beta v_o + \frac{1}{\tau})v_1 = -\frac{e}{m} E_1 + i \frac{D}{n_o\tau} \beta n_1 \tag{IV-17}$$

The current density separates into two terms

$$J = -env = -en_o v_o - e(n_o v_1 + v_o n_1)e^{i(\omega t-\beta z)} = J_o + J_1 e^{i(\omega t-\beta z)} \tag{IV-18}$$

$$J_o = -en_o v_o \tag{IV-19}$$

$$J_1 = -e(n_o v_1 + v_o n_1) \tag{IV-20}$$

The dc equations (IV-16,19) constitute Ohm's law:

$$J_o = \sigma_o E_o \tag{IV-21}$$

$$\sigma_o = \frac{e^2 n_o \tau}{m} \tag{IV-22}$$

To find the ac susceptibility (IV-2) we use the continuity equation

$$\frac{\partial J}{\partial z} = e \frac{\partial n}{\partial t} \tag{IV-23}$$

which has an ac part:

$$n_1 = -\frac{\beta}{e\omega} J_1 \tag{IV-24}$$

Equations (IV-17,20,24) are then solved for J_1, in terms of E_1, resulting in:

$$\chi_p(\beta,\omega) = \frac{ie^2 n_o \tau/m}{(\beta v_o - \omega) + i[D\beta^2 - \tau(\beta v_o - \omega)^2]} \tag{IV-25}$$

We use the following definitions and identities: The plasma frequency

$$\omega_p = \left(\frac{n_o e^2}{\varepsilon m}\right)^{1/2} \tag{IV-26}$$

Thermal velocity is defined by:

$$v_T \equiv \frac{k_B T}{m} \tag{IV-27}$$

The Einstein relation is assumed to connect the diffusion coefficient D and the mobility μ ($v_o = \mu E_o$):

$$D = -\frac{k_B T}{e}\mu \tag{IV-28}$$

which, using (IV-16) can be written as

$$D = \frac{k_B T \tau}{m} \tag{IV-29}$$

or

$$D = v_T^2 \tau \tag{IV-30}$$

so we can write (IV-25) in the form

$$\chi_p(\beta,\omega) = \frac{i\omega_p^2 \varepsilon\tau}{(\beta v_o - \omega) + i\tau[v_T^2\beta^2 - (\beta v_o - \omega)^2]} \equiv$$

$$\equiv \frac{i\sigma_o}{(\beta v_o - \omega) + i\tau[v_T^2\beta^2 - (\beta v_o - \omega)^2]} \tag{IV-31}$$

and consequently the plasma dielectric constant response (IV-6) is

$$\varepsilon_p(\beta,\omega) = \frac{(\beta v_o - \omega) + i\tau[v_T^2\beta^2 + \omega_p^2 - (\beta v_o - \omega)^2]}{(\beta v_o - \omega) + i\tau[v_T^2\beta^2 - (\beta v_o - \omega)^2]} \tag{IV-32}$$

Eqs. (IV-31,32) can now be directly substituted in Eqs. (IV-9, 10) to result in the coupled modes dispersion equation and its first order solution respectively. But before doing this, it is interesting to check our results at some familiar limits. In the limit $\tau \to \infty$ Eq. (IV-32) reduces into

$$\varepsilon_p(\beta,\omega) = 1 + \frac{\omega_p^2}{v_T^2\beta^2 - (\beta v_o-\omega)^2} \qquad \text{(IV-33)}$$

which is the dielectric constant of collisionless drifting plasma including diffusion effect. When $v_T = v_o = 0$ we get the familiar expression

$$\varepsilon_p(\beta,\omega) = 1 - \frac{\omega_p^2}{\omega^2} \qquad \text{(IV-34)}$$

An interesting limit to check is the case of the conventional traveling wave tube amplifier. In this case $\tau = \infty$, $v_T = 0$ (zero temperature) and $v_o \approx \frac{\omega}{\beta_1} \neq 0$. We show in Appendix IV-A that in this case our results reduce to the conventional traveling wave equation (IV-A3,A8).

Coming back to our results in the general case ($\tau \neq \infty$, $T \neq 0$), we realize that $\varepsilon_p(\beta,\omega)$ (Eq. IV-32) does not have real roots. Hence $\varepsilon_p(\beta_1,\omega) \neq 0$ and we usually may use the first order solution of the dispersion equation (IV-10). Directly substituting (IV-31,32) in (IV-10) we get

$$\Delta\beta = \frac{1}{2} K_1 S \beta_1^2 \omega \; \frac{i\sigma_o}{(\beta_1 v_o-\omega) + i\tau\,[v_T^2\beta_1^2+\omega_p^2 - (\beta_1 v_o-\omega)^2]} \qquad \text{(IV-35)}$$

and particularly

$$\mathrm{Im}\beta = \frac{1}{2} K_1 \sigma_o S \beta_1^2 \omega \; \frac{\beta_1 v_o - \omega}{(\beta_1 v_o-\omega)^2 + \tau^2[v_T^2\beta_1^2 + \omega_p^2 - (\beta_1 v_o-\omega)^2]^2} \qquad \text{(IV-36)}$$

This can be written as

$$\mathrm{Im}\beta = \frac{Q_1\beta_1}{2} \frac{S_1 - 1}{(S_1-1)^2 + A^2[(S_1-1)^2 - B^2]^2} \qquad \text{(IV-37)}$$

where

$$S_1 \equiv \frac{\beta_1 v_o}{\omega} \equiv \frac{v_o}{v_{ph1}} \qquad \text{(IV-38)}$$

or when $\beta_o << \beta_1 \simeq 2\pi/L$:

$$S_1 = \frac{v_o}{c} \frac{\lambda}{L} \qquad \text{(IV-39)}$$

$$A \equiv \omega\tau \qquad \text{(IV-40)}$$

$$B \equiv [(v_T\beta_1/\omega)^2 + (\omega_p/\omega)^2]^{1/2} \qquad \text{(IV-41)}$$

and

$$Q_1 = S\beta_1 K_1 \sigma_o = wd\beta_1 K_1 \sigma_o \qquad \text{(IV-42)}$$

When the conducting layer thickness is $d = L/2\pi \simeq 1/\beta_1$, (see Fig. 8) it can be simplified to

$$Q_1 = wK_1\sigma_o \qquad \text{(IV-43)}$$

The curve describing the gain dependence on drift velocity [Eq. (IV-37)] is shown in Fig. 19. It is a typical S-shaped curve which turns from negative (attenuation) to positive (gain) at the beam-electromagnetic wave synchronism point $S_1 = 1$ providing gain at the Cerenkov condition (III-25,27).

Such an S shaped curve is typical to coupled wave problems with dissipation present [Barybin 1974]. When there is no dissipation an exact phase matching condition of the interacting waves can be found and the first order solution (IV-10) is not valid.

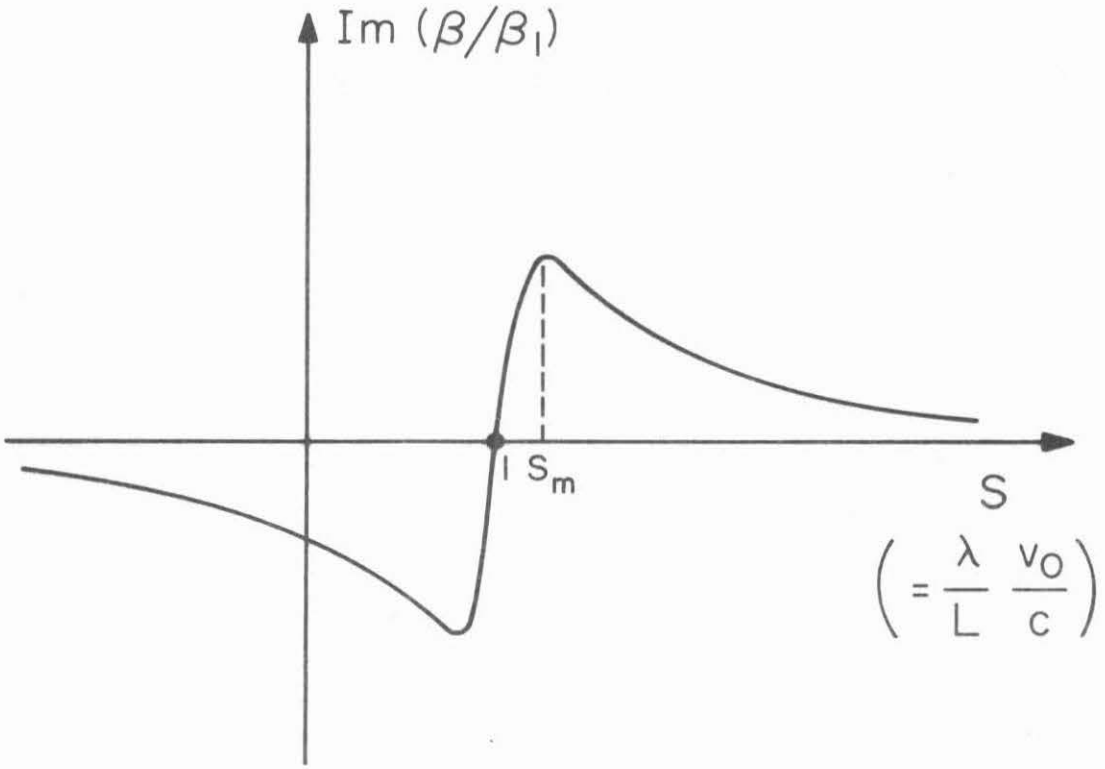

Fig. 19 Gain curve of the traveling wave amplifier in conditions $T \neq 0$ $\tau \neq \infty$. Describes the gain vs. drift velocity v_o (for fixed λ).

At a fixed frequency ω, the gain as given by Eq. (IV-37) reaches its extreme at

$$S_{1_m} - 1 = \pm \frac{2A^2B^2-1 + [(2A^2B^2-1)^2 + 12A^4B^4]^{1/2}}{6A^2} \qquad \text{(IV-44)}$$

The parameter $A^2B^2 = \tau^2(\omega_p^2 + v_T^2\beta_1^2)$ is independent of frequency. For cases when $2A^2B^2 >> 1$, Eq. (IV-44) simplifies into

$$S_{1_m} - 1 = B = \frac{[\omega_p^2 + (v_T\beta_1)^2]^{1/2}}{\omega} \qquad \text{(IV-45)}$$

and the maximum exponential gain constant is

$$g_{1_m} = 2(Im\beta)_1 = \frac{Q_1\beta_1}{B} = Q_1\beta_1 \frac{\omega\tau}{\tau[(v_T\beta_1)^2 + \omega_p^2]^{1/2}} \qquad \text{(IV-46)}$$

For the case when $2A^2B^2 << 1$, Eq. (IV-44) gives

$$S_{1_m} - 1 = AB^2 = \frac{\tau^2[(v_T\beta_1)^2 + \omega_p^2]}{\omega\tau} \qquad \text{(IV-47)}$$

and from Eq. (III-37)

$$g_{1_m} = \frac{Q_1\beta_1}{2} \frac{\omega\tau}{\tau^2[(v_T\beta_1)^2 + \omega_p^2]} \qquad \text{(IV-48)}$$

4. Backward Wave Interaction

The analysis of the interaction of drifting carriers with the electromagnetic wave via the -1 space harmonic is similar to the analysis of the first order space harmonic. However, since the -1 harmonic (with $\beta_{-1} < 0$) has opposite phase and group velocities, unlike the first order space harmonic, there is some physical difference between the two cases. The first is a backward wave interaction, and the second a forward wave interaction. Using Pierce's analysis, [Pierce 1950, p. 158] leads in the case of a -1 order space harmonic to an expression similar to Eq. (IV-8) with an opposite sign:

$$E_{cz_{-1}} = -i \frac{\beta^2 \beta_{-1} K_{-1} S}{\beta_{-1}^2 - \beta^2} J_{z_{-1}} \qquad \text{(IV-49)}$$

where

$$K_{-1} = \frac{|E_{-1}|^2}{2\beta_{-1}^2 |P|} \qquad \text{(IV-50)}$$

where K_{-1} is defined positive. This relation can also be obtained from our analysis in the end of Section 6 of Chapter III (which is correct for backward wave as well as forward wave) considering the fact that the mode power P_A is negative for wave with negative group velocity.

Correspondingly we get for the case of interaction with the -1 order space harmonic instead of (IV-37):

$$(Im\beta)_{-1} = - \frac{Q_{-1}\beta_{-1}}{2} \frac{S_{-1} - 1}{(S_{-1}-1)^2 + A^2[(S_{-1}-1)] - B^2]^2} \qquad \text{(IV-51)}$$

where S_{-1}, A, B, Q_{-1} are given by Eqs. (IV-38, 40-42) with -1 substituting the index 1. In the present convention $\beta_1 >> \beta_o > 0$, hence $\beta_{-1} \simeq -|\beta_1| < 0$. In this case we can write

$$S_{-1} = \frac{\beta_{-1} v_o}{\omega} \equiv \frac{v_o}{v_{ph-1}} \simeq - \frac{v_o}{c} \frac{\lambda}{L} \qquad \text{(IV-52)}$$

$$Q_{-1} = wd\beta_{-1} K_{-1} \sigma_o \simeq -wK_{-1}\sigma_o \qquad \text{(IV-53)}$$

$S_{-1} = \frac{\beta_{-1} v_o}{\omega}$ is positive only for negative electron velocities. The gain dependence on drift velocity is again given by the curve of Fig. 9. Gain starts when $S_{-1} > 1$ which means negative drift velocity v_o which exceeds the negative phase velocity $v_{ph-1} = \omega/\beta_{-1}$ of the -1 harmonic. Note that negative $(Im\beta)_{-1}$ corresponds to gain, since $\beta_{-1} < 0$.

The condition of maximum gain is given again by Eq. (IV-44) and the maximum gain is given by Eqs. (IV-46) or (IV-48) (where Q_1 is replaced by $|Q_{-1}|$).

5. Interaction of an Electromagnetic Mode via More than One Space Harmonic

The model of interaction via a single space harmonic may be too simplified for high temperature electron beam and low gain. An electromagnetic wave which is propagating in the periodic waveguide consists of an infinite number of space harmonics. Each of these (even if they are not synchronous with the current) modulates to some extent the drifting carriers with a different space charge wave. Each of the space charge waves interacts back with all of the space harmonics and through them amplifies or attenuates the total electromagnetic mode.

We will assume a model in which all the space harmonics except the main three: -1,0,1 , are neglected. Significant resonant interaction will take place only between a given space charge wave and its parent space harmonic. Our assumption is that the three interaction mechanisms may be treated independently, and the total gain of the electromagnetic mode will be given by the sum of the gains or attenuations due to the three coupling interactions.

The contribution of the interaction with the zero (fundamental) harmonic is always negative and should be related to the familiar free carrier loss. We can try to use the analysis of Section 3 to describe this interaction, substituting the subscript 0 instead of 1. The variable $S_o = \beta_o v_o/\omega$ is very small, of the order of 10^{-3} (notice $c/n_g < \omega/\beta_o < c$ and $v_o \lesssim 2 \times 10^7$ cm/sec), hence we may assume $S_o \simeq 0$. Substituting these into Eq. (IV-37) we get

$$(Im\beta)_o = -\frac{Q_o\beta_o}{2} \frac{1}{1 + \omega^2\tau^2[1 - (v_T\beta_o/\omega)^2 - (\omega_p/\omega)^2]^2} \qquad \text{(IV-54)}$$

where

$$Q_o = wd\beta_o K_o \sigma_o \tag{IV-55}$$

Since $v_T << c/n_g < \omega/\beta_o$, the diffusion term $(v_T\beta_o/\omega)^2$ is negligible, and we obtain

$$(Im\beta)_o = -\frac{Q_o\beta_o}{2} \frac{1}{1 + \omega^2\tau^2(1-\omega_p^2/\omega^2)^2} \tag{IV-56}$$

Following Eq.(III-28), the fundamental interaction impedance may be defined as

$$K_o = \frac{|E_{z_o}|^2}{2\beta_o^2 P} \tag{IV-57}$$

We assume a power normalized TM mode (II-A33) so that P/w = 1 watt/cm and $E_{z_o} = \mathcal{E}_z(0)$ (the structure of Fig. 8 or Fig. 20 is assumed here). Then Eqs. (IV-55-57) result in

$$(Im\beta)_o = -\frac{d\sigma}{4} |\mathcal{E}_z(0)|^2 \frac{1}{1 + \omega^2\tau^2(1-\omega_p^2/\omega^2)^2} \tag{IV-58}$$

These expressions for $(Im\beta)_o$ are formally very close to the standard equation for free carrier loss except for the spurious term ω_p^2/ω^2 . This term results from the use of the Poisson equation during the derivation. Equation (IV-58) cannot account for the total free carrier losses, since it results from a one-dimensional model with longitudinal field (E_z) only, while for the case of the fundamental space harmonic the transverse field (E_x) is non-negligible. These points are broadly discussed and accounted for in Appendix IV-B .

The fundamental space harmonic travels with about the speed of light in the medium and can never be synchronous with the carriers, therefore, it will always contribute attenuation to the traveling wave interaction of the mode. The first or -1 order space harmonics can be synchronous with the drifting carriers for correspondingly positive or negative drift velocities. The synchronous component will contribute gain to the total interaction, but then necessarily the other two components contribute loss.

Suppose we choose operation conditions with positive drift velocity, so that a synchronous interaction via the first order harmonic takes place; then interaction with the -1 harmonic is asynchronous and lossy. From Eq. (IV-52) it is apparent that for a fixed drift velocity

$$S_{-1} = -S_1 \tag{IV-59}$$

If the conditions are such that the first order harmonic interaction is on the maximum gain condition $S_1 = S_{1m}$ (Eqs. IV-44,45,47), then to find the -1 harmonic contribution we should substitute $S_{-1} = -S_{1m}$ in Eq. (IV-51). This results in

$$(Im\beta)_{-1} = \frac{|Q_{-1}||\beta_{-1}|}{2} \frac{1 + S_{1_m}}{(1+S_{1_m})^2 + A^2[(1+S_{1_m})^2 - B^2]^2} \tag{IV-60}$$

where

$$S_{1_m} > 1 \tag{IV-61}$$

Since $\beta_{-1} < 0$ this positive $(Im\ \beta)_{-1}$ corresponds to attenuation.

For the case when the -1 harmonic is synchronous and on maximum gain condition, an equation similar to (IV-60) holds for $(Im\beta)_1$ with

the subscript -1 substituted by 1 and the sign reversed (indicating loss contribution).

6. Discussion and Illustrative Examples

Until this point the discussion was quite general and did not specify the analysis to a particular structure (except for Eq. (IV-58) which is the fundamental free carrier loss in the specific structure in Fig. 20). At this point we direct our discussion to specific examples and calculate the interaction parameters for the structure in Fig. 8a, whose interaction impedances were calculated in Sec. 3 of Chapter III (Eq . III-44):

$$K_{\pm 1}(0^-) = \sqrt{\frac{\mu_o}{\varepsilon_o}} \frac{n_a^8}{2n_{LO}^4 n_g^4 (n_g^2+n_a^2)^2} \frac{h_o^2 a^2}{\gamma_o^2 \beta_o k t_{eff} w} \left(g_1 \beta_o \pm \frac{n_{L1}^2 n_{LO}^2}{n_a^4} \gamma_o \right)^2 \qquad \text{(IV-62)}$$

To calculate the interaction impedance of the fundamental harmonic we use Eqs. (III-A20, A21, A31)

$$\mathcal{E}_z(0) = - \frac{i h_o}{\omega \varepsilon_o n_g^2} \sqrt{\frac{2}{t_{eff}}} \sqrt{\frac{2\omega\varepsilon_o}{\beta_o}} \qquad \text{(IV-63)}$$

and Eq. (IV-57)

$$K_o = \sqrt{\frac{\mu}{\varepsilon_o}} \frac{2}{n_g^4} \frac{h_o^2}{k\beta_o^3 t_{eff} w} \qquad \text{(IV-64)}$$

Eq. (IV-58) is then explicitly given by

$$(\mathrm{Im}\beta)_o = \sqrt{\frac{\mu}{\varepsilon_o}} \sigma d \frac{1}{n_g^4} \frac{h_o^2}{k\beta_o t_{eff}} \frac{1}{1 + \omega^2\tau^2(1-\omega_p^2/\omega^2)^2} = \qquad \text{(IV-65)}$$

$$= \frac{d\omega_p^2 \omega\tau}{n_g^2 c^2} \frac{(h_o t)^2}{(kt)^2(\beta_o t)(t_{eff}/t)} \frac{1}{1 + \omega^2\tau^2(1-\omega_p^2/\omega^2)^2}$$

The maximum value of K_1 was numerically computed in Appendix III-B for the first order mode in a symmetric waveguide $n_g = 3.5$ $n_a = 1$, and was found to be (Eq. III-50)

$$K_1(0^-) = 0.272 \frac{a^2}{\lambda w}\sqrt{\frac{\mu}{\varepsilon_o}} \qquad \text{(IV-66)}$$

This maximum is attained at choice of parameters $t/\lambda = 0.1448$. The mode parameters at this point were found to be: $ht = 2.783$, $kt = 0.91$, $\beta t = 1.549$, $\gamma t = 1.2535$, $t_{eff}/t = 0.1474$. At this point the -1 interaction impedance is given by

$$K_{-1}(0^-) = 0.23 \frac{a^2}{\lambda w}\sqrt{\frac{\mu}{\varepsilon_o}} \qquad \text{(IV-67)}$$

The interaction impedances increase proportionally to the square of the corrugation depth — a^2, so it is advantageous to use deep corrugation. However, technological difficulties are likely to limit the corrugation depth to something less than the period length*. We will choose in the following examples:

$$a = \frac{L}{2} \qquad \text{(IV-68)}$$

---

*A recent publication [Kendall 1975] reports application of preferential etch on Si wafers, achieving etch ratio of 1:400. Further development of such techniques for different semiconductors may allow fabrication of devices with large corrugation depth compared to the period length. Some approximations that we used during the present work will not apply to these structures.

Let us consider two illustrative examples:

Example 1:

$\lambda = 100\mu m$ ($\omega = 1.88 \times 10^{13}$ rad/sec), $\tau = 1.33 \times 10^{-14}$ sec,

$\omega_p = 1.6 \times 10^{13}$ rad/sec, $v_o = 2 \times 10^7$ cm/sec, $v_T = 1 \times 10^7$ cm/sec,

$L = 600\text{Å}$

When GaAs is used as the dielectric material (effective electron mass $m \simeq 0.08\ m_e$), the indicated ω_p, v_T are achieved (Eqs. IV-26,27) with $n_o = 7.9 \times 10^{16} cm^{-3}$ and $T = 53°K$.

The conditions of this example are in the regime where Eq.(IV-48) applies ($2A^2B^2 << 1$). Equations (IV-48), (IV-43), and (IV-66) are used to calculate the maximum first order gain contribution: $g_1 = 0.733\ cm^{-1}$. The -1 order contribution is calculated from Eqs. (IV-60,52,53,67): $g_{-1} = -0.11\ cm^{-1}$ and the o order contribution (Eq. IV-65) is $g_o = -0.45\ cm^{-1}$. The resultant gain is

$$g = g_1 + g_{-1} + g_o = 0.17\ cm^{-1} \qquad \text{(IV-69)}$$

Example 2:

$\lambda = 100\ \mu m$, $\tau = 1.7 \times 10^{-13}$ sec, $\omega_p = 1.3 \times 10^{13}$ rad/sec,

$v_o = 2 \times 10^7$ cm/sec, $v_T = 1 \times 10^7$ cm/sec, $L = 280\text{Å}$

For GaAs, the indicated ω_p, v_T are achieved with $n_o = 4.8 \times 10^{16} cm^{-3}$ and $T = 53°K$.

In this example we are in the regime of Eq. (IV-46) ($2A^2B^2 >> 1$). At maximum gain conditions we get $g_1 = 1.015\ cm^{-1}$, $g_{-1} = 4.3 \times 10^{-3} cm^{-1}$

and $g_0 = -0.142\ cm^{-1}$, resulting in:

$$g = g_1 + g_{-1} + g_0 = 0.87\ cm^{-1} \qquad \text{(IV-70)}$$

It should be pointed out that the equations derived above indicate a higher gain for a longer relaxation time τ, but at the collisionless regime $\omega\tau >> 1$ the applicability of the macroscopic equation analysis is doubtful. This regime, which requires different theoretical methods, will be treated separately in the following chapters.

Higher plasma frequency (viz., higher free carrier concentration) increases the gain due to the first order harmonic interaction. On the other hand it also increases the loss due to the interaction of the zero and -1 harmonics. In addition, skin penetration depth may become small enough to limit harmfully the field penetration into the conducting layer.

Appropriate choice of a semiconductor (possibly InSb) and the temperature, which may allow higher drift velocities and lower thermal velocities may appreciably increase the gain. However, in high mobility semiconductors, the small effective mass may require extremely low temperature in order to achieve sufficiently low thermal velocities.

In conclusion,we demonstrated in this chapter that a new approach to solid state traveling wave amplifiers based on existing and still developing techniques of semiconductor surface corrugation and thin film waveguiding may possibly provide new amplification and oscillation devices in the interesting regime of submillimeter and far infrared waves. However, the gain predicted in the illustrative examples is quite low,

and in practice will be masked by different loss mechanisms like phonon absorption and some free carrier absorption from unintentional impurities doping in the non-conductive portions of the waveguide. Also, the structural and physical parameters assumed in the examples are hard to realize in practice. Hence, it should be indicated that the structure of Fig. 8a and the material and parameter choice in this chapter are probably not satisfactory enough to produce an efficient amplifier. There is room for improvement in design parameters and in the structure. The structure of Fig. 8b or "superlattice" structures (discussed later in Appendix V-A) may be found more efficient.

The framework of traveling wave interaction analysis which we developed in this chapter will serve us in investigating the traveling wave interaction in different regimes (collisionless and quantum regimes) in the following chapters. The one-dimensional model makes it possible to employ a simple analysis that does not mask the main physical mechanism. It proved to be general enough to allow us to include in the analysis also interaction with nonsynchronous space harmonics. However, the underlying assumption of transversely uniform electric fields is certainly not satisfied in the structure that we analyzed (Fig. 8a). This model is much more rigorously applicable to structures like the ones discussed in Appendix V-A (Figs. 28,29) where there is small transverse field variation.

Evidence for gain in solid state traveling wave amplifiers was presented in [Sumi 1968]. Even though different structure and frequency regime were used in that experiment, one should expect

similar qualitative behavior. We note, however, that some important details of the experimental results differ from the basic theory. Higher gain was observed at the backward wave operation mode, also instead of "S" shaped gain curve (Figure 19) gain increased in some of the samples starting with zero applied field. We conclude that the question of the experimental observation of amplification in a circuit-solid state plasma interaction is still open.

Appendix IV-A: The Traveling Wave Dispersion Equation in the Limit $\tau = \infty \quad T = 0$

In the limit $\tau \to \infty \quad v_T = 0$ $(T = 0)$ we would expect that Eqs. (IV-9, 31, 32) will reduce into the conventional dispersion equation of vacuum electron beam traveling wave tube. Substituting $\tau = \infty$ $v_T = 0$ in (IV-31-33) one gets

$$\chi_p(\beta,\omega) = - \varepsilon \frac{\omega_p^2}{(\beta v_o - \omega)^2} \tag{IV-A1}$$

$$\varepsilon_p(\beta,\omega) = 1 - \frac{\omega_p^2}{(\beta v_o - \omega)^2} \tag{IV-A2}$$

When this is substituted in the general traveling wave dispersion equation (IV-9) one gets the conventional traveling wave tube equation (compare [Gewartowski 1965, p. 361], [Hutter 1960, p. 328]).

$$- \frac{\varepsilon K_1 S \beta_1 \beta^2 \omega \omega_p^2 / v_o^2}{(\beta^2 - \beta_1^2)([(\beta - \frac{\omega}{v_o})^2 - (\frac{\omega_p}{v_o})^2]} = 1 \tag{IV-A3}$$

This equation can be cast in terms of parameters customary in traveling wave tube theory. Define C, δ, b, Q by

$$\beta \equiv \frac{\omega}{v_o}(1 + iC\delta) \tag{IV-A4}$$

$$\beta_1 \equiv \frac{\omega}{v_o}(1 + Cb) \tag{IV-A5}$$

$$C^3 \equiv \frac{\varepsilon K_1 S \omega_p^2}{2 v_o} \tag{IV-A6}$$

$$Q \equiv \frac{\omega_p^2}{4\omega^2 C^3} \equiv \frac{v_o}{2\varepsilon K_1 \omega^2} \tag{IV-A7}$$

Assuming near synchronism condition $\beta \approx \beta_1 \approx \omega/v_o$, we get by substitution in (IV-A3)

$$(i\delta - b)(\delta^2 + 4Qc) = 1 \qquad \text{(IV-A8)}$$

which is the conventional normalized dispersion equation [Pierce 1950, Yariv 1958]. This is a third order algebraic equation which often must be solved accurately (see [Pierce 1950]) and first order solution is not employed.

Appendix IV-B: TM Mode Interaction with Free Carriers

In Section 5 we extended the traveling wave interaction analysis to the zero (fundamental) space harmonic. The result (Eq. IV-58) is formally close to what is usually assumed for free carriers loss. To understand the relation better we will calculate the free carriers loss of a TM mode in a dielectric waveguide with a thin doped layer (Fig. 20) using a standard approach. This structure is the same as Fig. 8 with the corrugation neglected and $n_s = n_a$.

We start from Maxwell equations:

$$\underline{\nabla} \times \underline{E} = -i\omega\mu\underline{H} \qquad \text{(IV-B1)}$$

$$\underline{\nabla} \times \underline{H} = i\omega\varepsilon\underline{E} + \underline{J} \qquad \text{(IV-B2)}$$

where there is nonvanishing current $\underline{J}$ only in the conducting layer. Even if the electrons in the conducting layer are drifting, they can be considered stationary relative to the phase velocity of the electromagnetic mode ($v_o << c$) hence we get instead of (IV-17,20) simpler expressions:

$$\underline{J} = -en_o\underline{v} \qquad \text{(IV-B3)}$$

$$\frac{d\underline{v}}{dt} = -\frac{e}{m}\underline{E} - \frac{1}{\tau}\underline{v} \qquad \text{(IV-B4)}$$

$$\underline{v} = -\frac{e}{m}\frac{1}{i\omega+1/\tau}\underline{E} \qquad \text{(IV-B5)}$$

$$\underline{J} = \frac{e^2 n_o \tau}{m}\frac{1}{1+i\omega\tau}\underline{E} = \sigma_o\frac{1}{1+i\omega\tau}\underline{E} = \varepsilon\omega_p^2\frac{1}{1+i\omega\tau}\underline{E} \qquad \text{(IV-B6)}$$

When this is substituted in Eq. (IV-B2) we can rewrite it as

$$\underline{\nabla} \times \underline{H} = i\omega\bar{\varepsilon}\underline{E} \qquad \text{(IV-B7)}$$

where we defined in the layer d (Fig. 20) a complex dielectric constant $\bar{\varepsilon}$ which includes the carriers contribution

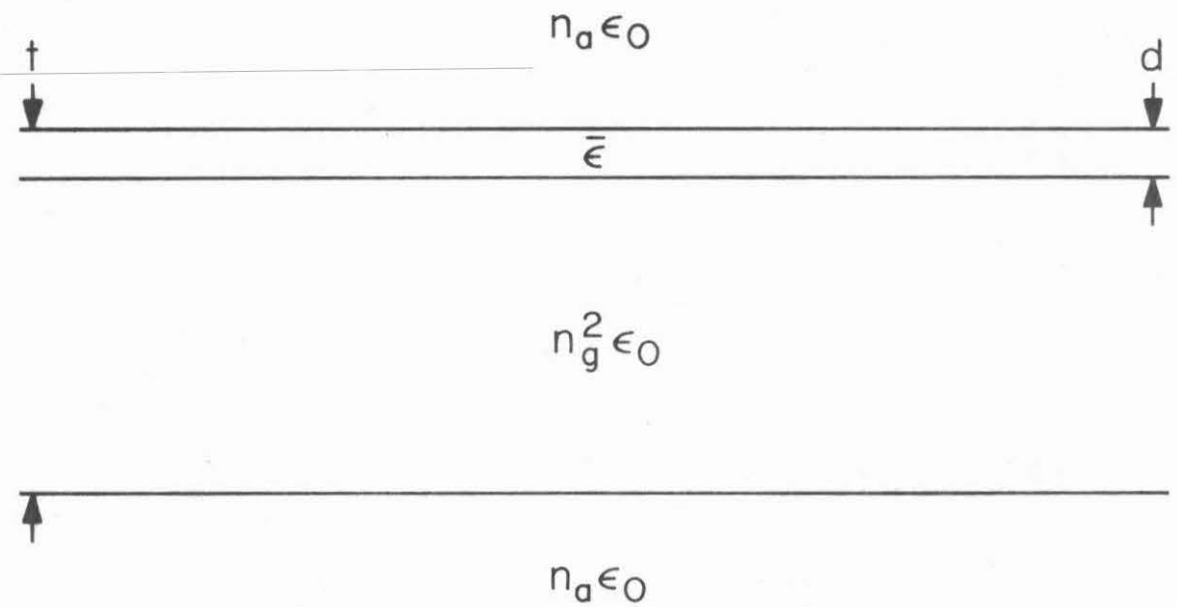

Fig. 20 A symmetric dielectric waveguide with thin conductive layer (corresponds to the structures of Fig. 8 with vanishing corrugation height).

$$\bar{\varepsilon} = (1 - i\frac{\omega_p^2\tau}{\omega}\frac{1}{1+i\omega\tau})\varepsilon = \bar{\varepsilon}_r + i\varepsilon_i \qquad \text{(IV-B8)}$$

$$\bar{\varepsilon}_r \equiv (1 - \frac{\omega_p^2\tau^2}{1+\omega^2\tau^2})\varepsilon \qquad \text{(IV-B9)}$$

$$\bar{\varepsilon}_i \equiv -\frac{\omega_p^2\tau}{\omega}\frac{1}{1+\omega^2\tau^2}\varepsilon \qquad \text{(IV-B10)}$$

This can readily be used to obtain the classical plane wave free carriers losses formula [Moss 1962]:

$$\alpha = 2(\mathrm{Im}\,\bar{\varepsilon}/\varepsilon)n\frac{\omega}{c} = n\frac{\bar{\varepsilon}_i}{\varepsilon}\frac{\omega}{c} = -\frac{n\omega_p^2\tau}{c}\frac{1}{1+\omega^2\tau^2} =$$

$$= -\sqrt{\frac{\mu}{\varepsilon}}\sigma\frac{1}{1+\omega^2\tau^2} \qquad \text{(IV-B11)}$$

We proceed to derive the free carrier attenuation for a TM mode in the dielectric waveguide (Fig. 20). The conducting layer d can be considered as a perturbation to the unperturbed waveguide (where $\omega_p = 0$). Hence we may use Eq. (III-C11) to find the change $\Delta\beta$ in the propagation parameter due to the perturbation $\Delta\varepsilon$

$$\Delta\beta = \frac{\omega}{4}\int_{-\infty}^{\infty}\Delta\varepsilon|\underline{\mathcal{E}}|^2dx \qquad \text{(IV-B12)}$$

In deriving (IV-B12) from (III-C11), we performed the integration over y: $\int dy = w$, assumed that the mode $\underline{\mathcal{E}}$ is power normalized as in Appendix II-A (P/w = 1 watt) and substituted $\Delta\varepsilon = \varepsilon_o\Delta n^2$.

In the present problem $\Delta\varepsilon = \bar{\varepsilon}-\varepsilon$ in the conductive layer and $\Delta\varepsilon = 0$ elsewhere, hence the imaginary part of (IV-B12) is

$$(\mathrm{Im}\Delta\beta)_o = (\mathrm{Im}\beta)_o = \frac{\omega\bar{\varepsilon}_i}{4}\int_{-d}^{o}|\underline{\mathcal{E}}|^2dx \qquad \text{(IV-B13)}$$

If the conductive layer d is thin enough so that the field variation across it is negligible, the integrand in Eq. (IV-B13) can be substituted by its value at $x = 0^-$. With the use of (IV-B10) one obtains

$$(\mathrm{Im}\beta)_o = -\frac{\omega_p^2 \tau \varepsilon d}{4} |\mathcal{E}(0^-)|^2 \frac{1}{1+\omega^2\tau^2} =$$

$$= -\frac{d\sigma}{4} (|\mathcal{E}_x(0^-)|^2 + |\mathcal{E}_z(0)|^2) \frac{1}{1+\omega^2\tau^2} \qquad \text{(IV-B14)}$$

There are striking similarities and dissimilarities between Eq. (IV-B13)and the corresponding expression that was derived in Section 5 for the free carrier attenuation of the fundamental harmonic of a TM mode (Eq. IV-58). The two equations have similar coefficients. Eq. (IV-B14) contains in addition to the term $|\mathcal{E}_z(0)|^2$ also a term with the x component of the electric field $|\mathcal{E}_x(0^-)|^2$. On the other hand Eq. (IV-58) contains a factor $(1 - \omega_p^2/\omega^2)$ which is absent in Eq. (IV-B14).

The absence of the term $|\mathcal{E}_x(0^-)|^2$ in Eq. (IV-58) is an expected result from the approximation of a one dimensional model in the analysis of the traveling wave interaction where transverse field components are ignored. On the other hand it seems that the presence of the factor $(1 - \omega_p^2/\omega^2)$ in (IV-58) indicates an interaction mechanism that is possibly omitted in the standard derivation of free carriers loss.

It is suggested that the usual separation of the electromagnetic wave into noninteracting rotational and longitudinal waves does not hold in the case of TM electromagnetic wave in a plasma loaded waveguide. It should be expected that in this case there will be coupling between the rotational wave and the longitudinal space charge plasma wave. This coupling is included in the traveling wave interaction analysis, and the coefficient $(1 - \omega_p^2/\omega^2)$ results there from the use of Poisson equation (IV-4). This coefficient is missing from Eq. (IV-B14) because the coupling process between the rotational and longitudinal wave is missing in the standard analysis.

The coupling between the rotational and longitudinal components in the case of a TM wave, traveling in a bounded structure which contains plasma, is an interesting effect, which may be detected in waveguiding experiments in plasma loaded waveguides or in ATR (attenuated total reflection) experiments [Kaplan 1974]. However we will avoid further investigation of this problem in the present work in order to not be carried away from the main research subject. It is suggested that the use of Eq. (IV-58) for the z field component loss contribution and Eq. (IV-B14) with $\mathcal{E}_z = 0$ for the x field component loss contribution, would be a reasonable estimate for the free carrier loss of the TM wave. In many cases the x component of the electric field may be considerably smaller than the z component and therefore its contribution will be negligible. In the present situation (Fig. 20), we find from Eqs. (II-A19÷A21,A28) that

$$|\mathcal{E}_x(0^-)|^2 = \left(\frac{\beta}{n_g^2\gamma}\right)^2 \mathcal{E}_z(0) \qquad \text{(IV-B15)}$$

for the choice of parameters used in Section 6 it is

$$|\mathcal{E}_x(0^-)|^2 = 10^{-2}\ |\mathcal{E}_z(0)|^2 \qquad \text{(IV-B16)}$$

so that the contribution of the x component is negligible and the use of Eq. (IV-58) or (IV-65) is a good approximation.

Finally we estimate the free carriers effect on the real part of the dielectric constant. From Eq. (IV-B9)

$$\Delta\varepsilon = \bar{\varepsilon}_r - \varepsilon = -\frac{\omega_p^2\tau^2}{1+\omega^2\tau^2}\,\varepsilon \qquad \text{(IV-B17)}$$

This contribution may be appreciable at low frequency ω. Moreover, if there is appreciable reduction in ε, the field penetration into the

conducting layer will be considerably reduced. In the simplified model that we used in Chapter IV this contribution was usually neglected in order to keep the analysis clear. In the examples used in Section 5 the change in the dielectric constant can be estimated as

$$\frac{\Delta\varepsilon}{\varepsilon} = -0.07$$

for example 1 and

$$\frac{\Delta\varepsilon}{\varepsilon} = -\ 0.44$$

for example 2.

CHAPTER V

TRAVELING WAVE INTERACTION IN THE COLLISIONLESS REGIME

1. Introduction

As Landau [1946] first demonstrated, plasma waves in a finite temperature plasma have features due to collective particle behavior which cannot be obtained from the macroscopic kinetic equation. Landau showed that the interaction of a plasma wave with particles traveling with velocities near its phase velocity could lead to damping of the wave even if the plasma is collisionless (relaxation time $\tau \to \infty$).

The goal of this chapter is to analyze the traveling wave interaction mechanism in the Landau regime, viz. $\omega\tau >> 1$. We should say in advance that the problem we consider here is different from the problem treated by Landau not only because the plasma is drifting, but also because of the existence of a slow wave structure which supports an electromagnetic mode whose field, acting on the plasma, is referred to as the external electric field. In the original Landau problem, by comparison, no external field exists in the plasma and the field solution there is the self-consistent solution of the plasma medium. Indeed it is possible to show that by itself, even when drifting (but with single peak in the velocity distribution function), a plasma does not give rise to unstable plasma waves [Stix 1972, Chapter 7].

In the two familiar traveling wave interaction problems - the conventional traveling wave tube problem [Pierce 1950] and the solid state traveling wave interaction in the collision dominated regime (Chapter IV), the charged particles are usually described by the moment

equations. This approach is valid for different reasons in the two systems. The TWT electron beam is nearly monochromatic; for such a beam, the Boltzmann equation reduces immediately to the moment equations. Even though the carriers in the solid state amplifier have a finite temperature, collisions are frequent enough that the effects discussed by Landau for a collisionless plasma are unimportant and the moment equations are again a good approximation.

If the frequency ω is sufficiently high, the drifting carriers in the solid state amplifier may be considered as a finite temperature, collisionless plasma ($\omega\tau >> 1$). The existing analysis of traveling wave interactions is not applicable to this case, since the moment equations used in it cannot correctly describe the Landau waves that propagate in a collisionless plasma. We intend, therefore, in this chapter, to extend the analysis of traveling wave interaction to this regime, employing the Boltzmann equation to describe the drifting plasma. This is an elaboration of a recent examination of this problem by Gover, Burrell and Yariv [1974].

A proper analysis of the solid state traveling wave interaction at high frequency is of special interest, since the availability of periodic structures with very short periods may allow amplification at frequencies in the collisionless regime. Such an analysis is also useful to describe the traveling wave interaction of a vacuum electron beam with wide thermal spread such that the Boltzmann equation describing the beam cannot be reduced to the moment equations.

2. The Plasma Response in the Collisionless Regime

We will use the derivation of the coupled mode dispersion equation presented in Section 2 of Chapter IV. However we use the Boltzmann equation to describe the plasma response. The linearized one dimensional Boltzmann equation is

$$(\frac{\partial}{\partial t} + u \frac{\partial}{\partial z}) f_1(z,u,t) = \frac{e}{m} E(z,t) \frac{\partial}{\partial u} f_o(u) \qquad (V-1)$$

Here u is the z component of the particle velocity. The zero and first order velocity distribution functions f_o and f_1, respectively, are calculated from the three dimensional distribution functions by integrating over the transverse velocities. E(z,t) is the longitudinal (z) local field at point z.

We may solve Eq. (V-1) by substituting harmonic time dependence $e^{i\omega t}$. To avoid the difficulties pointed out by Landau [1946] we need to define the z coordinate transformation carefully. We define a "rotated" Laplace transform of a function h(z) (z>0) by:

$$h(\beta) = \int_0^\infty dz\ h(z) e^{i\beta z} \qquad (V-2)$$

This transform is properly defined for values of β with an imaginary part large enough to ensure the convergence of the integral. Therefore the inverse transform must be defined by:

$$h(z) = \frac{1}{2\pi} \int_C d\beta\ h(\beta) e^{-i\beta z} \qquad (z > 0) \qquad (V-3)$$

where the contour of integration C (shown in Fig. 21a) is parallel to the real axis at Imβ large enough to contain all the poles in the lower half plane.

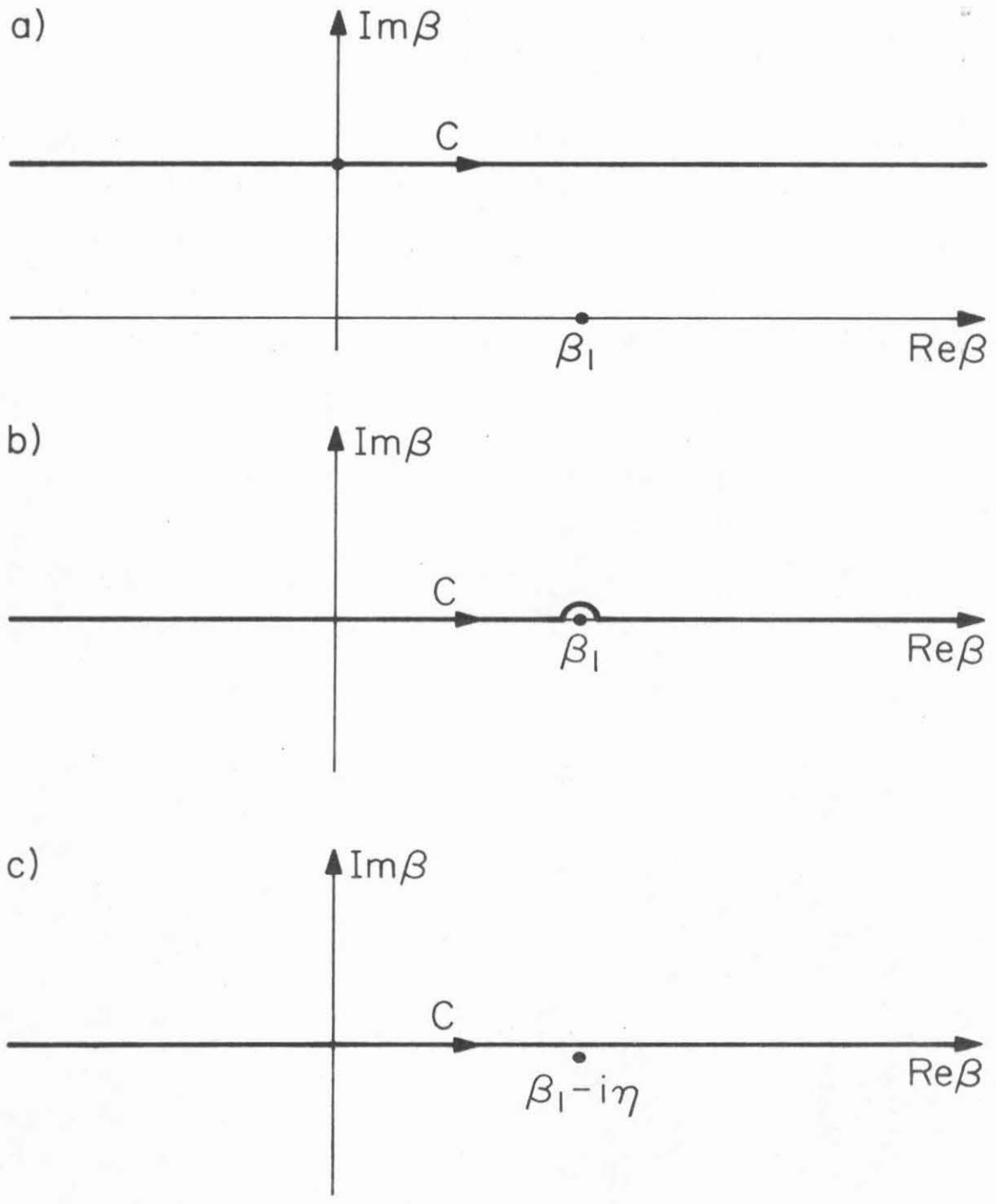

Fig. 21 Integration contours of the inverse transform (V-3).

As we will see later there will be a pole on the real β axis so that the integration contour cannot pass completely on the real axis but as in Fig. 21b. So the function is defined at the singularity by its analytical continuation from the lower half plane. An alternative way to define $h(\beta)$ properly is to translate the argument by an infinitesimal quantity $\beta \to \beta+i\eta'$. This will shift the pole below the real axis allowing integration along the real axis (Fig. 21c)

$$h(z) = \lim_{\eta'\to 0} \frac{1}{2\pi} \int_{-\infty}^{\infty} d\beta h(\beta+i\eta')e^{-i\beta z} \tag{V-4}$$

The integral is thus properly defined by an integration path passing above the pole.

Using this convention we get from the transform of Eq. (V-1)

$$(i\omega-i\beta u+\eta' u)f_1(\beta,u) = \frac{e}{m} E(\beta)f_0'(u) \tag{V-5}$$

or

$$f_1(\beta,u) = \frac{ie}{m\beta} \frac{f_0'(u)}{u - \omega/\beta + i\eta} E(\beta) \tag{V-6}$$

where $\eta \equiv \eta' u/\beta$ will be later set to the limit zero*.

The current induced in the plasma is then found to be:

$$J_z(\beta) = -e\int_{-\infty}^{\infty} du\, u\, f_1(\beta,u) = -\frac{ie^2}{m\beta}\int_{-\infty}^{\infty} du \frac{u\, f_0'(u)}{u-\omega/\beta + i\eta} E(\beta) =$$
$$= -\frac{ie^2\omega}{m\beta^2}\int_{-\infty}^{\infty} du \frac{f_0'(u)}{u-\omega/\beta + i\eta} E(\beta) \tag{V-7}$$

We have used the identities $u/(u+\alpha) = 1-\alpha/(u+\alpha)$ and $\int_{-\infty}^{\infty} du f_0'(u) = 0$ to put the integral in Eq. (V-7) in its present form. That $f_0(u)$

*An alternative presentation of the term $i\eta$ is made by adding an infinitesimal negative imaginary part to the frequency $\omega \to \omega - i\eta'$. This corresponds to turning on disturbance in the far past (adiabatic turning on). η can also be presented as a vanishing collision term.

should vanish as $|u| \to \infty$ is necessary for any reasonable distribution function. The integral in Eq. (V-7) would have been undefined if $\eta = 0$.

Comparing Eq. (V-7) with the definition of the susceptibility (Eq. IV-2) we find

$$\chi_p(\beta,\omega) = -\frac{e^2}{m\beta^2}\int_{-\infty}^{\infty} du\, \frac{f_o'(u)}{u-\omega/\beta+ i\eta} \tag{V-8}$$

We can now go back to the coupled mode analysis of the traveling wave interaction (Sect. 2 of Chap. IV) and readily use Eq. (V-8) in (IV-9) to get the coupled mode dispersion equation, or in (IV-11) to get the gain of the electromagnetic wave. However, before doing this we will pause for some further development of our result.

First we show that Eqs. (IV-5-7) can be derived directly from the Poisson equation

$$-i\beta E_p(\beta) = -\frac{e}{\varepsilon}\int_{-\infty}^{\infty} du\, f_1(\beta,u) \tag{V-9}$$

Using (V-6) in Eq. (V-9) and consequently using (V-8) we get

$$-i\beta E_p(\beta) = -\frac{ie^2}{\varepsilon m\beta}\int_{-\infty}^{\infty} du\, \frac{f_o'(u)}{u-\omega/\beta + i\eta} E(\beta)$$

$$E_p(\beta) = -\frac{\chi_p}{\varepsilon} E(\beta) \tag{V-10}$$

where (IV-3)

$$E(\beta) = E_p(\beta) + E_c(\beta) \tag{V-11}$$

$E(\beta)$ is the local field. $E_p(\beta)$ is the plasma space charge field and $E_c(\beta)$ is the external induced field (rotational field). From (V-10) and (V-11) we get

$$\varepsilon_p E(\beta) = E_c(\beta) \tag{V-12}$$

$$\varepsilon_p \equiv 1 + \chi_p/\varepsilon \tag{V-13}$$

Notice that we did not have to use the continuity equation which is implicit in the Boltzmann equation and only the Poisson equation (V-9) was used in addition to the Boltzmann equation.

To cast our result in a slightly more universal form, we define the following moments of the unperturbed distribution function: the carrier number density

$$n_o = \int_{-\infty}^{\infty} f_o(u)du \tag{V-14}$$

the drift (average) velocity

$$v_o = \frac{1}{n_o}\int_{-\infty}^{\infty} u\, f_o(u)du \tag{V-15}$$

and the temperature T and thermal velocity v_{th}

$$k_B T \equiv m v_{th}^2/2 \equiv \frac{m}{n_o}\int_{-\infty}^{\infty}(u-u_o)^2 f_o(u)du \tag{V-16}$$

Notice that the definition of thermal velocity v_{th} is different from v_T (Eq. IV-27), their relation is $v_{th} = \sqrt{2}\, v_T$. Also we define a normalized distribution function g(x)

$$f_o(u) \equiv \frac{n_o}{v_{th}}\, g\left(\frac{u-v_o}{v_{th}}\right) \tag{V-17}$$

The function g is defined so that its zero, first and second moments are 1, 0 and 1/2 respectively.

Using these definitions we proceed to define the plasma dispersion function

$$G(\zeta) = \int_{-\infty}^{\infty} \frac{g(x)}{x-\zeta}\, dx \qquad \text{Im}\ \zeta < 0 \tag{V-18}$$

This definition disagrees with the usual convention in plasma physics, where $\text{Im}\zeta > 0$ is usually taken.

Combining these definitions with (V-8),(V-13), (V-7) and (V-12) we find

$$\chi_p(\beta,\omega) = -\frac{1}{2}\,\varepsilon\,\frac{k_D^2}{\beta^2}\,G'(\zeta) \tag{V-19}$$

where

$$k_D \equiv \left(\frac{n_o e^2}{\varepsilon k_B T}\right)^{1/2} \equiv \sqrt{2}\,\frac{\omega_p}{v_{th}} \tag{V-20}$$

is the Debye wavenumber and

$$\zeta \equiv \frac{\omega/\beta - v_o - i\eta}{v_{th}} \tag{V-21}$$

and primes denote differentiation with respect to the argument.

$$\varepsilon_p(\beta,\omega) = 1 - \frac{1}{2}\,\frac{k_D^2}{\beta^2}\,G'(\zeta) \tag{V-22}$$

$$J_z(\beta) = -i\omega\,\frac{1}{2}\,\varepsilon\,\frac{k_D^2}{\beta^2}\,G'(\zeta)E(\beta) = -i\varepsilon\omega\,\frac{\frac{1}{2}\,\frac{k_D^2}{\beta^2}\,G'(\zeta)}{1-\frac{1}{2}\,\frac{k_D^2}{\beta^2}\,G'(\zeta)}\,E_c(\beta) \tag{V-23}$$

Eq. (V-22) is consistent with similar expressions for the plasma dielectric constant in [Steele 1969, p. 124].

3. Solution of the Dispersion Equation

When the derived expression for the susceptibility (V-19) is substituted in the general coupled mode dispersion equation (IV-9) and its first order solution (IV-10,11) we find

$$\frac{\varepsilon\omega\beta_1 K_1 S}{\beta_1^2-\beta^2}\,\frac{\frac{1}{2}k_D^2\,G'(\zeta)}{1-\frac{1}{2}\frac{k_D^2}{\beta^2}G'(\zeta)} = 1 \qquad \text{(V-24)}$$

$$\Delta\beta = -\alpha\,\frac{G'(\zeta_1)}{\varepsilon_p(\beta_1,\omega)} \qquad \text{(V-25)}$$

where

$$\zeta_1 = \frac{(\omega/\beta_1 - v_o)}{v_{th}} \qquad \text{(V-26)}$$

$$\alpha \equiv \frac{1}{4}\varepsilon\omega k_D^2 K_1 S \qquad \text{(V-27)}$$

and where we have finally taken the limit $\eta \to 0^+$.

Because β_1 is real we may write the real and imaginary parts of β as

$$\mathrm{Im}\beta = -\alpha\,\frac{\mathrm{Im}G'(\zeta_1)}{|\varepsilon_p(\beta_1,\omega)|^2} \qquad \text{(V-28)}$$

$$\mathrm{Re}\beta = \beta_1 - \frac{\alpha}{|\varepsilon_p(\beta_1,\omega)|^2}\left[\mathrm{Re}G'(\zeta_1) - \frac{1}{2}\frac{k_D^2}{\beta_1^2}|G'(\zeta_1)|^2\right] \qquad \text{(V-29)}$$

As a consequence of taking $\eta \to 0^+$

$$G'(\zeta_1) = (p)\int_{-\infty}^{\infty}\frac{g'(x)}{x-\zeta_1}\,dx - i\pi g'(\zeta_1) \qquad \text{(V-30)}$$

where (p) denotes principal value and the minus sign results in since we define the function at ζ_1 from its values at $\mathrm{Im}\zeta < 0$ (Eq. V-18).

From Eqs. (V-28) and (V-30) we see that the imaginary part of β

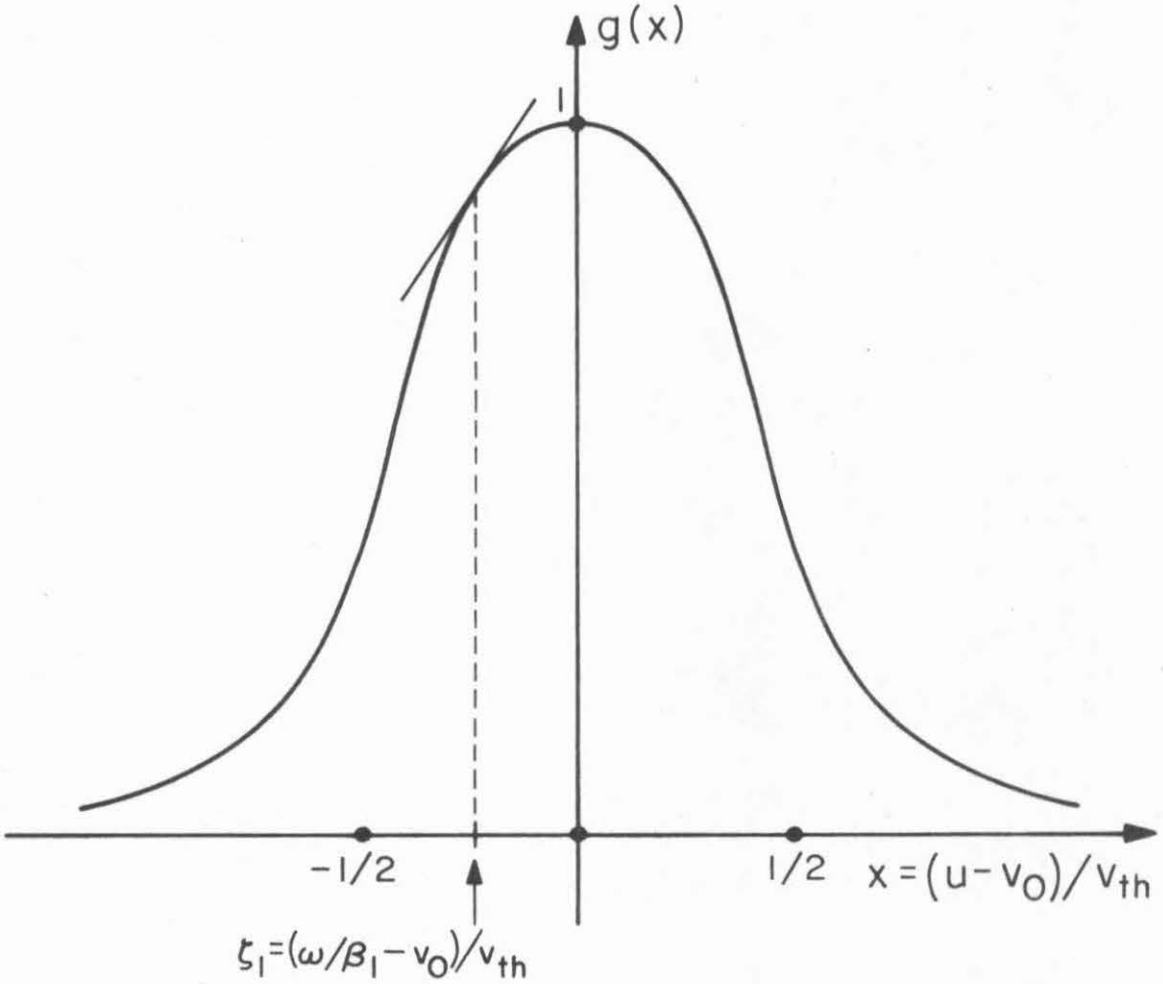

Fig. 22 A plot of g(x) (the function is not necessarily symmetric as in the picture). In this case $g'(\zeta_1) > 0$ for $\zeta_1 < 0$ or $v_0 > \omega/\beta_1$.

(and consequently the gain) is proportional to the derivative of the normalized zero order distribution function $g'(\zeta_1)$. Hence the system can support growing waves ($Im\beta > 0$) when this derivative is positive (see Fig. 22).

$$g'(\zeta_1) > 0 \tag{V-31}$$

This gain criterion is different from (III-25). Only when $g'(0) = 0$ $g''(0) < 0$ (which is the case when the maximum of the distribution function occurs at the drift velocity v_o). The gain condition can be written as $\zeta_1 < 0$ or (see V-26)

$$v_o > \omega/\beta_1 \tag{V-32}$$

which is identical with the Cerenkov condition(III-25).

Two limits of Eq. (V-28) are of interest. If $k_D^2/\beta_1^2 << 1$ then $\varepsilon_p \approx 1$ (Eq. V-22) and

$$Im\beta = -\alpha\, ImG'(\xi_1) = \alpha\pi g'(\zeta_1) \tag{V-33}$$

This corresponds to the limit of low electron density where the plasma has a negligible polarization effect and the local field $E(\beta)$ is approximately equal to the externally applied field $E_c(\beta)$. On the other hand if $k_d^2/\beta_1^2 \gtrsim 1$ we may be able to satisfy the condition

$$Re\,\varepsilon_p(\beta_1,\omega) = 1 - \frac{1}{2}\frac{k_D^2}{\beta_1^2} ReG'(\zeta_1) = 0 \tag{V-34}$$

which yields (using V-28,22,30)

$$Im\beta = -4\alpha \frac{\beta_1^4}{k_D^4} \frac{1}{ImG'(\zeta_1)} = \frac{4\alpha}{\pi} \frac{\beta_1^4}{k_D^4} \frac{1}{g'(\zeta_1)} \tag{V-35}$$

Physically, Eqs. (V-34,35) mean that maximum gain results when β_1 comes as close as possible to satisfying

$$\varepsilon_p(\beta_1,\omega) \simeq 0 \qquad \text{(V-36)}$$

which implies a good phase match between the electromagnetic wave (β_1,ω) and the collective plasma excitation (which is the exact solution of Eq. V-36). As Landau [1946] showed, no nonzero real β can satisfy the plasma wave dispersion relation (V-36) exactly, but the gain increases the closer β_1 comes to satisfying it.

Eq. (V-28) can be regarded as gain (or attenuation) due to <u>single electron interaction</u> since collective phenomena are not involved. On the other hand Eq. (V-35) describes gain (or attenuation) due to phase matched interaction of the electromagnetic wave with the collective plasma excitation. For this reason, we will call this case <u>electromagnetic wave-plasma wave coupling.</u> This will be further discussed also in the next chapter in the framework of the quantum mechanical analysis.

If the denominator in Eq. (V-35) can be made very small, one wonders whether our first order approximation to the dispersion relation, Eq. (IV-10), is valid. To check it, let us extend the solution for $\Delta\beta$ to second order, by expanding in Eq. (IV-9) $\beta^2-\beta_1^2$ and $\varepsilon_p(\beta,\omega) = 1 + \chi_p(\beta,\omega)/\varepsilon$ to first order about $\beta = \beta_1$. We obtain

$$A\left(\frac{\Delta\beta}{\beta_1}\right)^2 + B\left(\frac{\Delta\beta}{\beta_1}\right) + C = 0 \qquad \text{(V-37)}$$

where

$$A \equiv \beta_1 \frac{d}{d\beta_1} \chi_p(\beta_1,\omega)/\varepsilon \qquad \text{(V-38)}$$

$$B \equiv \varepsilon_p(\beta_1,\omega) = 1 + \chi_p(\beta_1,\omega)/\varepsilon \tag{V-39}$$

$$C \equiv -\frac{1}{2} K_1 S \beta_1^3 \omega \chi_p(\beta_1,\omega) \tag{V-40}$$

In the present case the collisionless plasma susceptibility is given by (V-19), so the parameters A, B, C can be written in terms of the plasma dispersion function $G'(\zeta)$

$$A = 2 + \frac{k_D^2 \omega}{2\beta_1^3 v_{th}} G''(\zeta_1) \tag{V-41}$$

$$B = 1 - \frac{1}{2}\frac{k_D^2}{\beta_1^2} G'(\zeta_1) \tag{V-42}$$

$$C = \frac{\alpha}{\beta_1} G'(\zeta_1) \tag{V-43}$$

The solution to Eq. (V-37) is

$$\frac{\Delta\beta}{\beta_1} = \frac{-B \pm (B^2-4AC)^{1/2}}{2A} \tag{V-44}$$

If

$$4|AC| \ll |B|^2 \tag{V-45}$$

which corresponds to poor plasma-electromagnetic wave phase matching ($B \neq 0$) or small interaction impedance, Eq. (V-44) reduces to

$$\frac{\Delta\beta}{\beta_1} = \frac{C}{B} \tag{V-46}$$

which is exactly the first order approximation (IV-10) or (specifically) (V-25). Consequently (V-45) is the criterion for the validity of the

first order approximation. If the matching between the electromagnetic wave and the plasma wave is good ($B \approx 0$), and the interaction impedance is large enough, we will be in the regime

$$4|AC| >> |B|^2 \tag{V-49}$$

where the amplifying solution to Eq. (V-44) reduces to

$$\frac{\Delta\beta}{\beta_1} = i\left(\frac{C}{A}\right)^{1/2} \tag{V-50}$$

It is of interest to check our derivation to find out if in the proper limit it reduces to that of the conventional traveling wave tube. In this case the electron beam is assumed to have no thermal velocity spread ($v_{th} = 0$) so that the normalized distribution function (V-17) reduces to

$$g(x) = \delta(x) \tag{V-51}$$

Used in (V-18) we get

$$G'(\zeta) = \frac{1}{\zeta^2} \qquad \zeta \neq 0 \tag{V-52}$$

which in Eqs. (V-19,22) results in

$$\chi_p(\beta,\omega) = -\varepsilon \frac{\omega_p^2}{(\beta v_o - \omega)^2} \tag{V-53}$$

$$\varepsilon_p(\beta,\omega) = 1 - \frac{\omega_p^2}{(\beta v_o - \omega)^2} \tag{V-54}$$

This result is identical with Eqs. (IV-A1,A2) and was shown in Appendix IV-A to lead to the conventional vacuum electron beam traveling wave equation (IV-A3 or IV-A8).

Eq. (V-24) is thus a generalization of the conventional traveling wave equation (IV-A3,A8) covering situations where the electron beam is not monoenergetic and can have some velocity distribution. If the wavenumber of the slow electromagnetic wave β_1 is quite different

from any of the plasma waves, Eq. (V-24) can be reduced into a first order algebraic equation for $\Delta\beta$ (V-25). When β_1 is close to one of the plasma wave solutions, a second order algebraic equation results in(Eq. V-37). In the case that both plasma wave solutions are close to each other also the second order approximation fails (this is not likely to happen in the examples analyzed in this work). In this case the full transcendental equation (V-24) should be solved. This equation reduces into a third order algebraic equation in $\Delta\beta$ (Eqs. IV-A3,A8) for a monoenergetic beam (Eq. V-51).

4. Discussion and Examples of Amplification

The present discussion of traveling wave interaction was kept up to this point general, so it could describe different systems. We now apply the analysis in the case of solid state traveling wave interaction. It is of particular interest to estimate the performance of such a structure in the gain regime where it may function as a submillimeter frequency amplifier and oscillator. This will be done in the present section. Operation at the attenuation regime is also of interest, providing tools for investigation of plasma waves and the carriers distribution function in solids. This will be discussed in the next section.

In order to estimate the amount of gain available from the solid state traveling wave amplifier, we need to know the velocity distribution function of the drifting carriers. We will use a drifting Maxwellian as a preliminary crude model of the distribution function. The real distribution function of drifting carriers in the solid is much more complicated than that, and not unambiguously measured. However, drifting Maxwellian is commonly used as a first order approximation with some experimental justification [Mooradian 1970].

Consequently we take

$$g(x) = \pi^{-1/2} e^{-x^2} \tag{V-55}$$

and the dispersion function (V-18) is then

$$G(\zeta) = \pi^{-1/2} \int_{-\infty}^{\infty} \frac{e^{-x^2}}{x-\zeta}\, dx \qquad \mathrm{Im}\zeta < 0 \tag{V-56}$$

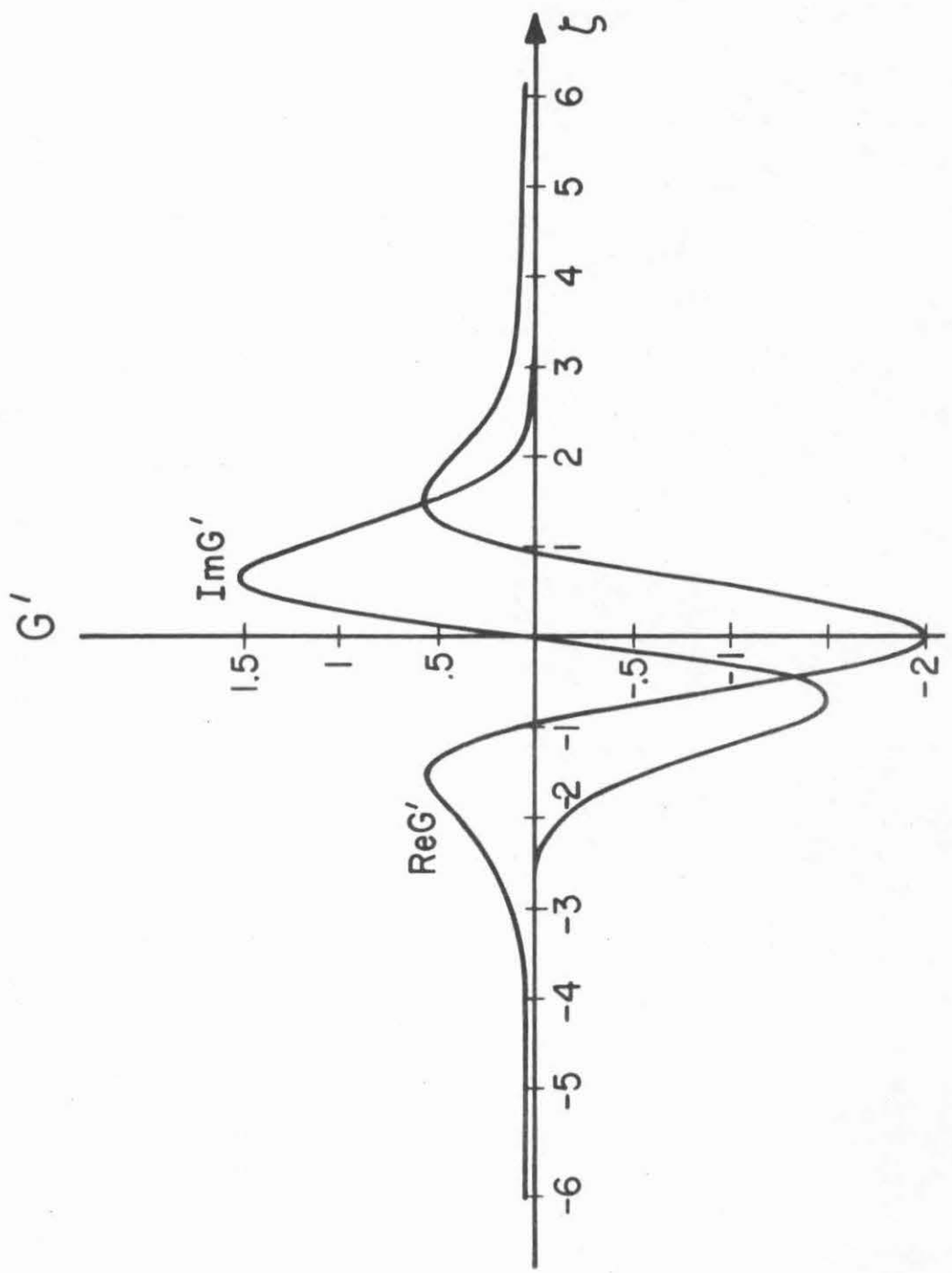

Fig. 23 The derivative of the plasma dispersion function $G'(\zeta)$ for Maxwellian distribution and real argument ζ.

The tabulated plasma function $Z(\zeta)$ which is defined by Fried and Conte [1971], has $Im\zeta > 0$ in its definition. For real ζ we have $G(\zeta) = Z^*(\zeta)$ (or Re $G(\zeta) = ReZ(\zeta)$, $ImG(\zeta) = -ImZ(\zeta)$). The function $G'(\zeta)$ is plotted in Fig. 23. A computer calculation of $Z'(\zeta)$ is listed in Appendix VI-B.

The function $ImG'(\zeta)$ shown in Fig. 23 is an S shaped curve like Fig. 19 (of course with a different functional dependence). It shows that the present $G'(\zeta_1)$ can support gain ($Im\beta>0$) whenever $\zeta_1 < 0$ (Eq. V-28). The Maxwellian, of course, is a symmetric function and satisfies $g'(0) = 0$; thus the gain condition $\zeta_1 < 0$ is equivalent in this case to the condition $v_o > \omega/\beta_1$ (Eq. V-32).

In Tables 24, 25 we present a few examples of solid state traveling wave amplifiers. The structures which are considered are shown in Figs. 8, 28, 29 and are discussed in Appendix V-A. In Table 24 we present examples in the regime $k_D^2/\beta_1^2 << 1$ where Eq. (V-33) applies. From Fig. 23 we see that $ImG'(\zeta)$ attains minimum value at $\zeta_1 = -0.65$, $ImG(-0.65) = -1.5$. We choose

$$\frac{k_D^2}{\beta_1^2} = \frac{1}{4}, \qquad a = \frac{L}{2}, \qquad \frac{v_o}{v_{th}} = 1.85, \qquad \frac{\omega/\beta_1}{v_{th}} = 1.2$$

resulting $\zeta_1 \equiv \omega/(\beta_1 v_{th}) - v_o/v_{th} = -0.65$. The calculated gain is given in Table 24 for two different dielectrics and three different structures along with some of the physical conditions necessary to attain that gain. For this calculation we assumed

$$\omega = 1.88 \times 10^{13} \text{ rad/sec} \qquad (\lambda = 100\mu)$$

Table 24. Example of Gain $k_D^2/\beta_1^2 << 1$

Parameter	Ge	GaAs	Unit
m/m_e	0.55	0.06	----
v_o	1.2×10^7	2×10^7	cm/sec
v_{th}	6.49×10^6	1.08×10^7	cm/sec
β_1	2.41×10^6	1.45×10^6	cm^{-1}
k_D	1.21×10^6	7.25×10^5	cm^{-1}
ω_p	5.54×10^{12}	5.54×10^{12}	rad/sec
n_o	6.51×10^{16}	9.47×10^{15}	cm^{-3}
T	77	31	°K
L	260	433.6	Å
Fig. 8a ($d = 1/\beta_1$) g	0.16	0.27	cm^{-1}
Fig. 28 (ϕ=65°, $n_{L1}^2/n_{LO}^2 = 0.1$) g	8	8	cm^{-1}
Fig. 29 (ϕ=90° n_{L1}^2/n_{LO}^2=0.1) g	4.1	4.1	cm^{-1}

Table 25. Example of Gain at Plasma-EM Wave Phase Matching Condition

Parameter	Ge	GaAs	Unit
m/m_e	0.55	0.08	-----
v_o	1.2×10^7	2×10^7	cm/sec
v_{th}	3.43×10^6	5.71×10^6	cm/sec
β_1	1.1×10^7	6.6×10^6	cm^{-1}
k_d	3.24×10^7	1.94×10^7	cm^{-1}
ω_p	2.52×10^{14}	7.85×10^{13}	rad/sec
n_o	1.3×10^{19}	1.9×10^{18}	cm^{-3}
T	21.3	8.6	°K
L	57.2	95.2	Å
Fig. 8b ($d=1/\beta_1$, $t=10u$, $n_{L1}^2/n_{L0}^2 = 0.3$, $\phi = 65^\circ$) g	18.6	31.1	cm^{-1}

and used for the calculation of the interaction impedance Eqs. (III-50), (V-A31) and V-A34).

In Table 25 we present an example in the regime $k_D^2/\beta_1^2 >> 1$ where increased interaction can be achieved due to phase matched coupling of the electromagnetic and plasma waves (Eqs. V-34, 35). We choose $\zeta_1 = -2.5$ which gives low value $ImG'(-2.5) = -1.71 \times 10^{-2}$. Also we get $ReG'(-2.5) = 0.231$. The ratio β_1^2/k_D^2 is chosen to satisfy the real part of the phase matching condition (Eq. V-34).

$$\beta_1^2/k_D^2 = \frac{1}{2} ReG'(\zeta_1) = 0.1154$$

We also choose $a=L/2$, $v_o/v_{th} = 3.5$, $\omega/(\beta_1 v_{th}) = 1$ (so that $\zeta_1 = \omega/(\beta_1 v_{th}) - v_o/v_{th} = -2.5$). In this example we operate in the regime $\omega < \omega_p$ (see discussion in Appendix V-A) hence we cannot use structures like in Figs. 28,29 which do not transmit the electromagnetic wave. We calculate the gain for the structure in Fig. 8b using Eq. (V-A16) to obtain the interaction impedance $K_1(0^+)$. The calculated gain is shown in Table 25 along with some of the physical conditions necessary to attain that gain. The frequency assumed was

$$\omega = 3.77 \times 10^{13} \text{ rad/sec} \qquad (\lambda = 50\mu)$$

The choice of the parameter $n_{L1}^2/n_{L0}^2 = 0.3$ would seem unpractical if one considers that the change between the dielectric constants of the different semiconductors used in heteroepitaxy is quite small. However, as was mentioned in Appendix V-A, a big change in dielectric constant can result if the epitaxially grown layer in Fig. 8b contains high density of free carriers so that $\omega < \omega_p$. In this case it is even possible to get $n_{L1}^2/n_{L0}^2 \simeq 1$, so that our choice is rather conservative. The choice

of effective thickness $d = 1/\beta_1 = L/2\pi$ is dictated by the decay length of the first order space harmonic. However if structures like those in Fig. 30 could be produced with thick periodic layer, interaction will take place across the whole thickness of the periodic layer, allowing considerably higher gain than that presented in Table 25.

In both examples considered the gain was calculated only from the contribution of the synchronous first order space harmonic. The nonsynchronous -1 order space harmonic contributes negligible attenuation. In our collisionless model $\tau = \infty$, and hence no free carriers loss due to the fundamental space harmonic is contributed. Of course loss due to collisionless traveling wave interaction (Landau damping) is negligible at the velocity of the fundamental space harmonic.

The physical conditions required in the two examples (especially the second one) are quite difficult. Finite collision relaxation time τ would affect the calculation (its effect is briefly discussed in Section 6). It is also not clear if drifting carriers distribution functions with high ratio v_o/v_{th} can be achieved in semiconductors (see discussion in Chapter VII Section 5).

5. Attenuation and the Traveling Wave Modulator

The traveling wave interaction in the solid can be applied in studying solid state plasma waves and the carrier velocity distribution function. In this case we may be interested in interaction also in the attenuation regime.

If one can measure $\Delta\beta$ experimentally, then the derivative of the normalized distribution function $g'(\zeta_1)$ can be found from Eqs. (V-25,30). However, since Re $\Delta\beta$ may be difficult to measure, especially in a solid, a series of measurements of Im $\Delta\beta$ for various

ω, β, k_D could furnish enough information to obtain $g'(\zeta_1)$ from Eq. (V-28) alone. If it is possible to work in parameter ranges where Eqs. (V-33) or (V-35) hold, then evaluation of $g'(\zeta_1)$ is straightforward when Im $\Delta\beta$ is known. It follows that it may be possible to measure directly the velocity distribution function of drifting carriers in some regimes. Such a method will measure the distribution of the velocities z components rather than the distribution of electron energies. Thus it may be complementary to other existing methods which measure velocity distribution [Mooradian 1970, Jantsch 1973].

Attaining attenuation, particularly with phase matching of the electromagnetic and the plasma waves (Eqs. V-34-36) is much easier than attaining amplification at similar conditions. The reason is that in order to get good phase matching we need $|\mathrm{Im}G'(\zeta_1)| \to 0$. This is possible for $|\zeta_1| >> 1$ which means operation at the tail of the distribution function (see Fig. 22). Physically, we know that at the tail of the distribution function the Landau damping of the plasma wave is diminishing and this is why it can match better an unattenuated electromagnetic wave. To get $\zeta_1 = (\omega/\beta_1 - v_o)v_{th} >> 1$ is possible with high frequency, low β_1 (long period) and low velocity v_o (even zero or negative velocity) and the contrary is when we want to get $\zeta_1 << 1$. As we see from Fig. 22 the derivative of the distribution function is negative in the first case (corresponding to attenuation) and positive in the second case (corresponding to amplification).

In Table 26 we present an example of attenuation under conditions of phase matching between the electromagnetic wave and the plasma wave.

As in the previous section, we assume for the distribution function a drifting Maxwellian (Eq. V-55) and use the plasma dispersion function (V-56). We choose the special case $v_o = 0$ (no DC voltage is applied). Choice of $\zeta_1 = \omega/(\beta_1 v_{th})=2.3$ gives low value $ImG'(2.3) = 4.11 \times 10^{-2}$. Also we find $ReG'(2.3) = 0.2913$. The ratio β_1^2/k_D^2 is chosen to satisfy the real part of the phase matching condition (Eq. V-34)

$$\beta_1^2/k_D^2 = \frac{1}{2} ReG'(\zeta_1) = 0.1456$$

We calculate the gain in the structures of Figs. 8a, 28, 29, using Eqs. (III-50), (V-A31) and (V-A34) to calculate the interaction impedances. The frequency of operation is chosen to be

$$\omega = 5.04 \times 10^{13} \text{ rad/sec}$$

Since the frequency is quite close to the plasma frequency a free carrier plasma correction to the dielectric constant was considered. Consequently using $n = 2.07$ for the average index of the waveguides in Figs. 28,29. In calculating the total attenuation we notice that both the first and -1 order harmonics contribute attenuations which add up.

The results of the calculations indicate considerable attenuation due to the phase matched interaction of the electromagnetic wave via the -1 and first order space harmonics. This attenuation may be superimposed on free carrier attenuation of the fundamental harmonic. However, unlike the fundamental free carriers attenuation the traveling wave attenuation occurs only at the phase matching condition (Eq. V-34). Hence it can be detected as a strong dip in the structure transmission when some parameter (like v_o or ω) is scanned about the phase matching condition (V-34).

Table 26. Example of Attenuation

at Plasma-EM Wave Phase Matching Condition

Parameter	Ge	GaAs	Unit
m/m_e	0.55	0.08	----
v_o	0	0	cm/sec
v_{th}	1.39×10^7	3.64×10^7	cm/sec
β_1	1.58×10^6	6.02×10^5	cm^{-1}
k_D	4.13×10^6	1.58×10^6	cm^{-1}
ω_p	4.06×10^{13}	4.06×10^{13}	rad/sec
n_o	4×10^{18}	6.7×10^{17}	cm^{-3}
T	350	350	°K
L	398	1044	Å
Fig. 8a ($d=1/\beta_1$)			
g_1	66.36	174	cm^{-1}
g_{-1}	56.11	147.13	cm^{-1}
$g=g_1+g_{-1}$	122.47	321.13	cm^{-1}
Fig. 28 ($\phi=30°$ $n^2_{L1}/n^2_{L0}=0.1$, $n_g=2.07$)			
$g=2g_1$	142.6	142.6	cm^{-1}
Fig. 29 ($\phi=90°$ $n^2_{L1}/n^2_{L0}=0.1$, $n_g=2.07$)			
$g=2g_1$	493.8	493.8	cm^{-1}

Let us check the sensitivity of the attenuation to changes from the phase matching condition. Assume that $\zeta_1 >> 1$ and that the phase matching condition (V-34) is satisfied for ζ_1. Then using (V-28)

$$\frac{g(\zeta_1+\Delta\zeta)}{|g(\zeta_1)|} = \alpha \frac{\mathrm{ImG}'(\zeta_1+\Delta\zeta)}{\left[1 - \frac{1}{2}\frac{k_D^2}{\beta_1^2}\mathrm{ReG}'(\zeta_1+\Delta\zeta)\right]^2 + \frac{1}{4}\frac{k_D^4}{\beta_1^4}[\mathrm{ImG}'(\zeta_1+\Delta\zeta)]^2} \frac{\frac{1}{4}\frac{k_D^4}{\beta_1^4}[\mathrm{ImG}'(\zeta_1)]^2}{\alpha\ \mathrm{ImG}'(\zeta_1)}$$

substituting $1/2\ k_D^2/\beta_1^2 = 1/\mathrm{ReG}'(\zeta_1)$

$$\frac{|g(\zeta_1+\Delta\zeta)|}{|g(\zeta_1)|} = \frac{\mathrm{ImG}'(\zeta_1)\mathrm{ImG}'(\zeta_1+\Delta\zeta)}{[\mathrm{ReG}'(\zeta_1+\Delta\zeta) - \mathrm{ReG}'(\zeta_1)]^2 + [\mathrm{ImG}'(\zeta_1+\Delta\zeta)]^2} \qquad \text{(V-57)}$$

Expand $G'(\zeta_1+\Delta\zeta)$ about ζ_1

$$\mathrm{ReG}'(\zeta_1+\Delta\zeta) = \mathrm{ReG}'(\zeta_1) + \mathrm{ReG}''(\zeta_1)\Delta\zeta \qquad \text{(V-58)}$$

$$\mathrm{ImG}'(\zeta_1+\Delta\zeta) = \mathrm{ImG}'(\zeta_1) + \mathrm{ImG}''(\zeta_1)\Delta\zeta \qquad \text{(V-59)}$$

The first order term in the expansion of $\mathrm{ImG}'(\zeta_1+\Delta\zeta)$ is negligible relative to the zero order term for

$$\zeta_1\Delta\zeta << 1 \qquad \text{(V-60)}$$

Substitution in (V-57) results in this limit in a Lorentzian function dependence

$$\frac{|g(\zeta_1+\Delta\zeta)|}{|g(\zeta_1)|} = \frac{1}{1 + (\Delta\zeta/\delta)^2} \qquad \text{(V-61)}$$

where

$$\delta \equiv \frac{\mathrm{ImG}'(\zeta_1)}{\mathrm{ReG}''(\zeta_1)} \qquad \text{(V-62)}$$

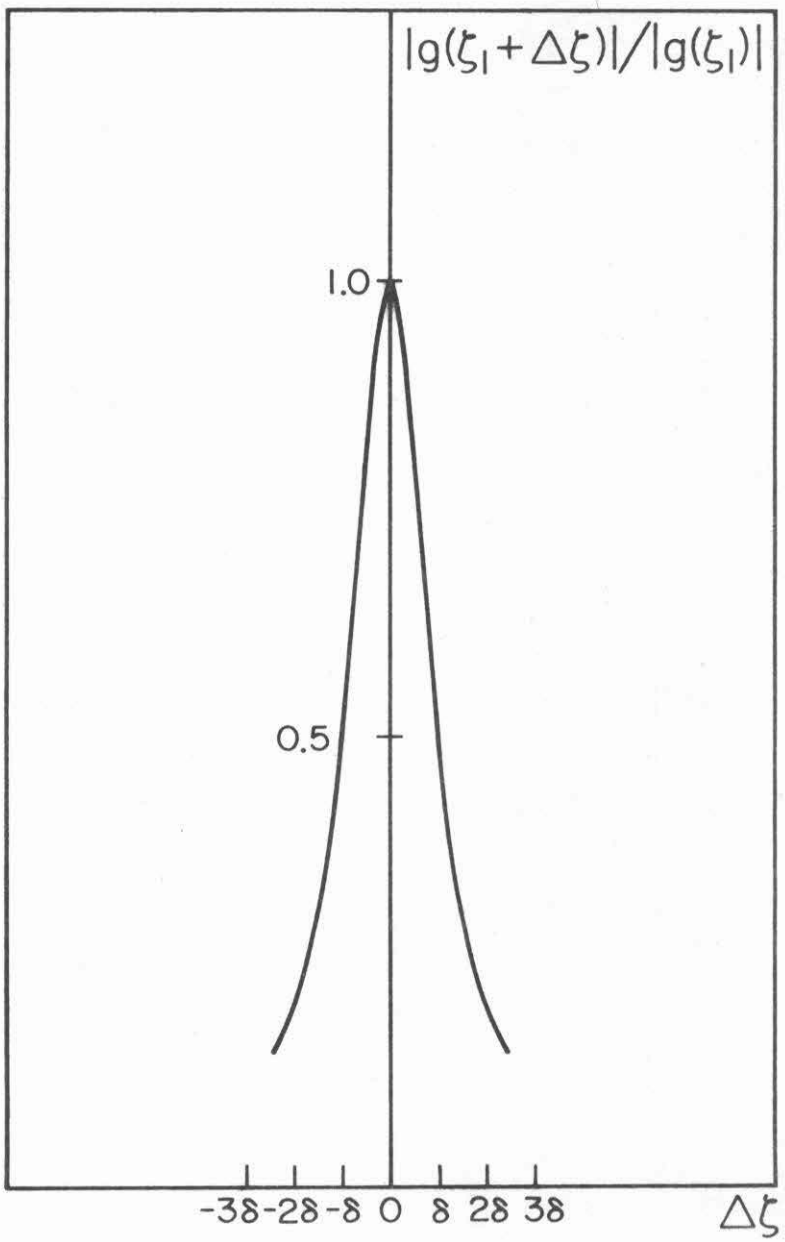

Fig. 27 Lorentzian function describing the relative attenuation as a function of deviation from the plasma-electromagnetic wave phase matching condition $\Delta\zeta(=-\Delta v_o/v_{th}$ or $\Delta\omega/(\beta_1 v_{th}))$.

The function $G''(\zeta_1)$ can be expressed in terms of the tabulated functions $G(\zeta_1)$ and $G'(\zeta_1)$ by differentiating the identity [Fried and Conte 1971]

$$G' = -2(1 + \zeta G) \tag{V-63}$$

which yields

$$G'' = -2(G + \zeta G') \tag{V-64}$$

A standard Lorentzian (Eq. V-61) is plotted in Fig. 27 as a function of the deviation from phase matching $\Delta\zeta$. If the change is caused by changing the drift velocity (see V-26) then

$$\Delta\zeta = -\frac{\Delta v_o}{v_{th}} \tag{V-65}$$

If it is caused by changing the frequency then

$$\Delta\zeta = \frac{\Delta\omega}{\beta_1 v_{th}} \tag{V-66}$$

The Lorentzian width δ (Eq. V-62) can be made very small for $\zeta_1 >> 1$ since $\mathrm{Im}G'(\zeta_1)$ decays strongly like a Gaussian, while $\mathrm{Re}G''(\zeta_1)$ decays asymptotically only like $1/\zeta_1^3$. In the example considered in this section $\zeta_1 = 2.3$ which corresponds to

$$\delta = 0.12$$

A change of 100% in the exponential gain constant (0.4343 gl db change in attenuation) is brought about by $\Delta\zeta = \delta/3 = 0.04$. Using the parameters of Table 26 we find that this corresponds to a driving current with drift velocity

$$\Delta v_o = v_o = 5.56 \times 10^5 \text{cm/sec (Ge)} \quad v_o = 1.46 \times 10^6 \text{cm/sec (GaAs)}$$

or to changing the frequency by

$$\frac{\Delta\omega}{\omega} = 0.017$$

The sensitivity of this effect to small changes should make its experimental observation easier. Also notice that the physical conditions required in Table 26 are much more convenient than those required in the previous examples.

From the device application point of view the sensitive control on the transmission at high values of the parameter ζ_1, looks attractive for use in modulation devices in the far infrared regime. Such a device may operate by changing the voltage across it so that the drift velocity of the carriers changes,and the device transmission changes. Contrary to modulators based on free carrier absorption by injected carriers [Moss 1962, Deb 1966, Benoit 1970] which are limited in speed by the minority carriers lifetime, this device is a majority carriers device and hence may operate as a high speed modulator.

6. The Effect of Collisions

In this chapter we presented traveling wave analysis in the collisionless regime ($\tau\to\infty$) only. A more general approach would include a collision term in the Boltzmann equation (V-1)

$$\frac{\partial f_1}{\partial t} + u\frac{\partial f_1}{\partial z} - \frac{e}{m}E\frac{\partial f_o}{\partial u} = \left(\frac{\partial f_1}{\partial t}\right)_{coll} \qquad (V\text{-}67)$$

$(\partial f_1/\partial t)_{coll}$ is the rate at which the number of particles in the class of particles with velocity u changes due to collisions. Collisions can

occur due to two particles interaction as well as interaction with impurities, phonons and other excitations.

The collision rate function $(\partial f_1/\partial t)_{coll}$ is usually very complicated. However it is quite customary to assume that it is independent of velocity and can be described by a phenomenological collision relaxation time parameter τ [Pines 196]]

$$(\frac{\partial f_1}{\partial t})_{coll} = - \frac{f_1}{\tau} \qquad \text{(V-68)}$$

τ in semiconductors is in the order of magnitude of $10^{-13} \div 10^{-12}$ sec at room temperature. The difficulty in this approximation is that it does not conserve particles. When we integrate (V-67) with (V-68) used, we get a contradiction to the continuity equation. We get that the total number of particles reduces in a rate corresponding to the collision relaxation time τ. The reason for this discrepancy is that the approximation (V-68) does not take into account the fact that particles, which are scattered from one class of velocities, will populate other classes and will not be scattered out of the system. A formal correction of this discrepancy was suggested by Bhatnagar et. al. [1954] (see also [Steele 1969, p. 123]). The limited validity of these approximations is sometimes not too disturbing, especially if the collision term is small, or when we deal with effects in which only a particular class of particle velocities participate.

Taking advantage of the simplicity of expression (V-68) we can use this approximation to extend our analysis and include collisions effect. When (V-68) is substituted in (V-67) and we apply Laplace and

Fourier transforms as in Section 2 we get instead of (V-5)

$$(i\omega - i\beta u + \frac{1}{\tau})f_1(\beta,u) = \frac{e}{m} E(\beta) f_o'(u) \tag{V-69}$$

Instead of the infinitesimal $\eta' u \equiv \beta\eta$ in Eq. (V-5) we get a finite $1/\tau$. We can simply extend our derivation to this case by substituting everywhere

$$\beta\eta = \frac{1}{\tau} \tag{V-70}$$

Hence ζ is automatically complex (V-21) and has nonvanishing negative imaginary part

$$\zeta = \frac{\omega/\beta - v_o}{v_{th}} - i \frac{1}{\tau\beta v_{th}} \tag{V-71}$$

$$Im\zeta < 0 \tag{V-72}$$

There is now no conceptual difficulty in the integration of Eq. (V-8) or (V-18) since there is no singularity along the line of integration.

Eqs. (V-28,29) still apply the way they are, but the imaginary and real parts of $G'(\zeta_1)$ are not given by Eq. (V-30) but instead we get from (V-18)

$$G'(\zeta_1) = \int_{-\infty}^{\infty} g'(x) \frac{x-\zeta_1^R}{(x-\zeta_1^R)^2+(\zeta_1^I)^2} dx - i\pi \int g'(x) \frac{|\zeta_1^I|/\pi}{(x-\zeta_1^R)^2+(\zeta_1^I)^2} dx \tag{V-73}$$

where

$$\zeta_1^R = \frac{\omega/\beta_1 - v_o}{v_{th}} \tag{V-74}$$

$$\zeta_1^I = \frac{1}{\tau\beta_1 v_{th}} \tag{V-75}$$

The effect of the collisions on $ImG'(\zeta_1)$ is such that instead of being proportional to $g'(\zeta_1)$ it is proportional to its convolution

with a standard normalized Lorentzian centered at $x = \zeta_1^R$, and of half width $|\zeta_1^I| \equiv 1/(\tau\beta_1 v_{th})$. The "smearing" effect of the convolution will not hurt very much in operation at the regime where Eq. (V-33) applies, and for small enough values of $|\zeta_1^I|$ there will be only a moderate reduction in $\mathrm{Im}G'(\zeta_1)$. The case of phase matched plasma electromagnetic wave interaction (Eqs. V-34-36) is much more sensitive to the presence of collisions. In this case the gain (or attenuation) is inversely proportional to the imaginary part of $G'(\zeta_1)$ (Eq. V-35), which with the absence of collisions goes strongly to zero for $\zeta_1 >> 1$. The convolution in (V-73) will cause $\mathrm{Im}G'(\zeta_1)$ to go to zero more slowly, thus resulting in lower gain or attenuation. The peak of the phase matched interaction gets wider then as well as lower (Eq. V-62), and so the attenuation due to a phase matched plasma-electromagnetic wave coupling is less sensitive to deviations from the phase matching condition (Eq. V-34), and the efficiency of the effect as a modulation process is reduced.

The criterion for ignoring collision effect is $\zeta_1^I << 1$ or

$$(\omega\tau)\ \frac{v_{th}}{(\omega/\beta_1)}\ >>1 \qquad \text{(V-76)}$$

This is somewhat different from the customary criterion $\omega\tau >> 1$ and indicates that this condition is harder to meet at high values of ζ_1. At the limit $\zeta_1^I \to 0$ the Lorentzian function in Eq. (V-73) turns into a Dirac delta function $\delta(x-\zeta_1^R)$, and the whole expression reduces into Eq. (V-30).

For a specific distribution function g(x), the function $G'(\zeta_1)$

is explicitly defined by Eq. (V-73). For the case of Maxwellian distribution (Eq. V-55) the integrals in the expression do not reduce into immediate integrals and the real and imaginary part of the plasma dispersion function must be computed numerically. For numerical computation of $G'(\zeta)$ in the complex field, a continued fraction iteration scheme presented previously by Burrell [1974] provides better convergence and accuracy than the numerical integration of Eq. (V-73) (see also Appendix VI-B).

Appendix V-A. Discussion on Interaction Impedances of Periodic Semiconductor Structures

The main purpose of the present work is to investigate different wave interaction mechanisms in periodic structures and to analyze them in different regimes and at different applications. Of particular interest is the traveling wave interaction between electrons and electromagnetic waves which is investigated here in different operation regimes.

Although the investigation of the interaction mechanisms is the primary goal, we try also to suggest some possible structures where the interaction can take place. In order to be able to estimate the interaction strength in the different regimes we must have in each case an estimate of the structure interaction impedance (Eq. III-28). Unfortunately the calculation of the interaction impedance and its optimization is often a very tedious and lengthy electromagnetic problem which we would like to avoid in the present work, as long as we can get at least a rough estimate of this parameter so that we can estimate the strength of the interaction.

In Chapter III we calculated the interaction impedance of a suggested slow wave structure (Fig. 8), utilizing the solution of the electromagnetic wave in a similar structure (Fig. 2) which was presented in Chapter II. Although the calculation is approximate and has limited validity when the corrugation depth a is large, it served satisfactorily in the estimation of the traveling wave interaction in the collision dominated regime (Chapter IV). However at the interaction regime which is investigated in the present chapter we have interest in operation

conditions in which the suggested structure is not efficient, or that the assumptions used to calculate the interaction impedance are not satisfied. In addition, some of the structural parameters which are required (like the corrugation period) become difficult to realize technologically.

A severe violation of the assumptions used in calculating the interaction impedance of the structure in Fig. 8a (Appendix III-B, Fig. 9) takes place when

$$\omega_p > \omega \qquad \text{(V-A1)}$$

since under this condition the free carriers effect on the real part of the dielectric constant in the conducting layer is not negligible. In the collisionless limit ($\omega\tau >> 1$) the real part of the dielectric constant (Eq. IV-B9) is:

$$\bar{\varepsilon}_r = \left(1 - \frac{\omega_p^2}{\omega^2}\right)\varepsilon \qquad \text{(V-A2)}$$

which is a negative number at condition (V-A1). However, in calculating the interaction impedance we assumed that the dielectric constant in the waveguide is $\varepsilon = n_g^2\varepsilon_o$, and that the fundamental space harmonic is equal to the solution of the three layer homogeneous waveguide (Fig. 2, a = 0).

The discrepancy at operating condition (V-A1) is a pertinent concern in this work. As it was noted in Section 3, appreciable gain can be achieved when phase matched photon-plasmon coupling is attained. A necessary condition to attain this coupling is $k_D >> \beta_1$. If we also expect gain the Cerenkov condition (Eq. V-32) should be satisfied $v_o > \omega/\beta_1$. Using the definition $k_D = \sqrt{2}\,\omega_p/v_{th}$ (Eq. V-20) this means

$$\omega_p >> \sqrt{2}\,\frac{v_{th}}{v_o}\,\omega \qquad \text{(V-A3)}$$

Since it is hard to get the drift velocity v_o appreciably larger than the thermal velocity, it means that usually when we want to get plasmon-photon coupling, we must operate at the troublesome regime (V-A1).

If one wants to calculate the interaction impedance in this case correctly then the solution of a four layer unperturbed waveguide (Fig. 8a with a = 0) must be found first, where the layers have relative dielectric constants as follows:

substrate - n_s^2

waveguide - n_g^2

collisionless plasma layer (thickness d) -

$$\varepsilon_L^R \equiv \frac{\bar{\varepsilon}_L}{\varepsilon_o} = \left(1 - \frac{\omega_p^2}{\omega^2}\right) n_g^2 < 0 \qquad \text{(V-A4)}$$

superstrate - n_a^2

and then the analysis of Chapter II should be repeated, in order to find the amplitudes of the space harmonics in this waveguide.

This calculation will not be attempted in the present work. We may see though without elaborate calculation that the effect of the plasma layer is to cause strong decay of the electromagnetic mode inside the layer. From Maxwell equations, an expression similar to (II-A24) is readily attained for the transverse decay parameter in the plasma layer:

$$\eta^2 = \beta^2 - \varepsilon_L^R k^2 = \beta^2 + |\varepsilon_L^R| k^2 \qquad \text{(V-A5)}$$

If $\omega_p >> \omega$ then from (V-A4) :

$$|\varepsilon_L^R| \simeq n_g^2 \frac{\omega_p^2}{\omega^2} \tag{V-A6}$$

$$\eta \simeq \frac{\omega_p}{\omega} n_g k = n_g \frac{\omega_p}{c} \tag{V-A7}$$

and

$$\eta >> n_g k > \beta, \gamma, h \tag{V-A8}$$

The effect will be that the mode will have suppressed amplitude at the corrugated surface of the waveguide (Fig. 8a) and will "sense" less the periodic corrugation. On the other hand, the first order Fourier coefficient is in this case

$$n_{L1}^2 = \frac{2}{\pi} (n_a^2 + |\varepsilon_L^R|) \tag{V-A9}$$

instead of Eq. (II-5). This is working towards increasing the amplitude of the first order space harmonic, and since the plasma layer can be very thin, the mode does not decay significantly through the plasma layer. Thus the final result may even be some improvement of the interaction impedance.

The Structure in Fig. 8b

With some approximative assumptions it may be possible to readily find the interaction impedance of the structure in Fig. 8b in the regime (V-A1) and to use it for the demonstration of examples in this regime.

To simplify the calculation, we will assume that the thickness d of the epitaxial layer is large enough so that the mode does not penetrate at all into the air medium. In this case we can apply the previous

derivation of $K_{\pm 1}(0^+)$ (Eq. III-43) and just use ε_L^R (Eq. V-A4) instead of n_a^2 for the relative dielectric constant of the superstrate. In this case we have instead of (II-A7):

$$\gamma^2 = \beta^2 - \varepsilon_L^R k^2 = \beta^2 + |\varepsilon_L^R| k^2 \approx$$

$$\beta^2 + n_g^2 \frac{\omega_p^2}{\omega^2} k^2 = \beta^2 + n_g^2 \frac{\omega_p^2}{c^2} \qquad \text{(V-A10)}$$

If $\omega_p >> \omega$ then

$$\gamma >> n_g \frac{\omega}{c} = n_g k > \beta, \gamma, h \qquad \text{(V-A11)}$$

and

$$\gamma \simeq n_g \frac{\omega_p}{c} \qquad \text{(V-A12)}$$

Using Eq. (V-A11) we can neglect the first term $g_1\beta_o$ inside the parentheses of Eq. (III-43) and thus avoid the difficulty resulting from the fact that g_1 (Appendix II-B) is not well defined for $\varepsilon_L^R < 0$. We obtain

$$K_{\pm 1}(0^+) = \frac{2}{n_g^4} \sqrt{\frac{\mu}{\varepsilon_o}} \frac{h_o^2 a^2}{\beta_o k t_{eff} w} \left(\frac{n_{L1}^2}{n_{L0}^2} \right)^2 \qquad \text{(V-A13)}$$

Under the present conditions the mode does not penetrate appreciably into the substrate and the superstrate which behave almost like metal reflectors (with skin effect field penetration). Assuming that the field is limited to the waveguide core we get (following Appendix II-A)

$$t_{eff} = t/n_g^2$$

and

$$h_o = n_g k \sin \phi \qquad \text{(V-A14)}$$

$$\beta_o = n_g k \cos\phi \qquad \text{(V-A15)}$$

where ϕ is the "zigzag angle" of the mode propagation. Eq. (V-A13) can then be written as

$$K_{\pm 1}(0^+) = \frac{2}{n_g}\sqrt{\frac{\mu}{\varepsilon_o}}\,\frac{a^2}{tw}\,\frac{\sin^2\phi}{\cos\phi}\left(\frac{n_{L1}^2}{n_{L0}^2}\right)^2 \qquad \text{(V-A16)}$$

where

$$n_{L1}^2 = \frac{2}{\pi}(n_g^2 - \varepsilon_L^R) = \frac{2}{\pi}(n_g^2 + |\varepsilon_L^R|) \qquad \text{(V-A17)}$$

$$n_{L0}^2 = \frac{1}{2}(n_g^2 + \varepsilon_L^R) = \frac{1}{2}(n_g^2 - |\varepsilon_L^R|) \qquad \text{(V-A18)}$$

and when $|\varepsilon_L^R| >> n_g^2$ we may get $(n_{L1}^2/n_{L0}^2)^2 \simeq 1$.

The Structure in Fig. 28.

The structure in Fig. 28 is an elementary example of periodic dielectric waveguide and easy to solve. By calculating its interaction impedance we can get another estimate of available and reasonable values for the interaction impedance in periodic semiconductor waveguide structures. Since the model is simpler we can proceed with fewer approximations and get a reliable estimate.

This structure has few other advantages. It provides an example of a case where the traveling wave interaction analysis of Section 2, Chapter IV holds as a good approximation. Since the periodic perturbation of the wave is distributed across the waveguide cross section, the tranverse profile of the space harmonics is moderately varying and the one dimensional model of Chapter IV holds well. In

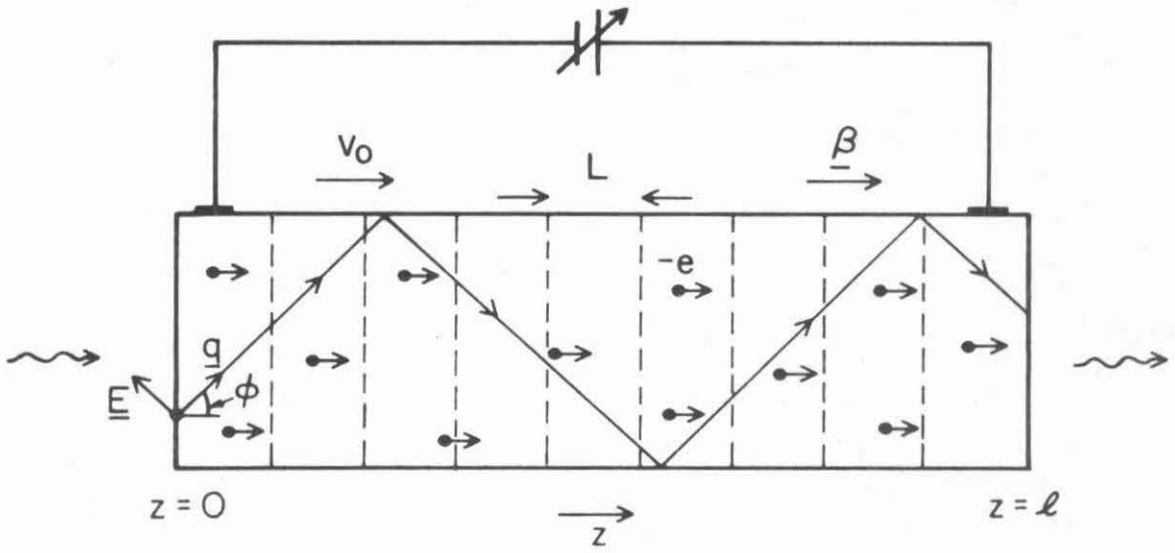

Fig. 28 A structure for solid state traveling wave amplifier with "bulk modulation" of the dielectric constant.

addition, this structure is expected to be more efficient, since interaction can take place all across the waveguide (and not in a narrow conducting layer as in Fig. 8).

The fabrication of this structure is difficult to accomplish with today's technological state of the art. The techniques of semiconductor corrugation and epitaxial growth [Garvin 1973, Nakamura 1974] could be used for this purpose if the technique of deep preferential etching [Kendall 1975] would be further developed. The development of the technique for superlattice growth by molecular beam epitaxy [Blakeslee 1970B, Alferov 1971, Woodall 1972, Chang 1973] may lend itself to the production of such structures with periods as short as 100Å which cannot be achieved today with the other techniques and the structures of Fig. 8.

We will calculate the interaction impedance of this structure starting from first principles. To do this we have to solve first the electromagnetic wave propagation problem in the structure of Fig. 28, and in particular to find the amplitude of the first and -1 order space harmonics. Let us further simplify the problem, assuming that the modes are well confined and can be described by two plane waves "zigzagging" along the waveguide by multiple reflection from the boundaries. The problem will then be equivalent to the problem of single plane wave traveling into a transversely unbound periodic stratified media. The angle that the propagation parameter of the plane wave $\underline{q}$ forms with the periodicity direction z, is equal to the "mode zigzag angle" ϕ.

In the periodic medium the electromagnetic field has a Floquet form

$$\underline{E}(\underline{r}) = \sum_m \underline{E}_m e^{i(\omega t - \underline{q}_m \underline{r})} \tag{V-A19}$$

where

$$\underline{q}_m = \underline{q}_o + m \frac{2\pi}{L} \hat{e}_z \qquad (m = 0, \pm 1, \pm 2, \ldots) \tag{V-A20}$$

where L is the period, $\hat{e}_z$ is a unit vector in the z direction, and

$$|\underline{q}_o| \simeq |\underline{q}| = n_g k = n_g \frac{\omega}{c} \tag{V-A21}$$

The first order Fourier expansion of the relative dielectric constant $\varepsilon^R \equiv \varepsilon/\varepsilon_o$ is

$$\varepsilon^R(z) = \varepsilon_o^R + \varepsilon_1^R \cos \frac{2\pi}{L} z \tag{V-A22}$$

where (compare Eqs. II-1-5)

$$\varepsilon_o^R = n_{LO}^2 \tag{V-A23}$$

$$\varepsilon_1^R = n_{L1}^2 \tag{V-A24}$$

The longitudinal field component can be calculated from the Poisson equation

$$\nabla \cdot [\varepsilon(z) \underline{E}(\underline{r})] = 0 \tag{V-A25}$$

By substituting Eqs. (V-A19, A22) in (V-A25) and using the orthogonality of the Fourier expansion we get

$$\varepsilon_o^R \, \underline{q}_m \underline{E}_m + \frac{1}{2} \varepsilon_1^R (\underline{q}_m \underline{E}_{m-1} + \underline{q}_m \underline{E}_{m+1}) = 0 \tag{V-A26}$$

We substitute in turn m = 1 and m = -1 in Eq. (V-A26) and assume that higher order space harmonics are negligible $|\underline{q}_{\pm 1}\cdot\underline{E}_{\pm 2}| << |\underline{q}_{\pm 1}\cdot\underline{E}_{o}|$. Also we assume that $2\pi/L >> |\underline{q}_{o}|$ so that

$$\underline{q}_{\pm 1} \simeq \underline{\beta}_{\pm 1} \equiv (\underline{q}_{\pm 1}\cdot\hat{e}_z)\hat{e}_z \tag{V-A27}$$

is in the z direction. Then we get from (V-A26)

$$E_{z\pm 1} \simeq -\frac{1}{2}\frac{\varepsilon_1^R}{\varepsilon_o^R} E_{z\,o} \tag{V-A28}$$

The electromagnetic mode power which is carried through a cross section S perpendicular to $\hat{e}_z$ is approximated by the power of the zero order space harmonic (which is approximately a plane wave)

$$\underline{P} = \frac{n_g}{2}\sqrt{\frac{\mu}{\varepsilon_o}}\, E_o^2 \cos\phi\, S \tag{V-A29}$$

Eqs. (V-A28, A29) and the relation

$$E_{z\,o} = E_o \sin\phi \tag{V-A30}$$

can now be substituted in the expression for the interaction impedance (III-28), resulting in

$$K_{\pm 1} = \frac{1}{n_g}\sqrt{\frac{\mu}{\varepsilon_o}}\;\frac{1}{S\beta_1^2}\,\frac{\sin^2\phi}{\cos\phi}\left(\frac{\varepsilon_1^R}{\varepsilon_o^R}\right)^2 \tag{V-A31}$$

There is striking similarity between Equations (V-A31) and (V-A16). In fact this similarity is even more apparent if we recall that the corrugation depth a is limited to (IV-68)

$$a = \frac{L}{2} \simeq \frac{\pi}{\beta_1} \tag{V-A32}$$

If this is used in Eq. (V-A16) together with the identities of Eqs. (V-A23, A24) and $S \equiv wt$ we get

$$K_{\pm 1}(0^+) = \frac{2\pi^2}{n_g} \sqrt{\frac{\mu}{\varepsilon_o}} \frac{1}{S\beta_1^2} \frac{\sin^2\phi}{\cos\phi} \left(\frac{\varepsilon_1^R}{\varepsilon_o^R}\right)^2 \qquad \text{(V-A33)}$$

which is different from Eq. (V-A31) only by a numerical factor $(2\pi^2)$.

This striking similarity between the expressions for the interaction impedance of very different structures is encouraging to believe that in spite of some crude approximations used through some of the derivations, the derived expressions have a physically sound dependence on parameters, which results from simple general considerations. Thus they can give numerical values which are reasonably representative of practical structures.

The Structure in Fig. 29

The technique of superlattice epitaxial growth by MBE (Molecular Beam Epitaxy) [Chang 1973, Dingle 1974] may make possible fabrication of periodic structures with periods in the order of 50-100Å [Esaki 1975] which is not presently attainable by other techniques. However fabrication of structures like those in Fig. 28 with a reasonable length is still unpractical with MBE techniques. A different version of this structure - Fig. 29 - is much more compatible with the MBE growth technique.

In this structure the periodicity and current flow direction is perpendicular to the electromagnetic mode propagation direction (z). Transverse traveling wave interaction is a mode of operation which is known also in conventional TWT amplifiers [Dunn 1956]. We would expect such a device to provide for more efficient interaction since the

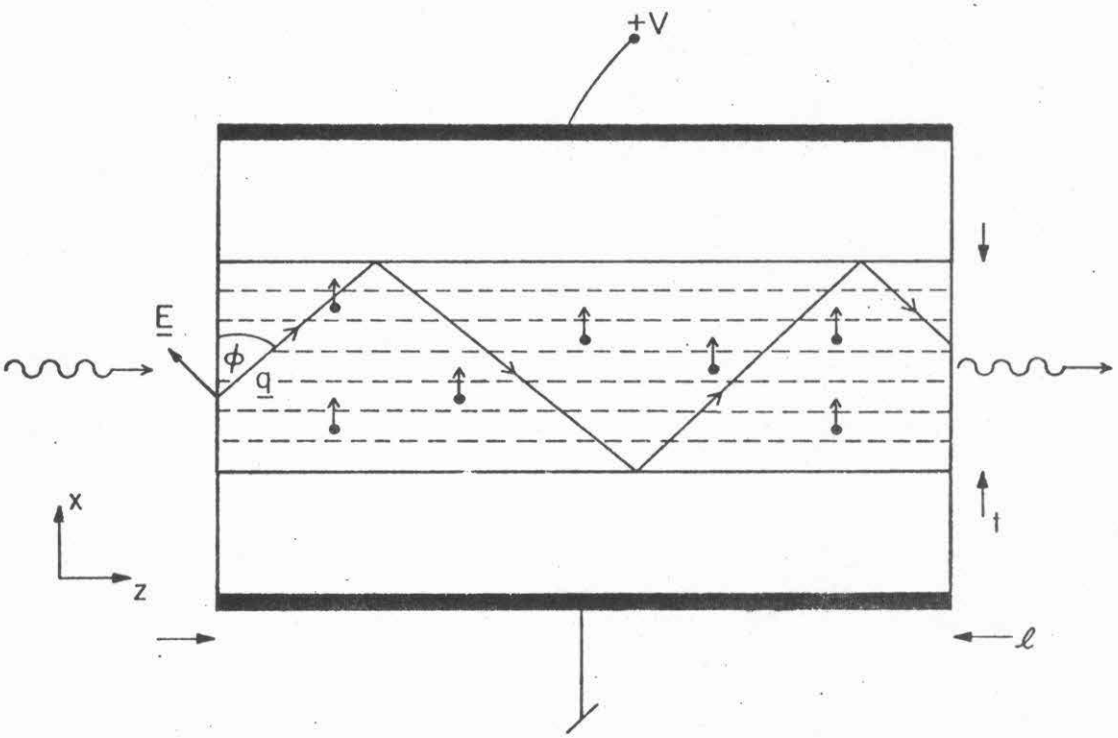

Fig. 29 A "superlattice" embodiment of solid state traveling wave amplifier.

electromagnetic field may have a larger component along the current flow direction.

The interaction in the structure of Fig. 29 can be analyzed by an entirely different approach from that of Section 2 Chapter IV. Since it is invariant to translation in the z direction, conventional waveguide coupled mode technique can be used to calculate the gain. However, in order to get just a reasonable estimate of the interaction impedance of this structure we can view the mode propagation in the structure as a zigzag propagation of a plane wave, and we assume that traversing this structure is equivalent to traversing multiple times a short segment of the structure in Fig. 28 whose length is t. (t is the waveguide width in Fig. 29.) So the gain of a structure like that in Fig. 29 whose length is ℓ equals the gain of the structure in Fig. 28 with length $t\cdot\ell/(t\cdot\tan\phi) = \ell/\tan\phi$, where $\ell/(t\cdot\tan\phi)$ is approximately the number of ray reflections from the waveguide boundaries. We conclude that the interaction impedance of the structure can be given by Eq. (V-A31) multiplied by a factor $1/\tan\phi$

$$K_{\pm 1} = \frac{1}{n_g}\sqrt{\frac{\mu}{\varepsilon_o}}\,\frac{1}{S\beta_1^{\,2}}\sin\phi\left(\frac{\varepsilon_1^R}{\varepsilon_o^R}\right)^2 \qquad \text{(V-A34)}$$

Notice that in order to conform with Fig. 28 the angle ϕ in Fig. 29 was chosen as the angle between the ray propagation direction and the periodicity or current flow direction (and not the z direction). S in Eq. (V-A34) is the cross section of the current (normal to the x orientation). It cancels out when the gain is calculated. An inherent assumption in the recent derivation was that the gain due to interaction of synchronous -1 order space harmonic is equal to that due to synchronous first order space harmonic. This is a justified assumption

since $|\beta_{-1}| \simeq \beta_1$ and $K_1 = K_{-1}$ in Eq. (V-A31).

Other Structures

The structures of Figs. 28, 29 may provide for more efficient interaction and they may be producible at short periods, but contrary to the structures in Fig. 8, they cannot operate (with gain) at the regime (V-A1) since at frequencies below the plasma frequency the electromagnetic wave will not penetrate at all into the waveguide. At this regime a combination of these two kinds of structures is proposed. For example, Fig. 30 shows a combination of the structure of Fig. 28 and a homogeneous dielectric waveguide. The periodic layer is doped by impurities to the extent that the plasma frequency exceeds the electromagnetic wave frequency (V-A1). Then the wave will propagate mostly in the undoped layer and will interact with the electrons through the skin effect evanescent tail. The thickness of the periodic layer is chosen to be approximately the decay depth of the mode in the plasma (see Eq. V-A12).

This structure is different from that of Fig. 8b in principle and in practice. In the structures of Fig. 8 we assumed that the periodic layer is very thin, and the interaction takes place out of the periodic layer in the evanescent tail of the space harmonic which decays at distance $L/2\pi$ from the corrugated surface. Conversely, in the structure of Fig. 30 the interaction takes place in the periodic layer itself. This layer is then as thick as the mode penetration depth and

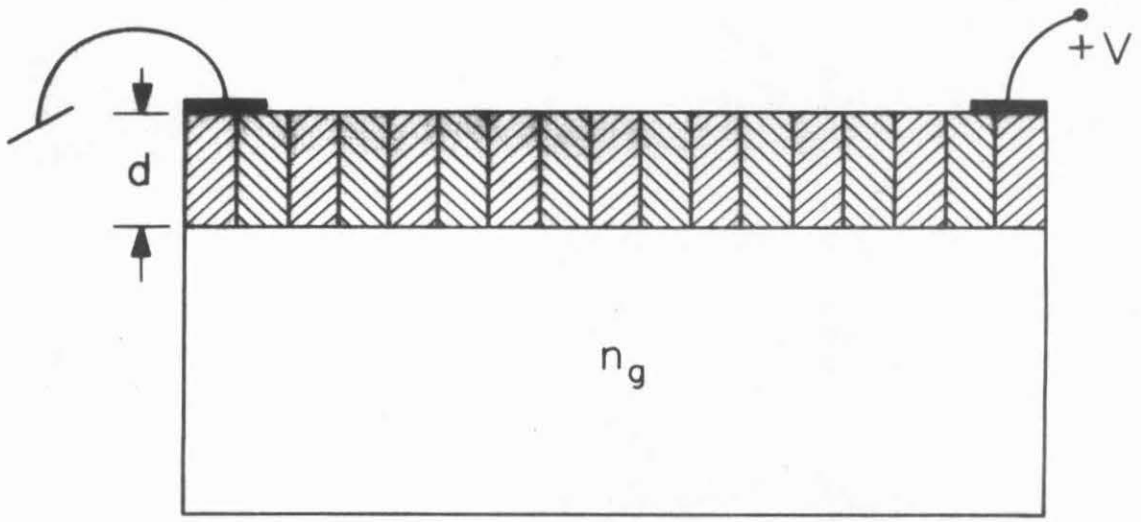

Fig. 30 A solid state traveling wave amplifier structure. The mode propagates mainly in the waveguide core (n_g), and the interaction takes place in the periodic layer whose thickness (d) is about the skin effect penetration of the mode.

may be much thicker than $L/2\pi$, thus providing more efficient interaction.

We will not attempt at present to calculate the interaction impedance of this structure.

The expressions that were derived for the interaction impedance of some of the periodic structures proposed here, allow rough estimate of the range of values to be expected, and will be used in the text for demonstrative examples.

CHAPTER VI

INTRABAND RADIATIVE TRANSITIONS IN PERIODIC STRUCTURES (TW INTERACTION IN THE QUANTUM REGIME)

1. Introduction

As indicated by the title of this chapter the familiar traveling wave interaction can be described in the quantum mechanical limit in quite different terms.

In the quantum mechanical limit the traveling wave interaction can be described as a stimulated radiative transition of a free electron. The transition involves photon emission (and consequently electromagnetic wave amplification) if the electron transition is from a high to a lower energy state, and it involves photon absorption (and consequently attenuation) if the transition is from a low energy state to a higher one.

As discussed in Chapter I, this process can be viewed as a three wave interaction involving the electron wave functions in the initial and final states and the electromagnetic wave. As we concluded there from quite general considerations (Eqs. I-5-7) the transition rate (essentially the Fermi golden rule) is appreciable only if energy and momentum are conserved during the transition

$$\mathcal{E}_{\underline{k}_i} - \mathcal{E}_{\underline{k}_f} = \hbar\omega \tag{VI-1}$$

$$\underline{k}_i - \underline{k}_f = \underline{q} \tag{VI-2}$$

We can show in a short derivation that in the case of free

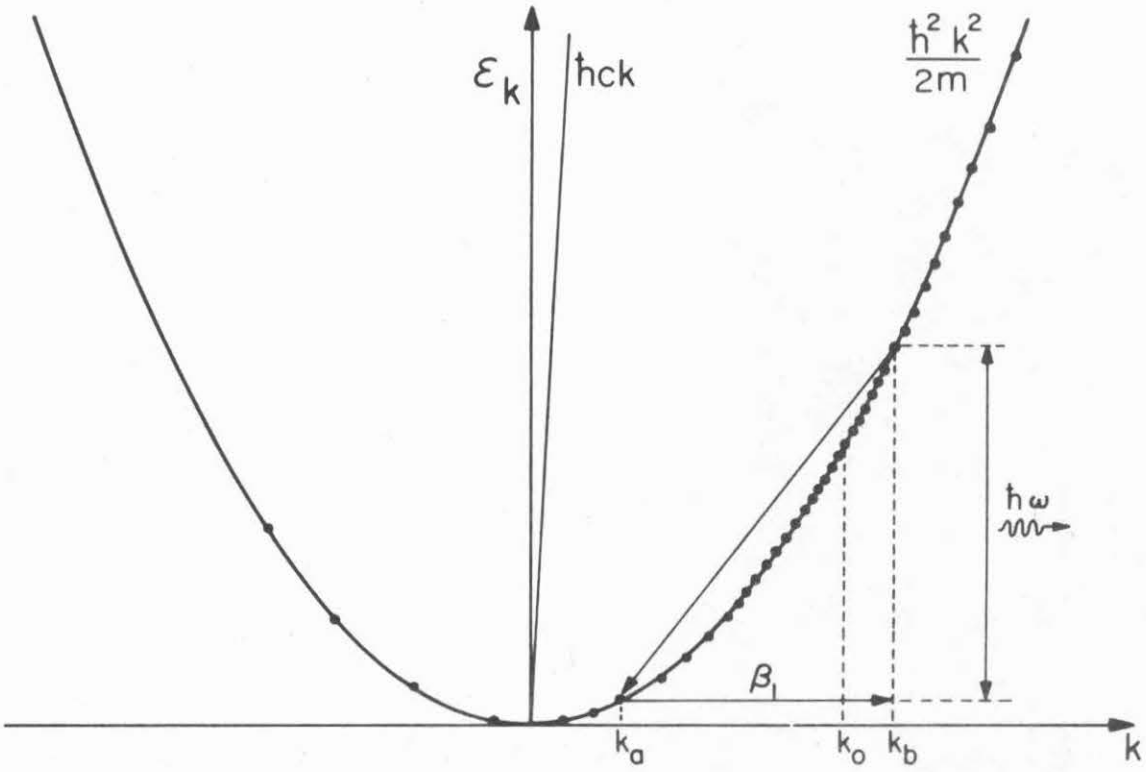

Fig. 31 Schematic intraband radiative transition in one dimension. The dots represent electron density. The oblique straight line is the dispersion function of a plane electromagnetic wave $\hbar\omega = \hbar ck$. Notice that the propagation parameter k of a plane wave is too small to account for the momentum change involved in the electronic transition.

electrons, simultaneous satisfaction of both conditions is not possible. Assume by way of contrast, that both conditions (VI-1,2) are satisfied. If $\mathcal{E}_{\underline{k}}$ is a continuous function of $\underline{k}$ with a continuous derivative, then a mathematical lemma assures the existence of a vectorial argument $\underline{k}^*$, such that $|\underline{k}^*|$ is bigger than the smaller of $|\underline{k}_i|$, $|\underline{k}_f|$ and smaller than the bigger of $|\underline{k}_i|,|\underline{k}_f|$, and

$$\mathcal{E}_{\underline{k}_i} - \mathcal{E}_{\underline{k}_f} = \nabla_{\underline{k}} \mathcal{E}_{\underline{k}} \Big|_{\underline{k}=\underline{k}^*} \cdot (\underline{k}_i - \underline{k}_f) \qquad \text{(VI-3)}$$

Substituting (VI-1) and (VI-2) and using the definition of the electron group velocity:

$$\underline{v}_{\underline{k}} = \frac{1}{\hbar} \nabla_{\underline{k}} \mathcal{E}_{\underline{k}} \qquad \text{(VI-4)}$$

we get

$$\omega = \underline{v}_{\underline{k}^*} \cdot \underline{q} \qquad \text{(VI-5)}$$

and consequently

$$|\underline{v}_{\underline{k}^*}| \geq \frac{\omega}{|\underline{q}|} = \frac{c}{n} \qquad \text{(VI-6)}$$

where c is the speed of light and n is the refraction index of the medium.

A situation like (VI-6) where the group velocity of the electron exceeds the speed of light is not possible in vacuum where n = 1. Excluding the case of very high energy (relativistic) electrons where inequality (VI-6) can exist inside matter (Cerenkov effect), we conclude that both Eqs. (VI-1,2) cannot be simultaneously satisfied.

This argument can be applied to free carriers in the conduction band (for electrons) or in the valence band (for holes). Intraband radiative transition cannot normally take place in a uniform medium, excluding of course, higher order transitions, which involve participation of additional waves like another photon or a phonon.

As was suggested in Chapter I, such intraband transitions are possible in an artificial periodic structure, where the "lattice momentum" of the structure is designed to provide the missing momentum needed to balance Eq. (VI-2), and makes the interaction possible. More specifically, the electromagnetic wave in the periodic structure assumes the Floquet form (I-8,9) which in the case of one dimensional periodicity in the z direction leads to

$$\underline{E}(\underline{r}) = \sum_m \underline{E}_m(x,y)e^{i(\omega t-\beta_m z)} \qquad \text{(VI-7)}$$

$$\beta_m = \beta_o + m\frac{2\pi}{L} \qquad \text{(VI-8)}$$

One of the space harmonics (say m = 1) may have a large enough propagation constant β_1 to balance the momentum equation (VI-2) and to allow an induced radiative transition at frequency ω. This process is illustrated schematically in Fig. 31.

In some of the periodic semiconductor structures discussed (Figs. 28-30), also the electron wave will have a Floquet-Bloch waveform, so that momentum conserving transitions can be possible involving the fundamental harmonic of the electromagnetic wave and higher space

harmonics of the initial or final electron waves* (compare this to the three waves interaction discussed in Section 2 of Chapter III in relation to nonlinear optical interaction). The analysis of traveling wave interaction through this mechanism is not attempted in the present work. We will assume that the periodic perturbation affects predominantly the electromagnetic wave. Indeed it is possible to have only the first mechanism present even in structures where the electrons pass through the periodic structure (like in Figs. 28-30). If the superlattice is produced by epitaxial growth of two alternating dielectric semiconductors we may get modulation of the dielectric constant. If the impurity doping level of the different layers is kept uniform, then the conduction band will "look" flat to an electron which traverses the device, and it will not be affected by the periodicity.

In the next sections we will present a more detailed analysis of the traveling wave interaction in the quantum mechanical regime, and get an estimate of the gain attainable by this process. The results, which were presented in the present section using general considerations, will follow explicitly from the analysis.

The one-dimensional analysis of traveling wave interaction presented in Section 2 of Chapter IV will be used here, but the expression for the plasma susceptibility which is used in that analysis will be derived quantum mechanically. We will study the interaction assuming a drifting Maxwellian, degenerate semiconductor (zero

---

*An alternative way to explain this mechanism is to present it as direct radiative transitions between extended Brillouin diagram minibands produced by the artificial periodic structure (superlattice).

temperature limit) and in presence of collisions. The effect of phase matched plasmon-photon coupling will be further discussed and some illustrative examples presented.

2. The Plasma Susceptibility

The quantum mechanical derivation of the free carrier plasma susceptibility was presented previously by several authors [Lindhard 1954]. We will basically follow the self-consistent field approach of Ehrenreich and Cohen [1959] or its extension to carriers in the crystal lattice [Adler 1962, Wiser 1963]. An MKS units system is used.

The Liouville equation for the electron density matrix ρ is

$$i\hbar \frac{\partial}{\partial t} \rho = [\mathcal{H}, \rho] \qquad \text{(VI-9)}$$

where $\mathcal{H}$ is the total single particle Hamiltonian of the free carriers, including the electromagnetic field contribution. Electrons in the conduction band of semiconductors are considered as free electrons with effective mass m

$$\mathcal{H} = \frac{1}{2m} (\underline{p} - e\underline{A}) + e\phi \qquad \text{(VI-10)}$$

where* $\underline{A} = \underline{A}(\beta)\exp i(\beta z-\omega t)$ is the electromagnetic vector potential. The scalar potential is set $\phi = 0$ by gauge choice. Neglecting second order terms in $\underline{A}$ we get

$$\mathcal{H} \simeq \mathcal{H}^{(0)} + \mathcal{H}^{(1)} \tag{VI-11}$$

$$\mathcal{H}^{(0)} \equiv \frac{1}{2m}\ \underline{p}^2 \tag{VI-12}$$

$$\mathcal{H}^{(1)} \equiv -\frac{e}{2m}\ (\underline{pA}+\underline{Ap}) \tag{VI-13}$$

The eigenmodes of the unperturbed Hamiltonian are

$$|\underline{k}\rangle = \frac{1}{\sqrt{v}}\ e^{\ i\underline{k}\underline{r}} \tag{VI-14}$$

satisfying

$$\mathcal{H}^{(0)}|\underline{k}\rangle = \mathcal{E}_{\underline{k}}|\underline{k}\rangle \tag{VI-15}$$

$$\rho^{(0)}|\underline{k}\rangle = f_o(\underline{k})|\underline{k}\rangle \tag{VI-16}$$

where $\mathcal{E}_{\underline{k}}$ is the electron energy in state $\underline{k}$, $\mathcal{E}_{\underline{k}} = \frac{\hbar^2}{2m}\ k^2$ for free electrons, $\rho^{(0)}$ and $f_o(k)$ are the density matrix and the quantum state occupation number (or the statistical distribution function) in the unperturbed system.

---

*This convention of time dependence was chosen in order to conform with the usual convention in quantum mechanics. However in the rest of this work we have assumed a time dependence $\exp(i\omega t)$, as customary in electromagnetic theory. The use of previously derived results in this context requires careful adaptation.

The density matrix can also be separated into zero and first order parts

$$\rho \simeq \rho^{(0)} + \rho^{(1)} \tag{VI-17}$$

where $\rho^{(1)}$ is the response to the perturbation $\underline{A}(\underline{r},t)$.

Substituting (VI-11,17) in (VI-9) we find that the perturbation $\rho^{(1)}$ satisfies

$$i\hbar \frac{\partial}{\partial t} \rho^{(1)} = [\mathcal{H}^{(1)},\rho^{(0)}] + [\mathcal{H}^{(0)},\rho^{(1)}] \tag{VI-18}$$

Once this equation is solved it can be used to calculate the current induced in the plasma

$$\underline{J}(\underline{r},t) = -e\, Tr[\rho^{(1)}\underline{J}^{(0)}_{op}(\underline{r}) + \rho^{(0)}\underline{J}^{(1)}_{op}(\underline{r},t)] \tag{VI-19}$$

where

$$\underline{J}^{(0)}_{op}(\underline{r}) \equiv \frac{1}{2}\left[\frac{\underline{p}_e}{m}\,\delta(\underline{r}-\underline{r}_e) + \delta(\underline{r}-\underline{r}_e)\frac{\underline{p}_e}{m}\right] \tag{VI-20}$$

and

$$\underline{J}^{(1)}_{op}(\underline{r}) \equiv -\frac{e}{m}\,\underline{A}(\underline{r},t)\delta(\underline{r}-\underline{r}_e) \tag{VI-21}$$

The detailed solution of this problem is presented in Appendix VI-A. It results in the following expression for the Fourier component of the current

$$\underline{J}(\underline{\beta},\omega) = i\,\frac{e^2 n_o}{m\omega}\,\underline{E}(\underline{\beta},\omega) - i\,\frac{e^2\hbar^2}{m^2 V\omega}\sum_{\underline{k}}\frac{f_o(\underline{k}+\underline{\beta}) - f_o(\underline{k})}{\hbar\omega - (\mathcal{E}_{\underline{k}+\underline{\beta}}-\mathcal{E}_{\underline{k}})+i\hbar\eta}\,x$$

$$(\underline{k}+\tfrac{1}{2}\underline{\beta})[(\underline{k}+\tfrac{1}{2}\underline{\beta})\cdot\underline{E}(\underline{\beta},\omega)] \tag{VI-22}$$

and particularly the longitudinal-longitudinal component is

$$J_z(\beta,\omega) = -i\omega \frac{e^2}{V\beta^2} \sum_{\underline{k}} \frac{f_o(\underline{k}+\underline{\beta}) - f_o(\underline{k})}{\hbar\omega - (\mathcal{E}_{\underline{k}+\underline{\beta}} - \mathcal{E}_{\underline{k}}) + i\hbar\eta'} E_z(\beta,\omega) \qquad \text{(VI-23)}$$

where $\underline{\beta} = \beta\hat{e}_z$ is in the z direction and we used

$$\underline{E} = i\omega\underline{A} \qquad \text{(VI-24)}$$

The plasma susceptibility χ_p defined by (IV-2) cannot be deduced by direct comparison to (VI-23) because of the different convention of time dependence. Appropriate conversion of Eq. (VI-23) to the previous convention is provided by taking the complex conjugate of Eq. (VI-23). We then get

$$\chi_p(\beta,\omega) = \frac{e^2}{V\beta^2} \sum_{\underline{k}} \frac{f_o(\underline{k}+\underline{\beta}) - f_o(\underline{k})}{\hbar\omega - (\mathcal{E}_{\underline{k}+\underline{\beta}} - \mathcal{E}_{\underline{k}}) - i\hbar\eta'} \qquad \text{(VI-25)}$$

consistently with $\exp(i\omega t)$ time dependence convention as used in the previous chapters.

Eq. (VI-25) is the conventional longitudinal susceptibility of free electron gas [Lindhard 1954]. Substituting $\sum_{\underline{k}} \to V/(2\pi)^3 \int d^3k$, it can be represented in an integral form

$$\chi_p(\beta,\omega) = \frac{1}{(2\pi)^3} \frac{e^2}{\beta^2} \int d^3k \frac{f_o(\underline{k}+\underline{\beta}) - f_o(\underline{k})}{\hbar\omega - (\mathcal{E}_{\underline{k}+\underline{\beta}} - \mathcal{E}_{\underline{k}}) - i\hbar\eta'} \qquad \text{(VI-26)}$$

3. The Gain in Traveling Wave Interaction

Expression (VI-26) can now be used in the dispersion equation of the coupled electromagnetic-plasma waves (Eq. IV-9) with $f_o(\underline{k})$ representing the distribution function of the drifting carriers. This dispersion equation was solved in Chapter IV in a first order approximation which resulted in the change in the propagation constant of the traveling electromagnetic wave due to its interaction with the plasma (Eq. IV-10). The imaginary part of this propagation constant is (Eq. IV-11)

$$\mathrm{Im}\beta = \frac{1}{2} K_1 S \beta_1^2 \frac{\mathrm{Im}\chi_p}{\left|1 + \chi_p(\omega,\beta_1)/\varepsilon\right|^2} \tag{VI-27}$$

Using (VI-26)

$$\mathrm{Re}\chi_p = \frac{1}{(2\pi)^3} \frac{e^2}{\beta_1^2} (p) \int d^3k \frac{f_o(\underline{k}+\underline{\beta}_1) - f_o(\underline{k})}{\hbar\omega - (\mathcal{E}_{\underline{k}+\underline{\beta}_1} - \mathcal{E}_{\underline{k}})} \tag{VI-28}$$

$$\mathrm{Im}\chi_p = \frac{\pi}{(2\pi)^3} \frac{e^2}{\beta_1^2} \int d^3k [f_o(\underline{k}+\underline{\beta}_1) - f_o(\underline{k})] \delta[\hbar\omega - (\mathcal{E}_{\underline{k}+\underline{\beta}_1} - \mathcal{E}_{\underline{k}})] \tag{VI-29}$$

where we have finally taken the limit $\eta' \to 0^+$.

Expression (VI-29) vividly demonstrates the general principles which were discussed in the introduction to this chapter and illustrated by Fig. 31. Only transitions which conserve both energy and momentum

$$\mathcal{E}_{\underline{k}_b} - \mathcal{E}_{\underline{k}_a} = \hbar\omega \tag{VI-30}$$

$$\underline{k}_b - \underline{k}_a = \underline{\beta}_1 \qquad \text{(VI-31)}$$

contribute to the integral (VI-29). Since the gain of the electromagnetic wave $g = 2\,\mathrm{Im}\beta$ is proportional to $\mathrm{Im}\chi_p$ (Eq. VI-27), we conclude that only transitions between states which fulfill Eqs. (VI-30,31) contribute to electromagnetic wave amplification (stimulated emission) or attenuation (stimulated absorption). Whether the net result is gain or attenuation depends on the difference in population between the higher states $\underline{k}_b = \underline{k}_a + \underline{\beta}_1$ and the lower states $\underline{k}_a$ (see Figs. 31,33). In an equilibrium carrier distribution there will be more carriers at the lower energy states, consequently leading to attenuation. Gain can be achieved only if there is higher population at the higher energy states $\underline{k}_b = \underline{k}_a + \underline{\beta}_1$ than in the lower states $\underline{k}_a$, which can be achieved for example by applying a dc field. For carriers in a solid such a situation may be referred to as <u>intraband population inversion</u>.

Since $\underline{\beta}_1 = \beta_1 \hat{e}_z$ is in the z direction,

$$\mathcal{E}_{\underline{k}+\underline{\beta}_1} - \mathcal{E}_{\underline{k}} = \frac{\hbar^2}{2m}(\beta_1^2 + 2\beta_1 k_z) = \frac{\hbar^2 \beta_1}{m}(k_z + \beta_1/2) \qquad \text{(VI-32)}$$

is independent of the transverse components k_x, k_y and we can simplify Eqs. (VI-26,28,29) by integrating transversely the three dimensional distribution function $f_o(\underline{k})$

$$f_o(k_z) = \frac{1}{(2\pi)^2} \int dk_x dk_y f_o(\underline{k}) \qquad \text{(VI-33)}$$

Using (VI-32,33) in Eq. (VI-26) we get

$$\chi_p(\beta_1,\omega) = -\frac{1}{2\pi}\frac{e^2 m}{\hbar^2\beta_1^3}\int_{-\infty}^{\infty}\frac{f_o(k_z+\beta_1) - f_o(k_z)}{k_z - k_a + i\eta}\,dk_z =$$

$$= -\frac{1}{2\pi}\frac{e^2 m}{\hbar^2\beta_1^3}\left[\int_{-\infty}^{\infty}\frac{f_o(k_z)}{k_z-k_b+i\eta}\,dk_z - \int_{-\infty}^{\infty}\frac{f_o(k_z)}{k_z-k_a+i\eta}\,dk_z\right] \qquad \text{(VI-34)}$$

where

$$\eta \equiv m\eta'/(\hbar\beta_1) \qquad \text{(VI-35)}$$

is infinitesimal, and

$$k_a = \frac{m}{\hbar}\frac{\omega}{\beta_1} - \frac{\beta_1}{2} \qquad \text{(VI-36)}$$

$$k_b = \frac{m}{\hbar}\frac{\omega}{\beta_1} + \frac{\beta_1}{2} = k_a + \beta_1 \qquad \text{(VI-37)}$$

$$\frac{\hbar^2 k_b^2}{2m} - \frac{\hbar^2 k_a^2}{2m} = \hbar\omega \qquad \text{(VI-38)}$$

Instead of (VI-28,29) we get at the limit $\eta \to 0^+$

$$\mathrm{Re}\chi_p = -\frac{1}{2\pi}\frac{e^2 m}{\hbar^2\beta_1^3}\left[(p)\int_{-\infty}^{\infty}\frac{f_o(k_z)}{k_z-k_b}\,dk_z - (p)\int_{-\infty}^{\infty}\frac{f_o(k_z)}{k_z - k_a}\,dk_z\right] \qquad \text{(VI-39)}$$

$$\mathrm{Im}\chi_p = \frac{1}{2}\frac{e^2 m}{\hbar^2\beta_1^3}[f_o(k_b) - f_o(k_a)] \qquad \text{(VI-40)}$$

Using (VI-27,40) we can write the condition for gain (population inversion condition) as

$$f_o(k_b) > f_o(k_a) \tag{VI-41}$$

In the limit

$$\beta_1 << k_a \tag{VI-42}$$

we have from (VI-36,37)

$$k_a \simeq k_b \approx \frac{m}{\hbar} \frac{\omega}{\beta_1} \tag{VI-43}$$

If the one dimensional distribution function $f_o(k_z)$ is such that it has a single maximum at k_o, where

$$k_o \equiv \frac{m}{\hbar} v_o \tag{VI-44}$$

then the gain condition Eq. (VI-41) is satisfied when

$$k_a, k_b < k_o \tag{VI-45}$$

which using (VI-43,44) gives

$$v_{ph1} = \frac{\omega}{\beta_1} < v_o \tag{VI-46}$$

Thus we have proved that the conditions of energy and momentum conservation (VI-30,31) lead to the equivalence of the quantum mechanical gain condition (VI-41) and the classical Cerenkov condition (III-25,V-32).

4. Nondegenerate Plasma

Let $f_o(k_z)$ represent the one dimensional distribution function of nondegenerate drifting carriers. Its zero, first and second order moments define the density n_o, drift momentum $\hbar k_o$ and thermal momentum spread in the z direction $\hbar k_{th}$:

$$n_o = \frac{1}{(2\pi)^3} \iiint f_o(\underline{k}) d^3k = \frac{1}{2\pi} \int_{-\infty}^{\infty} f_o(k_z) dk_z \tag{VI-47}$$

$$k_o = \frac{1}{2\pi n_o} \int_{-\infty}^{\infty} k_z f_o(k_z) dk_z \tag{VI-48}$$

$$k_{th}^2/2 = \frac{1}{2\pi n_o} \int_{\infty}^{\infty} (k_z - k_o)^2 f_o(k_z) dk_z \tag{VI-49}$$

Using the relation

$$k_z = \frac{m}{\hbar} u \tag{VI-50}$$

these definitions correspond to their classical counterparts Eqs. (V-14-16), where

$$\frac{m}{2\pi\hbar} f_o(k_z) = f_o(u) \tag{VI-51}$$

$$k_o = \frac{m v_o}{\hbar} \tag{VI-52}$$

$$k_{th} = \frac{m v_{th}}{\hbar} = \frac{\sqrt{2mk_B T}}{\hbar} \tag{VI-53}$$

As in (V-17) we may define a normalized distribution function

g(x) whose zero, first and second order moments are 1, 0 and 1/2 respectively:

$$f_o(k_z) = 2\pi \frac{n_o}{k_{th}} g\left(\frac{k_z - k_o}{k_{th}}\right) \tag{VI-54}$$

We can thus define the plasma dispersion function consistently with (V-18)

$$G(\zeta) = \int_{-\infty}^{\infty} \frac{g(x)}{x - \zeta} dx \qquad (Im\zeta < 0) \tag{VI-55}$$

Using these definitions, Eq. (VI-34) can be written as

$$\chi_p(\beta_1,\omega) = -\frac{1}{2}\varepsilon \frac{k_A^3}{\beta_1^3}[G(\zeta_b) - G(\zeta_a)] \tag{VI-56}$$

$$\zeta_b \equiv \frac{k_b - k_o - i\eta}{k_{th}} \tag{VI-57}$$

$$\zeta_a \equiv \frac{k_a - k_o - i\eta}{k_{th}} \tag{VI-58}$$

$$k_A^3 \equiv \frac{2\omega_p^2 m^2}{\hbar^2 k_{th}} \tag{VI-59}$$

In the limit $\eta \to 0^+$

$$\zeta_b = \frac{k_b - k_o}{k_{th}} \tag{VI-60}$$

$$\zeta_a = \frac{k_a - k_o}{k_{th}} \tag{VI-61}$$

$$Re\chi_p(\beta,\omega) = -\frac{1}{2}\varepsilon \frac{k_A^3}{\beta_1^3} Re[G(\zeta_b) - G(\zeta_a)] \tag{VI-62}$$

$$Im\chi_p(\beta,\omega) = -\frac{1}{2}\varepsilon \frac{k_A^3}{\beta_1^3} Im[G(\zeta_b) - G(\zeta_a)] = \pi\varepsilon \frac{\omega_p^2 m^2}{\hbar^2 \beta_1^3 k_{th}}[g(\zeta_b) - g(\zeta_a)] \tag{VI-63}$$

We can thus express Eq. (VI-27) in terms of the dispersion function $G(\zeta)$

$$\mathrm{Im}\beta = -\theta \frac{\mathrm{Im}[G(\zeta_b) - G(\zeta_a)]}{|\varepsilon_p(\beta_1,\omega)|^2} = \pi\theta \frac{g(\zeta_b) - g(\zeta_a)}{|\varepsilon_p(\beta_1,\omega)|^2} \tag{VI-64}$$

$$\varepsilon_p(\beta_1,\omega) = 1 - \frac{1}{2}\frac{k_A^3}{\beta_1^3}[G(\zeta_b) - G(\zeta_a)] \tag{VI-65}$$

$$\theta \equiv \frac{1}{4}\varepsilon\omega \frac{k_A^3}{\beta_1} K_1 S = \frac{1}{2}\varepsilon\omega \frac{\omega_p^2 m^2}{\hbar^2 \beta_1 k_{th}} K_1 S \tag{VI-66}$$

Let us consider the case where the distribution function is a shifted Maxwellian

$$f_o(\underline{k}) = (2\pi)^3 \frac{n_o}{(\sqrt{\pi}k_{th})^3} e^{-(\underline{k}-\underline{k}_o)^2/k_{th}^2} \tag{VI-67}$$

where $\underline{k}_o = k_o \hat{e}_z$. The one dimensional distribution function (Eq. VI-33) is

$$f_o(k_z) = 2\pi \frac{n_o}{\sqrt{\pi}k_{th}} e^{-(k_z-k_o)^2/k_{th}^2} \tag{VI-68}$$

and the normalized distribution function (VI-54) is

$$g(x) = \frac{1}{\sqrt{\pi}} e^{-x^2} \tag{VI-69}$$

Thus the definition of the plasma dispersion function $G(\zeta)$ (VI-55) is identical with (V-56). For real ζ

$$\mathrm{Re}G(\zeta) = \frac{1}{\sqrt{\pi}} (p) \int_{-\infty}^{\infty} \frac{e^{-x^2}}{x - \zeta} dx \tag{VI-70}$$

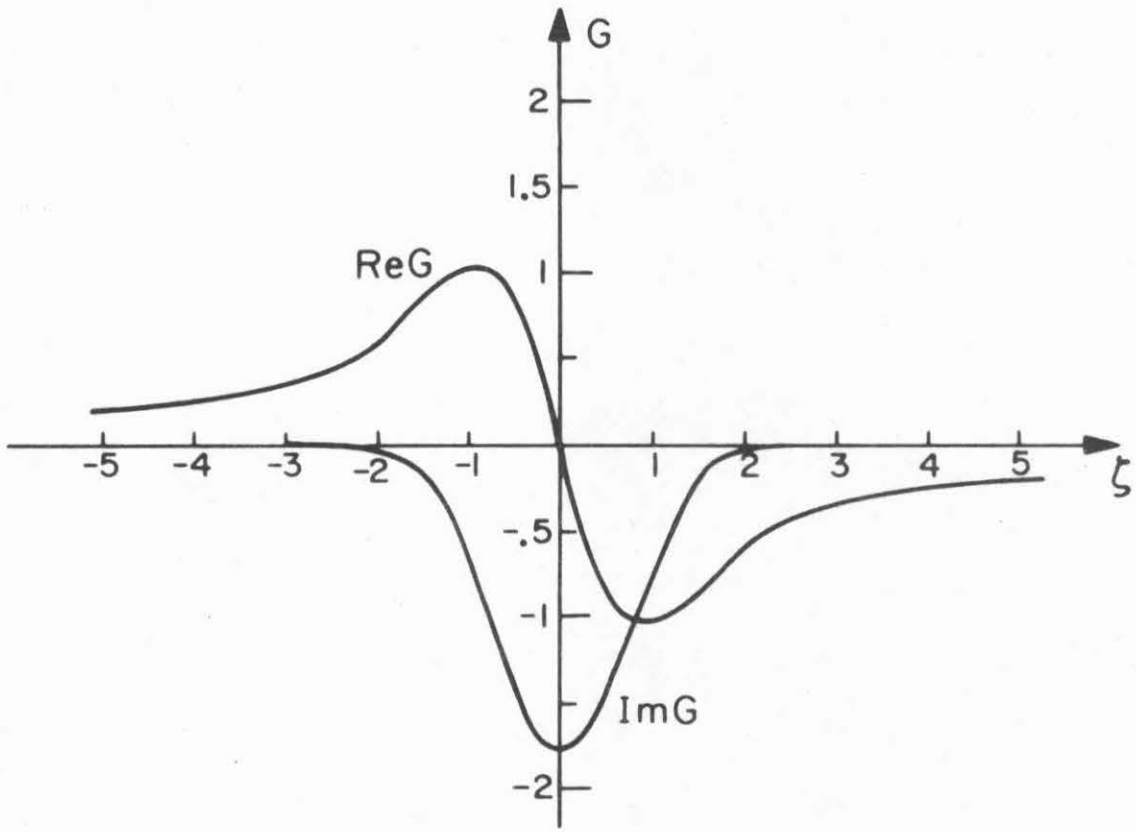

Fig. 32 The plasma dispersion function $G(\zeta)$ for a Maxwellian distribution and real argument ζ.

$$\mathrm{ImG}(\zeta) = -\sqrt{\pi}\, e^{-\zeta^2} \tag{VI-71}$$

These functions are plotted in Fig. 32 and tabulated in Appendix VI-B.

We see from Fig. 32 that $\mathrm{ImG}(\zeta_b) - \mathrm{ImG}(\zeta_a) < 0$ (which according to (VI-64) means conditions of gain) only if $(\zeta_b+\zeta_a)/2 > 0$. Using definitions (VI-60, 61, 36, 37) we find that this condition is equivalent to the classical Cerenkov condition (VI-46) even if we are not in the classical limit (VI-42). This is always true when the distribution function is symmetric as is the case with a Maxwellian.

In conclusion of this section it is in order to indicate that all the expressions in this section reduce to their classical counterparts in Chapter V in the limit (VI-42). In this limit we may have

$$f_o(k_z+\beta_1) - f_o(k_z) \simeq f_o'(k_z)\beta_1 \tag{VI-72}$$

$$G(\zeta_b) - G(\zeta_a) \simeq G'(\zeta_1)\frac{\beta_1}{k_{th}} \tag{VI-73}$$

$$g(\zeta_b) - g(\zeta_a) = g'(\zeta_1)\frac{\beta_1}{k_{th}} \tag{VI-74}$$

where

$$\zeta_1 \simeq \zeta_a \simeq \zeta_b \simeq \frac{\frac{m}{\hbar}\frac{\omega}{\beta_1} - k_o}{k_{th}} = \frac{\omega/\beta_1 - v_o}{v_{th}} \tag{VI-75}$$

For these approximations to be valid, β_1 must be small enough so that first order Taylor expansion of these functions is valid. Focusing our interest to the imaginary part of χ, it is enough to require

$$\beta_1 << \left|\frac{2f_o'(k_a)}{f_o''(k_a)}\right| \tag{VI-76}$$

in order to neglect second order expansion of $f_o(k_z)$ so that approximation (VI-72) will be valid. In terms of the normalized distribution function (VI-74) this can be written as

$$\beta_1 << \left| \frac{2g'(\zeta_1)}{g''(\zeta_1)} \right| k_{th} \qquad \text{(VI-77)}$$

In the case of a Maxwellian distribution (VI-69) the condition for reduction to the classical limit (VI-77) can be written as

$$\beta_1 << \frac{2|\zeta_1|}{|1-2\zeta_1^2|} k_{th} \qquad \text{(VI-78)}$$

This is in addition to condition (VI-42), which (using VI-43) can be written as

$$\beta_1^2 << \frac{m}{\hbar} \omega \qquad \text{(VI-79)}$$

5. Degenerate Plasma

If the density of carriers in the plasma is high enough and the temperature is low enough, the plasma may become degenerate, i.e. the effect of the Pauli exclusion principle will become appreciable enough so that the carriers will have to be described by Fermi statistics instead of Boltzmann statistics. Such a situation may be obtained in most semiconductors even at room temperature [Fistul 1969].

The carriers distribution function of degenerate plasma in equilibrium is given by the Fermi distribution function.

$$f(\underline{k}) = \frac{2}{1 + e^{(\mathcal{E}_{\underline{k}} - \mu)/k_B T}} \qquad \text{(VI-80)}$$

where we allowed for the possibility of two values of electron spin. The Fermi level μ is determined for a given carrier density n_o by Eq. (VI-A9) or its integral representation - the left hand side of Eq (VI-47).

In the limit of zero temperature T = 0, the Fermi distribution (VI-80) reduces to the form

$$f(\underline{k}) = \begin{cases} 2 & |\underline{k}| \leq k_F \\ 0 & |\underline{k}| > k_F \end{cases} \qquad \text{(VI-81)}$$

where k_F is defined by

$$\frac{\hbar^2 k_F^2}{2m} \equiv \mu \qquad \text{(VI-82)}$$

In an electron plasma in semiconductors, μ is measured relative to the bottom of the conduction band.

In a drifting degenerate plasma we will assume that the distribution function is equal to the equilibrium function shifted by k_o in the k_z direction. Thus the drifting Fermi distribution function will be

$$f_o(\underline{k}) = \frac{2}{1 + e^{-[(\underline{k}-\underline{k}_o)^2 - k_F^2]/k_{th}^2}} \qquad \text{(VI-83)}$$

where $\underline{k}_o = k_o \hat{e}_z$ and k_{th} are defined by Eqs. (VI-52) and (VI-53) respectively. The corresponding one dimensional distribution function (VI-33) is

$$f_o(k_z) = \frac{1}{(2\pi)^2} 2\pi \int_o^\infty \frac{2}{1+e^{-[(k_z-k_o)^2-k_F^2]/k_{th}^2} e^{-k_\rho^2/k_F^2}} k_\rho dk_\rho =$$

$$= \frac{k_{th}^2}{2\pi} \ln \left\{ 1 + e^{-[(k_z-k_o)^2 - k_F^2]/k_{th}^2} \right\} \qquad \text{(VI-84)}$$

where k_ρ is the transverse component of $\underline{k}$ in cylindrical coordinates. (See Fig. 33)

At zero temperature Eq. (VI-84) reduces into

$$f_o(k_z) = \begin{cases} \frac{1}{2\pi} [k_F^2 - (k_z-k_o)^2] & |k_z-k_o| \leq k_F \\ 0 & |k_z-k_o| > k_F \end{cases} \qquad \text{(VI-85)}$$

Equation (VI-84) or (VI-85) can be used in (VI-34,39,40) in order to calculate the susceptibility of the degenerate plasma.

We define a normalized function g(x) by

$$f_o(k_z) \equiv 2\pi \frac{n_o}{k_F} g\left(\frac{k_z-k_o}{k_F}\right) \qquad \text{(VI-86)}$$

so that

$$\int_{-\infty}^{\infty} g(x)dx = 1 \qquad \text{(VI-87)}$$

and proceed to define the degenerate plasma dispersion function $G_F(\xi)$.

Fig. 33 Three dimensional illustration of traveling wave interaction in the quantum regime. The example in the picture is of a shifted-Fermi-electron-plasma-distribution at T = 0. Transitions can take place between occupied states in circle b ($\underline{K}_b$) and empty states in the plane of circle a ($\underline{K}_a = \underline{K}_b - \underline{\beta}$), and vice versa. The different states in each circle have different energy, but since the corresponding states $\underline{K}_b$ and $\underline{K}_a$ have the same cylindrical component k_ρ, the energy difference between any two corresponding states $\underline{K}_b$ and $\underline{K}_a$ is fixed

$$\mathcal{E}_{\underline{k}_b} - \mathcal{E}_{\underline{k}_a} = \frac{\hbar^2}{2m}(k_b^2+k_\rho^2) - \frac{\hbar^2}{2m}(k_a^2+k_\rho^2) = \frac{\hbar^2}{2m}(k_b^2-k_a^2) = \mathcal{E}_{k_b} - \mathcal{E}_{k_a}$$

Since $k_b > k_a$, transitions from states in circle b to plane a (as indicated in the picture) correspond to the emission of a photon with energy $\hbar\omega = \mathcal{E}_{k_b} - \mathcal{E}_{k_a}$. The opposite transitions involve the absorption of a photon with the same energy. If the circle b is larger than the circle a ($k_o > (k_b+k_a)/2$), there will be radiative transitions only from the part of circle b which is not shadowed by circle a, and there will be no transitions from a to b (transitions to an occupied state are forbidden by the Pauli principle). Hence the net transition rate (and consequently the optical gain) is proportional to the difference in the area of the two circles $\pi[k_F^2-(k_b-k_o)^2] - \pi[k_F^2 - (k_a-k_o)^2]$. If the area of the circle b is smaller than circle a ($(k_b+k_a)/2 > k_o$) then we get optical absorption instead of gain.

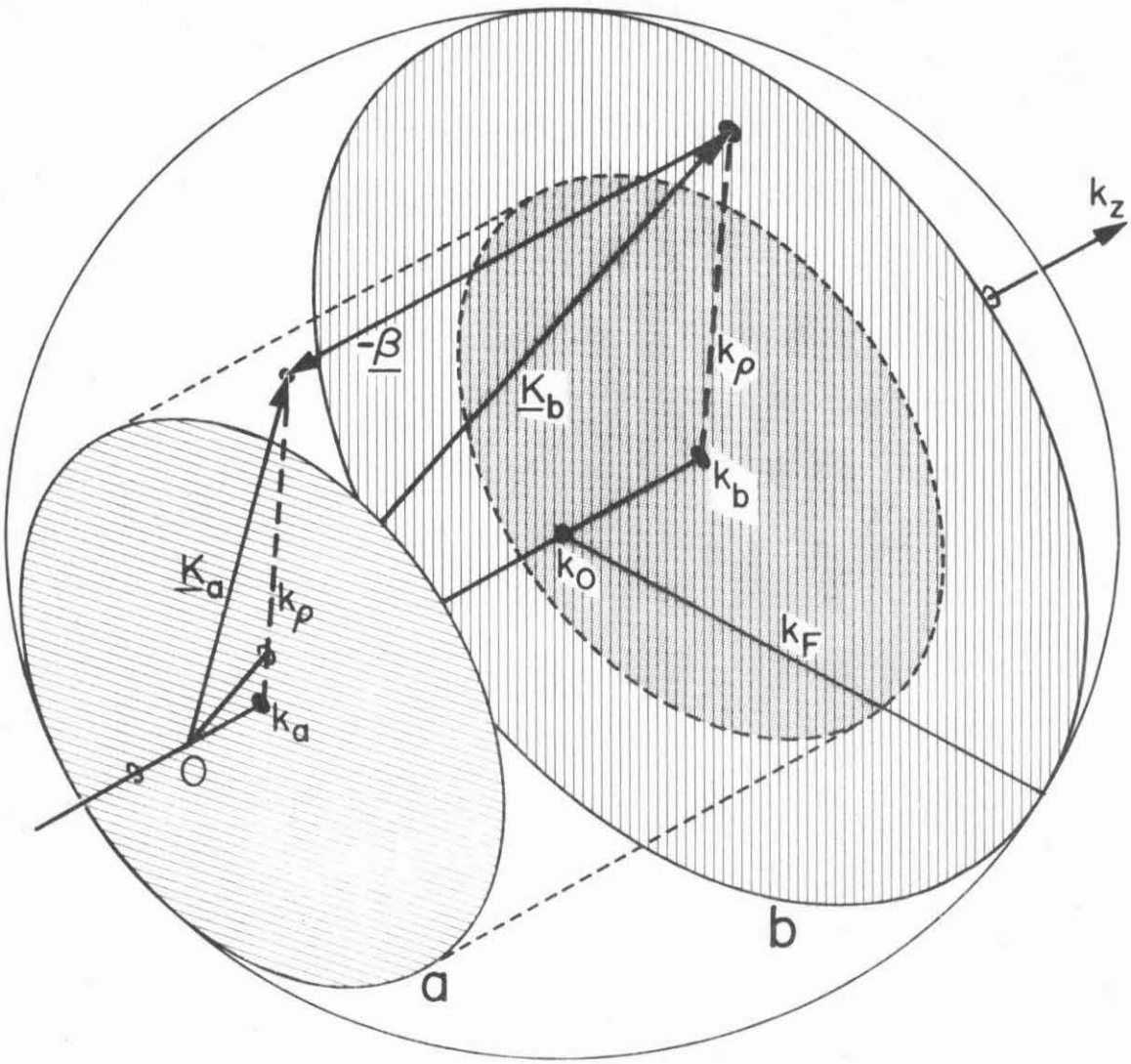
k_z
$-\underline{\beta}$
$\underline{K}_b$
k_ρ
k_b
k_O
k_F
$\underline{K}_a$
k_ρ
k_a
O
a
b

$$G_F(\xi) \equiv \int_{-\infty}^{\infty} \frac{g(x)}{x-\xi}\, dx \qquad \text{Im } \xi < 0 \tag{VI-88}$$

The plasma susceptibility (Eq. VI-34) can then be written as

$$\chi_p(\beta_1,\omega) = -\frac{1}{2}\,\varepsilon\,\frac{k_G^3}{\beta_1^3}\,[G_F(\xi_b) - G_F(\xi_a)] \tag{VI-89}$$

$$\xi_b \equiv \frac{k_b - k_o - i\eta}{k_F} \tag{VI-90}$$

$$\xi_a \equiv \frac{k_a - k_o - i\eta}{k_F} \tag{VI-91}$$

$$k_G^3 \equiv \frac{2\omega_p^2 m^2}{\hbar^2 k_F} \tag{VI-92}$$

where k_b, k_a are defined in Eqs. (VI-36,37).

In the limit $\eta \to 0^+$

$$\xi_b = \frac{k_b - k_o}{k_F} \tag{VI-93}$$

$$\xi_a = \frac{k_a - k_o}{k_F} \tag{VI-94}$$

$$\text{Re}\chi_p = -\frac{1}{2}\,\varepsilon\,\frac{k_G^3}{\beta_1^3}\,\text{Re}[G_F(\xi_b) - G_F(\xi_a)] \tag{VI-95}$$

$$\text{Im}\chi_p = -\frac{1}{2}\,\varepsilon\,\frac{k_G^3}{\beta_1^3}\,\text{Im}[G_F(\xi_b) - G_F(\xi_a)] \tag{VI-96}$$

where for real ξ the real and imaginary part separation is

$$G_F(\xi) = (p)\int \frac{g(x)}{x-\xi}\, dx - i\pi\, g(\xi) \tag{VI-97}$$

These expressions are identical with (VI-56-63) except that k_{th} is substituted by k_F, k_A by k_G, and ζ by ξ.

For the zero temperature distribution (Eq. VI-85), these expressions are explicitly given in terms of tabulated analytic functions

$$g(x) = \begin{cases} \frac{3}{4}(1 - x^2) & |x| \leq 1 \\ 0 & |x| > 1 \end{cases} \qquad \text{(VI-98)}$$

$$n_o = \frac{k_F^3}{3\pi^2} \qquad \text{(VI-99)}$$

For real ξ

$$\mathrm{Re}G_F(\xi) = -\frac{3}{2}\left[\xi + \frac{1}{2}(\xi^2-1)\ell n\left|\frac{1-\xi}{1+\xi}\right|\right] \qquad \text{(VI-100)}$$

$$\mathrm{Im}G_F(\xi) = \begin{cases} -\frac{3\pi}{4}(1 - \xi^2) & |\xi| < 1 \\ 0 & |\xi| > 1 \end{cases} \qquad \text{(VI-101)}$$

The real and imaginary parts of the susceptibility is found by substituting (VI-100,101) in (VI-95,96). The results are consistent with similar expressions which result in different plasma response problems, for example [Pines, 1964, p. 144, Spector 1965].

The traveling wave gain (or attenuation) is found by substitution in the first order solution of the dispersion equation (VI-27)

$$\mathrm{Im}\beta = -\kappa\frac{\mathrm{Im}[G_F(\xi_b)-G_F(\xi_a)]}{|\varepsilon_p(\beta_1,\omega)|^2} = \pi\kappa\,\frac{g(\xi_b)-g(\xi_a)}{|\varepsilon_p(\beta_1,\omega)|^2} \qquad \text{(VI-102)}$$

$$\varepsilon_p(\beta_1,\omega) = 1 - \frac{1}{2}\frac{k_G^3}{\beta_1^3}[G_F(\xi_b) - G_F(\xi_a)] \qquad \text{(VI-103)}$$

$$\kappa \equiv \frac{1}{4}\varepsilon\omega\frac{k_G^3}{\beta_1} K_1 S = \frac{1}{2}\varepsilon\omega\frac{\omega_p^2 m^2}{\hbar^2 \beta_1 k_F} K_1 S \qquad \text{(VI-104)}$$

For convenience $\mathrm{Re}G_F(\xi)$ and $\mathrm{Im}G_F(\xi)$ are plotted for real argument ξ in Fig. 34. Notice the similarity between Figs. 34 and 32. Gain is attained when $\mathrm{Im}G_F(\xi_b) < \mathrm{Im}G_F(\xi_a)$ (or $g(\xi_b) > g(\xi_a)$). In Fig. 34 $\mathrm{Im}G(\xi)$ vanishes for $|\xi| > 1$ so that the plasma dielectric function (VI-103) can be purely real if $|\xi_a|, |\xi_b| > 1$. This can be understood as an elimination of the Landau damping because the distribution function does not have any "tail."

When $\xi_a, \xi_b < 1$ (gain) or $\xi_a, \xi_b > 1$ (attenuation), exact phase matching of the plasma and electromagnetic waves can be achieved

$$\varepsilon_p(\beta_1,\omega) = 0 \qquad \text{(VI-105)}$$

In this case the first order solution of the dispersion equation (VI-102) is not valid any more, and we should resort to the second order solution (see Eqs. V-37-40, 44-50). In the present case, using VI-95,96 and assuming $\varepsilon_p(\beta_1,\omega) \approx 0$

$$A = 3 + \frac{1}{2}\frac{k_G^3}{\beta_1^3}[G_F'(\xi_b)\frac{k_a}{k_F} - G_F'(\xi_a)\frac{k_b}{k_F}] \qquad \text{(VI-106)}$$

$$B = \varepsilon_p(\omega,\beta_1) \simeq 0 \qquad \text{(VI-107)}$$

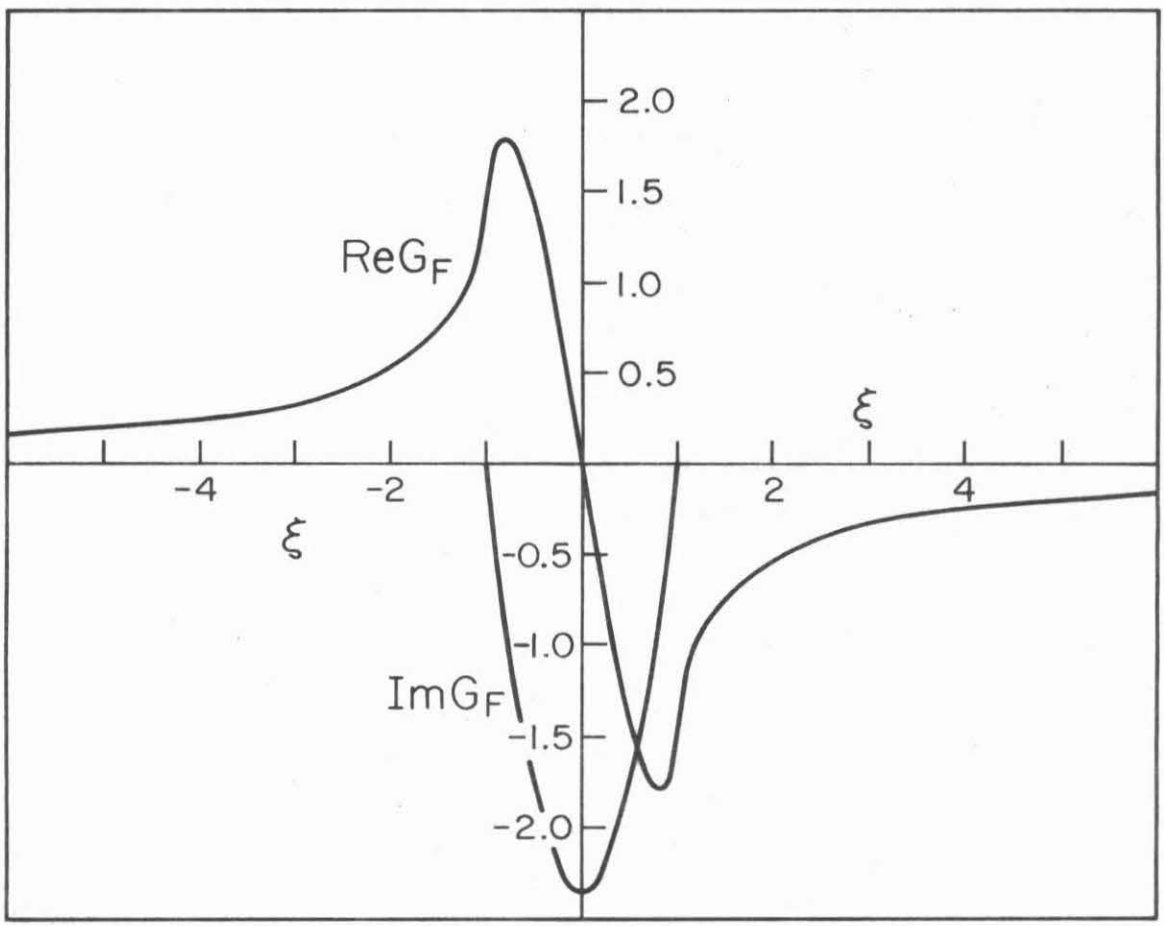

Fig. 34 The plasma dispersion function $G_F(\xi)$ for Fermi electron gas ($T = 0$).

$$C = \frac{\kappa}{\beta_1}\left[G_F(\xi_b) - G_F(\xi_a)\right] \tag{VI-108}$$

when $\varepsilon_p(\beta_1,\omega) = 0$ condition (V-49) is satisfied and the gain is (V-50)

$$\mathrm{Im}\beta = \beta_1\sqrt{\frac{C}{A}} \tag{VI-109}$$

6. The Effect of Collisions

The effect of collisions on the plasma susceptibility function and the traveling wave interaction was briefly discussed previously in section 6 of Chapter V in reference to the Boltzmann equation solution. Similarly to (V-67,68), a simple relaxation time approximation is frequently used in solving for the density matrix Liouville equation (VI-9 or VI-18)

$$i\hbar\frac{\partial}{\partial t}\rho^{(1)} = [\mathcal{H}^{(1)},\rho^{(0)}] + [\mathcal{H}^{(0)},\rho^{(1)}] - i\hbar\frac{\rho^{(1)}}{\tau} \tag{VI-110}$$

which can be written (using $e^{-i\omega t}$ harmonic dependence) as

$$\hbar(\omega + i\frac{1}{\tau})\rho^{(1)} = [\mathcal{H}^{(1)},\rho^{(0)}] + [\mathcal{H}^{(0)},\rho^{(1)}] \tag{VI-111}$$

Eq. (VI-111) is identical to (VI-A1) except that instead of the infinitesimal parameter η' we have a finite $1/\tau$. Hence with the substitutions

$$\eta' = \frac{1}{\tau} \tag{VI-112}$$

or (see VI-35)

$$\eta \equiv \frac{m}{\hbar\beta_1}\eta' = \frac{m}{\hbar\beta_1\tau} \qquad \text{(VI-113)}$$

Keeping $1/\tau$ finite throughout the derivation, the previously derived formulas can still be used.

Similar solution of plasma response problems with collisions is customary [Lindhard 1954, Tsu 1967, Kliewer 1969]. Kliewer [1969] also pointed out the limited validity of the simple relaxation time approximation, especially when longitudinal fields are present, and suggested some heuristic corrections to the Lindhard solution. Nevertheless we will use the simple relaxation time approximation in order to get an indication on the effect of collisions.

In our approximation the plasma susceptibility is still given by Eqs. (VI-56-59) for the nondegenerate plasma case, and Eqs. (VI-89-92) for the degenerate case, where η is substituted from Eq.(VI-113)
We define

$$\zeta_{a,b} = \zeta^R_{a,b} + i\,\zeta^I_{a,b} \qquad \text{(VI-114)}$$

$$\zeta^R_{a,b} = \frac{k_{a,b} - k_o}{k_{th}} \qquad \text{(VI-115)}$$

$$\zeta^I_{a,b} = -\frac{m}{\hbar k_{th}\beta_1\tau} = -\frac{1}{v_{th}\beta_1\tau} \qquad \text{(VI-116)}$$

$$\xi_{a,b} = \xi^R_{a,b} + i\,\xi^I_{a,b} \qquad \text{(VI-117)}$$

$$\xi^R_{a,b} = \frac{k_{a,b} - k_o}{k_F} \qquad \text{(VI-118)}$$

$$\xi^{I}_{a,b} = -\frac{m}{\hbar k_F \beta_1 \tau} = -\frac{1}{v_F \beta_1 \tau} \qquad \text{(VI-119)}$$

where the Fermi velocity v_F is defined by

$$v_F \equiv \frac{\hbar k_F}{m} \qquad \text{(VI-120)}$$

The plasma dispersion function $G(\zeta)$ can then be written as

$$G(\zeta) = \int_{-\infty}^{\infty} g(x) \frac{x-\zeta^R}{(x-\zeta^R)^2+(\zeta^I)^2}\, dx - i\pi \int_{-\infty}^{\infty} g(x) \frac{|\zeta^I|/\pi}{(x-\zeta^R)^2+(\zeta^I)^2}\, dx \qquad \text{(VI-121)}$$

and similarly for $G_F(\xi)$.

For the nondegenerate plasma case we find that Imβ is stil given by the left hand side of Eq. (VI-64), but instead of the right hand side, we have

$$\text{Im}\beta = \frac{\pi\theta}{|\varepsilon_p(\beta_1,\omega)|^2}\left[\int_{-\infty}^{\infty} g(x) \frac{|\zeta^I|/\pi}{(x-\zeta_b^R)^2+(\zeta^I)^2}\, dx - \int_{-\infty}^{\infty} g(x) \frac{|\zeta^I|/\pi}{(x-\zeta_a^R)^2+(\zeta^I)^2}\, dx\right] \qquad \text{(VI-122)}$$

where (VI-121) is used in calculating $\varepsilon_p(\beta_1,\omega)$ (Eq. VI-65). An identical expression results for the degenerate case from Eqs. (VI-102-104) with ζ substituted by ξ and θ by κ.

The physical meaning of Eq. (VI-122) is that the conservation of energy and momentum conditions (VI-30,31) are relaxed by the presence of collisions. Instead of transitions occurring only between states with $k_z=k_b$ and $k_z=k_a$ (Eqs. VI-36,37 , see Figs. 31,33 for illustration) there is finite (Lorentzian weighted) probability for transitions

between states with k_z around k_b and states with k_z around k_a. These transitions do not conserve energy and momentum. This effect is thus completely analogous to line broadening of atomic or molecular radiative transitions, which is brought about by the finite lifetimes of the quantum levels involved in the transitions. Also in that case the lineshape of the level is a Lorentzian.

The collisions have a harmful effect, mainly on the imaginary part of the dispersion function ImG. Instead of the curves of Figs. 32,34 which decay strongly to zero as $|\zeta| \gg 1$ $|\xi| > 1$, we get lower and wider curves which decay slowly to zero as $|\zeta|$, $|\xi| \gg 1$ (see Fig.35,37). This makes it difficult to achieve plasmon-photon phase matching, i.e.

$$|\varepsilon_p(\beta_1,\omega)| \simeq 0 \qquad \text{(VI-123)}$$

since even if the real part of $\varepsilon_p(\beta_1,\omega)$ (VI-65 or VI-103) vanishes, the imaginary part stays finite. Thus the traveling wave gain or attenuation (Eq. VI-122) cannot be made high by reducing the denominator $|\varepsilon_p(\beta_1,\omega)|^2$.

The plasma dispersion function $G(\zeta)$ for a Maxwellian distribution (VI-69) and complex argument was computed numerically as a function of ζ^R for few values of $|\zeta^I|$. Instead of numerical integration of Eq. (VI-121) better convergence and accuracy was obtained using a continued fraction iteration scheme [Burrell 1974] for direct computation of $G(\zeta)$ in the complex field. A computer listing of the computed functions for parameter values $|\zeta^I| = 0,\ 0.01,\ 0.066,$ 0.2 is given in Appendix VI-A. The functions $\mathrm{ImG}(\zeta^R)$ and $\mathrm{ReG}(\zeta^R)$

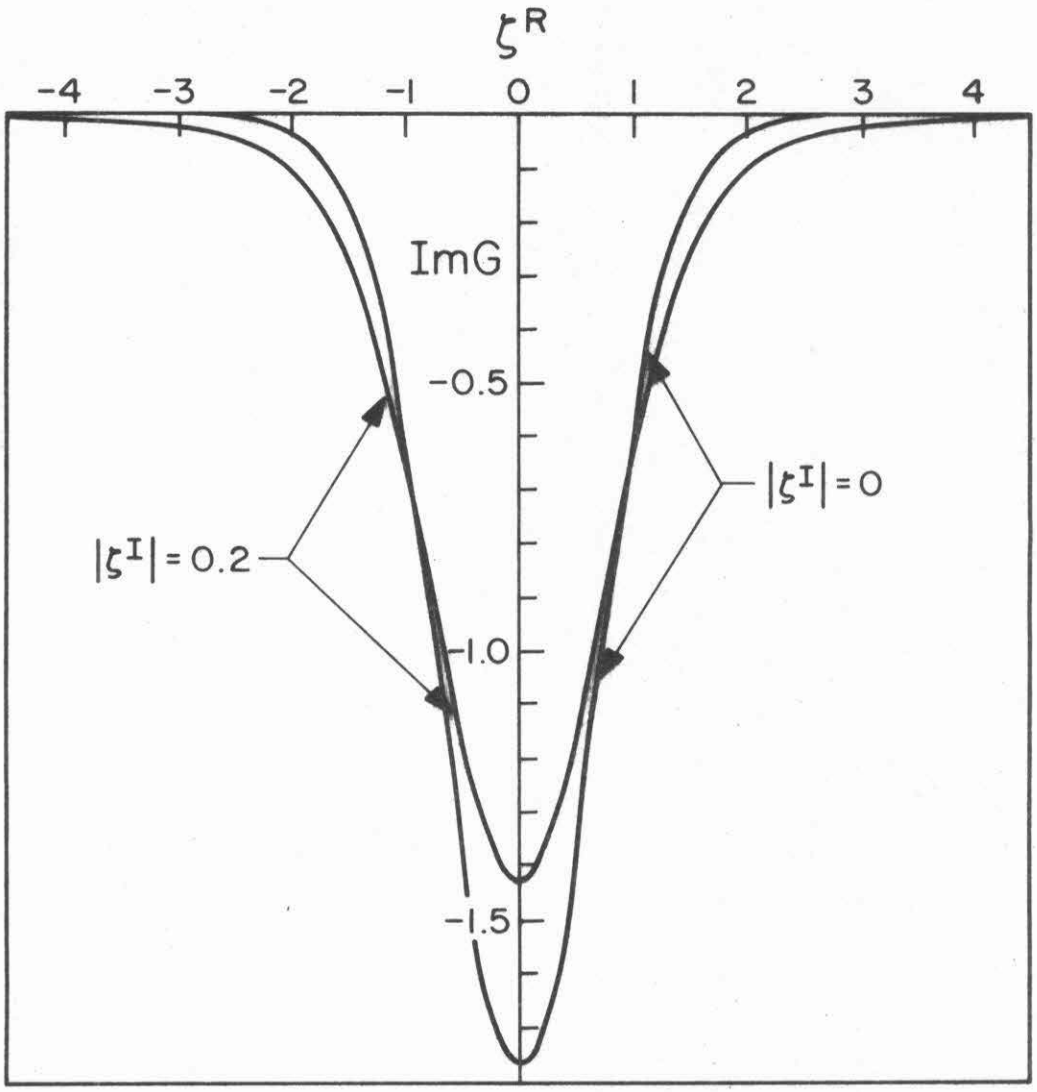

Fig. 35 The imaginary part of the plasma dispersion function $G(\zeta)$ for a Maxwellian distribution, plotted as a function of ζ^R for collision parameter values $|\zeta^I| = 0$ (no collisions) and $|\zeta^I| \equiv 1/(v_{th}\beta_1\tau) = 0.2$. Notice that ImG does not decay to zero rapidly at $|\zeta^R| >> 0$ when collisions are present.

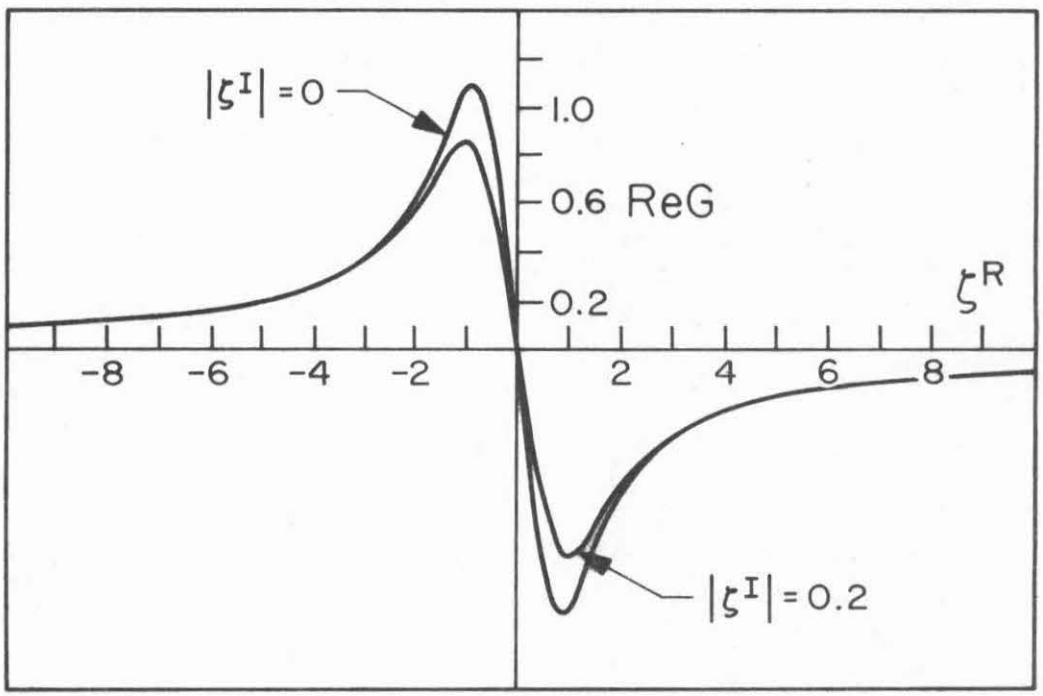

Fig. 36 The real part of the plasma dispersion function $G(\zeta)$ for Maxwellian distribution plotted as a function of ζ^R for collision parameter values $|\zeta^I| = 0$ (no collisions) and $|\zeta^I| = 1/(v_{th}\beta_1\tau) = 0.2$.

are plotted in Figs. 35, 36 for parameter values $|\zeta^I| = 0, 0.2$. The difference between the curves illustrates the effect of the collisions.

In the case of T = 0 degenerate plasma the dispersion function $G_F(\zeta)$ (VI-88,98) can be presented explicitly in terms of analytical functions also for complex ξ

$$\mathrm{Re}G_F(\xi) = -\frac{3}{4}\left\{2\xi^R+[(\xi^R)^2-(\xi^I)^2-1]\ln\left|\frac{\xi-1}{\xi+1}\right| +2\xi^R|\xi^I|[\arg(\xi-1)-\arg(\xi+1)]\right\} \quad \text{(VI-124)}$$

$$\mathrm{Im}G_F(\xi) = \frac{3}{4}\left\{2|\xi^I| +2\xi^R|\xi^I|\ln\left|\frac{\xi-1}{\xi+1}\right| - [(\xi^R)^2-(\xi^I)^2-1][\arg(\xi-1)-\arg(\xi+1)]\right\} \quad \text{(VI-125)}$$

where

$$\xi \equiv \xi^R - i|\xi^I| \quad \text{(VI-126)}$$

$$\arg(\xi-1)-\arg(\xi+1) = \tan^{-1}\left(\frac{-|\xi^I|}{\xi^R+1}\right) - \tan^{-1}\left(\frac{|\xi^I|}{\xi^R-1}\right) - \pi\eta(\xi^R) \quad \text{(VI-127)}$$

$$\eta(\xi^R)\equiv\begin{cases}1 & |\xi^R| \leq 1\\ 0 & |\xi^R| > 1\end{cases} \quad \text{(VI-128)}$$

and the $\tan^{-1}$ function is defined to accept values in the region $-\pi/2 < \tan^{-1}(x) < \pi/2$.

The mathematical derivation of these formulae is given in Appendix VI-C. An example with $|\xi^I| = 0.2$ is plotted in Figs. 37, 38 together with the curves for $|\xi^I| = 0$ in order to illustrate the effect of the collisions.

In the limit $|\zeta^I| \to 0$ the Lorentzian function in (VI-121) reduces into a Dirac delta function $\delta(x-\zeta^R)$. Consequently Eq. (VI-121) reduces into the collisionless expression (VI-70,71) and similarly for the degenerate plasma dispersion function. To neglect collisions we

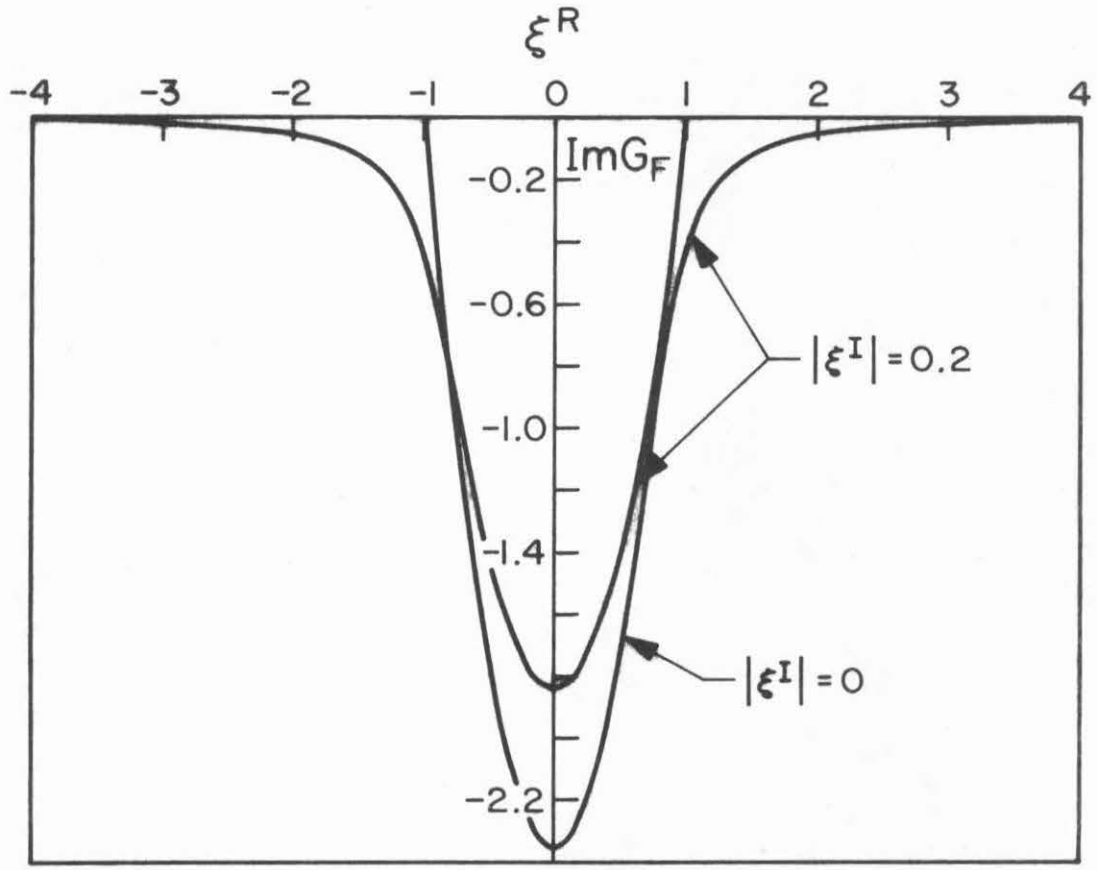

Fig. 37 The imaginary part of the plasma dispersion function $G_F(\xi)$ for a Fermi sphere distribution (T = 0), plotted as a function of ξ^R for collision parameter values $|\xi^I| = 0$ (no collisions) and $|\xi^I| \equiv 1/(v_F \beta_1 \tau) = 0.2$. The main effect of the collisions is that ImG does not decay rapidly to zero at $|\xi^R| > 1$.

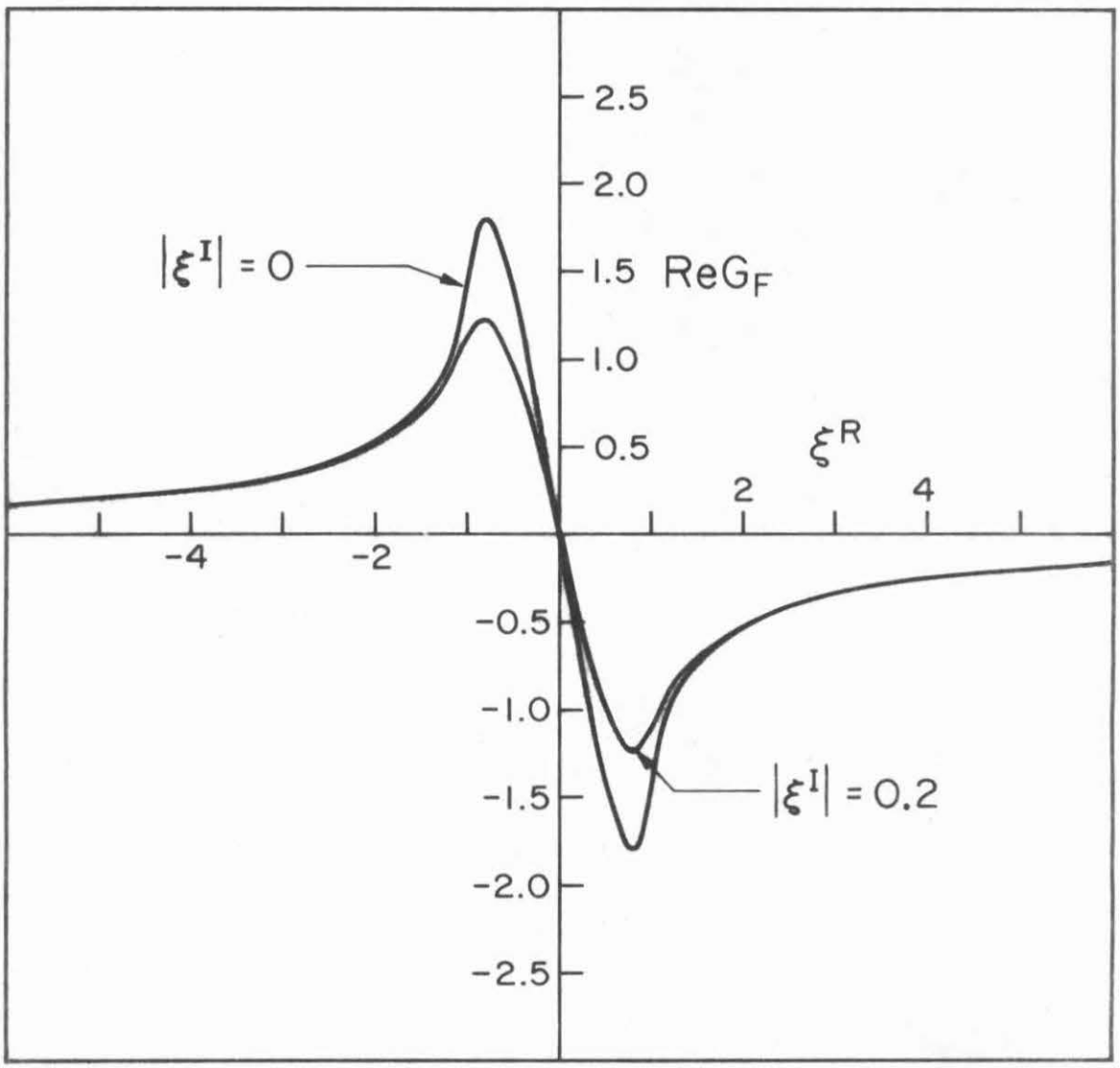

Fig. 38 The real part of the plasma dispersion function $G_F(\xi)$ for Fermi sphere distribution (T = 0), plotted as a function of ξ^R for collision parameter values $|\xi^I| = 0$ (no collisions) and $|\xi^I| = 1/(v_F\beta_1\tau) = 0.2$.

must require

$$|\zeta^I| << 1 \qquad |\xi^I| << 1 \tag{VI-129}$$

or

$$(\omega\tau)\,\frac{v_{th}}{(\omega/\beta_1)} >> 1 \tag{VI-130}$$

for nondegenerate plasma and

$$(\omega\tau)\,\frac{v_F}{(\omega/\beta_1)} >> 1 \tag{VI-131}$$

for degenerate plasma. These are somewhat different from the conventional criterion $\omega\tau >> 1$.

7. Discussion and Examples

The quantum mechanical analysis presented in this chapter provides a physical insight into the process of traveling wave interaction. We understand that the electromagnetic wave amplification is caused by stimulated radiative transitions of free electrons between states which conserve energy and momentum (Eqs. VI-30,31). The energy lost during an electron transition from a high to a lower state is transferred to an emitted photon. The momentum lost in this transition is transferred to the photon through one of its wave space harmonics. Thus, the traveling wave amplifier may be regarded as a free electron laser or maser.

Two independent effects are important:

i) Population inversion. This is the sitaution when there are more electrons in the higher energy states than in the lower energy states (Eq. VI-41), where we refer only to states which are connected by energy and momentum conservation (Fig. 31). In this case

there is higher probability for radiative electron transition emitting a photon than radiative transition which involves absorption of a photon, and thus the result is electromagnetic gain. In equilibrium population normally the lower energy states are more highly populated and thus the system exhibits electromagnetic attenuation.

We showed in Sections 3 and 4 that the population inversion condition (VI-41) is equivalent to the classical Cerenkov condition (VI-46) when the distribution function is symmetric, viz. population inversion is attained when the electrons average velocity exceeds the phase velocity of the space harmonic which participates in the interaction.

In terms of the normalized function (see Figs. 32,34) the gain condition (or population inversion condition) is that $\zeta_b + \zeta_a < 0$ or $\xi_b + \xi_a < 0$ so that Eqs. (VI-64) and (VI-102) respectively get positive value. Since the functions $\mathrm{Im}G(\zeta)$, and $\mathrm{Im}G_F(\xi)$ have their minimum at the zero argument point and $\zeta_b > \zeta_a$, $\xi_b > \xi_a$, a sufficient condition for gain (population inversion) is

$$\zeta_b, \zeta_a < 0 \qquad \text{(VI-132)}$$

or

$$\xi_b, \xi_a < 0 \qquad \text{(VI-133)}$$

ii) Plasmon-photon phase matched coupling. This is the situation when the propagation parameter and frequency of the electromagnetic space harmonic satisfy the plasma dispersion equation (VI-105) $\varepsilon_p(\beta_1, \omega) = 0$. When this happens, the electromagnetic wave is temporally and spatially phase matched to the plasma wave of the

system through one of the space harmonics, and there is strong interaction between the two waves.

When the plasmon-photon phase matching condition is closely satisfied, the electromagnetic gain (VI-64 or VI-102) gets very high since the denominator tends to vanish. Indeed in this case condition (V-45) may not be satisfied and the first order solution of the coupled modes dispersion equation (IV-10,11) fails. We thus have to resort to the second order solution (V-44) or (V-50).

In order to satisfy the phase matching condition (VI-105), both the real and imaginary parts of $\varepsilon_p(\beta_1,\omega)$ must vanish. For the Maxwellian distribution case (VI-65) these conditions can be explicitly written as

$$\mathrm{Re}\varepsilon_p = 1 - \frac{1}{2}\frac{k_A^3}{\beta_1^3}[\mathrm{ReG}(\zeta_b) - \mathrm{ReG}(\zeta_a)] = 0 \qquad \text{(VI-134)}$$

$$\mathrm{Im}\varepsilon_p = \frac{1}{2}\frac{k_A^3}{\beta_1^3}[\mathrm{ImG}(\zeta_b) - \mathrm{ImG}(\zeta_a)] = 0 \qquad \text{(VI-135)}$$

where $\mathrm{ReG}(\zeta)$, $\mathrm{ImG}(\zeta)$ are plotted in Fig. 32. For the T = 0 Fermi distribution case (VI-103) these conditions are

$$\mathrm{Re}\varepsilon_p = 1 - \frac{1}{2}\frac{k_G^3}{\beta_1^3}[\mathrm{ReG}_F(\xi_b) - \mathrm{ReG}_F(\xi_a)] = 0 \qquad \text{(VI-136)}$$

$$\mathrm{Im}\varepsilon_p = \frac{1}{2}\frac{k_G^3}{\beta_1^3}[\mathrm{ImG}_F(\xi_b) - \mathrm{ImG}_F(\xi_a)] = 0 \qquad \text{(VI-137)}$$

where $\mathrm{ReG}_F(\xi)$, $\mathrm{ImG}_F(\xi)$ are plotted in Fig. 34.

From Figs. 32, 34 we see that $|\mathrm{ReG}(\zeta)| < 1$ $|\mathrm{ReG}_F(\xi)| < 1.8$. Hence, a necessary condition for satisfying (VI-134, 136) is

$$k_A > \beta_1 \tag{VI-138}$$

$$k_G > \beta_1 \tag{VI-139}$$

Thus the presently defined parameters k_A, k_G (Eqs. VI-59,92) are useful in stating a necessary condition for plasmon-photon phase matching in nondegenerate (VI-138) and degenerate (VI-139) plasma. Another condition for the vanishing of the real part of ε_p (Eqs. VI-134,136) is that both ζ_a,ζ_b (or ξ_a,ξ_b) will have the same sign, otherwise $\mathrm{ReG}(\zeta_b) - \mathrm{ReG}(\zeta_b) < 0$ (or $\mathrm{ReG_F}(\xi_b)-\mathrm{ReG_F}(\xi_a) < 0$) and Eqs. (VI-134,136) cannot be satisfied.

In order to get also the imaginary part of $\varepsilon_p(\beta_1,\omega)$ to vanish (Eqs. VI-135,137) we must require also $|\zeta_a|,|\zeta_b| >> 1$ (see Fig. 32) or $|\xi_a|,|\xi_b| > 1$ (see Fig. 34). Furthermore, ζ_a,ζ_b (or ξ_a,ξ_b) must have the same sign in order that also the real part of $\varepsilon_p(\beta_1,\omega)$ will vanish. Thus we may have plasmon-photon phase matching either when

$$\zeta_a,\zeta_b << 1 \tag{VI-140}$$

$$\xi_a,\xi_b < 1 \tag{VI-141}$$

in which situation also population inversion and gain are attained (see Eqs. VI-132, 133), or when

$$\zeta_a,\zeta_b >> 1 \tag{VI-142}$$

$$\xi_a,\xi_b > 1 \tag{VI-143}$$

in which case the coupling involves attenuation of the electromagnetic wave.

Notice that in the limits (VI-140, 142) also the (positive) value of $\mathrm{ReG}(\zeta_b) - \mathrm{ReG}(\zeta_a)$ diminishes (see Fig. 32) even though not as fast as the imaginary part. Hence, in order to satisfy (VI-134) we must have

$$k_A \gg \beta_1 \tag{VI-144}$$

instead of (VI-138).

In the case of the zero temperature Fermi distribution, there is exact vanishing of the imaginary part of $\varepsilon_p(\beta_1,\omega)$ (Eq. VI-137) for $|\xi_a|,|\xi_b| > 1$ and a strong inequality is not needed. The gain in this case should be calculated from a second order solution of the dispersion equation which is explicitly given for this case by Eqs. (VI-106-109). In practice, the presence of collisions will cause $\mathrm{ImG}_F(\xi)$ to be finite for $|\xi| > 1$ even at $T = 0$ (see Fig. 37). Hence, also in the case of $T = 0$ distribution with collisions we may have to require instead of Eqs. (VI-141, 143, 139)

$$|\xi_a|,|\xi_b| \gg 1 \tag{VI-145}$$

$$k_G \gg \beta_1 \tag{VI-146}$$

so that the plasmon-photon phase matching condition may be attained.

In the classical limit (Eqs. VI-78, 79), the functions difference in Eqs. (VI-134, 135) may be substituted by a derivative, resulting in

$$1 - \frac{1}{2}\,\frac{k_D^2}{\beta_1^2}\,\mathrm{ReG}'(\zeta_1) = 0 \tag{VI-147}$$

$$\frac{1}{2}\,\frac{k_D^2}{\beta_1^2}\,\mathrm{ImG}'(\zeta_1) = 0 \tag{VI-148}$$

where

$$\zeta_1 = \frac{m\omega/(\hbar\beta_1)}{k_{th}} \equiv \frac{\omega/\beta_1}{v_{th}} \gtrsim \zeta_b \approx \zeta_a \qquad \text{(VI-149)}$$

$$k_D^2 \equiv \frac{k_A^2}{k_{th}} \qquad \text{(VI-150)}$$

From Fig. 23 we see that necessary conditions to get plasmon-photon phase matching in the classical regime (Eqs. VI-147, 148) are

$$|\zeta_1| \gg 1 \qquad \text{(VI-151)}$$

$$k_D \gg \beta_1 \qquad \text{(VI-152)}$$

which are the classical counterpart of Eqs. (VI-140, 142, 144).

In a similar way we may also find the classical analogue of Eqs. (VI-136, 137) in the limit

$$\frac{\beta_1}{k_F} \ll 1 \qquad \text{(VI-153)}$$

resulting in

$$\mathrm{Re}\varepsilon_p = 1 - \frac{1}{2}\frac{k_{FT}^2}{\beta_1^2}\,\mathrm{ReG}'(\xi_1) = 0 \qquad \text{(VI-154)}$$

$$\mathrm{Im}\varepsilon_p = \frac{1}{2}\,\frac{k_{FT}^2}{\beta_1^2}\,\mathrm{ImG}'(\xi_1) = 0 \qquad \text{(VI-155)}$$

where

$$\xi_1 = \frac{m\omega/(\hbar\beta_1)}{k_F} \equiv \frac{\omega/\beta_1}{v_F} \approx \xi_b \approx \xi_a \qquad \text{(VI-156)}$$

$$k_{FT}^2 \equiv \frac{k_G^3}{k_F} \qquad \text{(VI-157)}$$

where k_{FT} is the Fermi-Thomas wave number [Pines 1964] defined by (compare V-20):

$$k_{FT} \equiv \left(\frac{n_o e^2}{\varepsilon k_B T_F}\right)^{1/2} \equiv \sqrt{2}\,\frac{\omega_p}{v_F} \qquad \text{(VI-158)}$$

The "classical" counterpart of conditions (VI-145, 146) is thus

$$|\xi_1| >> 1 \qquad \text{(VI-159)}$$

$$k_{FT} >> \beta_1 \qquad \text{(VI-160)}$$

To illustrate the traveling wave interaction in the quantum regime we present in Table 39 an example of nondegenerate solid state traveling wave amplification in the gain regime but without plasmon-photon phase matching. It is relatively easy to satisfy Eq. (VI-132) in a semiconductor structure by drifting through the device a current so that $v_o > \omega/\beta_1$. It is much harder to meet condition (VI-140) for plasmon-photon phase matched amplification, since this requires $k_o >> k_{th}$ or $v_o >> v_{th}$.

From the parameters values listed in Table 39 and Eq. (VI-59) we find

$$k_A/\beta_1 = 0.657 < 1$$

so that plasmon-photon phase matching is not possible (VI-138).

We get

$$\zeta_b = \frac{k_b - k_o}{k_{th}} = 0.8417$$

$$\zeta_a = \frac{k_a - k_o}{k_{th}} = -1.3616$$

Table 39: An example of traveling wave gain ($k_A/\beta_1 < 1$)

parameter	value	unit
ω	3.5×10^{13}	rad/sec
n_o	8×10^{16}	cm^{-3}
T	50	°K
L	300	Å
ω_p	1.6×10^{13}	rad/sec
k_A	1.375×10^{6}	cm^{-1}
k_o	1.4×10^{6}	cm^{-1}
k_{th}	9.5×10^{5}	cm^{-1}
β_1	2.1×10^{6}	cm^{-1}
k_a	1.06×10^{5}	cm^{-1}
k_b	2.2×10^{6}	cm^{-1}
Fig. 28 ($\phi = 65°$ $n_{L1}^2/n_g^2 = 0.1$) g	2.1	cm^{-1}
Fig. 29 ($\phi = 90°$ $n_{L1}^2/n_g^2 = 0.1$) g	1	cm^{-1}

so that $\mathrm{ImG}(\zeta_b) < \mathrm{ImG}(\zeta_a)$ and net gain is obtained (Eq. VI-64). The real and imaginary part of $G(\zeta)$ are found from the computer listing in Appendix VI-B ($\zeta^I = 0$) , then the gain is calculated using Eqs. (VI-64-66). For the calculation of the interaction impedance of the structures in Figs. 28, 29 we used Eqs. (V-A31, A34).

The material considered in this example is GaAs, and so we use an effective electron mass $m/m_e = 0.08$ and an index of refraction $n = 3.1$ (including the free carrier contribution Eq. V-A2). The listed value of k_o corresponds to drift velocity $v_o = 2 \times 10^7$ cm/sec calculated from Eq. (VI-52). Eq. (VI-53) is used to find the thermal wave number k_{th} for the given temperature. Some useful equations for the calculation of some parameters are listed below (all parameters are assumed to have c.g.s. units).

$$\omega_p = 5.637 \times 10^4 \sqrt{\frac{n_o}{\varepsilon^R m/m_e}} \qquad \text{(VI-161)}$$

$$k_{th} = 4.77 \times 10^5 \sqrt{\frac{m}{m_e} T} \qquad \text{(VI-162)}$$

$$k_D = 1.4475 \times 10^{-1} \sqrt{\frac{n_o}{\varepsilon^R} T} \qquad \text{(V-163)}$$

$$k_A = 21.51 \left(\frac{n_o}{\varepsilon^R \frac{m_e}{m} T} \right)^{1/3} \qquad \text{(V-164)}$$

In the present example collisions were neglected. We find for the assumed parameters that the thermal velocity is $v_{th} = 1.38 \times 10^7$ cm/sec. Assuming $\tau = 10^{-12}$ sec, we find from Eq. (VI-116)

$$|\zeta^I| = \frac{1}{v_{th} \beta_1 \tau} = 0.035 << 1$$

so that the neglect of collisions is justified (Eq. VI-130). It is not justified of course for the fundamental space harmonic, which contributes background loss far exceeding the attained gain.

Examples of phase matched plasmon-photon coupling with gain or with attenuation are presented in the classical regime in Chapter V Sections 4,5. In most practical cases of plasmon-photon phase matching, the classical limit can be taken.

Operation in the degenerate regime can easily be attained in semiconductor structures with high carrier concentration and low temperature. A criterion for nondegeneracy is presented in Appendix VI-D (Eq. VI-D7)

$$n_o\left(\frac{m}{m_e}T\right)^{-3/2} < 4 \times 10^{15} \qquad \text{(VI-165)}$$

where n_o and T are expressed in units of $[cm^{-3}]$ and [°K] respectively. In the example presented in Table 39, assuming $m/m_e = 0.08$ we get

$$n_o\left(\frac{m}{m_e}T\right)^{-3/2} = 10^{16}$$

so that condition (VI-165) is violated and the semiconductor is slightly degenerate. This slight degeneracy is not expected though to change appreciably the numerical results presented there.

In the previous sections we derived explicit expressions for the plasma dispersion functions of the nondegenerate Maxwell distribution and the degenerate (T = 0) Fermi distribution with and without collisions. Previously derived expressions can be used to compute numerically the plasma dispersion function of the Fermi distribution with $T \neq 0$. This further elaboration is not attempted in the present work, and we also will not analyze examples in the degenerate regime.

Some comments about this case still may be in order.

In a degenerate semiconductor in which the carriers are introduced by impurity doping, the impurity level cannot be ignored. The impurity levels will be only partially ionized, and in order to find the concentration of free carriers in the conduction band n_o for a given donor concentration N_o and donor level $\mathcal{E}_d$, we have to solve a transcendental equation which results from the neutrality condition [Fistul 1969]. Indeed a zero temperature Fermi distribution like the one we analyzed in section 5 (Fig. 33) cannot be achieved at all at equilibrium by impurity doping, since at zero temperature all the carriers will populate the impurity levels. Distribution which is close to the Fermi sphere distribution may be attained at finite temperatures corresponding to thermal energy k_BT large enough to ionize the impurity level appreciably but still smaller than the Fermi energy. When a strong dc field is applied (for operation in the gain regime) the problem of carriers "freezing" in the impurity levels does not arise since the impurity levels will get strongly ionized by the mechanism of impact ionization [Conwell 1967]. The difficulty of "carriers freezing" may be completely avoided if the carriers are introduced by injection instead of impurity doping or if an appropriate semimetal can be used instead of a semiconductor.

As a theoretical model for the analysis of traveling wave amplification with drifting carriers at $T = 0$, we used a shifted Fermi distribution model (Fig. 33) to describe the carriers. This assumption is commonly used also in other semiconductor plasma response problems [Paranjape 1963, Spector 1965],

however it lacks experimental justification.

It is apparent that operation in the gain regime, especially when also photon-plasmon phase matching is desired (VI-140,141), is much easier to attain at low temperatures when the plasma is degenerate. The comparison of Figs. 32, 34 indicates that vanishing of $\mathrm{Im}\varepsilon_p(\beta_1,\omega)$ is much easier to attain at low temperatures. Furthermore, the collision relaxation time τ is considerably larger because of the scarcity of phonon collision events. Thus the imaginary part of ξ (VI-119) can get reduced, which again helps to attain vanishing of $\mathrm{Im}\varepsilon_p(\beta_1,\omega)$ and increase in gain. Though phonon scattering is considerably reduced at low temperature, impurities scattering may limit appreciable increase in the relaxation time τ. This is especially destructive when we wish to use high doping levels (this problem is avoided, of course, if the carriers are not introduced by impurity doping). It is worth noting, however, that the cross section of impurity scattering reduces with the applied electric field to the power 1 to 1.5 [Conwell 1967], thus longer collision relaxation time can be attained for the drifting carriers.

Appendix VI-A: Derivation of the Quantum Mechanical Plasma Response to Longitudinal Field

We first solve Eq. (VI-18) for $\rho^{(1)}$. The perturbation is assumed to have $e^{-i\omega t+\eta' t}$ time dependence where $\eta' \to 0^+$ is the adiabatic turning on parameter (see discussion in Chapter V, Section 2)

$$\hbar(\omega+i\eta')\rho^{(1)} = [\mathcal{H}^{(1)}\rho^{(0)}] + [\mathcal{H}^{(0)}\rho^{(1)}] \qquad \text{(VI-A1)}$$

A general matrix element k+q, q is found

$$[\hbar\omega+i\hbar\eta' - (\mathcal{E}_{\underline{k}+\underline{q}}-\mathcal{E}_{\underline{k}})] \langle \underline{k}+\underline{q}|\rho^{(1)}|\underline{k}\rangle =$$

$$-\frac{e}{2m}[f_o(\underline{k}) - f_o(\underline{k}+\underline{q})] \langle \underline{k}+\underline{q}|\underline{A}\underline{p} + \underline{p}\underline{A}|\underline{k}\rangle$$

$$\langle \underline{k}+\underline{q}|\rho^{(1)}|\underline{k}\rangle = \frac{e}{2m}\frac{f_o(\underline{k}+\underline{q}) - f_o(\underline{k})}{\hbar\omega - (\mathcal{E}_{\underline{k}+\underline{q}}-\mathcal{E}_{\underline{k}})+i\hbar\eta'} \langle \underline{k}+\underline{q}|\underline{A}\underline{p}+\underline{p}\underline{A}|\underline{k}\rangle \qquad \text{(VI-A2)}$$

where we made use of Eqs. (VI-13,15,16). Substituting

$$\underline{A}(\underline{r},t) = A(\underline{\beta},\omega)e^{i(\underline{\beta}\cdot\underline{r}-\omega t)} \qquad \text{(VI-A3)}$$

yields

$$\langle \underline{k}+\underline{q}|\rho^{(1)}(\underline{r},t)|\underline{k}\rangle = \frac{e}{2m}\frac{f_o(\underline{k}+\underline{q}) - f_o(\underline{k})}{\hbar\omega-(\mathcal{E}_{\underline{k}+\underline{q}}-\mathcal{E}_{\underline{k}}) + i\hbar\eta'}(2\hbar\underline{k}+\hbar\underline{\beta})\langle k+q|e^{i\underline{\beta}\cdot\underline{r}}|\underline{k}\rangle \underline{A}(\underline{\beta},t) =$$

$$= \frac{e\hbar}{m}\frac{f_o(\underline{k}+\underline{q}) - f_o(\underline{k})}{\hbar\omega-(\mathcal{E}_{\underline{k}+\underline{q}}-\mathcal{E}_{\underline{k}}) + i\hbar\eta'}(\underline{k}+\frac{1}{2}\underline{\beta})\cdot\underline{A}(\underline{\beta},t)\delta_{\underline{q},\underline{\beta}} \qquad \text{(VI-A4)}$$

In order to evaluate the induced current (Eq. VI-19) we need to first find the matrix elements of $\underline{J}_{op}^{(0)}(\underline{r})$ (Eq. VI-20), $J_{op}^{(1)}(\underline{r})$ Eq. (VI-21) and $\rho^{(0)}$ (Eq. VI-16).

$$\langle \underline{k}|J_{op}^{(0)}(\underline{r})|\underline{k}+\underline{q}\rangle = \frac{1}{2V}\iiint e^{-i\underline{k}\cdot\underline{r}_e}\left[\frac{\underline{p}_e}{m}\delta(\underline{r}-\underline{r}_e)+\delta(\underline{r}-\underline{r}_e)\frac{\underline{p}_e}{m}\right]e^{i(\underline{k}+\underline{q})\cdot\underline{r}_e}d^3r_e =$$

$$= \frac{1}{2mV}e^{i\underline{q}\cdot\underline{r}}(2\hbar\underline{k}+\hbar\underline{q}) = \frac{\hbar}{mV}e^{i\underline{q}\cdot\underline{r}}(\underline{k}+\frac{1}{2}\underline{q}) \qquad \text{(VI-A5)}$$

$$\langle \underline{k}|J_{op}^{(1)}(\underline{r},t)|\underline{k}+\underline{q}\rangle = -\frac{e}{mV}\iiint e^{-i\underline{k}\cdot\underline{r}_e}\delta(\underline{r}-\underline{r}_e)e^{i(\underline{k}+\underline{q})\cdot\underline{r}_e}d^3r_e A(\underline{r}t) =$$

$$= -\frac{e}{mV}e^{i\underline{q}\cdot\underline{r}}\underline{A}(\underline{r},t) \qquad \text{(VI-A6)}$$

$$\langle \underline{k}+\underline{q}|\rho^{(0)}|\underline{k}\rangle = f_o(\mathcal{E}_{\underline{k}})\delta_{\underline{q},0} \qquad \text{(VI-A7)}$$

Eqs. (VI-A4-A7) are then substituted in (VI-19), yielding

$$\underline{J}(\underline{r},t) = -e \sum_{\underline{k},\underline{q}} [\langle \underline{k}|\underline{J}^{(0)}_{op}(\underline{r})|\underline{k}+\underline{q}\rangle \langle \underline{k}+\underline{q}|\rho^{(1)}|\underline{k}\rangle +$$

$$+\langle \underline{k}|\underline{J}^{(1)}_{op}(\underline{r},t)|\underline{k}+\underline{q}\rangle \langle \underline{k}+\underline{q}|\rho^{(0)}|\underline{k}\rangle] =$$

$$= \frac{e^2 n_o}{m}\underline{A}(\underline{r},t) - \frac{e^2\hbar^2}{m^2 V}\sum_{\underline{k}} \frac{f_o(\underline{k}+\underline{\beta}) - f_o(\underline{k})}{\hbar\omega - (\mathcal{E}_{\underline{k}+\underline{\beta}} - \mathcal{E}_{\underline{k}}) + i\hbar\eta'} \times$$

$$(\underline{k} + \frac{1}{2}\underline{\beta})[(\underline{k}+\frac{1}{2}\underline{\beta})\cdot\underline{A}(\underline{r},t)] \qquad \text{(VI-A8)}$$

where we used for the particle density n_o the relation

$$n_o = \frac{1}{V}\sum_{\underline{k}} f_o(\underline{k}) \qquad \text{(VI-A9}$$

Eq. (VI-A8) results in Eq. (VI-22) when (VI-24) is substituted

$$\underline{J}(\underline{r},t) = -i\,\frac{e^2 n_o}{m\omega}\,\underline{E}(\underline{r},t) + i\,\frac{e^2\hbar^2}{m^2 V\omega}\sum_{\underline{k}}\frac{f_o(\underline{k}+\underline{\beta}) - f_o(\underline{k})}{\hbar\omega-(\mathcal{E}_{\underline{k}+\underline{\beta}}-\mathcal{E}_{\underline{k}}) + i\hbar\eta'}\ x$$

$$(\underline{k} + \tfrac{1}{2}\,\underline{\beta})[(\underline{k} + \tfrac{1}{2}\,\underline{\beta})\cdot\underline{E}(\underline{r},t)] \qquad \text{(VI-A10)}$$

To get the longitudinal-longitudinal response (VI-23) we substitute $\underline{E} = E_z\underline{\beta}/\beta$ and multiply (VI-A10) by $\hat{e}_z = \underline{\beta}/\beta$

$$J_z = -i\,\frac{e^2 n_o}{m\omega}\,E_z + i\,\frac{e^2\hbar^2}{4m^2 V\omega\beta^2}\sum_{\underline{k}}\frac{f_o(\underline{k}+\underline{\beta}) - f_o(\underline{k})}{\hbar\omega-(\mathcal{E}_{\underline{k}+\underline{\beta}}-\mathcal{E}_{\underline{k}}) + i\hbar\eta'}\ x$$

$$x\ [(2\underline{k}+\underline{\beta})\cdot\underline{\beta}]^2 E_z \qquad \text{(VI-A11)}$$

Using the relation

$$(2\underline{k}+\underline{\beta})\cdot\underline{\beta} = (\underline{k}+\underline{\beta})^2 - \underline{k}^2 = \frac{2m}{\hbar^2}\ (\mathcal{E}_{\underline{k}+\underline{\beta}}-\mathcal{E}_{\underline{k}}) \qquad \text{(VI-A12)}$$

we get

$$J_z = -i\,\frac{e^2 n_o}{m\omega}\,E_z + i\,\frac{e^2\hbar^2}{4m^2 V\omega\beta^2}\,\frac{2m}{\hbar^2}\sum_{\underline{k}}[f_o(\underline{k}+\underline{\beta})-f_o(\underline{k})]\ x$$

$$\left[\frac{\hbar\omega}{\hbar\omega-(\mathcal{E}_{\underline{k}+\underline{\beta}}-\mathcal{E}_{\underline{k}}) + i\eta'},\ -1\right][(2\underline{k}+\underline{\beta})\cdot\underline{\beta}]E_z =$$

$$= -i\,\frac{e^2 n_o}{mV\omega}\,E_z + \frac{ie^2\hbar^2}{4m^2 V\omega\beta^2}\left(\frac{2m}{\hbar^2}\right)^2\sum_{\underline{k}}[f_o(\underline{k}+\underline{\beta}) - f_o(\underline{k})]\ x$$

$$\hbar\omega\left[\frac{\hbar\omega}{\hbar\omega-(\mathcal{E}_{\underline{k}+\underline{\beta}}-\mathcal{E}_{\underline{k}}) + i\hbar\eta'} - 1\right]E_z - i\,\frac{e^2\hbar^2}{4m^2 V\omega\beta^2}\,\frac{2m}{\hbar^2}\ x$$

$$\sum_{\underline{k}}[f_o(\mathcal{E}_{\underline{k}+\underline{\beta}}) - f_o\mathcal{E}_{\underline{k}})](2\underline{k}\cdot\underline{\beta} + \beta^2)E_z \qquad \text{(VI-A13)}$$

Note that

$$\sum_{\underline{k}}[f_o(\underline{k}+\underline{\beta}) - f_o(\underline{k})] = \sum_{\underline{k}} f_o(\underline{k}) - \sum_{\underline{k}} f_o(\underline{k}) = 0$$

$$\sum_{\underline{k}}[f_o(\underline{k}+\underline{\beta}) - f_o(\underline{k})]\underline{k}\cdot\underline{\beta} = \sum_{\underline{k}} f_o(\underline{k})(\underline{k}-\underline{\beta})\cdot\underline{\beta} - \sum_{\underline{k}} f_o(\underline{k})\underline{k}\cdot\underline{\beta} =$$

$$= -\beta^2 \sum_{\underline{k}} f_o(\underline{k}) = -\beta^2 n_o V$$

When these are used in (VI-A13) we get cancellation of the first and third terms, resulting in

$$J_z = i\omega \frac{e^2}{V\beta^2} \sum_{\underline{k}} \frac{f_o(\underline{k}+\underline{\beta})-f_o(\underline{k})}{\hbar\omega - (\mathcal{E}_{\underline{k}+\underline{\beta}}-\mathcal{E}_{\underline{k}}) + i\hbar\eta\Gamma} E_z \qquad \text{(VI-A14)}$$

which we use in the text as Eq. (VI-23).

Appendix VI-B: The Plasma Dispersion Function $G(\zeta)$ for Complex Argument

The computation is based on continued fraction iteration scheme for the function $Z'(\zeta)$ [Burrell 1974, p. 126]. Subroutine G(z,zprime) calculates $Z'(\zeta)$ in the first complex quadrant. Subroutine convert (z_{in}, z_{out}), evaluates $Z'(\zeta)$ at any point in the complex plane and calculates the function $Z(\zeta)$, using the identity [Fried and Conte 1971]

$$Z(\zeta) = -\frac{1}{2\zeta} Z'(\zeta) - \frac{1}{\zeta} \qquad \text{(VI-B1)}$$

$Z(\zeta)$ is the conventional plasma dispersion function for Maxwellian velocity distribution [Fried and Conte 1971] which is usually defined in plasma physics for $e^{-i\omega t}$ harmonic time dependence. Its definition is identical to that of $G(\zeta)$ (Eqs. VI-55,69), but for $Im\zeta > 0$. The relation between $Z(\zeta)$ and the function used in the present work $G(\zeta)$ is

$$G(\zeta) = Z^*(\zeta^*) \qquad \text{(VI-B2)}$$

Calculated values of ReZ, ImZ, ReZ', ImZ' are listed for parameter values

$$\text{ETA} \equiv |\zeta^I| = 0,\ 0.01,\ 0.066,\ 0.2$$

$$\zeta^R = 0,\ 0.1,\ 0.2 \ \ldots\ 9.3$$

```
      SUBROUTINE G(Z,ZPRIME)
      INTEGER I,M
      COMPLEX Z,ZPRIME
      DOUBLE PRECISION A(20),B(20)
      REAL X,Y,X2,Y2,RE,IM,RZ2,IZ2,D,T,R
      DATA A/-1.772454D+00, 2.198389D-01, -1.92978D-01,-1.945556D-01
     &,-1.825269D-01,-1.703509D-01,-1.596796D-01,-1.505391D-01,
     & -1.428836D-01,-1.416862D-01, 7.879815D-03, 3.586354D-01,
     & -1.431593D-01, 4.567910D-01,-2.635771D-01, 5.235408D-01,
     & -3.600042D-01, 3.520949D-01, -2.531981D-01,-8.186648D-02/

      DATA B/1.14159D+00,7.469541D-02,
     & 4.508787D-02, 3.110716D-02, 2.362925D-02,1.901998D-02,
     & 1.590448D-02, 1.366566D-02, 1.185415D-02, 1.405589D-02,
     & -4.824088D-02, 5.540440D-02,-1.728404D-02, 1.182689D-01,
     &-8.085029D-03, 1.921583D-01,-5.804205D-03, 1.221379D-01,
     & -1.942373D-02,  1.742264D-01/

      X=REAL(Z)
      Y=AIMAG(Z)
      R=CABS(Z)
      IF(Y.GE.(4.75-X)*(0.112*X+0.369)) GO TO 50
      IF(R.NE.0.0) GO TO 10
      ZPRIME=(-2.0,0.0)
      RETURN
10    D=1.0/(R*R)
      X2=-Y*D
      Y2=-X*D
      M=3.05*R+4.79
      RE=X2+A(M)
      IM=Y2
30    M=M-1
      D=B(M)/(RE*RE+IM*IM)
      RE=X2+A(M)+D*RE
      IM=Y2-D*IM
      IF(M.GT.1)GO TO 30
      D=-2.0/(RE*RE+IM*IM)
      T=D*(RE*X2+IM*Y2)
      IM=D*(RE*Y2-IM*X2)
      RE=T
      ZPRIME=CMPLX(RE,IM)
      RETURN
50    RZ2=(X-Y)*(X+Y)
      IZ2=2.0*X*Y
      X2=2.0*RZ2-3.0
      Y2=2.0*IZ2
      I=18.45/R+2.12
      M=4*I
      I=2*I+2
      RE=X2-M
      IM=Y2
70    M=M-4
      I=I-2
      D=I*(I+1)/(RE*RE+IM*IM)
      RE=X2-M-D*RE
      IM=Y2+D*IM
      IF(M.GT.0) GO TO 70
      D=2.0/(RE*RE+IM*IM)
      RE=RE*D
      IM=-D*IM
      IF(Y.EQ.0.0 .AND. ABS(RZ2).LT. 180.0)IM=-3.54490770*I*EXP(-RZ2)
      ZPRIME=CMPLX(RE,IM)
      RETURN
      END
      SUBROUTINE CONVRT(ZIN,ZOUT)
      COMPLEX Z1,ZIN,ZOUT
      SIGNRE=1
      SIGNIM=1
      IF(REAL(ZIN) .LT. 0) SIGNRE=-1
      IF(AIMAG(ZIN) .LT. 0) SIGNIM=-1
      ZIN=CMPLX(ABS(REAL(ZIN)),ABS(AIMAG(ZIN)))
      CALL G(ZIN,Z1)
      ZOUT=CMPLX(0.0,1.772453)
      R=CABS(ZIN)
      IF(R .NE. 0.0) ZOUT=(Z1+2.)/ZIN/(-2.)
      ZOUT=CMPLX(SIGNRE*REAL(ZOUT),-SIGNIM*AIMAG(ZOUT))
      RETURN
      END
```

EIA= 0.0000

	Re Z	Im Z	Re Z'	Im Z'
0.0	0.000000E-01	1.77245E+00	-2.00000E+00	0.00000E-01
0.1	-1.98672E-01	1.75482E+00	-1.96027E+00	-3.52964E-01
0.2	-3.89503E-01	1.70295E+00	-1.84420E+00	-6.81182E-01
0.3	-5.65264E-01	1.61990E+00	-1.66084E+00	-9.71940E-01
0.4	-7.19887E-01	1.51038E+00	-1.42409E+00	-1.20851E+00
0.5	-8.48875E-01	1.38059E+00	-1.15113E+00	-1.38059E+00
0.6	-9.49526E-01	1.23660E+00	-8.60569E-01	-1.48392E+00
0.7	-1.02101E+00	1.08505E+00	-5.70598E-01	-1.52019E+00
0.8	-1.06424E+00	9.34601E-01	-2.57276E-01	-1.49556E+00
0.9	-1.08145E+00	7.88490E-01	5.33946E-02	-1.41928E+00
1.0	-1.07610E+00	6.52049E-01	1.52316E-01	-1.30410E+00
1.1	-1.05241E+00	5.28541E-01	3.15307E-01	-1.16279E+00
1.2	-1.01458E+00	4.19944E-01	4.34911E-01	-1.00707E+00
1.3	-9.66794E-01	3.27853E-01	5.13665E-01	-8.50338E-01
1.4	-9.13014E-01	2.49566E-01	5.56439E-01	-6.99064E-01
1.5	-8.56496E-01	1.86816E-01	5.69494E-01	-5.60448E-01
1.6	-7.99880E-01	1.37020E-01	5.59615E-01	-4.38403E-01
1.7	-7.45119E-01	9.85068E-02	5.33404E-01	-3.34923E-01
1.8	-6.93546E-01	6.94166E-02	4.96764E-01	-2.49900E-01
1.9	-6.45949E-01	4.79485E-02	4.54605E-01	-1.82204E-01
2.0	-6.02681E-01	3.24859E-02	4.10724E-01	-1.29856E-01
2.1	-5.63770E-01	2.15447E-02	3.67834E-01	-9.04877E-02
2.2	-5.29022E-01	1.46154E-02	3.27695E-01	-6.16662E-02
2.3	-4.98136E-01	5.93640E-03	2.91288E-01	-4.11074E-02
2.4	-4.70826E-01	5.58529E-03	2.59006E-01	-2.68094E-02
2.5	-4.46168E-01	3.42171E-03	2.30838E-01	-1.71085E-02
2.6	-4.24330E-01	2.85473E-03	2.06516E-01	-1.06846E-02
2.7	-4.04749E-01	1.20943E-03	1.85645E-01	-6.53094E-03
2.8	-3.87102E-01	6.97790E-04	1.67769E-01	-3.90762E-03
2.9	-3.71111E-01	3.94625E-04	1.52441E-01	-2.28882E-03
3.0	-3.56542E-01	2.18757E-04	1.39253E-01	-1.31254E-03
3.1	-3.43201E-01	1.15967E-04	1.27845E-01	-7.36975E-04
3.2	-3.32924E-01	6.33121E-05	1.17914E-01	-4.05197E-04
3.3	-3.19577E-01	3.30358E-05	1.09210E-01	-2.18168E-04
3.4	-3.09046E-01	1.69186E-05	1.01527E-01	-1.15046E-04
3.5	-2.99243E-01	8.48937E-06	9.47025E-02	-5.94256E-05
3.6	-2.90094E-01	4.17672E-06	8.86018E-02	-3.00724E-05
3.7	-2.81502E-01	2.01532E-06	8.31176E-02	-1.49153E-05
3.8	-2.73442E-01	9.54196E-07	7.81626E-02	-7.25189E-06
3.9	-2.65855E-01	4.43748E-07	7.36659E-02	-3.46124E-06
4.0	-2.58696E-01	2.02929E-07	6.96682E-02	-1.62343E-06

4,1	-2.51x25E-01	9.2129ØE-Ø8	6.58206E-Ø2	-7.55464E-Ø7
4,2	-2.45522E-01	4.17720E-Ø8	6.23819E-Ø2	-3.50885E-Ø7
4,3	-2.39444E-01	1.94179E-Ø8	5.92172E-Ø2	-1.66994E-Ø7
4,4	-2.33670E-01	9.54491E-Ø9	5.62968E-Ø2	-8.39952E-Ø8
4,5	-2.28177E-01	5.22655E-Ø9	5.35951E-Ø2	-4.70369E-Ø8
4,6	-2.22945E-01	3.45610E-Ø9	5.10899E-Ø2	-3.17961E-Ø8
4,7	-2.17953E-01	1.22276E-Ø9	4.87618E-Ø2	-1.17759E-Ø8
4,8	-2.13187E-01	1.74755E-10	4.65939E-Ø2	-1.67765E-Ø9
4,9	-2.08630E-01	6.62467E-11	4.45715E-Ø2	-6.49218E-10
5,0	-2.04268E-01	2.46157E-11	4.26815E-Ø2	-2.46157E-10
5,1	-2.00089E-01	8.96522E-12	4.09122E-Ø2	-9.14483E-11
5,2	-1.96082E-01	3.20075E-12	3.92532E-Ø2	-3.32878E-11
5,3	-1.92235E-01	1.12006E-12	3.76954E-Ø2	-1.18727E-11
5,4	-1.88540E-01	3.84192E-13	3.62305E-Ø2	-4.14927E-12
5,5	-1.84986E-01	1.29172E-13	3.48511E-Ø2	-1.42089E-12
5,6	-1.81567E-01	4.25696E-14	3.35505E-Ø2	-4.76780E-13
5,7	-1.78274E-01	1.37514E-14	3.23228E-Ø2	-1.56766E-13
5,8	-1.75100E-01	4.35420E-15	3.11624E-Ø2	-5.05087E-14
5,9	-1.72039E-01	1.35140E-15	3.00645E-Ø2	-1.59465E-14
6,0	-1.69085E-01	4.11125E-16	2.90245E-Ø2	-4.93350E-15
6,1	-1.66235E-01	1.22596E-16	2.80385E-Ø2	-1.49567E-15
6,2	-1.63476E-01	3.58340E-17	2.71026E-Ø2	-4.44341E-16
6,3	-1.60811E-01	1.02666E-17	2.62134E-Ø2	-1.29329E-16
6,4	-1.58232E-01	2.86319E-18	2.53682E-Ø2	-3.69048E-17
6,5	-1.55736E-01	7.93657E-19	2.45633E-Ø2	-1.03175E-17
6,6	-1.53316E-01	2.14145E-19	2.37968E-Ø2	-2.82671E-18
6,7	-1.50975E-01	5.66364E-20	2.32661E-Ø2	-7.58928E-19
6,8	-1.48704E-01	1.46824E-20	2.23692E-Ø2	-1.99681E-19
6,9	-1.46502E-01	3.73091E-21	2.17035E-Ø2	-5.14666E-20
7,0	-1.44366E-01	9.29277E-22	2.10673E-Ø2	-1.30099E-20
7,1	-1.42295E-01	2.26877E-22	2.04571E-Ø2	-3.22165E-21
7,2	-1.40286E-01	5.42937E-23	1.98772E-Ø2	-7.81829E-22
7,3	-1.38331E-01	1.27357E-23	1.93200E-Ø2	-1.85941E-22
7,4	-1.36434E-01	2.92826E-24	1.87852E-Ø2	-4.33382E-23
7,5	-1.34585E-01	6.59949E-25	1.82743E-Ø2	-9.89923E-24
7,6	-1.32784E-01	1.45789E-25	1.77834E-Ø2	-2.21600E-24
7,7	-1.31029E-01	3.15686E-26	1.73121E-Ø2	-4.86196E-25
7,8	-1.29320E-01	6.78037E-27	1.68579E-Ø2	-1.04526E-25
7,9	-1.27652E-01	1.39398E-27	1.64245E-Ø2	-2.20249E-26
8,0	-1.26026E-01	2.84269E-28	1.60064E-Ø2	-4.54829E-27
8,1	-1.24442E-01	5.69216E-29	1.56041E-Ø2	-9.20510E-28
8,2	-1.22879E-01	1.11306E-29	1.52157E-Ø2	-1.82582E-28
8,3	-1.21376E-01	2.13810E-30	1.48441E-Ø2	-3.54925E-29
8,4	-1.19912E-01	4.02491E-31	1.44849E-Ø2	-6.76185E-30
8,5	-1.18479E-01	7.42675E-32	1.41386E-Ø2	-1.26255E-30
8,6	-1.17082E-01	1.34324E-32	1.38040E-Ø2	-2.31038E-31
8,7	-1.15717E-01	2.38136E-33	1.34827E-Ø2	-4.14357E-32
8,8	-1.14382E-01	4.13819E-34	1.31718E-Ø2	-7.20321E-33
8,9	-1.13082E-01	7.04879E-35	1.28716E-Ø2	-1.25467E-33
9,0	-1.11814E-01	1.17668E-35	1.25817E-Ø2	-2.11853E-34
9,1	-1.10576E-01	1.92597E-36	1.23015E-Ø2	-3.50526E-35
9,2	-1.09369E-01	3.08951E-37	1.20306E-Ø2	-5.66470E-36
9,3	-1.08186E-01	4.85787E-38	1.17686E-Ø2	-9.03563E-37

EIA= 0.2100

0.0	-0.000000E+01	1.75263E+00	-1.96495E+00	0.00000E-01
0.1	-1.95275E+01	1.73539E+00	-1.92625E+00	-3.43173E-01
0.2	-3.82766E+01	1.68467E+00	-1.81320E+00	-6.66212E-01
0.3	-5.55655E+01	1.58342E+00	-1.63454E+00	-9.50941E-01
0.4	-7.07936E+01	1.49625E+00	-1.48373E+00	-1.18284E+00
0.5	-8.35210E+01	1.36894E+00	-1.13741E+00	-1.35224E+00
0.6	-9.34832E+01	1.22803E+00	-8.53641E-01	-1.45494E+00
0.7	-1.00595E+00	1.08015E+00	-5.70072E-01	-1.49209E+00
0.8	-1.04936E+00	9.31602E-01	-3.62363E-01	-1.46958E+00
0.9	-1.06737E+00	7.87908E-01	-6.29814E-02	-1.39689E+00
1.0	-1.06624E+00	6.50509E-01	1.30436E-01	-1.28575E+00
1.1	-1.04035E+00	5.31629E-01	3.03513E-01	-1.14875E+00
1.2	-1.00452E+00	4.24215E-01	4.19324E-01	-9.98025E-01
1.3	-9.58527E-01	3.32112E-01	4.99277E-01	-8.44326E-01
1.4	-9.06037E-01	2.55158E-01	5.42007E-01	-6.96321E-01
1.5	-8.54894E-01	1.92446E-01	5.56531E-01	-5.60320E-01
1.6	-7.95486E-01	1.42563E-01	5.48436E-01	-4.40281E-01
1.7	-7.41754E-01	1.03794E-01	5.24038E-01	-3.38064E-01
1.8	-6.91027E-01	7.43463E-02	4.69184E-01	-2.53826E-01
1.9	-6.44150E-01	5.24647E-02	4.48649E-01	-1.86484E-01
2.0	-6.01354E-01	3.59464E-02	4.26174E-01	-1.34166E-01
2.1	-5.62044E-01	2.45261E-02	3.64451E-01	-9.46089E-02
2.2	-5.28386E-01	1.72798E-02	3.29244E-01	-6.54632E-02
2.3	-4.97673E-01	1.18406E-02	2.80555E-01	-4.45134E-02
2.4	-4.70343E-01	8.10959E-03	2.57811E-01	-2.98062E-02
2.5	-4.45955E-01	5.72603E-03	2.30232E-01	-1.97107E-02
2.6	-4.24217E-01	4.11727E-03	2.09986E-01	-1.27256E-02
2.7	-4.04674E-01	3.06419E-03	1.85332E-01	-8.45314E-03
2.8	-3.87654E-01	2.37441E-03	1.67551E-01	-5.55558E-03
2.9	-3.71098E-01	1.91837E-03	1.52306E-01	-3.70495E-03
3.0	-3.56523E-01	1.61088E-03	1.39172E-01	-2.53402E-03
3.1	-3.43186E-01	1.39707E-03	1.27794E-01	-1.79808E-03
3.2	-3.30912E-01	1.24230E-03	1.17833E-01	-1.33244E-03
3.3	-3.19571E-01	1.12506E-03	1.08919E-01	-1.03400E-03
3.4	-3.08904E-01	1.03214E-03	1.01015E-01	-8.37679E-04
3.5	-2.99263E-01	9.59461E-04	9.45913E-02	-7.03517E-04
3.6	-2.90058E-01	8.92172E-04	8.85962E-02	-6.17628E-04
3.7	-2.81500E-01	8.40175E-04	8.31137E-02	-5.55525E-04
3.8	-2.73446E-01	7.82572E-04	7.81597E-02	-4.78730E-04
3.9	-2.65852E-01	7.37943E-04	7.36637E-02	-4.32280E-04
4.0	-2.58628E-01	6.99377E-04	6.96035E-02	-3.93155E-04
4.1	-2.51728E-01	6.66291E-04	6.59192E-02	-3.59434E-04
4.2	-2.45052E-01	6.38324E-04	6.26805E-02	-3.29977E-04
4.3	-2.38516E-01	6.15106E-04	5.97153E-02	-3.03934E-04
4.4	-2.32058E-01	5.96273E-04	5.69997E-02	-2.80768E-04

4,3	-2.2817cE-01	5.3b952E-04	2.35941E-02	-2.50048E-04
4,6	-2.2294cE-01	5.13898E-04	5.12890E-02	-2.41394E-04
4,7	-2.179[illegible]E-01	4.97415E-04	4.87612E-02	-2.24539E-04
4,8	-2.131[illegible]E-01	4.85936E-04	4.85932E-02	-2.79273E-04
4,9	-2.080[illegible]E-01	4.45713E-04	4.45739E-02	-1.95412E-04
5,0	-2.042[illegible]E-01	4.26813E-04	4.26602E-02	-1.82784E-04
5,1	-2.000[illegible]E-01	4.09120E-04	4.09116E-02	-1.71250E-04
5,2	-1.96[illegible]E-01	3.92530E-04	3.92527E-02	-1.60691E-04
5,3	-1.922[illegible]E-01	3.76953E-04	3.76949E-02	-1.51003E-04
5,4	-1.885[illegible]E-01	3.62304E-04	3.62301E-02	-1.42097E-04
5,5	-1.849[illegible]E-01	3.48510E-04	3.48507E-02	-1.33892E-04
5,6	-1.815[illegible]E-01	3.35504E-04	3.35502E-02	-1.26320E-04
5,7	-1.782[illegible]E-01	3.23227E-04	3.23225E-02	-1.19319E-04
5,8	-1.751[illegible]E-01	3.11623E-04	3.11621E-02	-1.12836E-04
5,9	-1.72[illegible]E-01	3.00644E-04	3.00642E-02	-1.06822E-04
6,0	-1.69[illegible]E-01	2.90244E-04	2.90243E-02	-1.01236E-04
6,1	-1.66[illegible]E-01	2.80384E-04	2.80382E-02	-9.60388E-05
6,2	-1.63[illegible]E-01	2.71025E-04	2.71023E-02	-9.11978E-05
6,3	-1.60[illegible]E-01	2.62134E-04	2.62132E-02	-8.66801E-05
6,4	-1.58[illegible]E-01	2.53679E-04	2.53678E-02	-8.24609E-05
6,5	-1.55[illegible]E-01	2.45632E-04	2.45631E-02	-7.85150E-05
6,6	-1.53[illegible]E-01	2.37968E-04	2.37966E-02	-7.48203E-05
6,7	-1.50[illegible]E-01	2.30661E-04	2.30659E-02	-7.13568E-05
6,8	-1.48[illegible]E-01	2.23689E-04	2.23688E-02	-6.81064E-05
6,9	-1.46[illegible]E-01	2.17033E-04	2.17032E-02	-6.50529E-05
7,0	-1.44[illegible]E-01	2.10672E-04	2.10671E-02	-6.21814E-05
7,1	-1.42[illegible]E-01	2.04591E-04	2.04590E-02	-5.94783E-05
7,2	-1.40[illegible]E-01	1.98772E-04	1.98771E-02	-5.69314E-05
7,3	-1.38[illegible]E-01	1.93200E-04	1.93199E-02	-5.45293E-05
7,4	-1.36[illegible]E-01	1.87861E-04	1.87860E-02	-5.22619E-05
7,5	-1.34[illegible]E-01	1.82743E-04	1.82742E-02	-5.01197E-05
7,6	-1.32[illegible]E-01	1.77833E-04	1.77832E-02	-4.80942E-05
7,7	-1.30[illegible]E-01	1.73121E-04	1.73120E-02	-4.61773E-05
7,8	-1.29[illegible]E-01	1.68595E-04	1.68594E-02	-4.43619E-05
7,9	-1.27[illegible]E-01	1.64245E-04	1.64243E-02	-4.26413E-05
8,0	-1.26[illegible]E-01	1.60063E-04	1.60062E-02	-4.10093E-05
8,1	-1.24[illegible]E-01	1.56041E-04	1.56040E-02	-3.94602E-05
8,2	-1.22[illegible]E-01	1.52169E-04	1.52168E-02	-3.79868E-05
8,3	-1.21[illegible]E-01	1.48443E-04	1.48442E-02	-3.65902E-05
8,4	-1.19[illegible]E-01	1.44848E-04	1.44846E-02	-3.52600E-05
8,5	-1.18[illegible]E-01	1.41386E-04	1.41385E-02	-3.39939E-05
8,6	-1.17[illegible]E-01	1.38048E-04	1.38047E-02	-3.27882E-05
8,7	-1.15[illegible]E-01	1.34827E-04	1.34826E-02	-3.16392E-05
8,8	-1.14[illegible]E-01	1.31718E-04	1.31716E-02	-3.05437E-05
8,9	-1.13[illegible]E-01	1.28716E-04	1.28715E-02	-2.94985E-05
9,0	-1.11[illegible]E-01	1.25817E-04	1.25816E-02	-2.85008E-05
9,1	-1.10[illegible]E-01	1.23015E-04	1.23014E-02	-2.75479E-05
9,2	-1.09[illegible]E-01	1.20303E-04	1.20302E-02	-2.66372E-05
9,3	-1.07[illegible]E-01	1.17684E-04	1.17683E-02	-2.57665E-05

ETA= 0.7650

0.0	-4.0000[illegible]E-01	1.6[illegible]781E+00	-1.7[illegible]49E+00	0.000002E-01
0.1	-1.77132[illegible]E-01	1.63258E+00	-1.74907E+00	-3.03134E-01
0.2	-3.47066[illegible]E-01	1.58773E+00	-1.65135E+00	-5.89208E-01
0.3	-5.05[illegible]E-01	1.51562E+00	-1.49661E+00	-8.42768E-01
0.4	-6.45[illegible]E-01	1.42072E+00	-1.29613E+00	-1.05136E+00
0.5	-7.63[illegible]E-01	1.3[illegible]734E+00	-1.0[illegible]37[illegible]E+00	-1.20653E+00
0.6	-8.57[illegible]E-01	1.18131E+00	-8.14873E-01	-1.30436E+00
0.7	-9.26572E-01	1.04836E+00	-5.64406E-01	-1.34540E+00
0.8	-9.70[illegible]E-01	9.13975E-01	-3.25848E-01	-1.33420E+00
0.9	-9.72[illegible]E-01	7.83011E-01	-1.1012[illegible]E-01	-1.27841E+00
1.0	-9.[illegible]E-01	6.59458E-01	7.[illegible]260E-02	-1.1[illegible]771E+00
1.1	-9.[illegible]E-01	5.46282E-01	2.25197E-01	-1.07264E+00
1.2	-9.[illegible]E-01	4.45396E-01	3.39173E-01	-9.43534E-01
1.3	-9.12[illegible]E-01	3.57731E-01	4.1[illegible]424E-01	-8.[illegible]717E-01
1.4	-8.67[illegible]E-01	2.83354E-01	4.6644[illegible]E-01	-6.78878E-01
1.5	-8.19[illegible]E-01	2.21602E-01	4.[illegible]E-01	-5.56799E-01
1.6	-7.70[illegible]E-01	1.71572E-01	4.8859[illegible]E-01	-4.47311E-01
1.7	-7.22[illegible]E-01	1.31710E-01	4.7352[illegible]E-01	-3.52459E-01
1.8	-6.76[illegible]E-01	1.00573E-01	4.4780[illegible]E-01	-2.72797E-01
1.9	-6.33[illegible]E-01	7.[illegible]62[illegible]E-02	4.15693E-01	-2.07756E-01
2.0	-5.93[illegible]E-01	5.[illegible]57[illegible]E-02	3.[illegible]E-01	-1.5[illegible]009E-01
2.1	-5.[illegible]E-01	4.[illegible]7[illegible]E-02	3.46[illegible]E-01	-1.15804E-01
2.2	-5.[illegible]E-01	3.[illegible]E-02	3.13914E-01	-8.52363E-02
2.3	-4.[illegible]E-01	2.77599E-02	2.79165E-01	-6.24447E-02
2.4	-4.[illegible]E-01	2.[illegible]E-02	2.52[illegible]E-01	-4.57[illegible]E-02
2.5	-4.[illegible]E-01	1.[illegible]E-02	2.24857E-01	-3.[illegible]E-02
2.6	-4.[illegible]E-01	1.55573E-02	2.02411E-01	-2.50410E-02
2.7	-4.[illegible]E-01	1.[illegible]E-02	1.[illegible]E-01	-1.89181E-02
2.8	-3.[illegible]E-01	1.17143E-02	1.65883E-01	-1.45820E-02
2.9	-3.[illegible]E-01	1.[illegible]E-02	1.51167E-01	-1.15012E-02
3.0	-3.[illegible]E-01	2.[illegible]E-03	1.38385E-01	-9.[illegible]E-03
3.1	-3.[illegible]E-01	8.[illegible]E-03	1.27244E-01	-7.[illegible]E-03
3.2	-3.[illegible]E-01	7.[illegible]E-03	1.17489E-01	-6.[illegible]E-03
3.3	-3.[illegible]E-01	7.[illegible]E-03	1.[illegible]E-01	-5.[illegible]E-03
3.4	-3.[illegible]E-01	6.71202E-03	1.01293E-01	-4.86909E-03
3.5	-2.[illegible]E-01	6.25453E-03	9.[illegible]E-02	-4.[illegible]E-03
3.6	-2.[illegible]E-01	5.[illegible]E-03	8.84547E-02	-3.83494E-03
3.7	-2.[illegible]E-01	5.[illegible]E-03	8.[illegible]E-02	-3.44583E-03
3.8	-2.[illegible]E-01	5.15[illegible]E-03	7.[illegible]E-02	-3.11532E-03
3.9	-2.[illegible]E-01	4.86042E-03	7.[illegible]E-02	-2.[illegible]E-03
4.0	-2.[illegible]E-01	4.[illegible]E-03	6.[illegible]E-02	-2.[illegible]E-03
4.1	-2.[illegible]E-01	4.[illegible]E-03	6.[illegible]E-02	-2.[illegible]E-03
4.2	-2.[illegible]E-01	4.11592E-03	6.23221E-02	-2.17434E-03
4.3	-2.[illegible]E-01	3.[illegible]E-03	5.[illegible]E-02	-2.[illegible]E-03
4.4	-2.[illegible]E-01	3.71455E-03	5.62493E-02	-1.[illegible]E-03

4.3	-2.28121E-01	3.53633E-03	5.35524E-02	-1.71509E-03
4.6	-2.22892E-01	3.37109E-03	5.10513E-02	-1.59218E-03
4.7	-2.17904E-01	3.21750E-03	4.87268E-02	-1.48114E-03
4.8	-2.13141E-01	3.07450E-03	4.65622E-02	-1.38055E-03
4.9	-2.08587E-01	2.94109E-03	4.45427E-02	-1.28914E-03
5.0	-2.04229E-01	2.81640E-03	4.26552E-02	-1.20586E-03
5.1	-2.00052E-01	2.69967E-03	4.08881E-02	-1.12980E-03
5.2	-1.96047E-01	2.59023E-03	3.92312E-02	-1.06015E-03
5.3	-1.92203E-01	2.48745E-03	3.76752E-02	-9.96257E-04
5.4	-1.88513E-01	2.39080E-03	3.62119E-02	-9.37510E-04
5.5	-1.84957E-01	2.29950E-03	3.48342E-02	-8.83392E-04
5.6	-1.81540E-01	2.21399E-03	3.35347E-02	-8.33443E-04
5.7	-1.78246E-01	2.13329E-03	3.23081E-02	-7.87204E-04
5.8	-1.75067E-01	2.05642E-03	3.11486E-02	-7.44497E-04
5.9	-1.72001E-01	1.98348E-03	3.00519E-02	-7.04828E-04
6.0	-1.69063E-01	1.91505E-03	2.90126E-02	-6.67976E-04
6.1	-1.66212E-01	1.85030E-03	2.80275E-02	-6.33692E-04
6.2	-1.63459E-01	1.78855E-03	2.70924E-02	-6.01748E-04
6.3	-1.60792E-01	1.72988E-03	2.62039E-02	-5.71949E-04
6.4	-1.58214E-01	1.67409E-03	2.53591E-02	-5.44114E-04
6.5	-1.55717E-01	1.62099E-03	2.45552E-02	-5.18081E-04
6.6	-1.53302E-01	1.57042E-03	2.37890E-02	-4.93706E-04
6.7	-1.50966E-01	1.52220E-03	2.30588E-02	-4.70855E-04
6.8	-1.48699E-01	1.47620E-03	2.23621E-02	-4.49410E-04
6.9	-1.46498E-01	1.43228E-03	2.16969E-02	-4.29264E-04
7.0	-1.44363E-01	1.39031E-03	2.10612E-02	-4.10318E-04
7.1	-1.42287E-01	1.35018E-03	2.04534E-02	-3.92484E-04
7.2	-1.40267E-01	1.31178E-03	1.98716E-02	-3.75679E-04
7.3	-1.38302E-01	1.27501E-03	1.93149E-02	-3.59831E-04
7.4	-1.36389E-01	1.23979E-03	1.87814E-02	-3.44870E-04
7.5	-1.34524E-01	1.20601E-03	1.82698E-02	-3.30736E-04
7.6	-1.32708E-01	1.17361E-03	1.77791E-02	-3.17371E-04
7.7	-1.30939E-01	1.14251E-03	1.73083E-02	-3.04723E-04
7.8	-1.29216E-01	1.11264E-03	1.68556E-02	-2.92745E-04
7.9	-1.27538E-01	1.08394E-03	1.64209E-02	-2.81391E-04
8.0	-1.25901E-01	1.05634E-03	1.60024E-02	-2.70623E-04
8.1	-1.24311E-01	1.02980E-03	1.56008E-02	-2.60401E-04
8.2	-1.22671E-01	1.00425E-03	1.52138E-02	-2.50692E-04
8.3	-1.21166E-01	9.79642E-04	1.48411E-02	-2.41463E-04
8.4	-1.19702E-01	9.55959E-04	1.44820E-02	-2.32686E-04
8.5	-1.18271E-01	9.33091E-04	1.41360E-02	-2.24332E-04
8.6	-1.17075E-01	9.11059E-04	1.38022E-02	-2.16376E-04
8.7	-1.15711E-01	8.89803E-04	1.34803E-02	-2.08794E-04
8.8	-1.14377E-01	8.69288E-04	1.31693E-02	-2.01565E-04
8.9	-1.13077E-01	8.49479E-04	1.28694E-02	-1.94668E-04
9.0	-1.11809E-01	8.30344E-04	1.25796E-02	-1.88085E-04
9.1	-1.10573E-01	8.11853E-04	1.22994E-02	-1.81796E-04
9.2	-1.09368E-01	7.93976E-04	1.20286E-02	-1.75787E-04
9.3	-1.08194E-01	7.76686E-04	1.17667E-02	-1.70041E-04

ETA= 0.2000

0.0	0.0000E-01	1.43395E+00	-1.42642E+00	0.00000E-01
0.1	-1.41847E-01	1.42251E+00	-1.40253E+00	-2.27764E-01
0.2	-2.78990E-01	1.38878E+00	-1.33289E+00	-4.43918E-01
0.3	-4.07050E-01	1.33447E+00	-1.22198E+00	-6.37863E-01
0.4	-5.22259E-01	1.26225E+00	-1.07730E+00	-8.00893E-01
0.5	-6.21690E-01	1.17553E+00	-9.08097E-01	-9.20855E-01
0.6	-7.03402E-01	1.07822E+00	-7.24629E-01	-1.01250E+00
0.7	-7.66484E-01	9.74386E-01	-5.37168E-01	-1.05755E+00
0.8	-8.11019E-01	8.67988E-01	-3.56174E-01	-1.06437E+00
0.9	-8.37968E-01	7.62635E-01	-1.86604E-01	-1.03756E+00
1.0	-8.48902E-01	6.61396E-01	-3.74624E-02	-9.83197E-01
1.1	-8.46235E-01	5.66684E-01	8.83978E-02	-9.08209E-01
1.2	-8.32146E-01	4.80207E-01	1.89233E-01	-8.19639E-01
1.3	-8.09623E-01	4.04988E-01	2.65175E-01	-7.24081E-01
1.4	-7.79837E-01	3.35432E-01	3.17856E-01	-6.27255E-01
1.5	-7.46537E-01	2.77426E-01	3.49983E-01	-5.33743E-01
1.6	-7.13466E-01	2.28161E-01	3.64875E-01	-4.46888E-01
1.7	-6.73619E-01	1.87754E-01	3.64085E-01	-3.68836E-01
1.8	-6.37589E-01	1.54363E-01	3.57057E-01	-3.00672E-01
1.9	-6.02641E-01	1.27282E-01	3.42950E-01	-2.42616E-01
2.0	-5.69547E-01	1.05517E-01	3.22394E-01	-1.94248E-01
2.1	-5.38679E-01	8.81876E-02	2.97538E-01	-1.54723E-01
2.2	-5.10062E-01	7.43136E-02	2.73997E-01	-1.22955E-01
2.3	-4.83824E-01	6.33271E-02	2.50919E-01	-9.77753E-02
2.4	-4.59837E-01	5.45773E-02	2.29050E-01	-7.80303E-02
2.5	-4.37959E-01	4.72738E-02	2.08822E-01	-6.26855E-02
2.6	-4.18012E-01	4.19248E-02	1.97430E-01	-5.08043E-02
2.7	-3.99810E-01	3.73232E-02	1.73905E-01	-4.16212E-02
2.8	-3.83171E-01	3.35317E-02	1.59171E-01	-3.45091E-02
2.9	-3.67921E-01	3.03590E-02	1.46090E-01	-2.89719E-02
3.0	-3.53973E-01	2.76278E-02	1.34499E-01	-2.46252E-02
3.1	-3.41077E-01	2.54141E-02	1.24226E-01	-2.11767E-02
3.2	-3.29023E-01	2.34399E-02	1.15103E-01	-1.84072E-02
3.3	-3.17923E-01	2.17156E-02	1.06951E-01	-1.61535E-02
3.4	-3.07505E-01	2.01960E-02	9.97239E-02	-1.42951E-02
3.5	-2.97754E-01	1.88464E-02	9.32151E-02	-1.27452E-02
3.6	-2.88936E-01	1.76394E-02	8.73544E-02	-1.14317E-02
3.7	-2.80464E-01	1.65537E-02	8.20556E-02	-1.03116E-02
3.8	-2.72503E-01	1.55720E-02	7.72496E-02	-9.34592E-03
3.9	-2.65000E-01	1.46803E-02	7.28722E-02	-8.50645E-03
4.0	-2.57916E-01	1.38672E-02	6.88728E-02	-7.77145E-03
4.1	-2.51214E-01	1.31231E-02	6.52071E-02	-7.12386E-03
4.2	-2.44864E-01	1.24400E-02	6.18376E-02	-6.55015E-03
4.3	-2.38838E-01	1.18110E-02	5.87320E-02	-6.03940E-03
4.4	-2.33110E-01	1.12303E-02	5.58623E-02	-5.58271E-03

4.5	-2.27054E-01	1.06929E-02	5.32045E-02	-5.17276E-03
4.6	-2.22463E-01	1.01944E-02	5.07374E-02	-4.80343E-03
4.7	-2.17585E-01	9.73104E-03	4.84428E-02	-4.46963E-03
4.8	-2.12769E-01	9.29945E-03	4.63045E-02	-4.16703E-03
4.9	-2.08240E-01	8.89672E-03	4.43081E-02	-3.89194E-03
5.0	-2.03903E-01	8.52025E-03	4.24411E-02	-3.64120E-03
5.1	-1.99748E-01	8.16776E-03	4.06923E-02	-3.41210E-03
5.2	-1.95761E-01	7.83719E-03	3.90517E-02	-3.20228E-03
5.3	-1.91934E-01	7.52673E-03	3.75103E-02	-3.00972E-03
5.4	-1.88256E-01	7.23473E-03	3.60601E-02	-2.83263E-03
5.5	-1.84719E-01	6.95974E-03	3.46940E-02	-2.66945E-03
5.6	-1.81315E-01	6.70042E-03	3.34054E-02	-2.51882E-03
5.7	-1.78036E-01	6.45559E-03	3.21885E-02	-2.37952E-03
5.8	-1.74875E-01	6.22417E-03	3.10379E-02	-2.25049E-03
5.9	-1.71826E-01	6.00519E-03	2.99489E-02	-2.13079E-03
6.0	-1.68883E-01	5.79774E-03	2.89171E-02	-2.01956E-03
6.1	-1.66041E-01	5.60102E-03	2.79384E-02	-1.91606E-03
6.2	-1.63294E-01	5.41429E-03	2.70093E-02	-1.81963E-03
6.3	-1.60637E-01	5.23687E-03	2.61263E-02	-1.72965E-03
6.4	-1.58067E-01	5.06816E-03	2.52865E-02	-1.64559E-03
6.5	-1.55579E-01	4.90758E-03	2.44871E-02	-1.56697E-03
6.6	-1.53168E-01	4.75460E-03	2.37254E-02	-1.49334E-03
6.7	-1.50833E-01	4.60875E-03	2.29991E-02	-1.42431E-03
6.8	-1.48568E-01	4.46960E-03	2.23061E-02	-1.35952E-03
6.9	-1.46370E-01	4.33672E-03	2.16442E-02	-1.29864E-03
7.0	-1.44236E-01	4.20975E-03	2.10117E-02	-1.24139E-03
7.1	-1.42167E-01	4.08833E-03	2.04067E-02	-1.18749E-03
7.2	-1.40155E-01	3.97215E-03	1.98278E-02	-1.13670E-03
7.3	-1.38201E-01	3.86089E-03	1.92734E-02	-1.08880E-03
7.4	-1.36300E-01	3.75430E-03	1.87422E-02	-1.04358E-03
7.5	-1.34451E-01	3.65210E-03	1.82328E-02	-1.00085E-03
7.6	-1.32653E-01	3.55405E-03	1.77440E-02	-9.60440E-04
7.7	-1.30902E-01	3.45994E-03	1.72748E-02	-9.22200E-04
7.8	-1.29197E-01	3.36954E-03	1.68242E-02	-8.85981E-04
7.9	-1.27537E-01	3.28268E-03	1.63911E-02	-8.51650E-04
8.0	-1.25918E-01	3.19915E-03	1.59746E-02	-8.19085E-04
8.1	-1.24341E-01	3.11880E-03	1.55739E-02	-7.88172E-04
8.2	-1.22803E-01	3.04147E-03	1.51882E-02	-7.58808E-04
8.3	-1.21303E-01	2.96699E-03	1.48168E-02	-7.30896E-04
8.4	-1.19839E-01	2.89524E-03	1.44589E-02	-7.04347E-04
8.5	-1.18411E-01	2.82608E-03	1.41140E-02	-6.79077E-04
8.6	-1.17016E-01	2.75939E-03	1.37813E-02	-6.55010E-04
8.7	-1.15654E-01	2.69504E-03	1.34603E-02	-6.32075E-04
8.8	-1.14324E-01	2.63294E-03	1.31504E-02	-6.10206E-04
8.9	-1.13024E-01	2.57297E-03	1.28512E-02	-5.89340E-04
9.0	-1.11753E-01	2.51504E-03	1.25622E-02	-5.69422E-04
9.1	-1.10511E-01	2.45905E-03	1.22829E-02	-5.50396E-04
9.2	-1.09296E-01	2.40493E-03	1.20128E-02	-5.32214E-04
9.3	-1.08108E-01	2.35258E-03	1.17516E-02	-5.14829E-04

Appendix VI-C: The Zero Temperature Plasma Dispersion Function for Complex Argument

In order to obtain an explicit expression for $G_F(\xi)$ we may either integrate Eq. (VI-121) with (VI-98) for $g(x)$, or directly evaluate $G_F(\xi)$ from its definition in the complex half plane $Im\xi < 0$ (VI-88). We will use the second method. The mathematical steps are straightforward but care should be taken in the definition of the logarithmic function which is a multivalued function in the complex field. For a function $\ell n z$ we will choose the branch cut as

$$Im z = 0 \qquad -\infty < Re z < 0 \tag{VI-C1}$$

so that $arg z$ receives values in the principal branch

$$-\pi < arg z < \pi \tag{VI-C2}$$

The direct integration of (VI-88) with (VI-98) results in

$$G_F(\xi) = -\frac{3}{4}\left[2\xi + (\xi^2-1)\ell n \frac{\xi-1}{\xi+1}\right] \qquad Im\xi < 0 \tag{VI-C3}$$

Breaking $G_F(\xi)$ into its real and imaginary parts results in

$$Re G_F(\xi) = -\frac{3}{4}\left\{2\xi^R + [(\xi^R)^2-(\xi^I)^2-1]\ell n\left|\frac{\xi-1}{\xi+1}\right| + 2\xi^R|\xi^I|[arg(\xi-1)-arg(\xi+1)]\right\} \tag{VI-C4}$$

$$Im G_F(\xi) = \frac{3}{4}\left\{2|\xi^I| + 2\xi^R|\xi^I|\ell n\left|\frac{\xi-1}{\xi+1}\right| - [(\xi^R)^2-|\xi^I|^2-1][arg(\xi-1)-arg(\xi+1)]\right\} \tag{VI-C5}$$

Defining the function $\tan^{-1}(x)$ in the section $-\frac{\pi}{2} < x < \frac{\pi}{2}$, bearing in mind that $Im\xi = -|\xi^I| < 0$, we get as a result of the branch cut (VI-C1)

$$\arg(\xi-1) = \begin{cases} \tan^{-1}\left(\dfrac{-|\xi^I|}{\xi^R-1}\right) & \xi^R > 1 \\ \tan^{-1}\left(\dfrac{-|\xi^I|}{\xi^R-1}\right) - \pi & \xi^R < 1 \end{cases} \qquad \text{(VI-C6)}$$

$$\arg(\xi+1) = \begin{cases} \tan^{-1}\left(\dfrac{-|\xi^I|}{\xi^R+1}\right) & \xi^R > -1 \\ \tan^{-1}\left(\dfrac{-|\xi^I|}{\xi^R+1}\right) - \pi & \xi^R < -1 \end{cases} \qquad \text{(VI-C7)}$$

or

$$\arg(\xi-1)-\arg(\xi+1) = \tan^{-1}\left(\frac{|\xi^I|}{\xi^R+1}\right) - \tan^{-1}\left(\frac{|\xi^I|}{\xi^R-1}\right) - \pi\eta(\xi^R) \qquad \text{(VI-C8)}$$

where

$$\eta(\xi^R) = \begin{cases} 1 & |\xi^R| < 1 \\ 0 & |\xi^R| > 1 \end{cases} \qquad \text{(VI-C9)}$$

At the limit $|\xi^I| \to 0$ Eq. (VI-C8) reduces to $-\pi\eta(\xi^R)$ and Eqs. (VI-C4,C5) reduce into (VI-100,101).

An HP25 program for calculating the real and imaginary parts of $G_F(\xi)$ (Eqs. VI-C4,C5) is listed below. The examples, $|\xi^I| = 0$, $|\xi^I| = 0.2$ are plotted for comparison on the same axes in Figs. 37, 38.

HP25 Program to calculate $ImG_F(\xi)$ for complex argument

Preliminary	Storage			
g rad	0	$\lvert\xi^I\rvert$	3	ξ^R-1
Store 0 to 5	1	$\lvert\xi^I\rvert^2$	4	ξ^R+1
	2	ξ^R	5	.75

Program

00	10 +	20 x	30 $\tan^{-1}$	40 x
01 RCL3	11 ÷	21 RCL6	31 -	41 RCL1
02 ENTER	12 $\sqrt{}$	22 +	32 RCL3	42 -
03 x	13 ℓn	23 RCL0	33 x > 0	43 x
04 RCL1	14 RCL0	24 RCL4	34 GTO 48	44 -
05 +	15 2	25 ÷	35 R↓	45 RCL5
06 RCL4	16 x	26 $\tan^{-1}$	36 π	46 x
07 ENTER	17 STO6	27 RCL0	37 -	47 GTO 0
08 x	18 x	28 RCL3	38 RCL3	48 R↓
09 RCL1	19 RCL2	29 ÷	39 RCL4	49 GTO 38

HP25 Program to calculate $ReG_F(\xi)$ for complex argument

Preliminary	Storage			
g rad	0	$\lvert\xi^I\rvert$	3	ξ^R-1
store 0 to 5	1	$\lvert\xi^I\rvert^2$	4	ξ^R+1
	2	ξ^R	5	-.75

Program

00	10 +	20 RCL2	30 RCL3	40 RCL0
01 RCL3	11 ÷	21 2	31 ÷	41 x
02 ENTER	12 $\sqrt{}$	22 x	32 $\tan^{-1}$	42 RCL6
03 x	13 ℓn	23 STO6	33 -	43 x
04 RCL1	14 RCL3	24 +	34 RCL3	44 +
05 +	15 RCL4	25 RCL0	35 x ≥ 0	45 RCL5
06 RCL4	16 x	26 RCL4	36 GTO 48	46 x
07 ENTER	17 RCL1	27 ÷	37 R↓	47 GTO 00
08 x	18 -	28 $\tan^{-1}$	38 π	48 R↓
09 RCL1	19 x	29 RCL0	39 -	49 GTO 40

Appendix VI-D: Degeneracy Criterion

The number of electrons in the conduction band of a semiconductor is given by [Fistul 1969, Sze 1969]

$$n_o = N_c \frac{2}{\sqrt{\pi}} F_{1/2}\left(\frac{\mu}{k_B T}\right) \qquad \text{(VI-D1)}$$

where μ is the Fermi energy level measured in reference to the conduction band bottom. N_c is the effective density of states in the conduction band

$$N_c = 2\left(\frac{2\pi m k_B T}{h^2}\right)^{3/2} \qquad \text{(VI-D2)}$$

and $F_{1/2}(\frac{\mu}{kT})$ is the Fermi-Dirac integral

$$F_{1/2}\left(\frac{\mu}{k_B T}\right) = \int_0^\infty \frac{\sqrt{x}\ dx}{1 + \exp(x - \frac{\mu}{k_B T})} \qquad \text{(VI-D5)}$$

This function is tabulated in [Fistul 1969].

We define a criterion for degeneracy as the condition when the Fermi level exceeds the bottom of the conduction band ($\mu > 0$). To be in the nondegenerate regime we must satisfy

$$n_o < N_c \frac{2}{\sqrt{\pi}} F_{1/2}(0) \qquad \text{(VI-D6)}$$

which when numerically computed, results in the condition

$$n_o\left(\frac{m}{m_e} T\right)^{-3/2} < 4 \times 10^{15} \qquad \text{(VI-D7)}$$

where n_o and T are expressed in units of [cm^{-3}] and [°K] respectively.

Chapter VII

DISCUSSION ON WAVE INTERACTIONS IN PERIODIC STRUCTURES

1. Introduction

In the present chapter we present in further detail some conclusions which result from our generalized treatment of traveling wave interaction. We also discuss some other effects and topics which have relevance to the present investigation and give reference to some other investigations which are related to this work.

The implication of our generalized analysis to traveling wave interaction with vacuum accelerated electron beams is discussed in the second section, and the limits of the conventional traveling wave interaction analysis are indicated. In the third section we discuss briefly the Smith-Purcell radiation and the Cerenkov radiation and their relation to the present traveling wave analysis.

The implication of the present theory to the case when the periodic structure is the crystal lattice is discussed in Section 4. We calculate the amplitude of optical space harmonics in the crystal lattice, and discuss the single crystal distributed feedback X-ray laser and the possibility of traveling wave interaction in the crystal lattice.

The possibility of a solid state traveling wave amplifier is discussed in Section 5. Previous research is reviewed, and the design considerations and limitations are indicated. Finally, the limitations of the present theory and of the models used are pointed out in Section 6.

2. Traveling Wave Interaction with Vacuum Accelerated Electron Beam of Finite Temperature

The most obvious example of a finite temperature electron beam is the solid state plasma, therefore in the extensions of the conventional theory of traveling wave interaction we refer mostly to this example. However, even a vacuum tube accelerated electron beam has a finite velocity distribution width, and it will be of interest to investigate the theoretical limits of the conventional theory in this case.

In this section we will summarize the results of our traveling wave interaction theory in the different operational regimes, show the consistency of the different expressions, their implication to the case of vacuum electron beams and their reduction to the conventional traveling wave interaction theory [Pierce 1950].

It is apparent that even in the conventional traveling wave tube there are operating regimes which cannot be explained by the conventional (macroscopic plasma equations) theory. If the electromagnetic wave component moves synchronously with the electron beam or within its velocity spread width, the beam will not "look" monochromatic to the wave. The kinetic (Boltzmann) plasma theory or even quantum theory may be then necessary to explain the interaction. Fortunately, as we will see later, at the optimal operation conditions (maximum gain) the wave is slightly out of synchronism with the electron beam. This slight out of synchronism condition is usually enough to make the beam "look" practically monoenergetic, and the extended theories reduce into the conventional one for most practical cases of conventional traveling wave tube amplifiers.

The constant interest in extending the operating frequency of vacuum traveling wave devices [e.g., Mizuno 1973, Yariv 1973A] raises the need to examine and define the limits of the conventional theory and provide appropriate extensions. Yariv and Armstrong [1973A] recently suggested a possible backward wave oscillator operating at the optical frequency regime (λ = 10 μm) utilizing a periodic dielectric waveguide structure (Fig. 7). Operation at this high frequency may be close to the limits where conventional theory ceases to apply and the extended theory should be used. This limit will be defined in more detail in the following.

There are a few other known physical effects which involve interaction of radiation and electron beams in slow wave structures and have apparent relation to the conventional traveling wave interaction. One of them is the Smith-Purcell radiation effect [Smith 1953] discussed in the next section, which operates in the visible light regime. Another related subject is the idea of "free electron laser" [Madey 1971, Elias 1975] which operates at optical wavelength λ = 10 μm. Yet a third intriguing possibility is the interaction of an electron beam with an electromagnetic beam, utilizing the natural periodicity of the crystal lattice (discussed later in Section 4). All these problems call for extension of the traveling wave theory to high frequencies and to short periodicities.

The theory extensions which were presented in the previous chapters make it easier to discuss the relation of these effects to the conventional traveling wave interaction.

Before proceeding, it may be in order at this point to discuss briefly the characteristics of the vacuum electron beam velocity distribution. This is done in more detail in Appendix VII-A. A typical distribution function of a vacuum tube diode is plotted in Fig. 41, following the model of Poritsky [1953] (see Eq. VII-A8). The velocity distribution is quite different from a Gaussian distribution. It has an abrupt step on its slow side and a Gaussian tail on its fast side. Nevertheless we can still talk about the beam average velocity and temperature defined in terms of the distribution function moments (V-15,16).

It is important to notice that the beam's longitudinal temperature, which is an important parameter in the theory, reduces considerably with its acceleration (VII-A5,A7),

$$v_{th} = \frac{1}{2} \frac{(v_{th})_i^2}{v_o} \tag{VII-1}$$

$$T = \frac{k_B}{4} \frac{T_i^2}{eV} = 2.156 \times 10^{-5} \frac{T_i^2}{V} \tag{VII-2}$$

or

$$T = \frac{k_B}{2m} \frac{T_i^2}{v_o^2} = 8.425 \times 10^{-11} \frac{T_i^2}{(v_o/c)^2} \tag{VII-3}$$

where in (VII-2,3) the units are [T] = °K, [V] = volt

A typical vacuum tube electron beam has an initial temperature which is about the temperature of the cathode electron emitter. A reasonable estimate is T_i = 1500°K. If accelerated to V = 6 kV, its temperature becomes $T = 8 \times 10^{-3}$°K. The thermal velocity of this

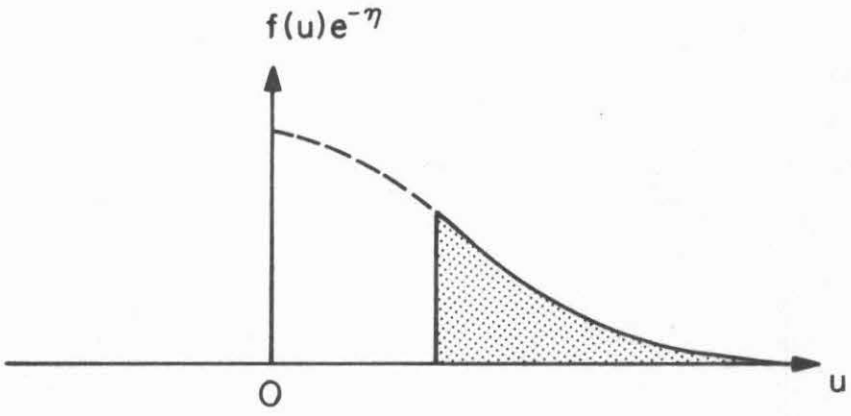

Fig. 41 The longitudinal velocity distribution of an electron beam in a vacuum tube diode (the dotted area). The velocity distribution at the potential minimum (near the cathode) includes also the area under the broken line. The parameter η is defined in Appendix VII-A.

beam is $v_{th} = 4.9 \times 10^4$cm/sec which is exceedingly low relative to the beam velocity $v_o = 4.55 \times 10^9$cm/sec ($v_{th}/v_o = 1.06 \times 10^{-5}$). We thus see that the beam's longitudinal temperature is many orders of magnitude smaller than the cathode temperature. In practice the beam may be thermalized by different effects like nonuniformity of the accelerating field, electron optics aberrations, noise, etc.

Also, the density of the electron plasma reduces with the acceleration (VII-A3)

$$n_o = \frac{I/S}{ev_o} \qquad \text{(VII-4)}$$

For example, a high current tube ($I/S = 1000A/cm^2$) operating at 6 KeV energy ($v_o = 4.55 \times 10^9$cm/sec) has electron density $n_o = 1.37 \times 10^{12}$ cm^{-3} calculated from (VII-4).

It is interesting to notice that the parameters k_D (Eq. V-20) and k_A (Eq. VI-59) are independent of the electron acceleration, since both n_o and v_{th} (Eqs. VII-1,4) have the same dependence on v_o ! Thus effects and criteria which depend on these parameters do not change by accelerating the beam, and are solely determined by the current density and the initial temperature of the beam.*

The temperature decrease of a relativistic electron beam is much stronger than that of (VII-1-3). Instead,we get Eqs. (VII-A18-A21). Pantell [1968] quotes as "reasonable" characteristics for

---

*Also the parameter k_G can be shown to be independent of v_o; but to show this, some modification of the analysis leading to Eq. (VI-92) must be made, in order to take into account the anisotropy of the electron beam plasma.

carefully filtered electron beams from high current accelerators in the low megavolt range $\Delta\mathcal{E}/\mathcal{E} = 10^{-4}$, $n_o = 10^8 cm^{-3}$. The first parameter gives for a 5 MeV beam (using VII-A19-A21) $v_{th} \simeq 30000$ cm/sec, $T \simeq 3 \times 10^{-3}$°K. On the other hand, Piestrup [1972] suggests a value of $\Delta\mathcal{E}/\mathcal{E} < 10^{-3}$ as a typical value for a 2 MeV, 600 amp electron gun. This corresponds to $v_{th} < 1.9 \times 10^6$cm/sec and $T < 12$°K.

The discussion up to this point gave us some indication about the characteristics of typical electron beams, although it should be understood that a variety of instruments with different characteristics exist. We can now proceed in summarizing the extended theory of traveling wave interaction and its relation to interactions with electron beams.

Our basic model, stated in Section 2 of Chapter IV, consists of one-dimensional (longitudinal) coupling between a slow electromagnetic wave component, which is excited by a plasma a-c current according to Pierce's equation (IV-8), and a plasma current which is induced in the plasma by the electromagnetic component according to a general linear plasma response law, including local field effect (IV-7). The result of the coupling is the traveling wave dispersion equation (IV-9)

$$\frac{K_1 S\, \beta_1 \beta^2 \omega}{\beta^2 - \beta_1} \; \frac{\chi_p(\beta,\omega)}{1 + \chi_p(\beta,\omega)/\varepsilon} = 1 \qquad \text{(VII-5)}$$

where $\chi_p(\beta,\omega)$, the plasma susceptibility, was calculated according to different plasma models in different operating regimes (Chapters IV to VI).

Finite Temperature Plasma in the Collision Regime

Using the macroscopic plasma equations, we derived in Chapter IV an expression for the plasma susceptibility (IV-31):

$$\chi_p(\beta,\omega) = \frac{i\varepsilon\omega_p^2}{(\beta v_o-\omega) + i\tau[v_T^2\beta^2 - (\beta v_o-\omega)^2]} \qquad \text{(VII-6)}$$

This expression was used in Chapter IV to obtain the dispersion equation (VII-5) of the traveling wave excitation.

In the limit $\tau \to \infty$, $T \simeq 0 \simeq V_T$ we showed in Appendix IV-A that Eq. (VII-6) reduces into

$$\chi_p = -\varepsilon \frac{\omega_p^2}{(\beta v_o-\omega)^2} \qquad \text{(VII-7)}$$

$$\varepsilon_p(\beta,\omega) \equiv 1 + \chi_p/\varepsilon = 1 - \frac{\omega_p^2}{(\beta v_o - \omega)^2} \qquad \text{(VII-8)}$$

When substituted into Eq. (VII-5), this results in the conventional traveling wave tube dispersion equation (IV-A3)

$$-\frac{K_1 S\, \beta_1 \beta^2 \omega\, \omega_p^2/v_o^2}{(\beta^2-\beta_1^2)[(\beta - \frac{\omega}{v_o})^2 - (\frac{\omega_p}{\omega})^2]} = 1 \qquad \text{(VII-9)}$$

or its reduced form (see IV-A8).

In a vacuum accelerated electron beam collisions are usually negligible. The main collision mechanism is electron-electron scattering. The reduction to the collisionless finite temperature limit is thus justified. In some related effects like the Cerenkov radiation, the electrons propagate in matter. Obviously collisions are severe in that case and cannot be neglected.

Kinetic (Boltzmann equation) description of the plasma

In the finite temperature collisionless regime we derived in Chapter V the drifting plasma susceptibility and dielectric constant (V-19,22)

$$\chi_p(\beta,\omega) = -\frac{1}{2}\,\varepsilon\,\frac{k_D^2}{\beta^2}\,G'(\zeta) \qquad \text{(VII-10)}$$

$$\varepsilon_p(\beta,\omega) = 1 - \frac{1}{2}\,\frac{k_D^2}{\beta^2}\,G'(\zeta) \qquad \text{(VII-11)}$$

We showed in Chapter V that when (VII-10) applies, the electromagnetic-like solution ($\beta \simeq \beta_1$) of the dispersion equation (VII-5) exhibits gain when (assuming a symmetric distribution function)

$$\zeta_1 \equiv \frac{\omega/\beta_1 - v_o}{v_{th}} < 0 \qquad \text{(VII-12)}$$

and attenuation, when

$$\zeta_1 > 0 \qquad \text{(VII-13)}$$

It was also shown that when

$$k_D >> \beta \qquad \text{(VII-14)}$$

it is possible to find operating conditions where the electromagnetic-like solution of the dispersion equation (VII-5) nearly satisfies the plasma dispersion equation

$$\varepsilon_p(\beta,\omega) = 0 \qquad \text{(VII-15)}$$

Then strong interaction occurs with the plasma wave, which can result in strong gain in case (VII-12), or strong attenuation (the "Kompfner dip") in case (VII-13).

We showed in Section 3 of Chapter V that Eq. (VII-5) with (VII-10,11) reduces into Eq. (VII-9) in the limit of monoenergetic electron beam $g(x) = \delta(x)$. We will now assume that the electron beam has a finite longitudinal velocity spread and show in this case the conditions for reduction to the conventional theory.

In the limit

$$|\zeta| \gg 1 \tag{VII-16}$$

we can asymptotically expand the function $G(\zeta)$

$$G(\zeta) \simeq -\frac{1}{\zeta} \tag{VII-17}$$

$$G'(\zeta) \simeq \frac{1}{\zeta^2} \tag{VII-18}$$

This expansion is a good approximation for large enough values of ζ so that $g(x) \simeq 0$ for $|x| > |\zeta|$. In this case, the contribution of the pole to the integral (V-18) is negligible and one can neglect x relative to ζ in the denominator. Equation (VII-17) is then obtained straightforwardly using the normalization of $g(x)$.

Using (VII-18) and (V-21), Eqs. (VII-10,11) can be written as

$$\chi_p(\beta,\omega) = -\frac{1}{2}\varepsilon\frac{k_D^2}{\beta^2}\frac{v_{th}^2}{(\omega/\beta - v_o)^2} = -\varepsilon\frac{\omega_p^2}{(\beta v_o - \omega)^2} \tag{VII-19}$$

$$\varepsilon_p(\beta,\omega) = 1 - \frac{\omega_p^2}{(\beta v_o - \omega)^2} \qquad \text{(VII-20)}$$

where we used the identity

$$k_D^2 = \frac{n_o e^2}{\varepsilon k_B T} = 2\,\frac{\omega_p^2}{v_{th}^2} \qquad \text{(VII-21)}$$

Equations (VII-19,20) are identical with (VII-7,8) and therefore, as before, reduce (VII-5) to the conventional expression (VII-9).

It is apparent now that Equations (VII-19,20) do not apply universally for any operation conditions ω, β, v_o because they were derived with the assumption (VII-16). Since $\zeta \equiv (\omega/\beta - v_o)/v_{th}$, it means that Equations (VII-19,20,9) do not apply when

$$|\omega/\beta - v_o| \lesssim v_{th} \qquad \text{(VII-22)}$$

which means that the phase velocity of the excitation is synchronous with the beam velocity within its thermal spread.

We may show, however, that for operational conditions where the electromagnetic wave is phase matched to the plasma wave (which is the case of most practical interest, since then the interaction is the strongest) the expansion condition (VII-16) is always satisfied and hence the conventional equation (VII-9) applies. Indeed, when β satisfies Equations (VII-15,20) we get

$$\beta = \frac{\omega}{v_o} \pm \frac{\omega_p}{v_o} \qquad \text{(VII-23)}$$

hence

$$|\zeta| = \frac{|\omega/\beta - v_o|}{v_{th}} = \frac{\omega_p/\beta}{v_{th}} = \frac{1}{\sqrt{2}} \frac{k_D}{\beta} \qquad \text{(VII-24)}$$

Since we assumed that phase matching to the plasma wave is attained, the necessary condition (VII-14) must have been satisfied (it is always satisfied in traveling wave tubes). Substituting (VII-14) in (VII-24) we find that (VII-16) is automatically satisfied and the use of Equations (VII-9,19,20,23) is thus a posteriori satisfied near the operation condition (VII-23).

A discussion on the transition from a monoenergetic beam case to the finite temperature case in relation to the double stream amplifier can be found in [O'Neil 1968].

Quantum mechanical description of the plasma

In Chapter VI we have treated the plasma response problem using a quantum mechanical model. We received in the case of nondegenerate plasma (the degenerate case is not relevant to the present discussion) the following expressions for the plasma susceptibility and dielectric function (VI-56)

$$\chi_p(\beta,\omega) = -\frac{1}{2}\,\varepsilon \frac{k_A^3}{\beta^3} [G(\zeta_b) - G(\zeta_a)] \qquad \text{(VII-25)}$$

$$\varepsilon_p(\beta,\omega) = 1 - \frac{1}{2} \frac{k_A^3}{\beta^3} [G(\zeta_b) - G(\zeta_a)] \qquad \text{(VII-26)}$$

where ζ_a, ζ_b, k_A are defined by (VI-57-59,36,37).

The traveling wave dispersion equation in this regime results from substituting (VII-25) in (VII-5). We concluded that the solution

for the electromagnetic-like mode exhibits gain in the population inversion condition

$$g(\zeta_b) > g(\zeta_a) \tag{VII-27}$$

where $g(x)$ is the normalized distribution function (VI-54). In the case of a symmetric $g(x)$ this condition can be written as

$$\frac{1}{2}(\zeta_a + \zeta_b) \equiv \zeta_1 < 0 \tag{VII-28}$$

which is equivalent to (VII-12) or the classical Cerenkov condition (VI-46). We also concluded that strong coupling can occur when conditions for phase matched photon-plasmon interaction are obtained, viz., Eq. (VII-15) is closely satisfied with $\varepsilon_p(\beta,\omega)$ given by (VII-26). This was broadly discussed in Section 7 of Chapter VI, where we indicated that conditions for phase matched photon-plasmon coupling are (VI-140, 142, 144, 164).

$$\beta_1 << k_A = 21.51 \left(\frac{n_o}{\sqrt{T}}\right)^{1/3} \tag{VII-29}$$

$$|\zeta_a|, |\zeta_b| >> 1 \tag{VII-30}$$

where ζ_a and ζ_b have the same sign (if negative, gain is obtained; if positive, we get attenuation.)

The units in (VII-29) are all c.g.s. For example when $n_o = 1.37 \times 10^{12} cm^{-3}$, $T = 8 \times 10^{-3} °K$, we get $k_A = 5.32 \times 10^5 cm^{-1}$, which means that condition (VII-29) does not forbid collective interaction (photon-plasmon phase matching) down to optical grating period lengths $2\pi/\beta_1 >> 0.15$ μm.

The reduction of the quantum mechanical expressions to the classical kinetic theory was discussed in Sections 4 and 7 of Chapter VI. The classical regime is obtained by replacing the functions' difference $G(\zeta_b) - G(\zeta_a)$ by the derivative, evaluated at $\zeta_1 \simeq \zeta_a \simeq \zeta_b$ (compare (VII-25,26) to VII-10,11). Necessary conditions for this reduction are (VI-42)

$$\beta_1 << k_a \simeq k_b \simeq \frac{m}{\hbar} \frac{\omega}{\beta_1} \tag{VII-31}$$

which can be written in the form

$$\beta_1^2 << \frac{m}{\hbar} \omega \tag{VII-32}$$

Also (VI-77)

$$\beta_1 << \left| \frac{2g'(\zeta_1)}{g''(\zeta_1)} \right| k_{th} \tag{VII-33}$$

which in the case of Maxwellian distribution can be written as (VI-78)

$$\beta_1 << \frac{2|\zeta_1|}{|1 - 2\zeta_1^2|} k_{th} \tag{VII-34}$$

where

$$\zeta_1 = \frac{\omega/\beta_1 - v_o}{v_{th}} \tag{VII-35}$$

We can see from (VII-33,34) that the quantum mechanical regime can be obtained with vacuum accelerated electron beams under practical situations. In the discussion above we found that the thermal velocity of a 6 KeV, T_i = 1500°K electron beam in a diode tube is $v_{th} = 4.95 \times$

10^4cm/sec. This corresponds to $k_{th} = 4.3 \times 10^4 cm^{-1}$. From criterion (VII-34), assuming a Gaussian distribution and $|\zeta_1| >> 1$ we get that the condition for reduction to the classical limit is

$$\beta_1 << 4.17 \times 10^4 cm^{-1}/\zeta_1 \quad \text{or} \quad 2\pi/\beta_1 >> \zeta_1 \times 1.5\ \mu m$$

We thus find that under the above conditions the quantum regime applies to periodic structures with periods in the micron range. Certainly quantum effects will dominate in interactions involving shorter periods (like the crystal lattice) or beams with smaller thermal spread (higher acceleration).

The actual electron distribution function is quite different from a Gaussian and therefore, the more general criterion (VII-33) should be used. Examining Fig. 41 we realize that strong quantum effect may be obtained if the slow electromagnetic wave component is synchronous with the step-like slow edge of the velocity distribution. In this case the difference $g(\zeta_b) - g(\zeta_a)$ cannot be substituted by a differential, or using condition (VII-33) we note that $g'(\zeta_1)$ is so large at this point that the inequality is not satisfied even at quite small values of k_{th} (or long periods of the periodic structure.)

We showed that under the appropriate conditions the quantum mechanical theory reduces into the classical kinetic (Boltzmann equation) theory. We also showed that the latter can be reduced to the conventional traveling wave tube dispersion equation (VII-9). It thus follows that the quantum mechanical derivation is consistent with the conventional traveling wave theory. It is, however, of interest to examine directly how and under what conditions the quantum mechanical

analysis reduces to the conventional traveling wave tube expressions.

Substituting (VII-25) into (VII-5), one gets the quantum mechanical expression of the traveling wave interaction dispersion equation

$$\frac{-2\beta_1\theta[G(\zeta_b) - G(\zeta_a)]}{(\beta^2-\beta_1^2)\{1 - \frac{1}{2}\frac{k_A^3}{\beta_1^3}[G(\zeta_b) - G(\zeta_a)]\}} = 1 \qquad \text{(VII-36)}$$

where θ is given by Equation (VI-66).

In order to reduce (VII-36) to the conventional expression (VII-9), we would like to use the asymptotic expansion (VII-17) of $G(\zeta_a)$ and $G(\zeta_b)$. However, if β_1/k_{th} is large enough, it is possible to get a situation where the expansion condition (VII-16) is satisfied for only one of ζ_a, ζ_b. If, for example, only $|\zeta_a| \ll 1$ we get a "mixed" expression

$$-2\beta_1\theta \frac{G(\zeta_b) + 1/\zeta_a}{(\beta^2 - \beta_1^2)\{1 - \frac{1}{2}\frac{k_A^3}{\beta_1^3}[G(\zeta_b) + 1/\zeta_a]\}} = 1 \qquad \text{(VII-37)}$$

We may have a situation where both ζ_b and ζ_a satisfy (VII-16) even if they are quite different from each other (large value of β_1/k_{th}).

$$|\zeta_a|, |\zeta_b| \gg 1 \qquad \text{(VII-38)}$$

$$2\beta_1\theta \frac{1/\zeta_b - 1/\zeta_a}{(\beta^2-\beta_1^2)\{1 + \frac{1}{2}\frac{k_A^3}{\beta_1^3}[1/\zeta_b - 1/\zeta_a]\}} = 1 \qquad \text{(VII-39)}$$

After substituting ζ_a, ζ_b and θ (Eqs. VI-60,61,36,37,66) in (VII-39) we get

$$-\frac{\varepsilon K_1 S\ \beta_1 \beta^2 \omega\ \omega_p^2/v_o^2}{(\beta^2-\beta_1^2)[(\beta-\frac{\omega}{v_o})^2-(\frac{\hbar\beta^2}{2mv_o})^2-\frac{\omega_p^2}{v_o^2}]} = 1 \qquad \text{(VII-40)}$$

Equation (VII-40) is almost identical to (VII-9) except for an extra "quantum mechanical" term $(\hbar\beta^2/2mv_o)^2$ in the denominator. Equation (VII-40), like (VII-9), can also be reduced into Pierce's third order normalized equation (IV-A8) (assuming $\beta \simeq \beta_1$).

The condition for neglecting the quantum mechanical effect is that the term $(\hbar\beta^2/2mv_o)^2$ will be negligible relative to the classical term ω_p^2/v_o^2. This can be written in one of the forms

$$\frac{\hbar\beta^2}{2m} \ll \omega_p \qquad \text{(VII-41)}$$

$$\mathcal{E}_\beta \ll \hbar\omega_p \qquad \text{(VII-42)}$$

$$\beta^2 \ll \frac{2e}{\hbar}\sqrt{\frac{mn_o}{\varepsilon_o}} = 2.73 \times 10^4 \sqrt{n_o} \qquad \text{(VII-43)}$$

where β and n_o are expressed in (VII-43) in units $[cm^{-1}]$ and $[cm^{-3}]$ respectively.

For $n_o = 10^{12} cm^{-3}$ criterion (VII-43) gives $\beta \ll 3.12 \times 10^5$ cm^{-1} (or $2\pi/\beta \gg 0.2\ \mu m$). For $n_o = 10^8 cm^{-3}$, $\beta \ll 3.12 \times 10^4$ $(2\pi/\beta \gg 2\mu m)$.

Charge continuity limit

In the limit when the wavelength of the collective oscillation

is smaller than the average distance between the electrons, the space charge analysis of the traveling wave tube which is based on hydrodynamic modeling of the plasma charge fails. To get traveling wave interaction with isotropic electron plasma we must require that the bunching period be longer than the average spacing between electrons*

$$2\pi/\beta_1 > \ell_\alpha \equiv n_o^{-1/3} \qquad \text{(VII-44)}$$

For the example $n_o = 1.37 \times 10^{12}$, $T_i = 1500°K$, $V = 6$ KV we get $\ell_\alpha = 0.9\mu m$. So, under these conditions, interaction with space charge waves can take place down to bunching periods in the micron range. It seems that in practice the charge continuity condition is the strongest limitation for obtaining traveling wave interaction with space charge waves (electromagnetic-plasma wave phase matching) at short wavelengths.

It should be noticed that the analysis in Chapters V and VI started from a single electron interaction, and the only place where violation of Eq. (VII-44) is disrupting is where we used the Poisson equation and assumed an average modulated space charge (Eq. IV-4). When condition (VII-44) is violated, we may say that the electrons are so diluted that the local field in the plasma E_z, is equal to the external field E_{cz} (see Eq. IV-3). Thus the Poisson equation should not be used in this case. The result is that in Eq. (IV-7), and consequently in (VII-5), one should replace $\varepsilon_p \equiv 1 + \chi_p/\varepsilon$ by 1. With this modification, the analysis in this work still holds even beyond

---

*This condition can be shown to be equivalent with the requirement that the electron bunching energy is larger than the Coulomb repulsion energy of individual electrons (I am indebted to Dr. A. Rose for pointing out this fact to me.)

the regime (VII-44). However, in this case only the single electron interaction is obtained, and collective interaction (electromagnetic-plasma wave phase matched interaction) cannot be obtained. In contrast, the conventional traveling wave interaction fails when condition (VII-44) is violated, since it is based on a space charge wave analysis.

The optical traveling wave oscillator

Is there a theoretical limitation to operation of traveling wave amplifiers at optical frequencies? Does space charge wave analysis still apply then?

As an example we may examine the optical traveling wave oscillator suggested by Yariv and Armstrong [1973A]. This device which operates in the infrared regime ($\lambda = 10\mu$) utilizes a periodically corrugated dielectric waveguide to guide the electromagnetic wave. The structure, operating as a backward wave oscillator, is shown in Fig. 7 and its interaction impedance $K_{-1}(0^+)$ was derived and calculated in Chapter II (Eqs. III-43, 49, Fig. 9, Appendix III-B).

The analysis in [Yariv 1973A] is based on the conventional theory of space charge wave interaction, using a coupled mode formalism. For parameter values $a = 1\mu$, $\lambda = 10\mu$, $t = 1.43\mu$, $L = 0.8\mu$, $V = 2.5$ KV, $I/S = 1000 A/cm^2$, we get from Eq. (III-49)

$$wK_{-1}(0^+) = 2.16 \times 10^{-3} \Omega \text{ cm}$$

for which [Yariv 1973A] would predict a start oscillation condition at device length $\ell = 154$ μm.

The parameter values of some commercial or laboratory demonstrated devices are listed in Table 42 (after[Mizuno 1975]*). Some additional beam parameters which were discussed in the present chapter are also listed, providing practical case parameter values for the investigation of the conventional theory limits.

For wavelength λ = 10μm and v_o/c = 1/10 [Yariv 1973A] we have

$$|\beta_{-1}| \simeq \frac{\omega}{v_o} = \frac{2\pi}{\lambda}\frac{c}{v_o} \simeq 6 \times 10^4 \text{cm}^{-1}$$

$$2\pi/|\beta_1| \simeq 10^{-4}\text{cm}$$

Comparison of these values with the examples of parameter values listed in Table 42 indicates that the conditions for collective interaction (VII-14) or (VII-29) and the charge continuity condition (VII-44) may be practically satisfied. Hence the theoretical limitations are avoided, and a space charge wave analysis, as presented in [Yariv 1973A], can still apply at these conditions ($2\pi/\beta_1$ = 1μm). There may be, though, some practical difficulties in implementing the structure of Fig. 7 to operate at these conditions.

The condition (VII-44) is getting difficult to satisfy with practical electron tubes and a period range of $2\pi/\beta_1 \gtrsim$ 1μm or less. At this regime only single electron interaction can take place and the extended analysis (Chapters V, VI) should be used. Notice also that for $\beta_1 \gtrsim 6 \times 10^4 \text{cm}^{-1}$, Table 42 indicates $\beta_1 \gtrsim k_{th}$; hence, in conditions

*Mizuno and Ono [1975] overlooked the effect of reduction in the electron beam longitudinal velocity spread (VII-A-3) which led them to overly pessimistic predictions. This was corrected here in Table 42.

Table 42. The Beam Parameters of Some TWT Devices

	Ledatron (SWM)	Reflex Klystron (Philips)	Backward-Wave Oscillator (Thomson-CSF)	Unit
f	210	120	300	GHz
λ	1.43	2.5	1	mm
I/S	30	300	1000	A/cm^2
V	10	2.5	6	KV
v_o	5.84×10^9	2.95×10^9	4.55×10^9	cm/sec
k_o	5.04×10^9	2.55×10^9	3.93×10^9	cm^{-1}
n_o	3.2×10^{10}	6.36×10^{11}	1.37×10^{12}	cm^{-3}
ω_p	1×10^{10}	4.5×10^{10}	6.6×10^{10}	rad/sec
T	5×10^{-3}	2×10^{-2}	8.24×10^{-3}	°K
v_{th}	3.9×10^4	7.8×10^4	5×10^4	cm/sec
k_{th}	3.36×10^4	6.72×10^4	4.31×10^4	cm^{-1}
k_A	1.65×10^5	3.55×10^5	5.32×10^5	cm^{-1}
k_D	3.66×10^5	8.16×10^5	1.87×10^6	cm^{-1}
ℓ_α	3.14×10^{-4}	1.16×10^{-4}	9×10^{-5}	cm
$\beta_1 \simeq \frac{\omega}{v_o}$	2.25×10^2	2.56×10^2	4.14×10^2	cm^{-1}
$2\pi/\beta_1$	2.78×10^{-2}	2.46×10^{-2}	1.52×10^{-2}	cm

of single particle interaction, quantum mechanical behavior (Chapter VI) may be observed.

At short enough wavelength when the space charge wave analysis can no longer apply, the optical traveling wave oscillator can still work on the mechanism of single electron interaction discussed in Chapters V, VI, and its gain is given by Eqs. (V-28, 33) or (VI-64).

3. Relativistic Beam Interaction, Smith-Purcell and Cerenkov Radiation and the Free Electron Laser

In 1953 it was discovered by S. J. Smith and E. M. Purcell that when an energetic electron beam travels in close proximity to an optical grating, light is emitted from the grating in the visible region [Smith 1953]. The Cerenkov radiation is an electromagnetic radiation at different frequency regimes (from microwave to U.V.), which is observed when an energetic electron beam passes through matter at a speed faster than the speed of the electromagnetic radiation in the same medium (see for example [Jackson 1962]). The analysis of electron-electromagnetic wave interaction in periodic structures, which was presented in this work is obviously related to these effects. This relation will be briefly discussed in the present section; however, we should first examine the effect of special relativity on our previously derived results.

In the relativistic regime the quantum mechanical analysis of traveling wave interaction should be modified, and instead of the Schrödinger equation one should use the Dirac equation to describe the electron wave [Heitler 1936], or if spin can be ignored the Klein-Gordon equation

$$\nabla^2\psi - \frac{1}{c^2}\frac{\partial^2}{\partial t^2}\psi = \frac{m_o c^2}{h^2}\psi \qquad \text{(VII-45)}$$

can be used [Marcuse 1970].

It is not intended in the present work to pursue this extension. In addition, at high values of v/c the neglect of coupling through transverse field components, which is done in our one dimensional model, may not be justified. This is especially true in the case of

Cerenkov radiation (see for example [Piestrup 1972, Rose 1966A, p. 135] for three dimensional analysis). In spite of these differences, we would still expect that some of the conclusions which resulted from the analysis of Chapter VI are correct also in the relativistic regime. In particular, the conditions of energy and momentum conservation during the electronic transition should be satisfied

$$\mathcal{E}_{\underline{k}_i} - \mathcal{E}_{\underline{k}_f} = \hbar\omega \qquad \text{(VII-46)}$$

$$\underline{k}_i - \underline{k}_f = \underline{q} \qquad \text{(VII-47)}$$

The only difference is that $\mathcal{E}_{\underline{k}}$ is given by the relativistic expression

$$\mathcal{E}_{\underline{k}} = \sqrt{(\hbar \underline{k} c)^2 + (m_o c^2)^2} \qquad \text{(VII-48)}$$

instead of the usual parabolic relation. The transition process is still illustrated by Fig. 31 but the parabolic energy curve plotted there should be substituted by the curve of the function (VII-48). Also in the present case there is a much smaller energy spread of the beam than what is presented in the figure and most electrons populate the states around $\underline{k}_i$.

In the limit

$$|\underline{q}| << |\underline{k}_i| \simeq |k_f| \qquad \text{(VII-49)}$$

the energy difference in Eq. (VII-46) can be replaced by a differential

$$\mathcal{E}_{\underline{k}_i} - \mathcal{E}_{\underline{k}_f} = \nabla_{\underline{k}} \mathcal{E}_{\underline{k}^*} \cdot \underline{q} = \hbar\omega \qquad \text{(VII-50)}$$

or

$$\underline{v}_{\underline{k}^*} \cdot \underline{q} = \omega \qquad \text{(VII-51)}$$

where

$$\underline{v}_{\underline{k}^*} \equiv \frac{1}{\hbar} \nabla_{\underline{k}} \mathcal{E}_{\underline{k}^*} \tag{VII-52}$$

is the group velocity at $\underline{k}^*$, such that $|\underline{k}_f| < |\underline{k}^*| < |\underline{k}_i|$ (assuming $|\underline{k}_f| < |\underline{k}_i|$). Hence

$$|\underline{v}_{\underline{k}_i}| > |\underline{v}_{\underline{k}^*}| \geq \frac{\omega}{|\underline{q}|} \tag{VII-53}$$

If $\underline{k}_i$ is the peak of the electron distribution, and we define $\underline{v}_{\underline{k}_i} \equiv \underline{v}_o$, then the electronic transition involves photon emission and Eq. (VII-53) is the Cerenkov condition (VI-46).

$$v_o > v_{ph\,\underline{q}} \tag{VII-54}$$

As we showed in section 1 of Chapter VI, condition (VII-54) cannot be satisfied in free space where

$$\frac{\omega}{|\underline{q}|} = c \tag{VII-55}$$

It can be satisfied, however, in a periodic structure, where due to the lattice momentum $\underline{G}$ we may have for space harmonic $\underline{G}$

$$\frac{\omega}{|\underline{q}_{\underline{G}}|} < c \tag{VII-56}$$

where

$$\underline{q}_{\underline{G}} = \underline{q}_o + \underline{G} \tag{VII-57}$$

which in the case of one dimensional (z direction) periodicity can be written as

$$\underline{q}_{\underline{G}} = \underline{q}_o + m \frac{2\pi}{L} \hat{e}_z \tag{VII-58}$$

where m is an integer. Eq. (VII-54) may be satisfied also in the case when the light passes in a material with index of refraction $n > 1$, so that

$$\frac{\omega}{|\underline{q}|} = \frac{c}{n} < c \qquad \text{(VII-59)}$$

Thus we conclude that the traveling wave interaction of an electron with a slow electromagnetic wave space harmonic, which was analyzed in the present work, is equivalent to the Cerenkov radiation effect. In the Cerenkov effect the material with index of refraction $n > 1$ functions as "the slow wave structure" instead of the periodic structure, and instead of interacting only with one wave component (space harmonic) as in the latter case, the interaction is with the whole wave.

Usually the energetic electron beam used in the Cerenkov effect is too dilute to support space charge waves in the wavelength of the radiation (except possibly at the long wavelength region of radio or microwave wavelengths). This makes it similar to the traveling wave amplifier operating at the single particle interaction regime (off the photon-plasmon phase matching condition). The traveling wave tube amplifier in its normal operation point exhibits collective interaction (phase matched electromagnetic-plasma wave) in addition to satisfying the Cerenkov condition (VII-54), and in this sense it is different from the Cerenkov radiation effect. The statement made by D. Marcuse [1970, p. 173], "It is perfectly legitimate to think of the radiation emitted by the traveling wave tube as a stimulated emission of Cerenkov radiation" and similar statements made by Ginzburg et al [1965] and others, are very confusing. It is my opinion that these statements are correct only within a broad sense of notations. It is true that traveling wave interaction in a traveling wave tube can be

viewed as a special case of stimulated Cerenkov radiation. However, in its normal operation condition there is in the traveling wave tube amplification of both space charge wave and rotational electromagnetic wave, in addition to satisfying the Cerenkov condition (VII-54). By contrast, in the conventional Cerenkov radiation no space charge wave is involved. In a broad sense of notations [Ginzburg 1965], amplification of space charge waves can be regarded as a "Cerenkov effect" of space charge waves.

Usually Cerenkov radiation is a spontaneous effect. The emitted radiation is carried away from the narrow beam and does not continue to interact with it. A comprehensive discussion of Cerenkov radiation at microwave frequencies is given in [Lashinsky 1961]. Several suggestions of structures in which stimulated Cerenkov interaction can take place are presented in this reference. Some structures incorporate cavities for the microwave radiation; others confine the microwave radiation in a dielectric waveguide so that it is propagating collinearly with the electron beam, which also propagates in the waveguide or very close to its surface. This latest possibility is completely analogous to the optical traveling wave amplifier shown in Fig. 7, again stressing the similarity between the two effects.

High power device for Cerenkov microwave generation which is intensified by prebunching of the electron beam was reported by Coleman and Enderby [1960]. This is, however, still a spontaneous radiation device.

Piestrup [1972] analyzed and experimented with stimulated Cerenkov radiation in the visible and UV frequency regime, using an

optical resonator. His analysis consists of solving the kinetic Boltzmann equation in a three dimensional model, obtaining dispersion equations similar to the conventional traveling wave equation [Pierce 1950].

Let us discuss now the Smith-Purcell radiation effect and its relation to the traveling wave interaction. Smith and Purcell interpreted their result by a simple classical physics argument. The electron charges, traveling across the metallic optical grating, were assumed to induce positive charge images which bounce up and down as the electrons move across the grating rulings. The relation between the beam velocity v_o, the period L, the wavelength λ, and the direction (θ) of the radiation is

$$m\lambda = L\left(\frac{c}{v_o} - \cos\theta\right) \qquad (m = 1,2,\ldots) \qquad \text{(VII-60)}$$

and follows from a simple Huygens construction. This equation agreed well with the experimental observation.

By eliminating v_o from (VII-60) we get

$$v_o = \frac{\omega}{\frac{2\pi}{\lambda}\cos\theta + m\frac{2\pi}{L}} = \frac{\omega}{\beta_o + m\frac{2\pi}{L}} = \frac{\omega}{\beta_m} = v_{ph_m} \qquad \text{(VII-61)}$$

where β_o is the z component of the propagation parameter of a plane wave propagating in angle θ to the grating plane, and β_m can be viewed as the propagation parameter of its m order space harmonic.

Equation (VII-61) means that there is exact velocity synchronism between the electron beam and the m-th order electromagnetic wave space harmonic. This is somewhat different from the ordinary Cerenkov

or population inversion condition (VII-54) which requires inequality

$$v_o > v_{ph_m} \tag{VII-62}$$

However, since condition (VII-49) is certainly satisfied in this experiment, or rather

$$\beta_m << k_f \lesssim k_i \tag{VII-63}$$

it turns out that v_{ph_m} is only slightly smaller than $v_{k_i} \equiv v_o$ and slightly larger than v_{k_f}. Therefore in addition to the inequality (VII-54)

$$v_o > \frac{\omega}{\beta_m} = v_{ph_m} \tag{VII-64}$$

we also have

$$v_o \simeq \frac{\omega}{\beta_m} = v_{ph_m} \tag{VII-65}$$

The slight amount by which $v_{ph_m} = \omega/\beta_m$ is smaller than v_o is a small quantum effect which could not be detected in this experiment and therefore the equality (VII-61) was measured instead of (VII-64,65).

We thus conclude that the Smith-Purcell radiation effect is exactly a spontaneous traveling wave interaction of the kind discussed in the previous chapter. As in that case we would expect that the interaction would take place predominantly with a TM electromagnetic wave. This was confirmed by Smith and Purcell who reported that the light emitted was strongly polarized with the electric vector perpendicular to the grating.

To check if the traveling wave interaction in the Smith Purcell experiment could possibly include collective interaction (phase matching to the space charge wave) let us examine in some more detail the experimental conditions in which the effect was measured.

The investigators used a small Van de Graaf generator and an electron accelerator tube. A 5 microampere beam, focused electrostatically and magnetically to a diameter of 0.15 mm, and diverging less than 0.004 radian, was adjusted by deflection coils to pass over the grating, just grazing its surface. The energies used were in the range V = 309 ÷ 340 KV. The observed radiation was about $\lambda = 0.5\mu m$ for the first order (m = 1) line. The grating period was $L = 1.67\mu m$.

From this information we find that the current density was

$$I/S = 2.8 \times 10^{-2}\ A/cm^2$$

The beam velocity (using VII-A22)

$$v_o \simeq 2.35 \times 10^{10} cm/sec$$

and the electron density

$$n_o = 7.4 \times 10^{6} cm^{-3}$$

It is difficult to estimate the velocity spread (or the longitudinal temperature) of the beam. Using Pantell's estimate (see discussion after Eq. VII-4) $\Delta\mathcal{E}/\mathcal{E} \simeq 10^{-4}$, we get (using Eqs. VII-A18, V-16 and VI-53) T = 11°K, $k_{th} = 1.6 \times 10^{6} cm^{-1}$. Taking even a more optimistic estimate:

$$T = 1°K$$

we get from Eqs. (VI-163,164, VII-44,65)

$$k_A = 4.2 \times 10^{3} cm^{-1}$$

$$k_D = 3.9 \times 10^{2} cm^{-1}$$

$$\ell_\alpha \equiv n_o^{-1/3} = 5.1 \times 10^{-3}\ cm$$

$$\beta_1 \simeq \frac{\omega}{v_o} = \frac{2\pi}{\lambda}\frac{c}{v_o} = 1.6 \times 10^{5} cm^{-1}$$

and neither of conditions (VII-14), (VII-29) or (VII-44) is satisfied. So the Smith-Purcell experiment could not involve collective interaction with space charge waves (phase matched plasma-electromagnetic wave).

We thus conclude that the Smith-Purcell experiment was essentially traveling wave interaction of the kind discussed in the previous chapters, operating at the single electron interaction regime, and could not involve interaction with space charge waves (plasma-electromagnetic wave phase matching).

In the Smith-Purcell experiment, the generated light is radiated away from the grating and does not continue to interact with the electron beam, in contrast to the structures analyzed in the previous chapters and the TWT amplifier. Indeed, if the emitted radiation will be confined in a waveguide (for example, a structure like Fig. 7 or an evacuated metallic corrugated waveguide), then much stronger light generation and amplification will be demonstrated.

We may conclude that even in operation and frequency regions where space charge waves do not exist (and conventional traveling wave tube theory may not hold), gain can still be attained in traveling wave amplifiers by the single electron interaction mechanism, which we might call the Smith-Purcell mechanism.

The single electron (Smith-Purcell) interaction gain is simply given by the first order solution of the dispersion equation (Eqs. V-28, 33) in the classical case, and Eq. (VI-64) in the quantum case. Examination of these equations, assuming (III-49) for the interaction impedance reveals that highest gain is attained when k_D is still kept to be of the order of magnitude of β_1 (even though we may have $k_D < \beta_1$

and are far from phase matching to the plasma wave). If this condition is kept we find that the gain increases inversely with the radiation wavelength, so that this mechanism is more efficient at short wavelengths. For a wavelength of $\lambda \simeq 10\mu$ and $v_o/c \simeq 1/10$ [Yariv 1973A] gain of the order of a few inverse centimeters was calculated. So even in regimes where space charge waves do not exist, the optical TW oscillator (Fig. 7) may operate as a "Smith-Purcell oscillator."

Most of the existent literature on Smith-Purcell radiation is based on a classical model, solving the Maxwell equations with the appropriate boundary conditions and a current source of a single moving electron of fixed energy (see for example [Barnes 1966, Van den Berg 1973A, 1973B, Lalor 1973]). Palocz and Oliner [Palocz 1962, 1964, 1965, 1967] solved this problem using a model of leaky space charge waves and equivalent electrical networks. It is noteworthy that the structures analyzed by them confined the electromagnetic wave to propagate collinearly with the electron beam and they actually solved the mutual electron-electromagnetic wave interaction self consistently. In some of these references and some others of interest ([Hessel 1964, Bradshaw 1959]), space charge wave effects are also included (our definition of the Smith-Purcell effect excludes interaction with space charge waves).

Another interesting related effect of electron interaction with electromagnetic wave in a periodic structure is the "free electron laser" suggested by Madey et al.[1971, 1973] and recently demonstrated experimentally [Elias 1975]. In this experiment a 20-30 MeV electron beam was passed through a 5.2m long superconducting helix of period

L = 3.2 cm. The electrons, passing through the center of the helix, experienced a periodically varying transverse magnetic field with period L = 3.2 cm. The workers observed both spontaneous and stimulated radiative emission at wavelength λ = 10μm.

The effect was explained by Madey et al. using a model which presents the interaction as a Compton Scattering of virtual photons, which are the result of the periodic static magnetic field, when viewed in the electron rest mass. This interesting point of view allowed the use of well known equations of Compton Scattering for the calculation of the electromagnetic gain obtained in this interaction.

The emission wavelength was found to be (for relativistic electrons)

$$\lambda \simeq \frac{L}{2\gamma^2}\left[1 + \left(\frac{1}{2\pi}\right)^2 \frac{L^2 r_o B^2}{m_o c^2}\right] \qquad \text{(VII-66)}$$

This condition can be shown to be equivalent to the conservation of energy and momentum conditions in the limit (VII-49). In the limit of small magnetic field (B $\approx$ 0) the second term in (VII-66) is negligible and we can show that Eq. (VII-66) can be deduced from (VII-65). Substituting

$$\beta_1 = \frac{2\pi}{\lambda} + \frac{2\pi}{L} \qquad \text{(VII-67)}$$

into (VII-65), we get after short manipulation

$$\lambda \simeq L\,\frac{1-v_o/c}{v_o/c} \simeq L\,\frac{1-v_o^2/c^2}{2} = \frac{L}{2\gamma^2} \qquad \text{(VII-68)}$$

which is identical to the first term of (VII-66), and we used $v_o \approx c$ in the relativistic limit.

This interesting recent experiment is different from the traveling wave interaction discussed previously in three points:

(1) The periodicity affects only the electrons and not the electromagnetic wave. In this sense this effect can be described as "coherent bremsstrahlung", while the previously discussed effects are "generalized Cerenkov radiation" effects (where only the electromagnetic wave is affected by a slow wave structure). (2) When the magnetic field is strong enough, it affects the free electron trajectory, resulting in the term proportional to B^2 in (VII-66). (3) The electromagnetic wave in this experiment is a TEM wave and the coupling of the electromagnetic field to the electron beam is a transverse coupling*.

In spite of the differences, the free electron laser, like the stimulated Smith-Purcell and Cerenkov radiation, can be described by the framework of the traveling wave interaction model developed in the previous chapters. Even though our model is quite simplified, it has the advantage of being general, and reveals the connection between the different effects. Thus, we can, for example, answer a question which was left open by Madey et al. [Madey 1973, Kroll 1975] who wondered at the fact that the calculated expression for gain in the "free electron laser" does not reduce to the conventional expression of gain in a traveling wave tube amplifier, and especially at the different dependence on the electron density (or current density). The answer is that the conventional traveling wave tube operates usually in the collective interaction mode where the electromagnetic wave is coupled

---

*The transverse coupling of a TEM wave to a collinear electron beam can be obtained if in Eq. (VI-10) we keep the second order of A, and use the periodic magnetostatic field in the perturbation Hamiltonian.

to the slow space charge wave or both space charge waves (see the discussion in Section 2). On the other hand the "free electron laser" is basically a single electron interaction device. In this regime, the traveling wave model predicts that the gain is proportional to the electron density (or current density) (V-28, 27, 20, VI-64, 66), in agreement with Madey's expression for the free electron laser gain.

The traveling wave interaction model is capable of describing many of the electron-electromagnetic wave interactions discussed. However appropriate extensions of the model may be necessary in order to calculate the expected gain in specific cases. The demonstrations of the Smith-Purcell radiation effect, the "free electron laser" and other related works [Friedman 1973, Bartell 1965] give hope, that amplification of electromagnetic wave by stimulated emission from free electrons in periodic structures--in which the electromagnetic wave is confined, and efficiently interacts with the electron beam--will be further developed in the future. Thus possible new amplifiers and oscillators in the visible and U.V. regimes may evolve [see also Kroll 1975].

It is suggested that short period structures (gratings) which affect the electromagnetic wave and confine it in a waveguide, so that it efficiently interacts with the electron beam, are easier to produce than short period periodic magnetic field structures. Thus shorter wavelengths with lower electron energies may be attained in the first structure, possibly also with stronger (longitudinal) coupling and higher gain, compared to the low gain reported by Elias et al. [1975] for the free electron laser.

4. Wave Interactions in the Crystal Lattice

After extensive discussion on wave interactions in artificial periodic structure, it is natural to wonder about the implications of this theory in the case of the crystal lattice - nature's ready-made periodic structure.

The theories of electron bands in the solid, electron and x-ray diffraction in the crystal lattice and other waves interaction with the crystal lattice, are well developed. Nevertheless, new concepts and effects, developed recently for interactions in artificial periodic structures, provide a new outlook on different possible wave interactions in the crystal lattice, like x-ray DFB lasers and traveling wave interaction in the crystal lattice.

As pointed out by P. P. Ewald [1965], in spite of the extensive research on x-ray diffraction in the lattice since its discovery by von Laue in 1912, only at few points, novel features of x-ray optical theory were introduced. The successful application of x-ray diffraction to the analysis of crystal structures, overshadowed any other research on the basic features of x-ray diffraction in the crystal lattice. For this application and others, the fairly primitive "kinematic" theory of x-ray diffraction has been always used in the same way originally conceived by Laue. The kinematic theory is based on the assumption that a plane optical wave is passing through the crystal essentially unmodified, causing each atom to radiate independently according to the primary excitation by the plane wave; double and triple scattering is neglected. In contrast the "dynamical" theory of x-ray theory is based on the self consistent solution of the x-ray

wave propagation in the crystal lattice and its oscillating atoms.

The use of the dynamical theory is important in order to understand the wave propagation inside the crystal. Only by using a dynamical theory it is possible to explain the "Borrman effect" which consists of extraordinary high transmission of x-rays by perfect crystals near the Bragg condition; the transmitted beams are also characterized by a very narrow angular spread [Ewald 1965, Batterman 1964]. The Borrman effect explanation is based on recognizing that the Bragg diffracted wave is important, near the Bragg condition, as much as the primary impinging plane wave. Self consistent solution of the primary and diffracted waves in the lattice results in a possible mode of propagation in the crystal lattice, which has vanishing field at the lattice atom sites where losses are high. In the one dimensional case, the dynamical theory is equivalent to the coupled mode theory of a thin film Bragg reflector [Yariv 1973B] or to the "two harmonics" Floquet mode analysis (Chapter III, Section 6).

The X-ray DFB Laser

When gain is introduced into a Bragg reflector it can turn into an oscillator [Yariv 1974B], where the Bragg reflection is the oscillator's feedback mechanism. This is the principle of the optical distributed feedback laser, originally suggested by Kogelnik et al. [1972].

It was suggested by Yariv [1974C,1974D] that the idea of distributed feedback (DFB) laser can be extended to the x-ray regime, where a perfect crystal lattice is used as the feedback providing

periodic structure. What is necessary is that the atoms in the crystal will have an atomic transition in the x-ray regime, which can be inverted, and which produces radiation of wavelength that satisfies the Bragg condition. In the case of retro-Bragg coupling the interacting waves are collinear, and the problem is completely analogous to the conventional one dimensional DFB laser theory. In this case the Bragg condition is

$$m \frac{\lambda}{2} = d(h,k,\ell) \qquad (m = 1,2,\ldots) \qquad \text{(VII-69)}$$

where $d(h,k,\ell) \equiv 2\pi/|\underline{G}(h,k,\ell)|$ is the spacing between adjacent $|h,k,\ell|$ lattice planes (see Fig. 43). The retro-reflection scheme was discussed and analyzed in Yariv [1974D] from the point of view of optical index modulation. The retro-reflection scheme is not only easier to manipulate theoretically, but also is essential for attaining low threshold, efficient pumping and directionality of the laser beam.

This new promising approach to x-ray lasers did not yet get a comprehensive theoretical analysis which will present self consistently the active dynamical x-ray diffraction together with the quantum mechanics of the electronic transitions. Besides the simple analysis of Yariv [1974D], the DFB laser has been qualitatively examined from the points of view of loss modulation [Fisher 1974A,B], laser structure design [Spiller 1974, Yariv 1974E] and different host crystals [Elachi 1975, Farkas 1974]. First experimental observation of stimulated emission at Bragg condition was reported by Das Gupta [1973A, 1973B].

The main expected obstacle in the practical realization of a DFB x-ray laser is the problem of the laser pumping. There is

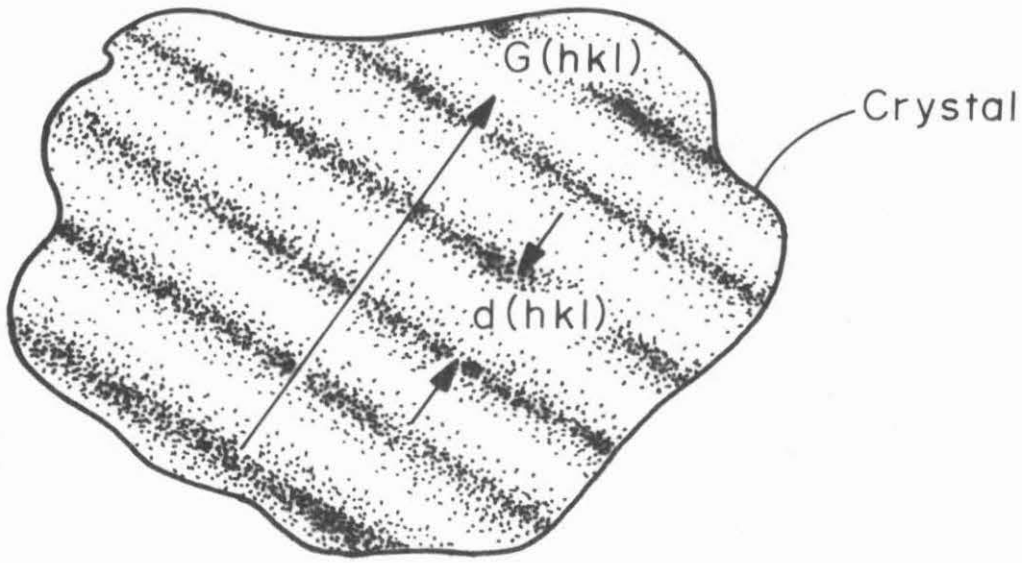

Fig. 43 The effective index modulation associated with the reciprocal lattice vector $\underline{G}(h,k,\ell)$.

extensive research on different approaches to x-ray laser pumping and population inversion [e.g. Lax 1972, McCorkle 1972, Duguay 1973, Freund 1974, Bohn 1974, Elton 1974]. It is sometimes claimed that the high transmission loss of x-rays in high mass materials will require a very high amount of pumping in order to overcome the losses in the x-ray laser. It may happen though that in the case of the DFB x-ray laser this problem is much less severe than usually considered. The major loss mechanism in incoherent transmission of x-rays is photoexcitation of electrons and conversion to longer wavelength rays. However, in the case of a coherent standing wave in a single crystal DFB laser, losses may be expected to decrease considerably, since the nodes of the standing wave can adjust relative to the atom sites as in the Borrman effect. It is encouraging to notice that the x-ray transmission in the Borrman effect was measured in some cases to be eight orders of magnitude higher from what is expected from simple "mass action"! [Ewald 1965]

For a full understanding and optimal design of a DFB x-ray laser, the x-ray dynamic diffraction and the quantum mechanical stimulated and spontaneous emission by the atomic electronic transitions, should be solved self consistently. The atom is stimulated to emit radiation by a particular standing wave and not by a general plane wave as usually is assumed in the theory of stimulated emission. An optimal situation would be such that the x-ray standing wave suffers low loss (its nodes coincide with the atom sites) and at the same time has good overlap with the electronic states which participate in the transition (i.e. the amplitude of the electronic transition matrix element, with the standing wave used in it has maximum value).

A comprehensive analysis may result in some new results. For example, it may be speculated that normally forbidden transitions ($\Delta\ell = 0$) may be preferable for the lasing transition. Such a transition may be stimulated by an x-ray standing wave with nodes in the atom sites which keep the matrix element $\langle f|\underline{A}(\underline{r})\cdot\underline{p}|i\rangle$ nonvanishing. Even if the transition rate of such a transition is smaller than a permitted ($\Delta\ell = 1$) transition, the advantage of low loss of the x-ray mode and longer lifetime of the excited level (which makes the pumping easier) may be dominant factors. A more quantitative detailed quantum analysis is necessary to get conclusive theoretical predictions. The point of the present discussion was just to stress the necessity of self consistent analysis of the quantum mechanical transition problem and the x-ray dynamic diffraction problem, and to suggest that favorable results may result from such an approach.

Finally it is pointed out that the DFB approach is a natural solution to the problem of very short lifetime of x-ray transitions. Estimates of inner shell levels lifetimes are in the range of 10^{-15} to 10^{-13} sec [Elton 1974, Das Gupta 1973A]. For self terminating amplified spontaneous emission [Elton 1974] this corresponds to coherence length of (0.1-10)μm. For ultrashort pulses (10 ps) a coherence length of 1mm results. This means that Fabry-Perot mirrors approach may require to set the mirrors inconveniently close so that the transit time of the laser beam will not exceed the gain duration time. In contrast, in the DFB x-ray laser the resonator length can be considered to be in the range of a few unit cell lengths, and the problem does not arise.

Optical Space Harmonics in the Crystal Lattice

It is well known that electromagnetic waves in any frequency regime have in the crystal lattice (like in any periodic structure) the Floquet-Bloch form (I-8,9)*

$$E(\underline{r},t) = \sum_{\underline{G}} \underline{E}_{\underline{G}}(\underline{q}_o,\omega) e^{i(\underline{q}_{\underline{G}}\cdot\underline{r}-\omega t)} \qquad \text{(VII-70)}$$

$$\underline{q}_{\underline{G}} = \underline{q}_o + \underline{G} \qquad \text{(VII-71)}$$

where a single Fourier component of temporal frequency ω is assumed in (VII-70). Nevertheless, the crystal is usually viewed in the optical frequency regime as a macroscopically uniform medium; so that instead of (VII-70) a single plane wave is assumed with single propagation constant which is determined by the average dielectric constant of the crystal.

The direct observation of the electromagnetic wave space harmonics is usually impossible, since they have low phase velocity and short spatial oscillation period (of the order of the crystal lattice constant). Only a very small fraction of a space harmonic ($\underline{G}\neq 0$) can radiate out of the crystal and possibly be seen. This is because of the smallness of the transverse component of the field of any space harmonic ($\underline{G}\neq 0$), and because of the big difference between its propagation constant $|\underline{q}_{\underline{G}}|$ and the vacuum propagation constant ω/c, which causes very high reflection at the crystal surface [Johnson 1975]. Detection of the optical space harmonics inside the crystal

*Here again we use the harmonic time-space dependence exp $i(\underline{q}\cdot\underline{r}-\omega t)$ which is customary in physics, instead of the electrical engineering convention exp $i(\omega t-\underline{q}\cdot\underline{r})$ which was used in previous chapters.

by means of parametric mixing with an x-ray wave was suggested by Freund [1969] but it has not, to date, been measured experimentally.

Even though the individual space harmonics are hard to detect, they certainly are not negligible and have an appreciable effect in determining the macroscopic optical dielectric constant of crystals via the local field effect [Adler 1962, Wiser 1963].

Due to a local field effect, the field at any point in the crystal is affected by the field (and the consequent polarization) at neighboring points. Thus, in a microscopic model, the field is a solution of Maxwell equations with an "induced" source term :

$$\underline{\nabla} \times \underline{E} = i\omega\mu\underline{H} \tag{VII-72}$$

$$\underline{\nabla} \times \underline{H} = -i\omega\varepsilon_o\underline{E} + \underline{J}^{ind} \tag{VII-73}$$

$$\underline{\nabla}\cdot\underline{E} = \rho^{ind}/\varepsilon_o \tag{VII-74}$$

$$\underline{\nabla}\cdot\underline{H} = 0 \tag{VII-75}$$

where

$$\underline{J}^{ind}(\underline{r},t) = -i\omega \int_V \underline{\chi}(\underline{r},\underline{r}',\omega)\underline{E}(\underline{r}',t)d^3\underline{r}' \tag{VII-76}$$

$$\rho^{ind}(\underline{r},t) = -\frac{i}{\omega}\underline{\nabla}\cdot\underline{J}^{ind} = -\int_V \underline{\nabla}_{\underline{r}}\cdot\underline{\chi}(\underline{r},\underline{r}',\omega)\underline{E}(\underline{r}',t)d^3r \tag{VII-77}$$

where we assumed a single Fourier frequency component (ω). The current (or polarization) at each point is induced by the spatially distributed field according to a nonlocal dependence (VII-76). The field in turn is determined by the Maxwell equations (VII-72,73), which must be solved self consistently with (VII-76). Only in the case of uniform

medium

$$\underline{\underline{\chi}}(\underline{r},\underline{r}',\omega) = \underline{\underline{\chi}}(\underline{r},\omega)\delta(\underline{r}-\underline{r}') \qquad \text{(VII-78)}$$

and the extended dependence (VII-76) reduces into a local one (IV-2)

$$\underline{J}^{ind}(\underline{r},t) = -i\omega\underline{\underline{\chi}}(\underline{r})\underline{E}(\underline{r},t) \qquad \text{(VII-79)}$$

Using the Floquet theorems, (VII-70,71) and

$$\underline{J}^{ind}(\underline{r},t) = \sum_{\underline{G}} \underline{J}^{ind}_{\underline{G}}(\underline{q}_o,\omega)e^{i(\underline{q}_{\underline{G}}\cdot\underline{r}-\omega t)} \qquad \text{(VII-80)}$$

and Fourier transforming (VII-76,77), we get

$$\underline{J}^{ind}_{\underline{G}}(\underline{q}_o,\omega) = -i\omega \sum_{\underline{G}'} \underline{\underline{\chi}}_{\underline{G},\underline{G}'}(\underline{q}_o,\omega)\underline{E}_{\underline{G}'}(\underline{q}_o,\omega) \qquad \text{(VII-81)}$$

$$\rho^{ind}(\underline{r},t) = \sum_{\underline{G}} \rho^{ind}_{\underline{G}}(\underline{q}_o,\omega)e^{i(\underline{q}_{\underline{G}}\cdot\underline{r}-\omega t)} \qquad \text{(VII-82)}$$

$$\rho^{ind}_{\underline{G}}(\underline{q}_o,\omega) = -i\underline{q}_{\underline{G}}\cdot\sum_{\underline{G}'}\underline{\underline{\chi}}_{\underline{G},\underline{G}'}(\underline{q}_o,\omega)\underline{E}_{\underline{G}'}(\underline{q}_o,\omega) \qquad \text{(VII-83)}$$

$\underline{\underline{\chi}}_{\underline{G},\underline{G}'}(\underline{q}_o,\omega) \equiv \underline{\underline{\chi}}(\underline{q}_{\underline{G}},\underline{q}_{\underline{G}'},\omega)$ is the general susceptibility matrix element (notice that each matrix element is by itself a 3 x 3 tensor). When Eqs. (VII-72,70,80,81) are substituted in (VII-73) we get

$$\underline{q}_{\underline{G}} \times \underline{q}_{\underline{G}} \times \underline{E}_{\underline{G}}(\underline{q}_o,\omega) = -\omega^2\mu \sum_{\underline{G}'}\underline{\underline{\varepsilon}}_{\underline{G},\underline{G}'}(\underline{q}_o,\omega)\underline{E}_{\underline{G}'}(\underline{q}_o,\omega) \qquad \text{(VII-84)}$$

where $\underline{\underline{\varepsilon}}_{\underline{G},\underline{G}'}$ is the dielectric matrix element, defined by

$$\underline{\underline{\varepsilon}}_{\underline{G},\underline{G}'}(q_o,\omega) \equiv \varepsilon_o\underline{\underline{I}} + \underline{\underline{\chi}}_{\underline{G}\underline{G}'}(\underline{q}_o,\omega) \qquad \text{(VII-85)}$$

and $\underline{\underline{I}}$ is the 3 x 3 unit tensor.

The dielectric matrix elements can be derived in the RPA approximation. Their longitudinal-longitudinal components are found

to be [Adler 1962, Wiser 1963]

$$\bar{\varepsilon}_{\underline{G},\underline{G}'} \equiv \hat{e}_{\underline{q}_{\underline{G}}} \cdot \underline{\underline{\varepsilon}}_{\underline{q}_{\underline{G}}} \cdot \hat{e}_{\underline{q}_{\underline{G}}} = \varepsilon_o \delta_{\underline{G},\underline{G}'} - \frac{e^2}{V|\underline{q}_{\underline{G}}||\underline{q}_{\underline{G}'}|} \sum_{\underline{k},\ell,\ell'} \frac{f_o[\mathcal{E}_{\ell'}(\underline{k}+\underline{q}_o)] - f_o[\mathcal{E}_{\ell}(\underline{k})]}{\mathcal{E}_{\ell'}(\underline{k}+\underline{q}_o) - \mathcal{E}_{\ell}(\underline{k}) - \hbar\omega + i\hbar\eta}$$

$$\times \langle \underline{k}+\underline{q}_o,\ell'| e^{i\underline{q}_{\underline{G}}\cdot\underline{r}} |\underline{k},\ell\rangle\langle\underline{k},\ell| e^{-i\underline{q}_{\underline{G}}\cdot\underline{r}} |\underline{k}+\underline{q}_o,\ell'\rangle \qquad \text{(VII-86)}$$

where $\hat{e}_{\underline{q}_{\underline{G}}}$ is a unit vector in the direction of $\underline{q}_{\underline{G}}$, $|k,\ell\rangle$ and $\mathcal{E}_{\ell}(\underline{k})$ are the Bloch eigenstates and eigenvalues of the unperturbed crystal Hamiltonian; ℓ is the band index, and V is the crystal volume (compare Eq. VII-86 to the expression for the free electron gas response VI-25). In the optical frequency regime

$$|\underline{q}_o| \ll |\underline{G}| \neq 0 \qquad \text{(VII-87)}$$

Hence

$$\hat{e}_{\underline{q}_{\underline{G}}} \simeq \hat{e}_{\underline{G}} \qquad (\underline{G} \neq 0) \qquad \text{(VII-88)}$$

Also it turns out then, that the dielectric matrix element tensor $\underline{\underline{\varepsilon}}_{\underline{G},\underline{G}'}$ is approximately scalar [Johnson 1974], hence

$$\bar{\varepsilon}_{\underline{G},\underline{G}'} \simeq \varepsilon_{\underline{G},\underline{G}'} \quad (\hat{e}_{\underline{G}} \cdot \hat{e}_{\underline{G}'}) \qquad \text{(VII-89)}$$

Once the matrix elements $\underline{\underline{\varepsilon}}_{\underline{G},\underline{G}'}$ are known, the self consistent Floquet mode solution of the electromagnetic wave in the crystal may be rigorously found by solving the infinite set of equations (VII-84) for the Floquet components $\underline{E}_{\underline{G}}$. Even though this solution is almost straightforward, it does not seem to have drawn interest from solid state physicists who work in this field. They would calculate the matrix elements mostly for the purpose of using them to obtain the

macroscopic dielectric constant with the local field effect: $\varepsilon_{macro} = 1/[\bar{\varepsilon}^{-1}_{\underline{G},\underline{G}'}]_{00}$ [e.g. Van Vechten 1972, Louie 1975]. For this reason, until recently, the off-diagonal matrix elements $\bar{\varepsilon}_{\underline{G},\underline{G}'}$ $(\underline{G},\underline{G}' \neq 0,0)$ were never reported.

Only recently, Johnson [1974] has reported the calculated values of the dielectric matrix elements $\bar{\varepsilon}_{\underline{G},\underline{G}'}$ of the diamond crystal at optical frequency ($\hbar\omega$ = 1.5 eV), and Louie et al [1975] reported these values for silicon crystal. Johnson [1975] also presented an approximate solution for the transverse components of the space harmonics amplitudes $|\hat{e}_{q_{\underline{G}}} \times \underline{E}_{\underline{G}}|$. He has found in the case of diamond that these components are quite small relative to the fundamental harmonic $|\underline{E}_o|$. Our goal in the following short analysis is to find the longitudinal components of the space harmonics $\hat{e}_{q_{\underline{G}}} \cdot \underline{E}_{\underline{G}}$. This follows from a very simple derivation analogous to the one used to derive Eq. (V-A28). It turns out that the longitudinal components of the space harmonics, in contrast to the transverse components, have appreciable magnitude relative to the fundamental harmonic.

The longitudinal components are found straightforwardly by either substituting Eqs. (VII-70,82,83) in (VII-74), or simply by scalar multiplication of (VII-84) by $\hat{e}_{q_{\underline{G}}}$ resulting in

$$\sum_{\underline{G}'} \hat{e}_{q_{\underline{G}}} \cdot \underline{\underline{\varepsilon}}_{\underline{G},\underline{G}'} \cdot \underline{E}_{\underline{G}'} = 0 \qquad \text{(VII-90)}$$

or using (VII-87-89)

$$\sum_{\underline{G}'} \varepsilon_{\underline{G},\underline{G}'} (\hat{e}_{\underline{G}} \cdot \underline{E}_{\underline{G}'}) = 0 \qquad \text{(VII-91)}$$

Using the assumptions $|\varepsilon_{\underline{G},\underline{G}}| >> |\varepsilon_{\underline{G},\underline{G}' \neq \underline{G}}|$ and $|\underline{E}_o| >> |\underline{E}_{\underline{G} \neq 0}|$, we get from (VII-91) an approximate expression for the longitudinal

component (compare to V-A28)

$$(\hat{e}_{\underline{G}} \cdot \underline{E}_{\underline{G}}) \simeq - \frac{\varepsilon_{\underline{G},0}}{\varepsilon_{\underline{G},\underline{G}}} (\hat{e}_{\underline{G}} \cdot \underline{E}_0) \qquad \text{(VII-92)}$$

From Johnson's calculation for diamond [Johnson 1974] we have for example $\varepsilon_{111,111} = 1.3858$, $\varepsilon_{111,000} = -0.2469$, and consequently

$$(\hat{e}_{111} \cdot \underline{E}_{111}) \simeq 0.18(\hat{e}_{111} \cdot \underline{E}_0)$$

which shows that the longitudinal components of optical space harmonics in the crystal lattice may be comparable in magnitude to the fundamental space harmonic!

The components of optical space harmonics in the crystal lattice have not been measured experimentally. They may possibly be measured using parametric mixing with x-rays, as suggested by Freund [1969], or by using traveling wave interaction with energetic charged particles passing through the crystal. The latter suggestion is particularly appropriate for detecting the longitudinal components of the space harmonic, and may be favorable, because of the large size of these components. Direct observation of space harmonics radiation out of the crystal ("the optical Borrman effect") suggested by Johnson [1975], seems to be a too small effect to be measurable (it also is incapable of detecting the longitudinal components of the space harmonics).

Traveling Wave Interaction in the Crystal Lattice

The high amplitude of the longitudinal components of electromagnetic wave space harmonics in the crystal lattice may make possible traveling wave interaction of the kind discussed in Chapter VI between these space harmonics and charged particles (electrons) channeling through the crystal lattice. In addition to this process one would also expect a process in which radiative transitions occur via the electron wave space harmonics (instead of the electromagnetic wave space harmonics). This effect is sometimes called "coherent Bremsstrahlung" or "resonant radiation."

Coherent Bremsstrahlung was discussed by a number of workers [Dyson 1955, Überall 1956, Belyakov 1971] and was also demonstrated experimentally [Walker 1970]. The contribution of the electromagnetic wave space harmonics to the interaction was not taken into account in these references.

The analysis of this section indicates that the magnitude of the electromagnetic space harmonics is not negligible. Hence, I suggest that in addition to the "Bremsstrahlung" mechanism discussed in the mentioned references, there will be also a "traveling wave" mechanism in the crystal. This mechanism and its contribution are described by the analysis of Chapter VI (in the nonrelativistic limit).

Further examination of this effect as a possible source for coherent radiation in the x-ray regime should be of appreciable interest. I suggest that Zeolites (a family of crystals with naturally occurring longitudinal channels [Smith 1963]), may be an excellent candidate for such experiments. These crystals were originally suggested by Elachi et al [1975] for use as DFB x-ray laser resonators.

5. The Solid State Traveling Wave Amplifier

A substantial part of the analysis developed in this report deals with the case of solid state traveling wave interaction (and amplification). Therefore we discuss in this section the state of the art of research in this field, and the difficulties and the prospects of developing solid state traveling wave interaction devices.

A short review of previous work on the solid state traveling wave amplifier was given in Section 1 of Chapter IV. In general, previous analyses were based on classical models and on solution of a macroscopic plasma equation similar to the conventional traveling wave tube analysis [Pierce 1950]. Also, the structures which were proposed and tried were basically similar to the conventional traveling wave tube, composed of metallic helix or meander line, which operates as an external slow wave circuit, electrically insulated from a semiconductor rod which is placed in close proximity to the circuit [e.g., Solimar 1966, Sumi 1966, 1967, 1968, Ettenberg 1970, Freeman 1973]. Hines and Swanenburg suggested using insulated metallic mosaic patterns [Hines 1969, 1971] and interdigital electrode structures [Swanenburg 1972, 1973], in order to improve the coupling of the electromagnetic wave to the drifting carriers. All these structures are designed for radio or microwave operation and are not suitable at higher frequencies.

Few workers have reported experimental observation of solid state traveling wave amplification. Sumi and Suzuki [1968] reported observation of amplifying traveling wave interaction in devices made of InSb semiconductor and helix or meander line circuits operating

at 77°K. Freeman et al [1973] observed traveling wave amplification in structures made of InSb or Ge semiconductors and metallic meander line circuits operating at 4°K. In both cases the measured effect was quite small. A third worker [Swanenburg 1972] reported observation of negative conductance and high frequency oscillation in a somewhat different but related device (an interdigital electrode structure).

In the present work, the analysis and the devices examined were oriented more towards high frequency operation (submillimeter, far infrared). Instead of an external slow wave structure, monolithic structures which incorporate the slow wave periodic circuit in the semiconductor rod were suggested, so that closer coupling between the electromagnetic wave and the drifting carriers can take place. One kind of these devices (Fig. 8) consists of a semiconductor dielectric waveguide with a periodically corrugated boundary [Gover 1974A, Yariv 1974A]. The other kind (Figs. 28-30) consists of superlattice structures [Gover 1975]. The interaction impedance of these structures was calculated in Chapter III and in Appendix V-A.

Traveling wave interaction was analyzed in this work in three different regimes--in the collision dominated regime where macroscopic equations describe the plasma, in the kinetic classical regime where the plasma behavior is describable by the Boltzmann equations, and in the quantum regime. In all these regimes the theory was applied to various examples of high frequency solid state traveling wave amplifiers of the structures mentioned above.

In the analysis we distinguished between two possible modes of operation, one which involves individual interaction with the drifting

carriers, the other involves collective interaction with the carriers space charge wave. Both mechanisms require satisfaction of a population inversion condition (VI-41) or Cerenkov condition (VI-46) in order to obtain gain. The collective mechanism, which is equivalent to the regular operation mechanism in the conventional traveling wave tube amplifier, is potentially capable of providing stronger gain, but for this, a condition of a high ratio of drift to thermal velocity spread must be satisfied by the drifting carriers. It is not clear if such condition may ever be attained in semiconductor plasma.

Usually the drift velocity in semiconductors is smaller than one thousandth of the speed of light. This means that the electromagnetic wave should be slowed down by about two orders of magnitude compared to the conventional traveling wave amplifier. A priori, this is likely to reduce the efficiency of the solid state traveling wave interaction considerably compared to the TWT amplifier. On the other hand, attainability of very high carrier density in semiconductors is an inherent advantage that the solid state amplifier has over the conventional TWT amplifier.

Considerations in optimizing the operation of the solid state traveling wave amplifier were presented in Section 7 of Chapter VI. It is found that low temperature operation is advantageous for achieving gain for many reasons. In the first place it results in longer collision relaxation time τ. This permits better phase matching of the electromagnetic wave to the plasma wave, permitting higher gain in the phase matched plasma-electromagnetic wave operational mode. Also, in the single electron interaction mode higher maximum gain is attained. At low carrier-temperature the velocity distribution tail

diminishes until at T = 0 it vanishes for $|v-v_o| > v_F$ (Figs. 33,34). Thus Landau damping of the plasma wave is reduced, and better phase matching and gain in the collective interaction operation mode can be attained. At low temperatures it is sufficient to get v_o only slightly larger than v_{th} or v_F in order to attain phase matching to slow space charge wave and amplification (providing collisions are negligible). In addition, at low temperature the mobility of the semiconductor (IV-16) increases appreciably so that high drift velocities can be attained at lower voltages. This also has the advantage of reducing power dissipation. The desirability of low temperatures dictates pulse operation in experimental investigation of the effect.

The effect of carrier concentration on the traveling wave interaction gain can be deduced from inspection of Eqs. (V-33,27,35). Bearing in mind that k_D^2 is proportional to the carrier density n_o, we find that the gain increases proportionally to the carrier density in the case of single electron interaction (V-33) as would be expected. The dependence of the gain on the density n_o is less obvious in the case of phase matched plasma-electromagnetic wave coupling. This dependence should be derived from (V-34,35), (V-50) or (IV-A3), depending on the operating conditions; it is different in each case, but in general the gain grows with n_o. Higher carrier concentration also affects the net gain of the device by increasing the attenuation due to traveling wave interaction with nonsynchronous space harmonics of the electromagnetic wave, and free carrier absorption of the fundamental space harmonic (due to the finite collision relaxation time τ). Also, we

notice that if the carriers are introduced by impurity doping, high doping level will limit the collision relaxation time τ even at low temperature, since impurity scattering mechanism will become dominant. This, as we explained before, has a negative effect on the gain. This difficulty is avoided if the carriers are introduced by injection.

In the choice of material for the solid state traveling wave amplifier, the attainability of high drift velocity and low thermal velocity spread should be a major criterion. Low band gap semiconductors have lower effective mass and correspondingly higher mobility (IV-16), so that higher drift velocity can be attained at low fields. On the other hand, the thermal velocity is inversely proportional to the square root of the effective mass m (V-16) which makes it harder to attain low thermal velocity spread in low effective mass materials.

In general the drift velocity of drifting carriers in the solid is limited to a little higher than 10^7 cm/sec. The most stringent limiting factors are scattering of electrons by optical phonons (which are present in any solid with more than one atom per unit cell) and intervalley scattering in semiconductors with the appropriate band structure. Comprehensive discussions of the different loss mechanisms by which an electron loses its energy can be found in [Rose 1966A,1966B, 1967,1969,1972] and in [Conwell 1967]. The highest drift velocity reported in semiconductors is $v_o = 9 \times 10^7$ cm/sec measured in indium antimonide at 77°K [Glicksman 1963]. This makes this material a favorite candidate for application in solid state traveling wave amplifiers. In other semiconductors the maximum drift velocity was measured to be in the range 1×10^7 to 3×10^7 cm/sec. (See for

example: GaAs [Ruch 1968, 1970], GaAlAs [Immorlica 1974], InP [Glover 1972, Hayes 1974], CdTe [Canali 1971A], Si [Canali 1971B, 1973, Haas 1973, Scharfetter 1969], Ge [Chang 1968, Ottaviani 1973]).

Another important parameter of the carrier distribution function is the thermal velocity. Low thermal velocity spread is desirable for attaining gain, particularly if phase matched plasma-electromagnetic wave amplification is attempted. There is very little experimental data on the thermal velocity spread of drifting electrons or their detailed distribution function. Mooradian et al [1970] measured the velocity distribution of drifting carriers in GaAs by Raman scattering. At drift velocity $v_o = 1.3 \times 10^7$ cm/sec, the distribution function fitted a shifted Gaussian with a carriers' temperature of the order of 300°K to 400°K, far exceeding the lattice temperature (40°K). By contrast, Southgate et al [1970A,1970B,1971] measured the distribution function by measuring the shift in radiative recombination photoluminescence. Their measurements fitted a shifted Gaussian with a carriers' temperature of 77°K which was the same as the lattice temperature.

It is difficult to estimate with the limited experimental data available the maximum attainable ratio of drift to thermal velocity v_o/v_{th}. However it seems that a ratio v_o/v_{th} appreciably higher than unity may be hard to attain with any material even under pulsed conditions. Glicksman and Hicinbothem [1963] estimated in their experiment in InSb that they attained relatively high ratios of drift to thermal velocity (0.7) and drift to transverse thermal velocity (1.5) at 77°K.

The estimates of attainable traveling wave interaction made in this work are quite low. Relatively high gain may be attained in the collective interaction operation mode (see Chapter V, Table 25). However, the conditions for this case (thermal velocity smaller than the drift velocity) may be unattainable. In the examples which were presented in this work (predominantly in order to illustrate the theory) we also ignored the fact that the semiconductors discussed may have high background fundamental lattice and free carrier absorption at the operation frequency, so that net gain may not be attained.

The estimates which result from the different examples which were presented in this work do not rule out the possibility that a practical solid state traveling wave amplifier or oscillator may be produced in the future, and operate with net gain in the submillimeter or infrared regime. It is apparent, however, that successive research efforts should be made to find better operational conditions and higher gains. Analytical research can provide a better estimate of expected gain in the different regimes by assuming more general models, three dimensional analysis and interaction through higher order harmonics. Important new results and estimates may result from considering traveling wave interaction through electron wave space harmonics in superlattice structures (see discussion in Appendix VII-B). Experimental and theoretical investigation of different materials (possibly other than semiconductors), different ways to introduce the carriers (possibly injection), different structures and operating conditions, may make the embodiment of a practical device possible in the future.

Finally we should mention that there exists a similarity between the analysis of solid state traveling wave interaction in the different regimes and the acoustoelectric effect. In the acousto-electric effect an acoustic wave interacts with the drifting electrons instead of an electromagnetic space harmonic. The low velocity of the acoustic wave makes it unnecessary to use a periodic slow wave structure. The coupling of the acoustic waves to the drifting electrons may be longitudinal or transverse, depending on the kind of acoustic wave and the crystal. Noting the analogy between the traveling wave interaction and the acoustoelectric effect may help in the investigation of each case. A detailed discussion on the acoustoelectric effect can be found in [Rose 1966A, 1966B, 1967, 1969, 1972]. As in the present report, the acoustoelectric effect has been analyzed in the three different regimes: using macroscopic plasma equations [e.g.White 1962, Blotekjaer 1964, Barybin 1968]; using the Boltzmann kinetic equation [e.g. Tsu 1965]; and using quantum mechanical model [e.g. Paranjape 1963, Spector 1965, Tsu 1967]. An original generalized quantum mechanical discussion on amplification of any kind of negative enrgy quanta in drifting plasma was presented by Musha [1963, 1964].

6. Limitations of the Present Analysis of Traveling Wave Interaction

In concluding this chapter it is in order to point out some of the limitations of the analyses presented in this work, and especially in their application to the problem of the solid state traveling wave amplifier.

Perhaps the most limiting assumption was the use of a one dimensional model, assuming only longitudinal coupling and no transverse variation of the field. In the case of solid state traveling wave amplifier, this may have very limited validity in structures where the periodic perturbation is on the surface of the device (Fig. 8). However in devices where the periodic perturbation is distributed throughout the bulk (Figs. 28, 29), these assumptions are quite valid. The one dimensional model gave us a clear description of the traveling wave interaction mechanism, allowing extension to different regimes, and providing information on both the single particle and collective interaction mechanisms. All this could have been lost in a more complicated formulation, including transverse variation and transverse field coupling. When the problem is analyzed in a three dimensional model it is found that also some beam parameters, and particularly the plasma frequency ω_p are modified, because of the finite width of the carriers' stream [e.g. Hutter 1960, p. 169]. Extension of the one dimensional analysis in the case of classical macroscopic plasma equations is given in [Sumi 1967, Steele 1969].

The expressions for the interaction impedance of the various structures, which were calculated in Chapter III and in Appendix V-A, have limited validity. They are based on a first order approximate

solution of Maxwell equations. In the case of the surface perturbed structures (Fig. 8), the approximation fails at large corrugation depth. In this case, higher order approximation or numerical solution for the amplitude of the space harmonics is required, in order to calculate the interaction impedance.

Another limitation is the use of a drifting Gaussian approximation to describe the carrier distribution in some of the examples presented. This however is not a limitation of the analysis, because any other known carrier distribution could be used in the equations. In principle one can calculate numerically the theoretical distribution function of drifting carriers and use it in the present model. However, as we pointed out in the previous section, the limited experimental data on the drifting carriers distribution function justifies in many cases the use of the Gaussian distribution approximation.

The extension of the analyses of Chapters V, VI to include collisions may have limited validity when the collisions are very frequent, a situation which, unfortunately, is often unavoidable in practice. The use of a single, energy-independent collision relaxation time τ, is then incorrect. To solve the problem exactly one would have to include all the collision mechanisms in the model which will make it very elaborate.

If the carriers plasma is introduced into the semiconductor by impurity doping, the impurity levels will have a negative effect by scattering carriers and by "freezing" carriers at low temperatures. In addition quantum transitions of excited electrons from conduction

band states to impurity level states is a process which may also compete with the intraband transition process. This effect was not taken into account in the present (except for possibly including the effect in τ). This problem can be avoided if the carriers are introduced by other ways (like injection).

In structures where the periodic structure is in the path of the carriers (especially in the superlattice structures, Figs. 28-30), the electron wave as well as the electromagnetic wave may be affected by the periodicity and have an appreciable contribution to the traveling wave interaction process. This effect is qualitatively discussed in Appendix VII-B, but was not quantitatively analyzed in this work. Notice that it is possible in principle to avoid an "electronic contribution" even in superlattice structures. For example, in a heterojunction superlattice structure which is doped uniformly by donors, the conduction band will be flat in space, and the electrons will not "sense" the periodicity but the electromagnetic wave will. However, in order to attain a stronger effect it may be preferable to use conditions where the electronic wave is affected, and there is then need for extension of the analysis of this work.

Finally there is the limitation of "pump depletion" or "gain saturation." This is the situation when the gain and the power density of the amplified radiation is high enough to cause a reduction of the population inversion of the electronic states between which transitions take place. This situation is not likely to be attained in the case of solid state traveling wave interaction. For traveling wave interaction with vacuum accelerated electrons, extension of the analysis to include the pump depletion effect may be of interest.

Appendix VII-A. The Distribution Function of the Vacuum Tube Electron Beam

The electron beam in the classical traveling wave interaction theory is usually considered monoenergetic. In order to investigate the limits of the classical theory we must have some estimate of the electron beam velocity distribution.

The first three moments of the beam distribution can be estimated by some simplified considerations (assume a non-relativistic electron beam). The average velocity is found from the beam kinetic energy

$$v_o = \sqrt{\frac{2\mathcal{E}}{m}} = \sqrt{\frac{2\ eV}{m}} \qquad \text{(VII-A1)}$$

where $\mathcal{E}$ is the electron kinetic energy

$$\mathcal{E} = eV \qquad \text{(VII-A2)}$$

and V is the acceleration potential. The electron density is computed from the given current density of the beam I/S.

$$n_o = \frac{I/S}{ev_o} \qquad \text{(VII-A3)}$$

Thus the beam becomes more diluted the more it is accelerated.

Some care is required in calculating the longitudinal temperature (which is the significant parameter in our model). All electrons gain the same energy eV during the acceleration, therefore the energy spread $\Delta\mathcal{E}$ stays the same before and after acceleration. This causes the velocity spread to change during the acceleration

$$mv_o\Delta v = \Delta\mathcal{E} \qquad \text{(VII-A4)}$$

Identifying Δv as a thermal velocity spread v_{th} and $\Delta\mathcal{E}$ with the initial thermal energy $k_B T_i \equiv m(v_{th})_i^2/2$ (Eq. V-16) we get

$$v_{th} = \frac{1}{2}\frac{(v_{th})_i^2}{v_o} \tag{VII-A5}$$

$$k_B T = \frac{1}{4}\frac{(k_B T)_i^2}{\mathcal{E}} \tag{VII-A6}$$

$$T = \frac{k_B}{4}\frac{T_i^2}{\mathcal{E}} = \frac{k_B}{2m}\frac{T_i^2}{v_o^2} \tag{VII-A7}$$

Thus the longitudinal thermal velocity v_{th} and beam temperature T reduce considerably as the beam is accelerated. This can be viewed as cooling down of the plasma gas due to its expansion (reduction of n_o).

In practice the electron beam distribution can hardly be considered a Gaussian distribution which is characterized by its first three moments. A detailed analysis of the electron beam distribution in a diode is given in [Poritsky 1953].

Assuming that the electrons emitted from the cathode obey a Gaussian distribution with temperature T_i (about the cathode temperature), and then noting that only electrons with some minimum initial velocity leave the cathode without being repelled back, it is found that the one dimensional (z direction) velocity distribution is an abruptly starting function (see Fig. 41) given by

$$f(u) = \begin{cases} 2n_i e^{\frac{e(V-V_m)}{k_B T_i}} \left(\frac{m}{2\pi k_B T_i}\right)^{1/2} e^{-\frac{mu^2}{k_B T_i}} & u > u_\ell \\ 0 & u < u_\ell \end{cases} \tag{VII-A8}$$

$$u_\ell \equiv \left[\frac{2e}{m}(V-V_m)\right]^{1/2} \tag{VII-A9}$$

where V_m is the potential minimum near the cathode where the velocity distribution is half a Gaussian with parameters $2n_i$ and T_i (see Fig. 41).

Even though the velocity distribution is quite different from a Gaussian it still may be useful to know the first three moments. Using the distribution (VII-A8) and definitions (V-14-16) one obtains

$$v_o \equiv \bar{u} = \frac{2k_B T_i}{m\pi} \frac{e^{-\eta}}{1 - \text{erf}\sqrt{\eta}} \tag{VII-A10}$$

$$n = n_i e^{\eta}(1-\text{erf}\sqrt{\eta}) = \frac{I}{ev_o} \tag{VII-A11}$$

$$T = \frac{m}{2k_B} v_{th}^2 \equiv \frac{m}{k_B}(\overline{u^2} - \bar{u}^2) =$$

$$= \left[1 + \frac{2\sqrt{\eta}\ e^{-\eta}}{\sqrt{\pi}(1-\text{erf}\sqrt{\eta})} - \frac{2e^{-2\eta}}{\pi(1-\text{erf}\sqrt{\eta})^2}\right] T_i \tag{VII-A12}$$

where

$$\eta \equiv \frac{e(V-V_m)}{k_B T_i} \tag{VII-A13}$$

As would be expected, Eqs. (VII-A10-A12) reduce into (VII-A1, A3,A7) in the limit $\eta >> 1$ (second order asymptotic expansion of $\text{erf}(\sqrt{\eta})$ must be used in (VII-A12)).

Finally, we will shortly present some equations for the relativistic electron beam case. The electron beam energy is given by

$$\mathcal{E} = \gamma m_o c^2 \tag{VII-A14}$$

where

$$\gamma = \frac{1}{\sqrt{1 - (v/c)^2}} \tag{VII-A15}$$

The beam velocity can be calculated from the acceleration potential which is equal to the gain in kinetic energy

$$\mathcal{T} = \mathcal{E} - m_o c^2 = (\gamma-1)m_o c^2 = eV \tag{VII-A16}$$

Instead of (VII-A4) we now have

$$\Delta\mathcal{E} = m_o c^2 \frac{d\gamma}{dv}\Delta v = \gamma^3 m_o v \Delta v \qquad \text{(VII-A17)}$$

or

$$\frac{\Delta v}{v} = \frac{1}{\gamma^2 - 1}\frac{\Delta\mathcal{E}}{\mathcal{E}} = \frac{(m_o c^2)^2}{\mathcal{E}^2 - m_o^2 c^4}\frac{\Delta\mathcal{E}}{\mathcal{E}} \qquad \text{(VII-A18)}$$

For a highly relativistic beam

$$\frac{\Delta v}{v} \simeq \left(\frac{m_o c^2}{\mathcal{E}}\right)^2 \frac{\Delta\mathcal{E}}{\mathcal{E}} \qquad \text{(VII-A19)}$$

We thus get correspondingly to (VII-A5,A7)

$$v_{th} = \frac{1}{2c}\frac{(v_{th})_i^2}{\gamma^3 v/c} \simeq \frac{1}{2c}\left(\frac{m_o c^2}{\mathcal{E}}\right)^3 (v_{th})_i^2 \qquad \text{(VII-A20)}$$

$$T = \frac{k_B}{2m_o c^2}\frac{T^2}{\gamma^6 v^2/c^2} \simeq \frac{k_B}{2m_o c^2}\left(\frac{m_o c^2}{\mathcal{E}}\right)^6 T_i^2 \qquad \text{(VII-A21)}$$

The velocity spread and the temperature of a relativistic electron beam reduces very strongly with the acceleration, even more so than in the nonrelativistic beam case. The carriers density n_o is calculated as in the nonrelativistic case (Eq. VII-A3).

A useful expression for the beam velocity can be readily derived from (VII-A15)

$$\frac{v}{c} = \sqrt{1 - \gamma^{-2}} = \sqrt{1 - \left(\frac{m_o c^2}{\mathcal{E}}\right)^2} =$$

$$= \sqrt{1 - \left(\frac{1}{1+eV/m_o c^2}\right)^2} = \sqrt{1 - \left(\frac{1}{1+V/512.437}\right)^2} \qquad \text{(VII-A22)}$$

where V is measured in KV.

Appendix VII-B: Superlattice Effects

In the solid state traveling wave structures suggested before (Figs. 8, 28-30) the periodic "slow wave circuit" is a monolithically integral part of the device and not only the electromagnetic wave but also the electron wave may "feel" the periodicity. This is particularly true for the superlattice structures (Figs. 28-30). This mechanism may make, in the appropriate conditions, a major contribution to the traveling wave interaction. However, its detailed analysis is not attempted at present; only some qualitative observations will be made in this Appendix, and related research on superlattice effects will be listed.

The single electron traveling wave interaction process was described in Chapter VI as a radiative electronic transition, in which an energetic electron makes a quantum transition to a lower energy quantum state (in the case of amplification), and emits in the process a photon. The conservation of momentum in this process is made possible by the fact that the electromagnetic wave in a periodic structure has components (space harmonics) with high momentum, e.g. $\beta_1 = \beta_o + 2\pi/L$ (see Fig. 31).

We realize that if also the electron wave has space harmonics, two more momentum conserving first order processes are possible: (1) a process involving a first order space harmonic of the lower electronic state wave function; (2) a process involving a -1 order space harmonic of the higher electronic state wave function. These two processes are schematically described in Fig. 43b,c. In addition an infinite number of higher order transitions exist too.

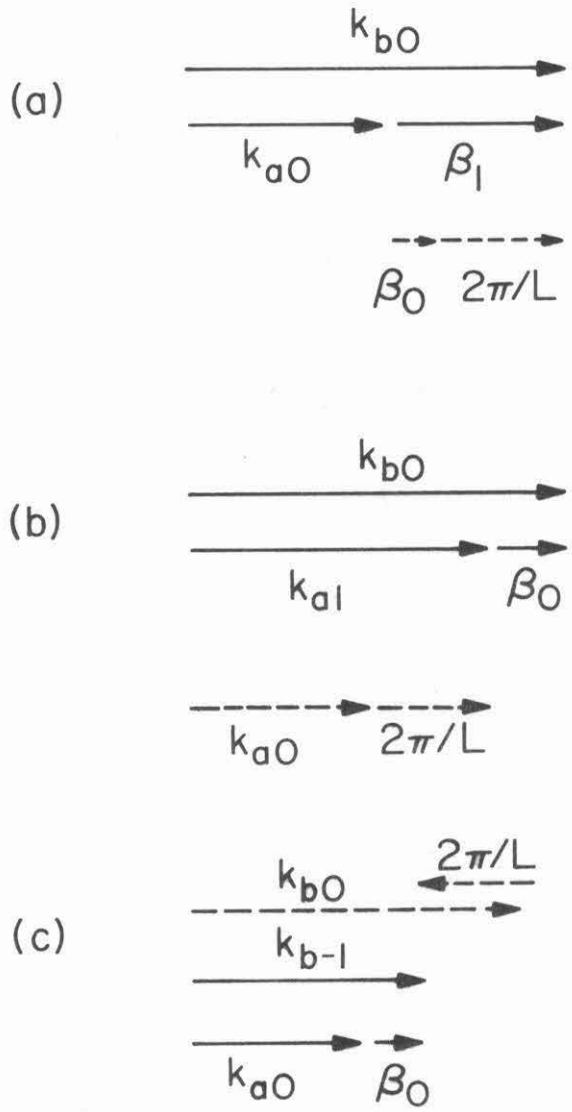

Fig. 43 The three first order processes of traveling wave interaction (intraband transitions in a superlattice). (a) is the conventional process involving a first order space harmonic of the electromagnetic wave (seeFig. 31). (b) and (c) involve first order and -1 order space harmonics of the initial and final electron wave respectively (see Fig. 44). Compare this scheme to the scheme of nonlinear optical mixing processes (Fig. 5).

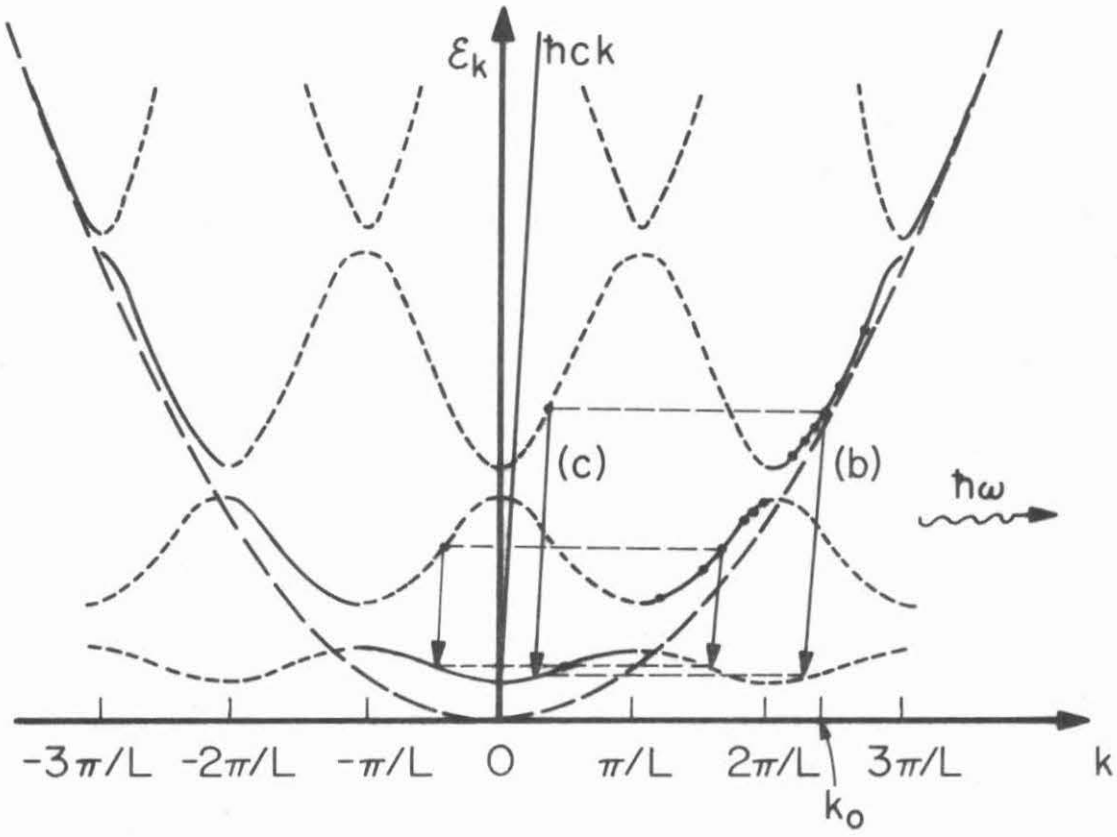

Fig. 44 The Brillouin band diagram of a superlattice. The first order transition processes (b) and (c) are explained schematically in Fig. 43. Also a transition from the second superlattice band to the first band is shown.

In the broader sense, we view the traveling wave interaction as a case of three wave interaction in a periodic structure. This case is analogous to a nonlinear optics parametric interaction of three optical waves, a particular case of which (second harmonic generation) was discussed in Section 2 of Chapter III. Fig. 43 should be compared to Fig. 5, and Eq. (III-17) expresses the different momentum conserving processes (which are, to first order, the three processes shown in Figure 43).

A Brillouin diagram description of the two processes of Fig. 43 b,c is presented in Fig. 44. The effect of the periodicity is to create mini-Brillouin zones associated with the superlattice. The processes (b) and (c) of Fig. 43 can be interpreted as direct electronic transitions between the superlattice mini-bands. Compare Fig. 44 to Fig. 31 which describes only the process (a) of Fig. 43. A process which involves transition between two adjacent superlattice bands is also shown in Fig. 43. Such a process is analogous to the backward phase matched nonlinear optical mixing scheme (Fig. 6).

The scheme of Fig. 44 can be viewed as a population inversion scheme in an artificial semiconductor. It operates analogously to a conventional semiconductor laser amplifier in the far infrared or submillimeter wavelengths. The population inversion is provided by simply applying a d-c field across the superlattice. Provided the superlattice-forbidden gaps are small enough and the field is high enough, the gaps will be surpassed by either of the effects of Zener tunneling, avalanching, and impact ionization. Assuming that the drifting carrier distribution is not modified strongly by the periodic perturbation, we see from Fig. 44 that a necessary condition for this

process to take place is

$$k_o > \frac{\pi}{L} \qquad \text{(VII-B1)}$$

For $k_o = 1.4 \times 10^6 cm^{-1}$ (corresponding to $v_o = 2 \times 10^7$cm/sec in GaAs $m = 0.08\ m_e$) this gives $L > 225\text{Å}$. For $k_o = 6.74 \times 10^6 cm^{-1}$ (corresponding to $v_o = 1.4 \times 10^7$cm/sec in Ge $m = 0.55\ m_e$) this gives $L > 47\text{Å}$.

In a broader sense, the scheme of Fig. 44 can describe also situations in which the population inversion is introduced by other means than drifting carriers by a d-c field (like optical or electrical carrier injection to higher superlattice bands). In this case condition (VII-B1) is not required, and the analogy to the conventional semiconductor laser or LED is even more complete.

We pointed out here how to extend the traveling wave analysis to include the effect of the periodicity on the electrons in superlattice structures. At present we will not pursue this analysis. The recently developed art of superlattice epitaxial growth by vapor phase epitaxy [Blakeslee 1970A,B] and most recently computer controlled molecular beam epitaxy [Chang 1973, Esaki 1974A, Dingle 1974], makes this extension necessary,and may open a new direction for the investigation of solid state traveling wave interaction devices.

Most of the research on superlattice effects (which evolved only in the last few years) is based on a different approach from the one presented here. The superlattice layers are usually assumed to introduce deep potential wells for the electrons, which the electrons populate at some distinct (in the periodicity direction) potential well quantum level. Effects of negative resistance and electromagnetic

wave amplification occur when an applied electric field tilts the potential wells so that the first energy level of the potential well overlaps the second energy level of the next potential well, so that strong tunneling between the wells can take place and consequently radiative transitions [Kazarinov 1971, Tsu 1973, Esaki 1975B]. This approach can be viewed as a "tightly bound electron" approximation, while the approach presented above can be regarded as a "nearly free electron" approximation, and is useful when the average energy of the drifting electrons is high relative to the depth of the potential well.

In addition to the references mentioned before, further research on superlattice effects was reported in the following references [Esaki 1970, Lebwohl 1970, Döhler 1972A, 1972B, 1975, Dingle 1974, Tsu 1975, Van der Ziel 1975].

REFERENCES

S. L. Adler, "Quantum Theory of the Dielectric Constant in Real Solids," Phys. Rev. 126, 413 (1962).

Zh. I. Alferov, Yu. V. Zhilyaev and Hu. V. Shmartsev, "Splitting of the Conduction Band in a Superlattice Based on GaP_xAs_{1-x}", Soviet Physics-Semiconductors 5, 174 (1971).

C. V. Barnes and K. G. Dedrick, "Radiation by an Electron Beam Interacting with a Diffraction Grating. Two-Dimensional Theory", J. Appl. Phys. 37, 411 (1966)

L. S. Bartell, H. B. Thompson and R. R. Raskos, "Observation of Stimulated Compton Scattering of Electrons by Laser Beam," Phys. Rev. Lett. 14, 851 (1965).

A. A. Barybin, "Application of the Theory of Coupled Waves to the Problem of the Interaction of Carrier Drift Flow with Acoustic Waves in Piezoelectric Semiconductors," Soviet Radio Engineering and Electronic Physics 13, 1783 (1968).

A. A. Barybin and L. T. Ter-Martirosian, "Analysis of Interaction between the Electron Beam and the Field of a Delay System," Soviet Radio Engineering and Electronic Physics 14, 237 (1969).

A. A. Barybin, "On the Coupling of Waves in Nondissipative and Dissipative Systems," IEEE Trans. ED21, 516 (1974).

B. W. Batterman, "Dynamical Diffraction of X-rays by a Perfect Crystal," Rev. of Mod. Phys. 36, 681 (1964).

V. A. Belyakov, "Coherent Radiation of Charged Particles Channelled in a Crystal," JETP Lett. 13, 179 (1971)

J. Benoit, "CO_2 Laser Modulation by Hole Injection in n-Type InSb," Appl. Phys. Lett. 16, 482 (1970)

P. L. Bhatnagar, E. P. Gross and M. Krook, "A Model for Collision Processes in Gases: I. Small Amplitude Processes in Charged and Neutral One-Component Systems," Phys. Rev. 94, 511 (1954).

G. C. Bjorklund, S. E. Harris, J. F. Young, "Vacuum Ultraviolet Holography," 25, 451 (1974).

A. E. Blakeslee, "Perfection of Vapor Grown $GaAs_{1-x}P_x$ Superlattice," Proc. of Intern. Symp. on GaAs and Related Compounds, Aachen, Germany, paper #34, October 5-7 (1970A).

A. E. Blakeslee, C. F. Aliotta, "Man-Made Superlattice Crystals," IBM Research & Develop. 14, 686 (1970B).

K. Blötekjaer and C. F. Quate, "The Coupled Modes of Acoustic Waves and Drifting Carriers in Piezoelectric Crystals," Proc. IEEE 52, 360 (1964)

W. L. Bohn, "Possible Population Inversions for VUV and Soft X-Ray Transitions in Hydrogen-like Ions," Appl. Phys. Lett. 24, 15 (1974).

G. D. Boyd, F. R. Nash, and D. F. Nelson, "Observation of Acoustically Induced Phase-Matched Optical Harmonic Generation in GaAs," Phys. Rev. Lett. 24, 1298 (1970).

J. A. Bradshaw, "A Millimeter Wave Multiplier Using the Purcell Radiator,", Symp. on Millimeter Waves, Polytechnic Inst. of Brooklyn, p. 223 (March 1959).

L. Brillouin, Wave Propagation in Periodic Structures, McGraw-Hill, New York (1946).

K. H. Burrell, An Investigation of the Resonance Cone Structure in Warm Anisotropic Plasmas, Ph.D. thesis, California Institute of Technology (1974).

C. Canali, M. Martini, G. Ottaviani and K. R. Zanio, "Transport Properties of CdTe", Phys. Rev. B 4, 422 (1971A).

C. Canali, G. Ottaviani and A. Alberigi Quaranta, "Drift Velocity of Electrons and Holes, and Associated Anisotropic Effects in Silicon," J. Phys. Chem. Solids 32, 1707 (1971B).

C. Canali, A. Loria, F. Nava and G. Ottaviani, "Negative Differential Mobility for Electrons in Silicon at Temperatures below 77°K," Solid State Commun. 12, 1017 (1973).

D. M. Chang and J. G. Ruch, "Measurement of the Velocity Field Characteristics of Electrons in Germanium," Appl. Phys. Lett. 12, 111 (1968).

L. L. Chang, L. Esaki, W. E. Howard, R. Ludeke, G. Schue, "Structures Grown by Molecular Beam Epitaxy," J. Vac. Sci. Technol. 10, 655 (1973).

P. D. Coleman and C. Enderby, "Megavolt Electronics Cerenkov Coupler for the Production of Millimeter and Submillimeter Waves, J. Appl. Phys. 31, 1695 (1960).

E. M. Conwell, High Field Transport in Semiconductors, Solid State Physics Supplement 9, Academic Press, New York (1967).

F. W. Dabby, A. Kestenbaum and U. C. Paek, "Periodic Dielectric Waveguides," Optics Comm. 6, 125 (1972).

F. W. Dabby, M. A. Saifi, A. Kestenbaum, "High Frequency Cutoff Periodic Dielectric Waveguides," Appl. Phys. Lett. 26, 190 (1973).

K. Das Gupta, "Evidence of Stimulation in X-Ray Emission," Colloq. Spectroscopicum Internationale XVII, Firenze, September 1973, ACTA Vol. II (1973A).

K. Das Gupta, "Nonlinear Increase in Bragg Peak and Narrowing of X-Ray Lines," Phys. Lett. 46A, 179 (1973B).

S. Deb, P. K. Choudhury, "Infrared and Submillimeter Wave Modulation Using Free Carrier Absorption in p-n Junction Diodes," Solid State Electr. 9, 113 (1966).

R. Dingle, W. Wiegmann and C. H. Henry, "Quantum States of Confined Carriers in Very Thin $Al_xGa_{1-x}As$-GaAs-$Al_xGa_{1-x}As$ Heterostructures," Phys. Rev. Lett. 33, 827 (1974).

G. H. Döhler, "Electron States in Crystals with nipi-Superstructure," Phys. Stat. Sol. B 52, 79 (1972A).

G. H. Döhler, "Electrical and Optical Properties of Crystals with nipi-Superstructure," Phys. Stat. Sol. B 52, 533 (1972B).

G. H. Döhler, R. Tsu and L. Esaki, "A New Mechanism for Negative Differential Conductivity in Superlattices," IBM Research Prepublication RC5234 (Jan. 27, 1975).

M. A. Duguay, "X-Ray Lasers: A Status Report," Laser Focus 9, 41 (1973).

D. A. Dunn, W. A. Harman, L. M. Field, G. S. Kino, "Theory of the Transverse-Current Traveling-Wave Tube, Proc. IRE 44, 879 (1956).

F. J. Dyson and H. Uberall, "Anisotropy of Bremsstrahlung and Pair Production in Single Crystals," Phys. Rev. 99, 605 (1955).

H. Ehrenreich and M. H. Cohen, "Self-Consistent Approach to the Many-Electron Problem," Phys. Rev. 115, 786 (1959).

C. Elachi, "Electromagnetic Wave Propagation and Source Radiation in Space-Time Periodic Media," AFOSR Scientific Report AFOSR-TR-0175 (Nov. 1971).

C. Elachi, "Electromagnetic Wave Propagation and Wave-Vector Diagram in Space-Time Periodic Media," IEEE Trans. on Antennas and Propagation, AP-20, 534 (1972).

C. Elachi, G. Evans and F. Grunthaner, "Proposed Distributed Feedback Crystal Cavities of X-ray Lasers," Appl. Optics 14, 14 (1975).

L. Elias, W. Fairbank, J. Madey, H. A. Schwettman and T. Smith, "Observation of Stimulated Emission of Radiation by Relativistic Electrons in a Spatially Periodic Transverse Magnetic Field," unpublished (June 1975).

R. C. Elton, "Analysis of X-Ray Laser Approaches: 2. Quasistationary Inversion on K-Alpha Innershell Transitions," Naval Research Laboratory Memo. Report 2906 (Oct. 1974).

L. Esaki and R. Tsu, "Superlattice and Negative Differential Conductivity in Semiconductors," IBM J. Res. Develop. 14, 61 (1970).

L. Esaki, "Computer Controlled Molecular Beam Epitaxy," Jap. Appl. Phys. Suppl. 52, 821 (1974A).

L. Esaki and L. L. Chang, "New Transport Phenomenon in a Semiconductor Superlattice," Phys. Rev. Lett. 33, 495 (1974B).

L. Esaki, IBM Watson Research Center, private communication (1975).

M. Ettenberg and J. S. Nadan , "The Theory of the Interaction of Drifting Carriers in a Semiconductor with External Traveling-Wave Circuits," IEEE Trans. ED-17, 219 (1970).

P. P. Ewald, "Crystal Optics for Visible Light and X-Rays," Rev. of Mod. Phys. 37, 46 (1965).

Gy. Farkas, Z. Gy. Horvath, "Metal Monocrystals as Possible DFB X-Ray Laser Materials in Preplasma State," Phys. Lett. 50A, 45 (1974).

W. Fawcett, "Recent Developments in the Calculation of Hot Electron Distribution Functions," Proc. 10th Int. Conf. on Phys. of Semiconductors, Cambridge, Mass., Aug. 1970, p. 51 (Washington, D.C. U.S. Atomic Energy Commission 1970).

R. A. Fisher, "On the Possibility of a Distributed Feedback X-Ray Laser," VIII International Quantum Electronics Conf. San Francisco, June 1974. Reprinted in J. Quantum Electronics QE-10, 779 (1974A).

R. A. Fisher, "Possibility of a Distributed-Feedback X-Ray Laser," Appl. Phys. Lett. 24, 598 (1974B).

V. I. Fistul, Heavily Doped Semiconductors, Plenum Press, New York (1969).

J. C. Freeman, V. L. Newhouse and R. L. Gunshor, "Interactions between Slow Circuit Waves and Drifting Carriers in InSb and Ge at 4.2°K", Appl. Phys. Lett. 22, 641 (1973).

I. Freund, "Parametric Conversion of X-Rays," Phys. Rev. Lett. 23, 854 (1969).

I. Freund, "Optically Stimulated X-Ray Laser," Appl. Phys. Lett. 24, 13 (1974).

B. D. Fried and S. D. Conte, The Plasma Dispersion Function, Academic Press, New York (1971).

M. Friedman and M. Herndon, "Generation of Intense Infrared Radiation from an Electron Beam Propagating through a Rippled Magnetic Field," Appl. Phys. Lett. 22, 658 (1973).

H. Garvin, E. Garmire, S. Somekh, H. Stoll and A. Yariv, "Ion Beam Micromachining of Integrated Optics Components," Appl. Opt. 12, 455 (1973).

J. W. Gewartowski and H. A. Watson, Principles of Electron Tubes, Van Nostrand, Princeton, N.J. (1965).

V. L. Ginzburg and V. V. Zheleznyakov, "On the Essential Identity of the Amplification of Longitudinal Plasma Waves and the Negative Absorption of Cerenkov Radiation in an Electron Stream," Phil. Mag. 11 (1965).

M. Glicksman and W. A. Hicinbothem Jr., "Hot Electrons in Indium Antimonide," Phys. Rev. 129, 1572 (1963).

G. H. Glover, "Microwave Measurement of the Velocity-Field Characteristic of n-Type InP," Appl. Phys. Lett. 20, 224 (1972).

R. W. Gould, "A Coupled Mode Description of the Backward Wave Oscillator and the Kompfner Dip Condition," IRE Trans. ED-2, 37 (1955).

A. Gover and A. Yariv, "Monolithic Solid-State Traveling-Wave Amplifier," J. Appl. Phys. 45, 2596 (1974A).

A. Gover, K. H. Burrell and A. Yariv, "Solid-State Traveling-Wave Amplification in the Collisionless Regime," J. Appl. Phys. 45, 4847 (1974B).

A. Gover and A. Yariv, "Intraband Radiative Transitions and Plasma-Electromagnetic Wave Coupling in Periodic Semiconductor Structures," J. Appl. Phys. 46, 3946 (1975).

G. A. Haas, T. Pankey, Jr., and F. H. Harris, "Temperature Dependence of Electron Drift Velocity in Silicon," J. Appl. Phys. 44, 2433 (1973).

R. E. Hayes, "Measurement of the Velocity-Field Characteristic of Indium Phosphide by the Microwave Absorption Technique," IEEE Trans. ED-21, 233 (1974).

W. Heitler, The Quantum Theory of Radiation, Oxford at the Clarendon Press (1936).

A. Hessel, "Resonances in the Smith-Purcell Effect," Canadian J. Phys. 42, 1195 (1964).

M. E. Hines, "Theory of Space-Harmonic Traveling-Wave Interactions in Semiconductors," IEEE Trans. ED-16, 88 (1969).

M. E. Hines, "High Power Solid State Microwave Device", U.S. Patent 3,555,444 (Jan. 12, 1971).

R.G.E. Hutter, Beam and Wave Electronics in Microwave Tubes, Van Nostrand, Princeton, N.J. (1960).

A. A. Immorlica, Jr. and G. L. Pearson, "Velocity Saturation in n-type $Al_xGa_{1-x}A_s$ Single Crystals," Appl. Phys. Lett. 25, 570 (1974).

J. D. Jackson, Classical Electrodynamics, John Wiley Inc., New York, (1962).

D. L. Johnson, "Local Field Effect and the Dielectric Response Matrix of Insulators: A Model," Phys. Rev. B 9, 4475 (1974).

D. L. Johnson, "Local Field Effects, X-Ray Diffraction, and the Possibility of Observing the Optical Borrman Effect: Solution to Maxwell's Equations in Perfect Crystals," Phys. Rev. B12, 3428 (1975).

H. Kaplan, E. D. Palik, R. Kaplan and W. Gammon, "Calculation of Attenuated-Total-Reflection Spectra of Surface Magnetoplasmas on Semiconductors," J. Opt. Soc. Am. 64, 1551 (1974).

R. F. Kazarinov and R. A. Suris, "Possibility of the Amplification of Electromagnetic Waves in a Semiconductor with Superlattice," Sov. Phys. Semicond. 5, 707 (1971).

D. L. Kendall, "On Etching Very Narrow Grooves in Silicon," Appl. Phys. Lett. 26, 195 (1975).

K. L. Kliewer and R. Fuchs, "Lindhard Dielectric Functions with Finite Electron Lifetime," Phys. Rev. 181, 552 (1969).

H. Kogelnik and C. V. Shank, "Coupled-Wave Theory of Distributed Feedback Lasers," J. Appl. Phys. 43, 2327 (1972).

N. M. Kroll, "Free-Electron Lasers," Chap. IIID (p.69) in "High Energy Visible and Ultraviolet Lasers," Stanford Research Institute Tech. Report JSR-74-1 (March 1975).

E. Lalor, "Three-Dimensional Theory of the Smith-Purcell Effect," Phys. Rev. A 7, 435 (1973).

L. Landau, "On the Vibration of the Electronic Plasma," J. Phys. USSR 10, 25 (1946).

H. Lashinsky, "Cerenkov Radiation at Microwave Frequencies," Advances in Electronics and Electron Physics, p. 265, Edited by L. Marton, Academic Press, New York (1961).

B. Lax and A. H. Guenther, "Quantitative Aspects of a Soft X-Ray Laser," Appl. Phys. Lett. 21, 361 (1972).

P. A. Lebwohl and R. Tsu, "Electrical Transport Properties in a Superlattice," J. Appl. Phys. 6, 2664 (1970).

J. Lindhard, "On the Properties of a Gas of Charged Particles," Kgl. Danske Viden Skab. Selskab, Mat. Fys. Medd. 28, no. 8 (1954).

S. G. Louie, J. R. Chelikoswky and M. L. Cohen, "Local Field Effects in the Optical Spectrum of Silicon," Phys. Rev. Lett. 34, 155 (1975).

H. Louisell, Coupled Modes and Parametric Electronics, J. Wiley, New York, (1960).

J.M.J. Madey, "Stimulated Emission of Bremsstrahlung in Periodic Magnetic Field," J. Appl. Phys. 42, 1906 (1971).

J.M.J. Madey, H. A. Schwettman and W. M. Fairbank, "A Free Electron Laser," Particle Accelerator Conf., San Francisco (March 1973).

D. Marcuse, "Mode Conversion Caused by Surface Imperfection of a Dielectric Slab Waveguide," BSTJ 48, 3187 (1969).

D. Marcuse, Engineering Quantum Electrodynamics, Harcourt Brace & World Inc. (1970).

D. Marcuse, Light Transmission Optics, Van Nostrand Reinhold, Princeton, New Jersey (1972).

D. Marcuse, "Coupling Coefficient for Imperfect Asymmetric Slab Waveguide," BSTJ 52, 63 (1973).

D. Marcuse, Theory of Dielectric Waveguides, Academic Press, New York (1974).

R. A. McCorkle, "Practicable X-Ray Amplifier," Phys. Rev. Lett. 29, 982 (1972).

M. Meyer and T. Van Duzer, "Travelling-Wave Amplification and Power Flow in Conducting Solids," IEEE Trans. ED-17, 193 (1970).

K. Mizuno, S. Ono and Y..Shibata, "Two Different Mode Interactions in Electron Tubes with a Fabry-Perot Resonator--The Ledatron", IEEE Trans. ED-20, 749 (1973).

K. Mizuno and S. Ono, "Comment on 'Traveling Wave Oscillation in the Optical Region: A Theoretical Examination'", J. Appl. Phys. 46, 1849 (1975).

A. Mooradian and A. L. McWhorter, "Light Scattering from Hot Electrons in Semiconductors, Proc. 10th Int. Conf. Phys. Semiconductors, Cambridge, Mass., p. 380 (1970).

T. S. Moss, "Methods for Modulating Infrared Beams," Infrared Physics 2, 129 (1962).

T. Musha, "Amplification of Waves Due to Electron Streams," J. Phys. Soc. Japan 18, 1326 (1963).

T. Musha, "Amplification of Waves Due to Quanta with Negative Energy," J. Appl. Phys. 35, 137 (1964).

J. S. Nadan, "Investigation of Solid State Traveling Wave Amplifier", Army Technical Report ECOM-2802 (Feb. 1967).

M. Nakamura, A. Yariv, H. W. Yen, S. Somekh, H. L. Garvin, "Optically Pumped GaAs Surface Laser with Corrugation Feedback," Appl. Phys. Lett. 22, 515 (1973).

M. Nakamura, K. Aiki, J. Umeda, A. Yariv, H. W. Yen and T. Morikawa, "Liquid Phase Epitaxy of GaAlAs on GaAs Substrates with Fine Surface Corrugation," Appl. Phys. Lett. 24, 466 (1974).

K. Ogawa, W.S.C. Chang, B. L. Sopori, F. J. Rosenbaum, "A Theoretical Analysis of Etched Grating Couplers for Integrated Optics," IEEE J. Quant. Electronics QE-9, 29 (1973).

T. M. O'Neil and J. H. Malmberg, "Transition of the Dispersion Roots from Beam-Type to Landau-Type Solutions," Phys. Fluids 11, 1754 (1968).

G. Ottaviani, C. Canali, F. Nava and J. W. Mayer, "Hole Drift Velocity in High Purity Ge," J. Appl. Phys. 44, 2917 (1973).

I. Palocz, "A Leaky Wave Approach to Cerenkov and Smith-Purcell Radiation," Ph.D. Dissertation, Polytechnic Institute of Brooklyn (1962).

I. Palocz and A. A. Oliner, "A Self-Consistent Theory of Cerenkov and Smith-Purcell Radiation," Symp. Quasi-Optics, Polytechnic Institute of Brooklyn, p. 217 (June 1964).

I. Palocz and A. A. Oliner, "Leaky Space-Charge Waves I: Cerenkov Radiation, Proc. IEEE, 53, 24 (1965).

I. Palocz and A. A. Oliner, "Leaky Space Charge Waves II: Smith-Purcell Radiation," Proc. IEEE 55, 46 (1967).

R. H. Pantell, G. Soncini and H. Puthoff, "S-9 Stimulated Photon-Electron Scattering," IEEE J. Quantum Electr. QE-4, 905 (1968).

B. V. Paranjape, "Amplification of Sound Waves in Semiconductors," Phys. Lett. 5, 32 (1963).

S. T. Peng, T. Tamir, H. L. Bertoni, "Leaky Wave Analysis of Optical Periodic Couplers," Elec. Comm. 9, 150 (1973).

S. T. Peng, H. L. Bertoni, T. Tamir, "Analysis of Periodic Thin Film Structures with Rectangular Profiles," Opt. Comm. 10, 91 (1974).

J. R. Pierce, Traveling Wave Tubes, Van Norstad, Princeton, N.J. (1950).

J. R. Pierce, "Coupling of Modes of Propagation," J. Appl. Phys. 25, 179 (1954).

J. R. Pierce, Almost All About Waves, MIT Press, Cambridge, Massachusetts (1974).

M. A. Piestrup, "An Ultraviolet Source Using Cerenkov Radiation," Ph.D. Thesis, Stanford University (1972).

D. Pines and R. Schrieffer, "Collective Behavior in Solid-State Plasma," Phys. Rev. 124, 1387 (1961).

D. Pines, Elementary Excitations in Solids, W. A. Benjamin, New York (1964).

A. H. Poritsky, "Electron Gas Equations for Electron Flow in Diodes," IRE Transac. on Elec. Devices PGED-2, 60 (1953).

Lord Rayleigh, "On the Maintenance of Vibrations by Forces of Double Frequency, and on the Propagation of Waves through a Medium Endowed with Periodic Structure," Phyl. Mag. 24, 145 (1887).

A. Rose, "The Acoustoelectric Effects and the Energy Losses by Hot Electrons,"

Part I, RCA Review 27, 98 (1966A).
Part II, RCA Review 27, 600 (1966B).
Part III, RCA Review 28, 634 (1967).
Part IV, RCA Review 30, 435 (1969).
Part V, RCA Review 32, 463 (1972).

J. G. Ruch and G. S. Kino, "Transport Properties of GaAs," Phys. Rev. 174, 921 (1968).

J. G. Ruch and W. Fawcett, "Temperature Dependence of the Transport Properties of GaAs Determined by a Monte Carlo Method," J. Appl.

Phys. 41, 3843 (1970).

K. Sakuda and A. Yariv, "Analysis of Optical Propagation in a Corrugated Dielectric Waveguide," Optics Communications 8, 1 (1973).

D. L. Scharfetter and T. E. Seidel, "Analysis of the I(v) Characteristics of p^{+}-n-π-p^{+} Structures for the Determination of Hole Velocity in Silicon," IEEE Transac. ED-16, 98 (1969).

R. V. Schmidt, D. C. Flanders, C. V. Shank, R. D. Standley, "Narrow-band Grating Filters for Thin-Film Optical Waveguides," Appl. Phys. Lett. 25, 651 (1974).

S. J. Smith and E. M. Purcell, "Visible Light from Localized Surface Charges Moving Across a Grating," Phys. Rev. 92, 1069 (1953).

J. V. Smith, "Structural Classification of Zeolites," Mineral Soc. Am. Special paper, 1, 281 (1963).

A. Solimar and E. A. Ash, "Some Traveling-Wave Interactions in Semiconductors-Theory and Design Considerations," Int. J. Electronics 20, 127 (1966).

S. Somekh and A. Yariv, "Phase Matching by Periodic Modulation of the Nonlinear Optical Properties," Opt. Commun. 6, 301 (1972A).

S. Somekh and A. Yariv, "Phase Matchable Nonlinear Optical Interactions in Periodic Thin Films," Appl. Phys. Lett. 21, 140 (1972B).

P. D. Southgate and D. S. Hall, "Radiative ecombination in n-GaAs from Field-Excited Hot Carriers," Appl. Phys. Lett. 16, 280 (1970A).

P. D. Southgate, "Field Dependence of Bulk Electroluminescence in Degenerate GaAs," J. of Luminescence 1,2,855 (1970B).

P. D. Southgate, D. S. Hall and A. B. Dreeben, "Hot-Electron Distribution in n-GaAs Derived from Photoluminescence Measurements

with Applied Electric Field," J. Appl. Phys. 42, 2868 (1971).

H. N. Spector, "Quantum Approach to Amplification of Optical Phonons in Semiconductors," Phys. Rev. 137A, A311 (1965).

E. Spiller and P. Zory, "X-Ray Laser Resonator," IBM Technical Disclosure Bulletin 16, 4093 (1974).

M. Steele and B. Vural, Wave Interactions in Solid State Plasmas, McGraw-Hill, New York (1969).

T. H. Stix, The Theory of Plasma Waves, McGraw-Hill, New York (1972).

H. Stoll, A. Yariv, "Coupled Mode Analysis of Periodic Dielectric Waveguides," Optics Comm. 8, 5 (1973).

H. Stoll, "Proton Implanted Optical Waveguides and Integrated Optical Detectors in GaAs," Ph.D. dissertation, Caltech (1974).

M. Sumi, "Traveling Wave Amplification by Drifting Carriers in Semiconductors," Appl. Phys. Lett. 9, 251 (1966).

M. Sumi, "Traveling Wave Amplification by Drifting Carriers in Semiconductors," Jap. J. of Appl. Phys. 6, 688 (1967).

M. Sumi and T. Suzuki, "Evidence for Directional Coupling between Semiconductor Carriers and Slow Circuit Waves," Appl. Phys. Lett. 13, 326 (1968).

T. J. B. Swanenburg, "Observation of Negative Conductance in an Interdigital Electrode Structure on an Oxidized Si-Surface," Physics Letters, 38, 311 (1972).

T. J. B. Swanenburg, "Negative Conductance of an Interdigital Electrode Structure on a Semiconductor Surface," IEEE Transac. ED-20, 630 (1973).

S. M. Sze, Physics of Semiconductor Devices, Wiley-Interscience, New York (1969).

T. Tamir, H. C. Wang and A. A. Oliver, "Wave Propagation in Sinusoidally Stratified Dielectric Media," IEEE Trans. on Microwave, MTT-12, 323 (1964).

P. K. Tien, R. J. Martin, S. L. Blank, S. H. Wemple and L. J. Varnerin, "Optical Waveguides in Single Crystal Garnet Films," Appl. Phys. Lett. 21, 207 (1972).

R. Tsu and D. L. White, "Interaction of Optical and Acoustic Phonons with Longitudinal Plasma Waves," Annals of Physics 32, 100 (1965).

R. Tsu, "Landau Damping and Dispersion of Phonon, Plasmon and Photon Waves in Polar Semiconductors, " Phys. Rev. 164, 380 (1967).

R. Tsu and L. Esaki, "Tunneling in a Finite Superlattice, "Appl. Phys. Lett. 22, 562 (1973).

R. Tsu, L. Koma and L. Esaki, "Optical Properties of Semiconductor Superlattice," J. Appl. Phys. 46, 842 (1975).

H. Überall, "High-Energy Interference Effect of Bremsstrahlung and Pair Production in Crystals," Phys. Rev. 103, 1055 (1956).

P. M. Van den Berg, "Smith-Purcell Radiation from a Line Charge Moving Parallel to a Reflection Grating," J. Opt. Soc. Am. 63, 689 (1973A).

P. M. Van den Berg, "Smith Purcell Radiation from a Point Charge Moving Parallel to a Reflection Grating, " J. Opt. Soc. Am. 63, 1558 (1973B).

J. P. Van der Ziel, R. Dingle, R. Miller, W. Wiegmann and A. Nordland, Jr. "Laser Oscillation from Quantum States in Very Thin GaAs-$Al_{0.2}Ga_{0.8}As$ Multilayer Structures," Appl. Phys. Lett. 26, 463 (1975).

J. A. Van Vechten and R. M. Martin, "Calculation of Local Effective Fields: Optical Spectrum of Diamond," Phys. Rev. Lett. 28, 446 (1972).

R. L. Walker, B. L. Berman, R. C. Der, T. M. Kavanagh, and J. M. Khan, "Channeling and Coherent Brehmsstrahlung Effects for Relativistic Positrons and Electrons," Phys. Rev. Lett, 25, 5 (1970).

D. A. Watkins, Topics in Electromagnetic Theory, John Wiley, New York (1960).

D. White, "Amplification of Ultrasonic Waves in Piezoelectric Semiconductors," J. Appl. Phys. 33, 2547 (1962).

N. Wiser, "Dielectric Constant with Local Field Effects Induced," Phys. Rev. 129, 62 (1963).

J. M. Woodall, "Solution Grown $Ga_{1-x}Al_xAs$ Superlattice Structures," J. of Crystal Growth 12, 32 (1972).

A. Yariv, "On the Coupling Coefficient in the Coupled-Mode Theory," Proc. of the IRE 46, 1956 (1958).

A. Yariv, Introduction to Optical Electronics, Holt, Rinehart and Winston, Inc. (1971).

A. Yariv and D. Armstrong, "Traveling Wave Oscillation in the Optical Region: A Theoretical Examination," J. Appl. Phys. 44, 1664 (1973A).

A. Yariv, "Coupled-Mode Theory for Guided Wave Optics," IEEE J. of Quantum Electronics QE-9, 919 (1973B).

A. Yariv and A. Gover, "Monolithic Solid State Traveling Wave Tunable Amplifier and Oscillator," U.S. Patent 3,835,407 (Sept. 10, 1974A).

A. Yariv, H. W. Yen, "Bragg Amplification and Oscillation in Periodic Optical Media," Optics Communications 10, 120 (1974B).

A. Yariv and A. Gover, "Distributed Feedback X-ray Lasers in Single Crystals," VIII International Quantum Electronics Conference, San Francisco, June 1974. Reprinted in IEEE J. of Quantum Electronics QE-10, 779 (1974C).

A. Yariv, "Analytical Considerations of Bragg Coupling Coefficients and Distributed Feedback X-ray Lasers in Single Crystals," Appl. Phys. Lett. 25, 105 (1974D).

A. Yariv, "An X-ray Laser with a Single Crystal Waveguide Structure," Patent Application CIT 1388 74/175 (1974E).

A. Yariv and A. Gover, "The Equivalence of the Coupled Mode and Floquet-Bloch Formalism in Periodic Optical Waveguides," Appl. Phys. Lett. 26, 537 (1975).

H. W. Yen, M. Nakamura, E. Garmire, S. Somekh, A. Yariv, "Optically Pumped GaAs Waveguide Lasers with a Fundamental 0.11μ Corrugation Feedback," Optics Comm. 9, 35 (1973).

B. Zotter, "Traveling Wave Amplification by Drifting Carriers in Semiconductors," Army R. and D. Report ECOM-2958 (April 1968).